VOLUME 32 FEBRUARY 1954 NUMBER 2

Canadian Journal of Chemistry

Published by THE NATIONAL RESEARCH COUNCIL
OTTAWA CANADA

CANADIAN JOURNAL OF CHEMISTRY

(Formerly Section B, Canadian Journal of Research)

The CANADIAN JOURNAL OF CHEMISTRY is published monthly by the National Research Council of Canada under the authority of the Chairman of the Committee of the Privy Council on Scientific and Industrial Research. The National Research Council publishes also: *Canadian Journal of Biochemistry and Physiology, Canadian Journal of Botany, Canadian Journal of Physics, Canadian Journal of Technology, Canadian Journal of Zoology.*

Matters of general policy concerning the Council's journals are the responsibility of a joint Editorial Board consisting of: the Editors of the journals; members representing the National Research Council of Canada and the Royal Society of Canada and two other scientific societies; and two ex-officio members.

The Chemical Institute of Canada has chosen the CANADIAN JOURNAL OF CHEMISTRY and the CANADIAN JOURNAL OF TECHNOLOGY as its medium of publication for scientific papers.

Manuscripts should be addressed to:

Dr. Léo Marion,
Editor-in-Chief,
Canadian Journal of Chemistry,
National Research Council,
Ottawa 2, Canada.

Subscriptions, renewals, and orders for back numbers should be addressed to:

Division of Administration,
National Research Council,
Ottawa 2, Canada.

Subscription rate: $6.00 a year; single numbers: 60 cents. Remittances should be made payable to the Receiver General of Canada, credit National Research Council.

CORRECTION

In Vol. 31, p. 1112. Equation [1] should read $c_2 = wD_2 - \frac{kdD_2}{dx}$.

Canadian Journal of Chemistry

Issued by THE NATIONAL RESEARCH COUNCIL OF CANADA

VOLUME 32 FEBRUARY, 1954 NUMBER 2

VISCOSITY AND MOLECULAR WEIGHT OF DEGRADED CARRAGEENIN[1]

BY C. R. MASSON AND G. W. CAINES

ABSTRACT

Viscosities and number average molecular weights of various carrageenin preparations, including thermally and photochemically degraded samples, have been measured. Aqueous solutions of carrageenin of low molecular weight are shown to exhibit viscosity characteristics which are entirely similar to those of other natural and synthetic polyelectrolytes. Solutions of carrageenin of high molecular weight exhibit plastic flow. The relationship between viscosity and molecular weight for the degraded polymer indicates that the molecular configuration in solution is that of a fairly stiff rod, even in the presence of salts.

INTRODUCTION

Carrageenin, the water-soluble polysaccharide obtained from the red alga *Chondrus crispus*, is of importance commercially as a gelling and suspending agent. The useful properties of this substance are undoubtedly due, in part, to the high viscosities which its solutions possess. Chemically, the polymer consists largely of D-galactose residues linked through positions 1 and 3 and carrying a negatively charged sulphate group on position 4. Solutions of carrageenin should therefore exhibit physical properties similar to those of other natural and synthetic polyelectrolytes.

In the course of an investigation of the kinetics of the degradation of carrageenin (9), the viscosities of various preparations in aqueous solution have been measured both in the presence and absence of salts. These measurements, along with corresponding molecular weight determinations, are described below.

EXPERIMENTAL

Details regarding the extraction of the carrageenin used in this study are given elsewhere (9). The sodium salt, prepared by means of ion-exchange techniques (9), was used in all experiments.

For most of the viscosity measurements Ostwald viscometers of similar dimensions were employed. The characteristics of these viscometers were as follows: capillary diameter 0.0515 cm.; volume of bulbs approx. 2 ml.; flow times for water 75 to 90 sec.; mean shear gradient for water 1100 to 1300 sec. $^{-1}$; kinetic energy correction less than 1%. The temperature of measure-

[1] *Manuscript received October 2, 1953.*
Contribution from the Maritime Regional Laboratory, National Research Council, Halifax, N.S., Canada. Issued as N.R.C. No. 3143.

ment was 25 ± 0.1°C. A few experiments were also performed using a commercial Stormer viscometer (A. H. Thomas Co.) equipped with a cylindrical rotor.

Molecular weights were determined osmotically at 25°C. using 0.1 *M* sodium chloride as solvent. The osmometer used here has been described elsewhere (10). Cellophane, grade P.T. 600 (kindly supplied by Canadian Industries Ltd., Montreal) was used as membrane. To avoid 'sticking' of the liquids in the osmometer capillaries, toluene was introduced into the capillaries after filling the osmometer cells, and the osmotic pressures were recorded as a head of this solvent using a cathetometer. A preservative consisting of a mixture of 1 part chlorobenzene plus 1 part dichloroethane plus 2 parts chlorobutane was added in small amounts to both solution and solvent. Osmotic equilibrium was generally attained overnight.

In the osmotic pressure measurements, a slight 'cell constant' or 'cell zero' was often observed with solvent in both half-cells, and corrections were applied for this effect. The cell constant was generally zero when a fresh membrane was used, or when solutions of high molecular weight polymer were measured. On prolonged use of the same membrane, however, or when degraded polymers of low molecular weight were employed, a small cell constant did develop.* If the necessary correction became greater than 0.05 cm., the membrane was discarded.

Concentrations were determined by weight, known portions of the solutions being evaporated to constant weight in an oven at 55°C. Further heating *in vacuo* at this temperature in an apparatus similar to that described by Grassie (7) did not lead to a significant decrease in weight of the residual polymer. Dilutions of highly viscous solutions were made by weight.

RESULTS

Fig. 1 shows the results of viscosity measurements on a relatively low molecular weight sample of carrageenin ($M = 120{,}000$) in three solvents. In aqueous solution, the reduced specific viscosity η_{sp}/c increases markedly with dilution. In the presence of a very low concentration of added salt (0.000231 *M* sodium bisulphate) the plot of η_{sp}/c against c passes through a maximum at a carrageenin concentration of approximately 0.03 gm. per 100 cc. At higher salt concentrations (0.1 *M* sodium chloride) the plot becomes linear.

These curves are entirely similar to those observed for other polyelectrolytes (4) and may be interpreted in terms of changes in molecular shape resulting from changes in the degree of ionization of the macromolecule. In dilute aqueous solution the molecule becomes rigidly extended as a result of the repulsive forces between neighboring charged groups, and the reduced viscosity increases accordingly. By analogy with the results of Fuoss and Strauss (4), the maximum observed in Fig. 1 at a low salt concentration

*These observations are in accordance with the idea that the cause of the cell constant is adsorption of polymer molecules on the membrane. It has recently been shown (S. Rothman, A. Schwebel, and S. G. Weissberg. J. Polymer Sci. 11: 381. 1953) that such adsorption does, in fact, take place on collodion membranes by radioactive dextran.

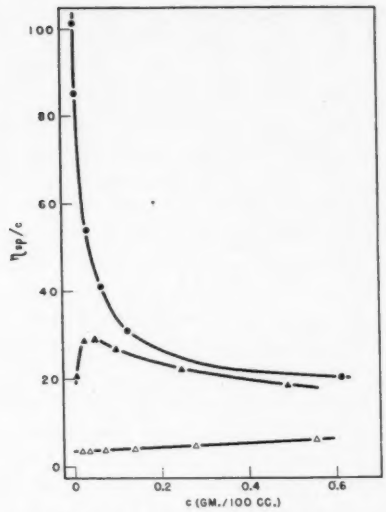

FIG. 1. η_{sp}/c vs. c for extract D in various solvents. ● water; ▲ 0.000231 M $NaHSO_4$; △ 0.1 M NaCl.

should occur when the concentration of sodium ions from the polyelectrolyte is of the same order of magnitude as the concentration of cations from the

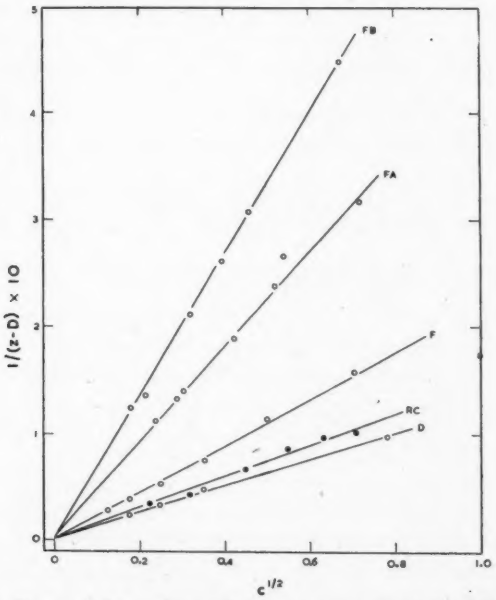

FIG. 2(*a*). $1/(z - D)$ vs. $c^{\frac{1}{2}}$ for various polymers in aqueous solution. ● Polymer of Rose and Cook.

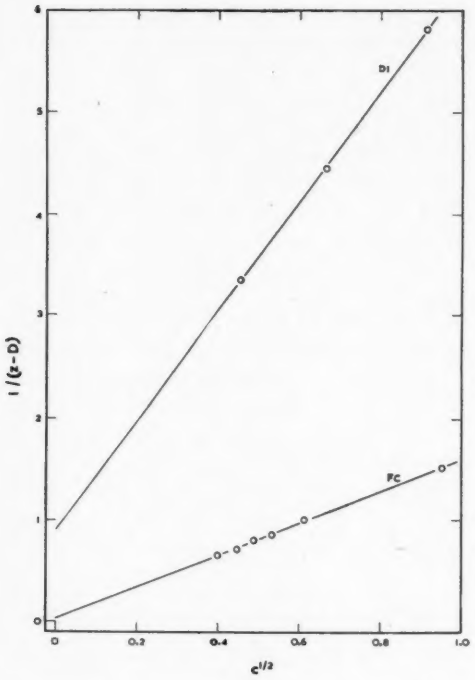

FIG. 2(*b*). $1/(z - D)$ vs. $c^{\frac{1}{2}}$ for two polymers in aqueous solution.

added salt. Assuming complete ionization of the salt, this implies that carrageenin is approximately 40% ionized at a concentration of 0.03 gm. per 100 cc. in this solvent.

The viscosities of aqueous solutions of carrageenin of low molecular weight may be adequately represented by the Fuoss (2, 3) equation

$$[1] \qquad \eta_{sp}/c = z = A/(1 + Bc^{\frac{1}{2}}) + D,$$

where A, B, and D are constants. This equation has been shown to represent the viscosity behavior of a wide variety of polyelectrolytes. Figs. 2(*a*) and 2(*b*) show plots of $1/(z - D)$ against $c^{\frac{1}{2}}$ for various samples of carrageenin. Included in Fig. 2(*a*) are points calculated from the experimental viscosity–concentration curve published by Rose and Cook (12) for an aqueous solution of a carrageen extract. Linear plots are obtained for all the polymers.

The samples designated FA, FB, and FC in these figures were prepared from the parent material F by heating a 1% solution, buffered at pH 7.0, at 90°C. for 14.3, 38.6, and 141.4 hr. respectively. The polymers were then precipitated with ethanol, washed with freshly distilled ether, and dried *in vacuo*. Solutions of these polymers were dialyzed under pressure to remove any low molecular-weight products of degradation before the viscosity and

molecular weight measurements were performed. As shown elsewhere (9), the sulphate content of the dialyzed polymer increases slightly (from 25.8% to 31.7%) as a result of this degradation.

Sample D1 was a photochemically degraded preparation, obtained by irradiating a 1% solution of extract D for 57 min. by means of a mercury resonance lamp immersed in the solution. Nitrogen was passed through the solution during this treatment to prevent possible photo-oxidation reactions. The polymer was precipitated with ethanol and sodium chloride, and dried as before. The solution of the degraded polymer was passed through ion-exchange columns before use, but was not dialyzed. The sulphate content of the degraded polymer was 25.7%.

The values of the constants A, B, and D in equation [1] have been determined for the polymers represented in Figs. 2(a) and 2(b). The slopes of the lines give the value of B/A for each polymer. The intercepts at $c^{\frac{1}{2}} = 0$ give the values of $1/A$. On account of the extremely small intercepts in Fig. 2(a), the values of A (and hence also of B) could not be determined directly for the polymers of highest molecular weight. For polymers FC and D1, however, measurable intercepts were obtained, from which values of B equal to 63 ($\pm$ 10) and 71 ($\pm$ 7) respectively were calculated. The fact that the value of B remains constant, within experimental error, for these two polymers is in accordance with the idea (3) that this constant is an electrostatic term whose value depends on the charge density along the polymer chain and is independent of molecular weight. Taking a mean value of $B = 67$, the values of A shown in Table I have been calculated for all the polymers. Included in this table are the values of D (obtained by extrapolating plots of η_{sp}/c against $c^{-\frac{1}{2}}$ to $c^{-\frac{1}{2}} = 0$) and, where measured, the intrinsic viscosities of the polymers in $M/30$ sodium phosphate buffer at pH 7.0. In this solvent, plots of η_{sp}/c against c were linear.

TABLE I

VISCOSITY CONSTANTS AND MOLECULAR WEIGHTS OF VARIOUS CARRAGEENIN PREPARATIONS

Polymer	$[\eta]$ in $M/30$ phosphate buffer (pH 7.0)	D	B/A	A	Osmotic molecular weight
D		10	0.12	558	120,000
RC*		14	0.15	446	
F	(2.48)	3.4	0.22	304	74,500
FA	1.75	2.2	0.45	149	42,900
FB	1.23	1.1	0.66	101	30,100
FC	0.74	0.75	1.57	42.6	21,800
D1		0.22	6.40	10.5	9,000

Polymer of Rose and Cook.

The results of the osmotic pressure measurements are shown in Fig. 3 where the reduced osmotic pressure π/c (π in cm. water) is plotted against concentration c (in gm. per 100 cc. solution). Molecular weights were calculated from the intercepts at zero concentration using the relationship

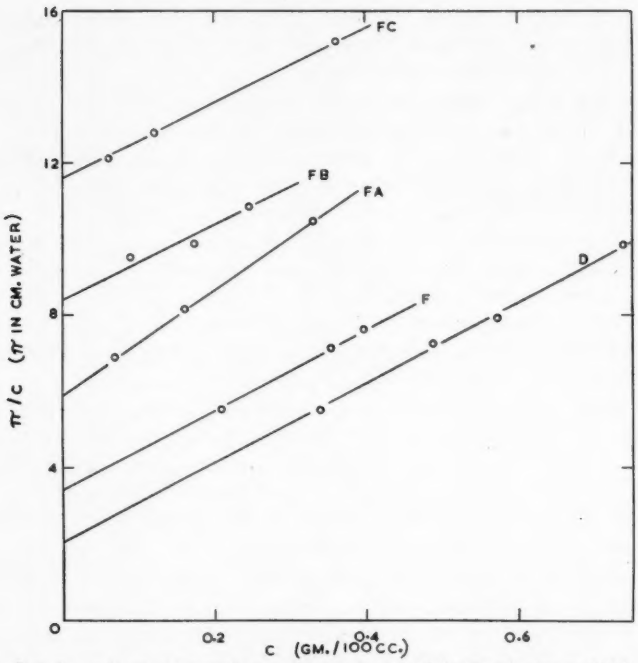

FIG. 3. π/c vs. c for various polymers in 0.1 M NaCl solution at 25°C.

$(\pi/c)_0 = 10330\ RT/M$. The values of M are given in Table I. The molecular weight of fraction D1 was so low that some diffusion of polymer through the membrane occurred, as witnessed by a slow downward drift in the osmotic pressure on standing. The approximate value of 9000 listed for the molecular weight of this fraction was obtained by using a dilute solution in the osmometer and extrapolating the osmotic pressure values back to the time of filling the osmometer.

DISCUSSION

On account of the low molecular weights observed, all the polymers described above must be considered as having been degraded to some extent. Degradation can occur either during extraction of the polymer from the seaweed (11), or upon subsequent storage of the solid extract (5). Both of these factors are believed to be responsible for the low molecular weights of extracts D and F. The molecular weight may also depend on the time of storage of the dried seaweed before extraction, although data are not yet available to test this point. Certain extracts of fresh seaweed have been found (8) to have an osmotic molecular weight of the order of 2×10^6, which is at the limit of the range of osmometric techniques.

For the low molecular weight extracts described above, viscosity measurements in the Stormer viscometer have shown that the solutions exhibit Newtonian flow, at least in the range of concentration and shear rate studied.

This is illustrated in Fig. 4(*a*) where the rate of rotation of the cylinder is plotted against the driving weight for various concentrations of extract F. The curves are essentially linear through the origin, characteristic of a Newtonian fluid. For an extract of higher viscosity, however, the curves shown in Fig. 4(*b*) were found. A 'yield point' is observed for these solutions, indicating that the flow is structual in nature, the curves being characteristic of a 'plastic' substance. Measurements in capillary viscometers at different rates of shear (6) confirm this behavior.

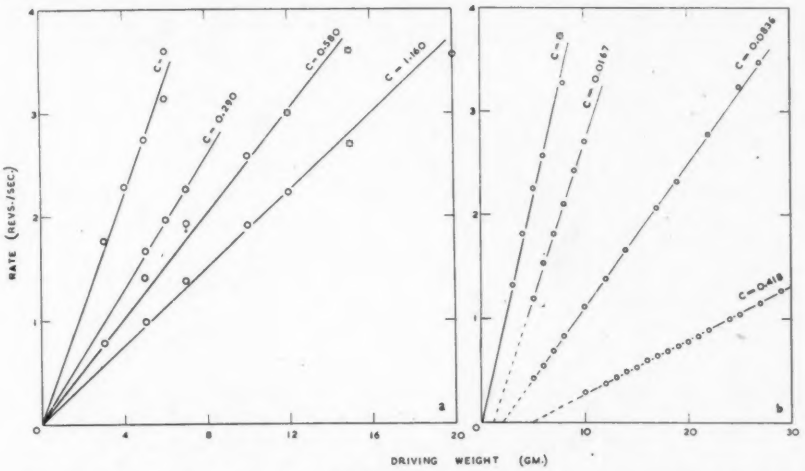

FIG. 4. Stormer viscosities. Rate of rotation of inner cylinder vs. driving weight for various concentrations of polymer. (*a*) Extract F (25°C.); (*b*) Extract A. (0°C.).

From the data in Table I an approximate value can be obtained for the constant α in the modified Staudinger equation $[\eta] = KM\alpha$ relating the intrinsic viscosity to the molecular weight. Unfortunately, the intrinsic viscosity of extract F in $M/30$ buffer was measured about two months after the other measurements had been performed. Subsequent measurements showed that degradation of the extract had taken place during storage, so that the viscosity and molecular weight values for this polymer are not exactly comparable. On the basis of the three measurements for the thermally degraded polymers, an approximate value of $\alpha = 1.28$ is obtained.

In assigning this value of α, the assumption is made that the samples have the same degree of polydisperity. Since these samples were prepared from the same parent material, and since, as shown elsewhere (9), the degradation proceeds mainly by a random process under the conditions employed, this assumption is probably justified. The high value of α should therefore have some significance, and indicates that, even in the presence of salt, the degraded carrageenin molecules exist in solution as fairly stiff rods. Since it is unlikely that this rigidity is due to the presence of ionized groups in the molecule at the salt concentration employed, the result must be interpreted in terms

of restricted rotation at the glycosidic linkage, and, possibly, an unbranched configuration for the degraded fragments. A similar conclusion concerning the structure of carrageenin of moderately low molecular weight has been reached by other workers (1).

According to equation [1], the quantity $(A + D)$ should be the value of the intrinsic viscosity of the polyelectrolyte in aqueous solution. Since the polymer molecules will be even more rigidly extended in aqueous solution than in the presence of salts, substitution of $(A + D)$ for $[\eta]$ in the Staudinger equation should result in an even higher value of α. Fig. 5 shows the plot of log $(A + D)$ vs. log M for all the polymers, from which a value of $\alpha = 1.58$ is obtained, in agreement with this consideration.

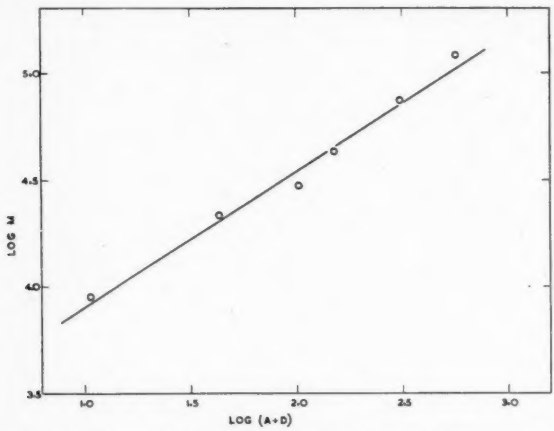

FIG. 5. L og $(A + D)$ vs. log M for degraded carrageenin.

ACKNOWLEDGMENTS

The authors are greatly indebted to Dr. L. A. McLeod of Polymer Corporation, Sarnia, Ont., for lending the osmometer used in this study. We wish to thank Dr. A. N. O'Neill of these laboratories for the extraction and purification of most of the carrageenin samples employed, and for performing the sulphate analyses. We wish also to thank Dr. E. Gordon Young for his interest and encouragement during this work.

REFERENCES

1. COOK, W. H., ROSE, R. C., and COLVIN, G. R. Biochim. et Biophys. Acta, 8: 595. 1952.
2. FUOSS, R. M. J. Polymer Sci. 3: 603. 1948.
3. FUOSS, R. M. and CATHERS, G. I. J. Polymer Sci. 4: 97. 1949.
4. FUOSS, R. M. and STRAUSS, U. P. J. Polymer Sci. 3: 602. 1948.
5. GORING, D. A. I. Private cnmmunication.
6. GORING, D. A. I. and MASSON, C. R. Unpublished.
7. GRASSIE, N. J. Polymer Sci. 6: 643. 1951.
8. MASSON, C. R. Unpublished.
9. MASSON, C. R. and O'NEILL, A. N. To be published.
10. MCLEOD, L. A. and MCINTOSH, R. Can. J. Chem. 29: 1104. 1951.
11. ROSE, R. C. Can. J. Research, F, 28: 202. 1950.
12. ROSE, R. C. and COOK, W. H. Can. J. Research, F, 27: 323. 1949.

CYCLIC THIOUREAS[1]

By A. F. McKay and G. R. Vavasour

ABSTRACT

1-β-Hydroxyethylimidazolidine-2-thione was prepared from 1-amino-5-hydroxy-3-azapentane and carbon disulphide. Since its properties differ from those claimed by Sergeyev and Kolychev (7) for this compound prepared from ethylene oxide and thiocyanic acid, its structure was confirmed by conversion to 1-β-hydroxyethyl-2-benzylamino-2-imidazoline. The latter compound was prepared for comparison from the known 1-β-hydroxyethyl-2-nitramino-2-imidazoline.

INTRODUCTION

Hofmann (4) found that ethylenediamine combined with carbon disulphide to give an intermediate addition product, which, on being boiled with water, evolved hydrogen sulphide to give ethylene urea. This intermediate was considered to be a dithiocarbamic acid inner salt (I). Later Yakubovich

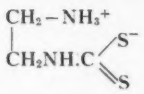

I

and Klimova (9) proved this assumption to be correct by obtaining compound II from the treatment of the addition product I with alkali and ethylchloro-

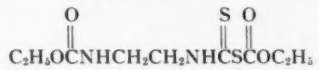

II

formate. On the other hand Goldenring (3) found that two mole equivalents of N-phenyltrimethylenediamine combined with one mole of carbon disulphide. This was also observed (2) with N-*p*-tolyltrimethylenediamine. In the present studies 1,3-diaminobutane with carbon disulphide gave an inner salt analogous to that obtained by Hofmann with ethylenediamine. This inner salt was converted by thermal decomposition into 4-methyl-hexahydropyrimidine-2-thione in good yield. Also 1-amino-5-hydroxy-3-azapentane was observed to combine with carbon disulphide to yield a solid addition product. This intermediate when heated in the dry state evolved hydrogen sulphide to give a new product. This new compound melted at 136.5–137.5°C. and gave analytical values in good agreement with the expected 1-β-hydroxyethyl-imidazolidine-2-thione (III). However, Sergeyev and Kolychev (7) previously had claimed to have prepared this compound from ethylene oxide and thiocyanic acid. Their product melted at 168.5°C. with decomposition. Because of this discrepancy in melting points it was considered necessary to confirm

[1] *Manuscript received October 21, 1953.*
Contribution from Defence Research Chemical Laboratories, Ottawa, Ontario. Issued as D.R.C.L. Report No. 136.

the identity of the compound prepared from 1-amino-5-hydroxy-3-azapentane and carbon disulphide.

1-β-Hydroxyethylimidazolidine-2-thione was converted to 1-β-hydroxyethyl-2-methylmercapto-2-imidazolinium iodide with methyl iodide.

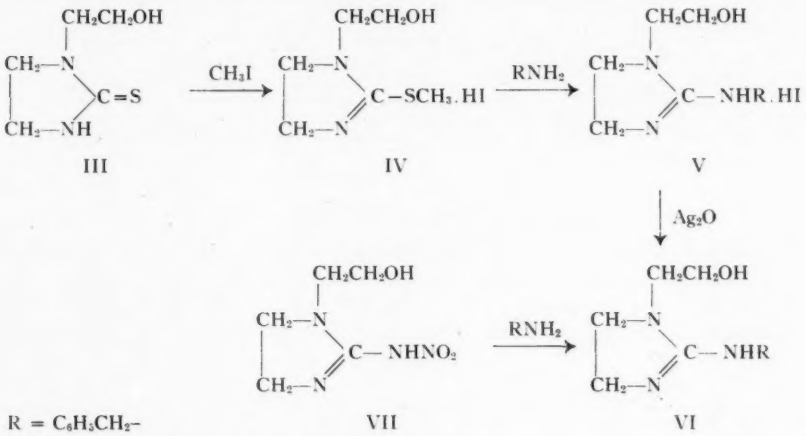

The iodide (IV) on treatment with benzylamine by the method of Aspinall and Bianco (1) gave the hydrogen iodide salt of 1-β-hydroxyethyl-2-benzylamino-2-imidazoline (V) which was isolated as its picrate. The same compound (VI) was obtained from the known 1-β-hydroxyethyl-2-nitramino-2-imidazoline (VII) (5) and benzylamine. The identity of these two products was established by a mixed melting point determination. The structure of 1-β-hydroxyethyl-2-nitramino-2-imidazoline was established previously (5,6) by nitration and hydrolysis to 1-β-nitroxyethyl-3-nitro-2-imidazolidone which was prepared also by the nitration of the known 1-β-hydroxyethyl-2-imidazolidone (6,8). These chemical reactions confirm the assignment of structure III to the cyclic thiourea from the reaction between aminoethylethanolamine and carbon disulphide.

EXPERIMENTAL[2]

4-Methyl-hexahydropyrimidine-2-thione

A solution of 8.8 gm. (0.1 mole) of 1,3-diaminobutane in 50 cc. of 95% ethanol was added dropwise to a solution of 25 cc. of carbon disulphide in 50 cc. of 95% ethanol. During the addition period the temperature was held below 40°C. with an ice–salt bath. The reaction mixture was allowed to stand at room temperature overnight in an open Erlenmeyer. At this time the viscous white oil had solidified, yield 12.65 gm. (77.2%). One gram of this γ-aminobutyldithiocarbamic acid inner salt was purified by solution in aqueous ammonia. On slow evaporation of ammonia from the solution white crystals separated. These crystals decomposed from 125–160°C. leaving a

[2] *All melting points were determined on a Kofler block. Microanalyses were performed by Micro-Tech Laboratories, Skokie, Illinois.*

residue which then melted at 175–178°C. Calc. for $C_5H_{12}N_2S_2$: C, 36.57; H, 7.32; N, 17.06; S, 39.02%. Found: C, 36.86; H, 7.55; N, 17.00; S, 38.72%.

The remaining inner salt (11.65 gm., 0.088 mole) was placed in an Erlenmeyer and heated in an oil-bath at 130–145°C. until the evolution of hydrogen sulphide ceased. The tan residue was crystallized from ethanol using charcoal for decolorizing the product, yield 8 gm. (87.4%). The melting point of 182–183°C. was increased to 183–184.5°C. after one further crystallization from ethanol. Calc. for $C_5H_{10}N_2S$: C, 46.15; H, 7.69; N, 21.52; S, 24.62%. Found: C, 46.35; H, 7.85; N, 21.88; S, 25.02%.

1-β-Hydroxyethylimidazolidine-2-thione

1-Amino-5-hydroxy-3-azapentane (40.0 gm., 0.38 mole) in 95% ethanol (100 cc.) was added dropwise with stirring into a solution of 100 cc. of carbon disulphide in 100 cc. of 95% ethanol. During the addition period, which required 30 min., the temperature was held below 15°C. The stirring was continued for one half hour after the addition period after which the solid was recovered by filtration, yield 67.0 gm. (96.9% based on formation of inner salt). This solid was heated in an oil bath at 145 ± 5°C. until the evolution of hydrogen sulphide had ceased. The residue was crystallized from 95% ethanol (250 cc.) to give 46.0 gm. (86.3% yield from inner salt) of crystals which melted at 136.5–137.5°C. Calc. for $C_5H_{10}N_2OS$: C, 41.10; H, 6.85; N, 19.16; S, 21.93%. Found: C, 41.34; H, 6.49; N, 19.16; S, 22.30%.

1-β-Hydroxyethyl-2-methylmercapto-2-imidazolinium Iodide

A mixture of 1-β-hydroxyethylimidazolidine-2-thione (14.6 gm., 0.1 mole) and methyl iodide (15.6 gm., 0.11 mole) in 50 cc. of absolute methanol was shaken at room temperature for 40 min., after which all the solid had dissolved. While the vigorous shaking was continued 200 cc. of anhydrous ether was added gradually. A dense white precipitate (m.p. 119–120°C.) was formed, yield 27.3 gm. (95%). This product was brought to a constant melting point of 120–121°C. after one crystallization from absolute ethanol (3.9 cc./gm.). However purification was unnecessary for further chemical reactions. Calc. for $C_6H_{13}IN_2OS$: C, 25.01; H, 4.55; I, 44.10%. Found: C, 25.35; H, 4.67; I, 43.63.

1-β-Hydroxyethyl-2-nitramino-2-imidazoline

1-β-Hydroxyethyl-2-nitramino-2-imidazoline (m.p. 131.5–132°C.) was prepared in 39% yield as previously described (5).

1-β-Hydroxyethyl-2-benzylamino-2-imidazoline

Method A

1-β-Hydroxyethyl-2-methylmercapto-2-imidazolinium iodide (2.5 gm., 0.0087 mole) and benzylamine (1.8 gm., 0.017 mole) were dissolved in 25 cc. water and allowed to stand overnight. The mixture then was heated on a steam bath for one hour after which it was taken to dryness. The residual oil gave no picrate or picrolonate under the usual conditions. This oil was redissolved in 25 cc. water and this solution shaken for one hour with 1.0

gm. (0.0044 mole) of silver oxide. After filtration to remove silver salts, the solution was taken to dryness *in vacuo*. The oil was dissolved in 25 cc. of water, filtered, and the filtrate treated with 200 cc. of 1% aqueous picric acid solution. A crystalline picrate (m.p. 120.5–122.5°C.) was obtained in 64.8% yield (2.48 gm.). One crystallization from absolute alcohol (25 cc.) gave 2.1 gm. of crystalline picrate with a constant melting point of 124–125°C. Calc. for $C_{18}H_{20}N_6O_8$: C, 48.21; H, 4.50; N, 18.74%. Found: C, 48.54; H, 4.26; N, 18.78%.

Method B

One gram (0.0057 mole) of 1-β-hydroxyethyl-2-nitramino-2-imidazoline and 8 cc. of benzylamine were refluxed for one hour in an apparatus protected from carbon dioxide. The excess benzylamine was distilled off under water pump vacuum at 100°C. The residual light yellow oil was dissolved in 30 cc. of 50% aqueous ethanol. One half of this solution was treated with 200 cc., of 1% aqueous picric acid solution. The crude picrate melted at 118–122°C., yield 0.93 gm. (72.4%). Two crystallizations from ethanol raised the melting point to 124–125°C. This melting point was not depressed on admixture with the picrate of 1-β-hydroxyethyl-2-benzylamino-2-imidazoline prepared above by Method A.

ACKNOWLEDGMENT

The authors wish to thank Mr. G. L. Rutherford for skillful technical assistance.

REFERENCES

1. ASPINALL, S. R. and BIANCO, E. J. J. Am. Chem. Soc. 73: 602. 1951.
2. FRÄNKEL, M. Ber. 30: 2497. 1897.
3. GOLDENRING, A. Ber. 23: 1168. 1890.
4. HOFMANN, A. W. Ber. 5: 240. 1872.
5. MCKAY, A. F., BRYCE, J. R. G., and RIVINGTON, D. E. Can. J. Chem. 29: 382. 1951.
6. MCKAY, A. F. and HATTON, W. G. Can. J. Chem. 30: 225. 1952.
7. SERGEYEV, P. G. and KOLYCHEV, B. S. J. Gen. Chem. (U.S.S.R.), 7: 1390. 1397.
8. WILSON, A. L. U.S. Patent No. 2,517,750. 1950.
9. YAKUBOVICH, A. Ya. and KLIMOVA, V. A. J. Gen. Chem. (U.S.S.R.), 9: 1777. 1939.

EFFECT OF FLUCTUATIONS OF FREE RADICAL CONCENTRATIONS ON THE CALCULATION OF RELATIVE RATE CONSTANTS[1]

By R. J. Cvetanovic and E. Whittle[2]

ABSTRACT

The effect of fluctuations in free radical concentrations on the values of relative reaction rate constants calculated from steady state expressions has been evaluated for a number of idealized model cases, representative of various conditions usually encountered in experiments.

INTRODUCTION

In many instances the concentration of free radicals or atoms participating in chemical reactions cannot be determined and it is then only possible to evaluate relative rate constants for two or more reactions competing for the same radical or atom. For mathematical simplicity calculations of the relative rate constants are as a rule carried out on the assumption of stationary concentrations of the free radicals or atoms involved. Time fluctuations, however, are usually inevitable and, as has been pointed out by Szwarc (8), introduce an error in the calculated relative rate constant when one of the two competing reactions is first order while the other is second order in the free radical. There may be some uncertainty (8,4) about the extent to which the error may affect the calculated values of rate constants and activation energies. In view of this, we have attempted to obtain more detailed information than is possible by mere inspection about the magnitude of this error, as well as of the similar error caused by concentration gradients.

Since, in general, the variation with time of the free radical concentration is not known, the treatment comprises a number of idealized model cases, believed to be sufficiently representative of various conditions usually encountered in experiments to allow an estimation of the magnitude of the effect.

Most of the systems for which relative rate data have been obtained in recent years are embraced by the following general reaction scheme, applicable also for radicals produced by other than photochemical methods:

$$\begin{aligned}
&\mathrm{A} + h\nu \rightarrow m\mathrm{X} + \mathrm{L} && \phi I_a \\
&\mathrm{X} + \mathrm{B} \rightarrow \mathrm{M} + \mathrm{K} && k_1 \\
&\mathrm{X} + \mathrm{B}' \rightarrow \mathrm{M}' + \mathrm{K}' && k_1' \\
&\mathrm{X} + \mathrm{B}'' \rightarrow \mathrm{M}'' + \mathrm{K}'' && k_1'' \\
&\cdots\cdots\cdots\cdots\cdots && \cdots\cdot \\
&\mathrm{X} + \mathrm{X} \rightarrow \mathrm{N} && k_2
\end{aligned}$$

where $m = 1$ or 2 and X is a free radical, the concentration of which will be

[1] *Manuscript received March 26, 1953.*
Contribution from the Divisions of Applied and Pure Chemistry, National Research Council, Ottawa, Canada. Issued as N.R.C. No. 3145.
[2] *Present address: Department of Chemistry and Chemical Engineering, University of California, Berkeley 4, California, U.S.A.*

denoted by x. The relative rate constant of Reaction (1), $k_1/k_2^{\frac{1}{2}}$, is usually calculated from the mean rates of formation of M and N ($\bar{R}_M$ and $\bar{R}_N$, respectively), and, neglecting concentration gradients, can be expressed in the form

$$[1] \qquad \frac{k_1}{k_2^{\frac{1}{2}}} = \frac{\bar{R}_M}{\bar{R}_N^{\frac{1}{2}}(B)} \cdot \delta \qquad \text{where } \delta = \frac{t^{\frac{1}{2}}\left(\int_0^t x^2\,dt\right)^{\frac{1}{2}}}{\int_0^t x\,dt}.$$

The effect of time fluctuations is, therefore, as was pointed out by Szwarc (8), that $\delta \geqslant 1$.

We have considered the effect on the value of δ of the time fluctuations of the following types: (*a*) steady drift in x, (*b*) sporadic fluctuations, (*c*) intermittent illumination; and of concentration gradients due to: (*i*) removal of radicals on the wall and (*ii*) nonuniform light absorption.

Steady Drift in the Free Radical Concentration

A drift in the free radical concentration may result, for example, from a gradual decline in the amount of light absorbed. The maximum and the minimum values of x will be denoted by x_0 and x_i respectively, so that $x = x_0(1 - \gamma t)$, and $0 \leqslant \gamma t \leqslant 1$. On integration it is found that

$$[2] \qquad \delta_a = \left\{1 + \frac{1}{3[(2/\alpha) - 1]^2}\right\}^{\frac{1}{2}}$$

where $\alpha = (x_0 - x_i)/x_0$, and $0 \leqslant \alpha \leqslant 1$. The values of δ_a for different values of α are shown in Fig. 1. The maximum value of δ_a is 1.15.

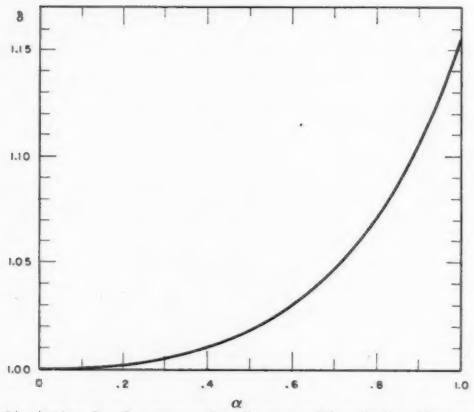

FIG. 1. Variation in the correction factor with relative fluctuation (α).

Sporadic Fluctuations

Sporadic fluctuations may result from technical imperfections in the control of experimental conditions, which are frequently unavoidable. These fluctuations can be expected to be for the most part relatively slow, and the

following model case chosen for mathematical simplicity, is probably adequate to give an idea of their possible importance.

The reaction time is divided into a large number of equal intervals and during each interval x is assumed to be constant, but in general varies from one interval to another. The variation in x is confined to a range between a maximum (x_0) and a minimum value (x_i). It is further assumed that, within this range, x can assume with equal probability any of $(n + 1)$ equally spaced discrete values. If $\alpha = (x_0 - x_i)/x_0$, it is found that

$$\delta_b = \left\{1 + \frac{1 + 2/n}{3[(2/\alpha) - 1]^2}\right\}^{\frac{1}{2}}. \qquad [3]$$

For large n Equation [3] reduces to the case of a steady drift. When both α and n are unity, δ_b becomes $\sqrt{2}$, which is its maximum value. Usually, however, α will be considerably smaller than unity and, consequently, δ_b will in general be close to unity.

Intermittent Illumination

The theory of the effect of intermittent illumination on the rate of a chain propagation step, has been extensively treated (1,2,3,5,7). The present problem is related to, though it differs in some respects from, the ones treated by Briers and Chapman (1) and by Rice (7). A simplified case, when x describes a linear and symmetrical zigzag curve, should provide a good first approximation (δ_c) for relatively fast light interruptions when the light and dark intervals are of equal duration. If, as before, the maximum and the minimum values of x are x_0 and x_i, respectively, and $\alpha = (x_0 - x_i)/x_0$, it is found, that δ_c also is given by Equation [2] and is, therefore, entirely determined by the relative fluctuation α. Determination of x_0 and x_i, however, requires a more elaborate treatment in which it is assumed that, during light intervals ϕI_a = const. and in dark intervals $\phi I_a = 0$, so that the light pulses are rectangular. Only the case when the light and the dark intervals are of equal duration ($p_l = p_d = p$) need be considered. It is assumed that x_0 and x_i immediately attain steady values, which is justifiable for the usual experimental reaction times.

It is convenient to express the value of x at any instant as a fraction (y) of the stationary value (x_s) corresponding to steady illumination, so that $y = x/x_s$. Introducing the notations

$$\epsilon = \left(1 + \frac{8\ mk_2\phi I_a}{\{k_1(\mathrm{B}) + k_1'(\mathrm{B}') + k_1''(\mathrm{B}'') + \ldots\}^2}\right)^{\frac{1}{2}},$$

$$\lambda = \{k_1(\mathrm{B}) + k_1'(\mathrm{B}') + k_1''(\mathrm{B}'') + \ldots\}\, p,$$

and

$$\eta = \left(y_0 + \frac{2}{\epsilon - 1}\right)\left(y_i + \frac{\epsilon + 1}{\epsilon - 1}\right) \Big/ \left(y_i + \frac{2}{\epsilon - 1}\right)\left(y_0 + \frac{\epsilon + 1}{\epsilon - 1}\right)$$

* $$y_0 = \frac{y_i\left(\frac{\epsilon + 1}{\epsilon - 1} + e^{\lambda\epsilon}\right) + \left(\frac{\epsilon + 1}{\epsilon - 1}e^{\lambda\epsilon} - 1\right)}{y_i\left(e^{\lambda\epsilon} - 1\right) + \left(\frac{\epsilon + 1}{\epsilon - 1}e^{\lambda\epsilon} + 1\right)}$$

$$y_i = \frac{2y_0}{y_0\,(\epsilon - 1)\,(e^{\lambda} - 1) + 2e^{\lambda}}$$

it is found that

$$[4] \qquad \delta = \frac{(\delta_N)^{\frac{1}{2}}}{\delta_M} = \left\{\tfrac{1}{2} - \frac{2}{\lambda(\epsilon-1)^2}\ln\eta\right\}^{\frac{1}{2}} \Big/ \left\{\tfrac{1}{2} + \frac{1}{\lambda(\epsilon-1)}\ln\eta\right\}$$

where $\delta_N = \bar{R}_N/k_2x_s^2$ and $\delta_M = \bar{R}_M/k_1(B)x_s$. In general $\delta_M \geqslant \frac{1}{2}$, $\delta_N \leqslant \frac{1}{2}$ and δ lies between unity (for very fast light interruptions) and $\sqrt{2}$ (for slow light interruptions).

The variation of the quantities of interest with duration of light and dark intervals is illustrated for the case when $\epsilon = 126.5$ by calculations given in Table I and presented graphically in Fig. 2. (The calculated quantities are

TABLE I
EFFECT OF VARIATION OF λ

Example	ϵ	λ	y_0	y_i	δ_M	δ_N	$\hat{\delta}$	δ_c
1	126.5	Large	1	0	.5	.5	1.414	1.155
2	"	4	1.0000	.00029	.5069	.4999	1.395	1.155
3	"	0.4	1.0000	.0309	.5482	.4992	1.289	1.138
4	"	0.04	0.9929	.2771	.6585	.4975	1.071	1.052
5	"	0.004	0.7710	.6438	.7041	.4967	1.001	1.002
6	"	0.0004	0.7110	.6983	.7042	.4967	1.001	1.000
7	"	0	0.7048	.7048	.7048	.4967	1.000	1.000

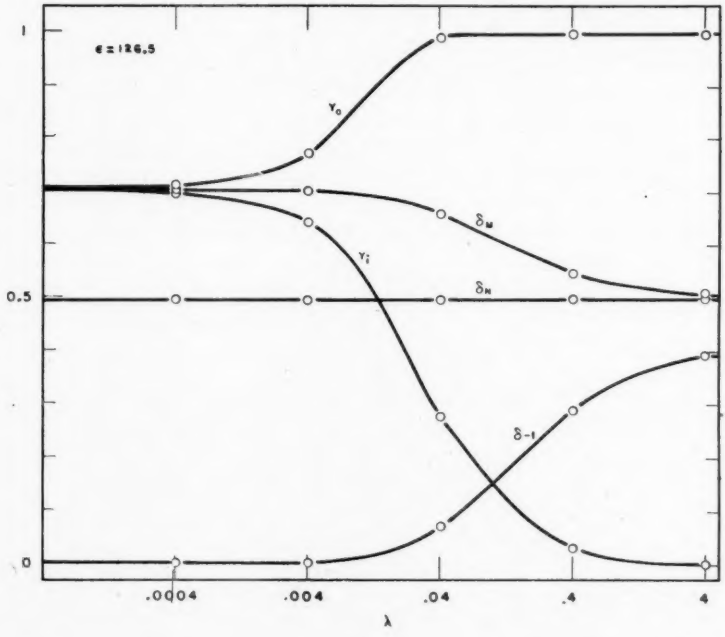

FIG. 2. Variation in the correction factors in the case of intermittent illumination.

indicated in Fig. 2 by circles.) The case corresponds, for example, to the following set of values: $\phi I_a = 10^{15}$ quanta/cc. sec., (B) = 10^{18} molecule/cc. ((B′) = (B″) = . . . = 0), $k_2 = 10^{-10}$ and $k_1 = 10^{-17}$ cc./molecule sec., with p varying from 4×10^{-1} to 4×10^{-5}. The quantities chosen are of magnitudes which may be encountered in experiments. The limiting values for $\lambda \rightarrow \infty$, irrespective of the value of ϵ, are $y_0 = 1$, $y_i = 0$, $\delta_M = \frac{1}{2}$, $\delta_N = \frac{1}{2}$, $\delta = (2)^{\frac{1}{2}}$. When $p \rightarrow 0$, $\delta = 1$, and for this particular case, $y_0 = y_i = \delta_M = .705$, $\delta_N = .497$. If a 60 cycle a.c. is used for the excitation of the light source, the corresponding duration of the light and dark intervals can be taken as $p_l = p_d = 4 \times 10^{-3}$ sec., which for the above set of values leads to $\lambda = 4 \times 10^{-2}$. In this case $\delta = 1.071$, so that an error of 7% is introduced when mean rates are used to calculate $k_1/k_2^{\frac{1}{2}}$ and no fluctuation in the radical concentration is taken into account.

The value of k_2 usually shows only slight or no temperature dependence. The value of k_1, on the other hand, may show a very pronounced temperature dependence. It is, therefore, important to see how the values of δ are affected by the variation in k_1, the other relevant quantities being kept constant. Table II gives calculations for the above set of data with $p = 4 \times 10^{-3}$ sec. and k_1 varying from 10^{-18} to 10^{-15} cc./molecule sec.

TABLE II

EFFECT OF VARIATION OF k_1 (WITH $\phi I_a = 10^{15}$, (B) = 10^{18}, (B′) = (B″) = . . . = 0 $k_2 = 10^{-10}$, $p = 4 \times 10^{-3}$; units: molecule (quanta), cc., sec.).

Example	k_1	λ	ϵ	y_0	y_i	δ_M	δ_N	δ	δ_c
1	10^{-18}	0.004	1265	.9930	.2826	.6607	.4997	1.070	1.050
2	10^{-17}	0.04	126.5	.9929	.2771	.6585	.4975	1.071	1.052
3	10^{-16}	0.4	12.69	.9925	.2284	.6354	.4768	1.089	1.063
4	10^{-15}	4	1.612	.9981	.0141	.5226	.4261	1.249	1.147

The last columns in Tables I and II give the values of δ_c calculated from Equation [2]. It is seen that δ_c is a good approximation for small values of p and not too large values of k_1.

DISCUSSION

The various model cases considered show that the effect of fluctuations in radical concentration on the calculated relative rate constant increases in general with increasing magnitude of the fluctuations relative to the average radical concentration. However, it is evident that sporadic fluctuations or drifts in the radical concentration under the usual experimental conditions will not affect the value of the relative rate constant to any appreciable extent. Thus, such fluctuations to the extent of as much as 40% cause an error in $k_1/k_2^{\frac{1}{2}}$ which is not greater than one per cent. Even under the most unfavorable experimental conditions the errors which may occur are not particularly great. In a similar manner, the use of 60 cycle a.c. for excitation of the light source will normally introduce an error of a few per cent only. The error increases for greater k_1(B), and can be estimated to the approximation of

rectangular light pulses. The case of rectangular pulses is more unfavorable than the actual conditions with a sinusoidal alternating current, and, therefore, provides an upper limit of the error.

The error in the activation energy (δ_E) obtained from the values of the rate constants at two temperatures is given by

$$\delta_E = R \frac{T_1 T_2}{T_1 - T_2} \ln \frac{\delta_{T_1}}{\delta_{T_2}},$$

where δT_1 and δT_2 are the values of the correction factor δ at the temperature T_1 and T_2 respectively. Evidently, the value of δ_E will be largely influenced by the value of $(T_1 - T_2)$. For temperature ranges of the order of 100°, the sporadic fluctuations and drifts in radical concentrations encountered under usual experimental conditions are unlikely to introduce an appreciable error in the calculated value of the activation energy. Sporadic fluctuations, such as may be caused, for example, by instability of the light source, are likely to introduce similar errors at the two temperatures and, consequently, not affect the activation energy. Drifts in the radical concentration would have to be very pronounced and different at the two temperatures in order to affect appreciably the activation energy. In the cases where pronounced drifts with time are encountered, the relative extent of the drift can be estimated from the drift in $\bar{R}_N$ and the error introduced by it can be evaluated from Equation [2]. Both in the case of sporadic fluctuations and drifts in the radical concentration the sign of δ_E is determined by the relative magnitudes of δ_{T_1} and δ_{T_2} and is not predictable *a priori*. It is, therefore, evident that the suggestion that, since in many instances the extent to which the reaction is allowed to proceed is greater at higher temperatures, the estimated activation energy will be slightly lower than its true value, cannot be expected to hold in general, except in the case of a very pronounced increase in the relative fluctuation at the higher temperature.

In the case of intermittent illumination, since k_2 is usually temperature independent and k_1 becomes greater with increasing temperature, a reference to Table II shows that the value of δ will usually be greater at higher temperature, provided ϕI_a, (B), and p remain unchanged, so that δ_E is positive. When k_1 is much smaller than k_2, k_1 will vary appreciably with temperature, but, on the other hand, the value of δ is only slightly affected and δ_E is small. As k_1 approaches k_2 the effect of its variation on δ becomes more pronounced but at the same time its temperature coefficient is reduced and for experimental convenience smaller concentrations of B are usually employed, so that the total effect may still remain relatively small. As an illustration we may consider two hypothetical cases, with $\phi I_a = 10^{15}$, (B) $= 10^{18}$, (B′) = (B″) = . . . $= 0$, $k_2 = 10^{-10}$, $p = 4 \times 10^{-3}$ (the units as given previously). Also it is assumed that $z_1 = 10^{-10}$ and that z_1 and k_2 are temperature independent. *Case 1*: At 400°K., $k_1 = 10^{-17}$, at 500°K., $k_1 = 10^{-16}$, and, therefore, $E = 9.15$ kcal./mole and the steric factor $s = 10^{-2}$. The values of δ for this case are given in Table II, examples 2 and 3 respectively, and it is found that $\delta_E =$ .07 kcal./mole. *Case 2*: At 400°K., $k_1 = 10^{-16}$, at 500°K., $k_1 = 10^{-15}$, and,

therefore, $E = 9.15$ kcal./mole and $s = 10^{-1}$. The respective values of δ are given by examples 3 and 4 in Table II, and, in this case $\delta_E = .55$ kcal./mole. It should, however, be borne in mind that the treatment presented here is strictly correct for the case of rectangular light pulses only. When sinusoidal a.c. is used for excitation of the light source, the maximum possible limits of error can be evaluated rather than the error itself.

The model cases considered are evidently highly idealized. They are, however, sufficiently representative of the types usually occurring in experiments to give an insight into the magnitude of the effects which can be expected. It is likely that in most cases the real conditions are much more favorable and the errors due to time fluctuations will normally be very small. More serious errors may arise, under certain circumstances, from space variations in the radical concentration. Such variations may be caused by a rapid consumption of free radicals on the reaction vessel walls or by a high extinction coefficient. The general effect is again that $\delta > 1$.

In order to evaluate the magnitude of the wall effect Noyes (6) has developed a mathematical solution of the diffusion equation, subject to certain simplifications. The solution is valid for a spherical distribution of the radical, with ϕI_a constant throughout the reaction vessel, and when the radical concentration is not affected by the first order homogeneous reaction or convection currents. It should, however, be applicable, as a first approximation, to the reaction scheme considered here and to a cylindrical reaction vessel of dimensions usually employed in vapor phase photolysis. If $a = (m\phi I_a/2k_2)^{\frac{1}{2}}$, $b = 1.15(m\phi I_a 2k_2/D^2)^{\frac{1}{2}}$, and R is the radius of the reaction vessel, Noyes finds that for $bR > 5.7$, $x = a[1 - \exp(-b(R - r))]$, if all radicals striking the wall are consumed. In the region of validity of this expression, it is found then that $\delta = (1 - 1.5/bR)^{\frac{1}{2}}/(1 - 1/bR)$ or, to a good approximation, $\delta \approx (1 + 0.25/bR)$. In view of the underlying assumptions this value of δ should represent an approximate upper limit. Thus, at a total pressure of 100 mm. the diffusion coefficient (D) may be of the order of 1.5 cm.^{2}/sec., $m\phi I_a$ 10^{12} to 10^{15} quanta/cc. sec., $2k_2$ 10^{-10} cc./molecule sec., and R 2 to 5 cm. For $R = 4$ cm. $\delta \leqslant 1.02$ when $m\phi I_a = 10^{12}$, and $\delta \leqslant 1.01$ when $m\phi I_a = 10^{13}$.

When wall effects, time fluctuations, and convection currents can be neglected, and if $s = 8\ m\phi k_2 q(\mathrm{A}) I_0/(\lambda/p)^2$ and $\beta = q(\mathrm{A})L$, the correction factor δ for the decreasing x along the length of the vessel (of total length L) due to an appreciable extinction coefficient (q) is

$$\delta = \frac{\beta^{\frac{1}{2}}\left\{s(1-e^{-\beta})/4 - (1+s)^{\frac{1}{2}} + (1+se^{-\beta})^{\frac{1}{2}} + \ln\{[(1+s)^{\frac{1}{2}}+1]/[(1+se^{-\beta})^{\frac{1}{2}}+1]\}\right\}^{\frac{1}{2}}}{(1+s)^{\frac{1}{2}} - (1+se^{-\beta})^{\frac{1}{2}} - \ln\{[(1+s)^{\frac{1}{2}}+1]/[(1+se^{-\beta})^{\frac{1}{2}}+1]\}}.$$

In the limiting case when $k_2 \ll \lambda/p$, $\delta = (\frac{1}{2}\beta)^{\frac{1}{2}}[(e^{\beta} + 1)/(e^{\beta} - 1)]^{\frac{1}{2}}$ and when $k_2 \gg \lambda/p$, $\delta = (\frac{1}{2}\beta/2)^{\frac{1}{2}}[(e^{\beta/2} + 1)/(e^{\beta/2} - 1)]^{\frac{1}{2}}$. The limiting curves and the curves for $s = 1$, 10, 100 are plotted against $(1 - e^{-\beta})$ in Fig. 3. For $s = 10^{-2}$ δ already practically coincides with curve I (Fig. 3), which gives an upper limit of the error. The error remains small to quite appreciable

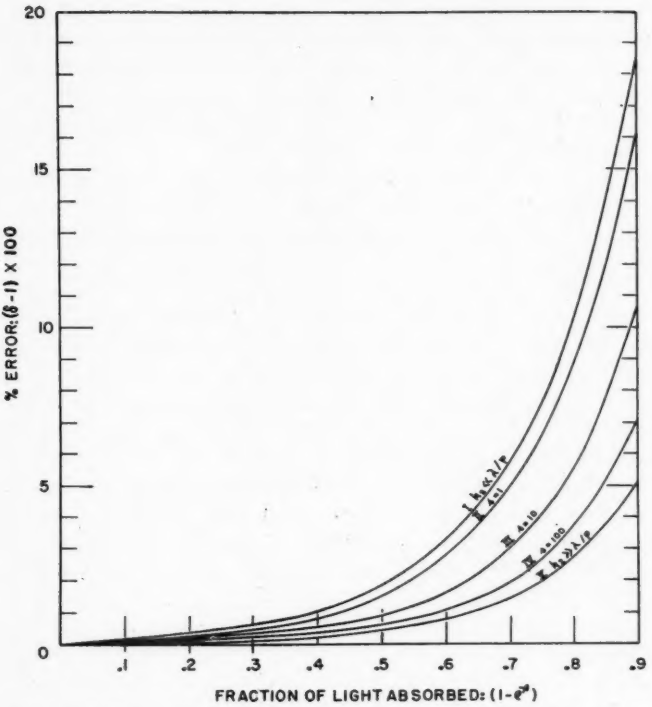

FIG. 3. Variation in the correction factor with the fraction of light absorbed.

absorptions and in actual experiments is further decreased by convection currents.

It is evident that while concentration gradients may under certain conditions have a serious effect, in many instances the limits of the errors can be evaluated and the experimental conditions adjusted so that the errors remain very small. Such conditions do prevail in many experimental determinations of relative rate constants.

REFERENCES

1. BRIERS, F. and CHAPMAN, D. L. J. Chem. Soc. 1802. 1928.
2. BRIERS, F., CHAPMAN, D. L., and WALTERS, E. J. Chem. Soc. 562. 1926.
3. BURNETT, G. M. and MELVILLE, H. W. Proc. Roy. Soc. (London), A, 189: 470. 1947.
4. DAVISON, S. and BURTON, M. J. Am. Chem. Soc. 74: 2307. 1952.
5. DICKINSON, R. G. *In* Photochemistry of gases *by* Noyes, W. A. and Leighton, P. A. Reinhold Publishing Corporation, New York. 1941. p. 202.
6. NOYES, R. M. J. Am. Chem. Soc. 73: 3039. 1951.
7. RICE, O. K. J. Chem. Phys. 10: 440. 1942.
8. SZWARC, M. J. Chem. Phys. 19: 256. 1951.

TEMPERATURE COEFFICIENTS FOR SELF-DIFFUSION IN SOLUTION[1]

By C. J. Krauss and J. W. T. Spinks

ABSTRACT

Coefficients of self-diffusion have been measured for aqueous solutions of sodium dihydrogen phosphates from 1 molar to 10^{-4} molar and at temperatures of 15, 25, 35, and 45°C. The activation energy of self-diffusion has been calculated for various concentrations. It decreases from 5.4 kcal./mole at 0.9 *M* to 4.3 kcal./mole. at infinite dilution.

INTRODUCTION

Self-diffusion has been described as "the diffusion of something into its exact counterpart" (13), and in the past few years isotopic tracers have often been used in studies of self-diffusion. While isotopes are obviously not exactly alike, the isotope effect in diffusion studies in solution is often small. For example, Adamson, Cobble, and Nielsen (1) found no detectable difference in the rates of diffusion of Na^{22} and Na^{24} ions in aqueous solutions of sodium chloride.

Various methods for measuring self-diffusion using tracer techniques have been developed. The diaphragm cell technique developed by McBain and Dawson (10) has been used extensively, and more recently Mysels and Stigter (11) have developed a method involving two fritted glass diaphragms. Anderson and Saddington developed a capillary cell method for studying self-diffusion in solution (2,4).

The capillary cell method was used in the present work for the determination of temperature coefficients for self-diffusion in aqueous solutions of sodium dihydrogen phosphate.

The equation for the diffusion coefficient for the capillary cell method is

$$[1] \qquad D = \frac{4L^2}{\pi^2 t} (\ln 8/\pi^2 - \ln R)$$

where D is the diffusion coefficient, L is the length of the capillary, t is the time, and R is the ratio of the activity (activity is used here in the sense of radioactivity) in the cell after diffusion to that in the cell before diffusion (4).

Various equations have been used to relate the diffusion coefficient to the temperature. One such equation is that of Stokes-Einstein:

$$[2] \qquad D = kT/6\pi\eta r$$

where k is the Boltzmann constant, T is the absolute temperature, η is the viscosity, and r is the radius of the diffusing particle. Another equation frequently used is

[1] *Manuscript received October 5, 1953.*
Contribution from Department of Chemistry, University of Saskatchewan, Saskatoon, Sask.
Paper is based on a thesis written in partial fulfillment of the requirements for the degree of Master of Arts, University of Saskatchewan, Saskatoon.

[3] $$D = Ae^{-E_D/RT}$$

where A is a constant, R is the gas constant, T is the absolute temperature, and E_D is the activation energy for self-diffusion.

The activation energy can be calculated from equation [3] and also from viscosity data (14) using equation [4].

[4] $$E_\eta = R\left(T - \frac{d \ln (1/\eta)}{d(1/T)}\right)$$

Wang and co-workers (14, 15, 19) have published a series of papers on "Self-diffusion and structure of liquid water." They used the capillary cell method and calculated the activation energy for self-diffusion in liquid water from a plot of log D vs. $1/T$. In another series of papers in which activation energies for self-diffusion were calculated from conductance data (16, 18, 17), Wang showed that diffusion data, viscosity data, and conductance data should yield the same activation energy.

Graupner and Winter (6) measured the self-diffusion coefficients for water, benzene, bromoethane, and ethanol using the diaphragm cell method and calculated activation energies for self-diffusion in each liquid.

Partington, Hudson, and Bagnall (12) determined self-diffusion coefficients and activation energies for self-diffusion for water and several aliphatic alcohols using the diaphragm cell method.

Hoffman (7) has determined the activation energy for self-diffusion in liquid mercury using the capillary cell method.

Table I lists the values from the literature cited, for the activation energy for self-diffusion calculated from diffusion data and from viscosity data.

TABLE I
ACTIVATION ENERGIES FOR SELF-DIFFUSION

Ref. No.	Ion or molecule	(kcal./mole) E_D	(kcal./mole) E_η	Temperature range, °C.
14	HDO	4.6	4.59	10–50
15	HHO^{18}	4.4		10–50
19	HTO	4.6		10–50
6	DDO and HHO^{18}	4.6	3.28	15–45
12	DDO	3.93	3.80	15–45
8	$H_2PO_4^-$ (∞ dilution)	4.3	4.6	15–45
12	Methanol	2.77	2.33	15–35
12	Ethanol	4.62	3.30	15–35
6	Ethanol	4.5	3.85	15–45
12	*n*-Propanol	4.25	4.31	15–45
12	*n*-Propanol	5.30	5.19	15–45
12	*n*-Butanol	4.60	4.57	25–45
12	*t*-Butanol	7.50	8.20	35–55
6	Benzene	2.1	2.4	15–45
6	Bromoethane	1.2	1.75	15–45
7	Mercury	1.16	1.25	0–90

The object of the present work was to determine self-diffusion coefficients for the $H_2PO_4^-$ ion in aqueous solutions of sodium dihydrogen phosphate at

different concentrations and at different temperatures. The value of the activation energy for self-diffusion of $H_2PO_4^-$ determined in the present work is included in Table I for purposes of comparison.

EXPERIMENTAL

Materials and Methods

Capillary cells about 3 cm. long and 0.1 cm. in diameter were made from glass capillary tubing of uniform bore. The uniformity of the bore was determined by accurately measuring the length of a mercury thread at overlapping intervals along the capillary tube. For a mercury thread of average length, 2.499 cm., the standard deviation of the length was 0.003 cm., indicating that the tubing was quite uniform (standard deviation in the radius is 0.07%). The cells contained 0.0250 ml. of solution when full.

The capillary cells were mounted vertically in a lucite holder (for details see (4, 8). The bottom ends of the capillaries were sealed. Three cells were used in each experiment. The cells were filled with radioactive solution of known concentration and then gently immersed in an inactive solution of the same concentration. The experiments were carried out at constant temperature. The time of diffusion, from two to six days, was measured to the nearest minute.

At the end of the diffusion period the cells were emptied and rinsed onto aluminum dishes and the solution evaporated to dryness. Five 0.0250 ml. samples of the undiffused radioactive solution were prepared as standards for each experiment. Fine pipettes were used to fill and empty the cells. The samples were analyzed for radioactivity using an end window Geiger-Mueller counter. The ratio of the activity of the diffused sample to the activity of the standard sample is equal to R in equation [1]. The experimental method for determining the self-diffusion coefficients was described in detail by Burkell and Spinks (4).

The diffusion apparatus was completely immersed in a constant temperature water bath. Measurements of temperature variation indicated that the temperature along the diffusion path did not fluctuate by more than 0.02°C. Experiments were carried out at 15, 25, 35, and 45°C.

Analyzed reagent grade $NaH_2PO_4 \cdot H_2O$ and distilled water were used to prepare a series of solutions of concentrations from 1 to 10^{-4} molar.

P^{32} in the form of $PO_4^{\equiv}$ in aqueous solution was obtained from the Atomic Energy Project at Chalk River. The radiochemical purity of the P^{32} was established by its half-life, 14.3 days, and its half-thickness, 117 cm./cm.^{2} The P^{32} solution was analyzed for $PO_4^{\equiv}$ and 1 ml. of solution containing originally 1 mc. of P^{32} was found to contain 28 mgm. of phosphorus. Radioactive solutions were prepared by adding sufficient radioactive phosphate to the inactive solution to give the 0.025 ml. standard sample an activity of about 2000 counts per minute. The weight of phosphorus introduced with the P^{32} was thus negligible even for the most dilute solution used (10^{-4} M).

All counting measurements were made with an end window Geiger-Mueller counter. Background corrections and resolving time corrections were applied

to all the measurements. Since the same weight of material was present in all the samples counted for individual experiments, and constant end-on geometry was maintained, and since only the ratio of the activities was used in the calculations, no corrections for back-scatter and self-absorption were necessary.

Viscosity Measurements

The viscosities of the sodium dihydrogen phosphate solutions were determined using an Ostwald viscometer. The results are plotted in Fig. 1. (The

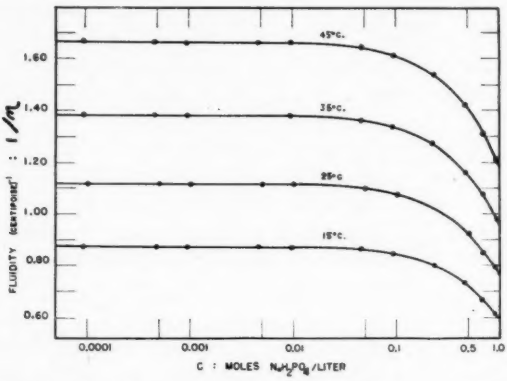

FIG. 1. Plot of fluidity ($1/\eta$) vs. log C for sodium dihydrogen phosphate solutions.

necessary densities at 15, 35, and 45°C. were determined, using the pyknometer method (8).) The densities of the solutions at 25°C. were obtained from Mason and Culvern (9).

pH Measurements

Measurements of pH on the sodium dihydrogen phosphate solutions were made using a Beckman pH meter. In solution, the $H_2PO_4^-$ ion dissociates, $H_2PO_4^- \rightleftarrows H^+ + HPO_4^=$, and it was of interest to know which ion was present in larger amount.

The ratio, X, of concentrations of the ions present is given by

$$X = \frac{(H_2PO_4^-)}{(HPO_4^=)} = \frac{(H^+)}{K_2} = \frac{(H^+)}{7.5 \times 10^{-8}}$$

where K_2 is the second ionization constant for phosphoric acid. Calculations from the pH measurements indicated that above 0.005 molar the diffusion measured was essentially that of the $H_2PO_4^-$ ion, while below 0.005 molar, both ions contributed appreciably (See Table II).

Effect of Stirring

One of the boundary conditions for the capillary cell method of determining diffusion coefficients was that the concentration of tracer at the upper end of the capillary be zero at all times during the experiment. To determine whether this condition was being fulfilled, the outer inactive solution was

TABLE II
DETERMINATIONS OF pH FOR SODIUM DIHYDROGEN PHOSPHATE SOLUTIONS AND VALUES OF $X = (H_2PO_4^-)/(HPO_4^=)$

Conc. (moles/liter)	15°C.		25°C.		35°C.		45°C.	
	pH	X	pH	X	pH	X	pH	X
0.9256	4.02	1270	4.03	1240	4.10	1060	4.13	988
0.694	4.12	1010	4.12	1010	4.19	861	4.22	804
0.463	4.20	841	4.22	802	4.27	716	4.31	653
0.231	4.32	639	4.37	568	4.40	530	4.44	484
0.0926	4.48	441	4.51	412	4.51	412	4.55	376
0.0463	4.57	358	4.59	343	4.61	327	4.65	299
0.00926	4.78	221	4.84	192	4.86	184	4.89	172
0.00463	5.08	111	5.10	106	5.10	106	5.15	95
0.000926	5.60	33	5.63	31	5.65	30	5.68	28
0.000463	5.88	18	5.90	17	5.86	18	5.90	17
0.0000926	6.15	9	6.22	8	6.35	6	6.46	5

stirred at 60 r.p.m. The diffusion coefficients obtained in these experiments were the same, within the expected standard deviation, as those obtained in parallel runs without stirring.

Effect of Immersion

The immersion error due to the lowering of the capillary cells into the inactive solution was estimated in diffusion experiments in which the time of diffusion was about one minute. The loss of activity by the cells in this operation was less than 0.5%. Thus, the actual immersion error in R was probably less than 0.5%.

RESULTS

The mean diffusion coefficients are plotted against the log of the concentration in Fig. 2. (Each point is the mean value of five determinations.)

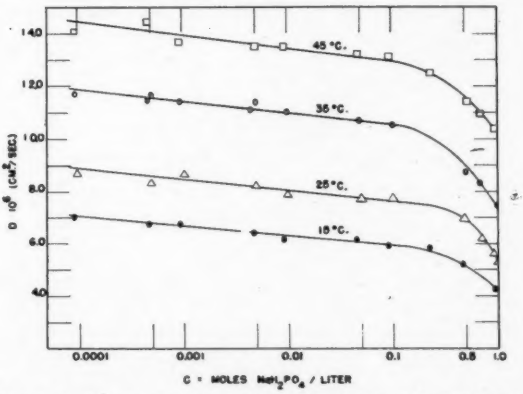

FIG. 2. Plot of $D \cdot 10^6$ vs. log C for sodium dihydrogen phosphate solutions.

For concentrations between 10^{-1} and 10^{-4} molar NaH_2PO_4 the variation of D with log C was found to be linear. The best fitting straight line for the data at each temperature was determined by the method of least squares.

S_D is the standard error of the estimate.
For 15°C., $D \cdot 10^6 = 5.60 - 0.364 \log C$; $S_D = 0.11$.
For 25°C., $D \cdot 10^6 = 7.22 - 0.412 \log C$; $S_D = 0.16$.
For 35°C., $D \cdot 10^6 = 10.14 - 0.450 \log C$; $S_D = 0.15$.
For 45°C., $D \cdot 10^6 = 12.49 - 0.492 \log C$; $S_D = 0.26$.
For the 25°C. curve, the results of Burkell (3) and the results obtained in the present work were used. The diffusion coefficient at infinite dilution was obtained by extrapolating the curves in the plot D vs. $\sqrt{C}$ (Fig. 3).

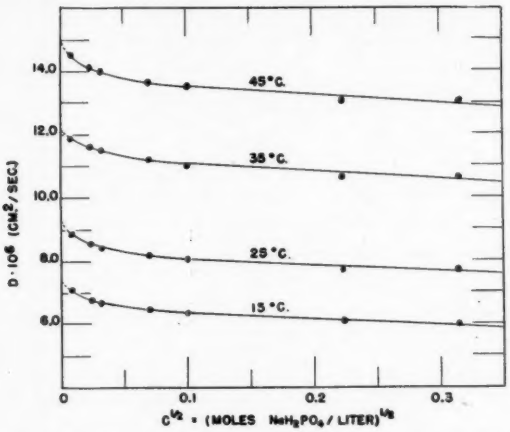

FIG. 3. Plot of $D \cdot 10^6$ vs. $\sqrt{C}$ for sodium dihydrogen phosphate solutions.

In order to obtain activation energies for self-diffusion, log D was plotted against $1/T$ for various concentrations (Fig. 4) and the best fitting straight

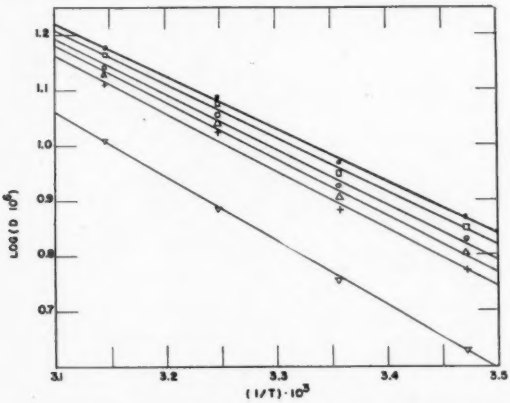

FIG. 4. Plot of log $(D \cdot 10^6)$ vs. $(1/T) \cdot 10^3$ for sodium dihydrogen phosphate solutions
● ∞ Dilution
□ 0.0001 molar
○ 0.001 molar
△ 0.01 molar
+ 0.1 molar
▽ 0.926 molar

lines determined using the method of least squares. The values of E_D were calculated from: $E_D = -2.3R\ (d(\log D/d(1/T))$. The slopes of the lines are recorded in Table III together with the activation energies calculated from viscosity data using the equation:

$$E_\eta = R\left(T - \frac{d \ln (1/\eta)}{d(1/T)}\right).$$

TABLE III

ACTIVATION ENERGIES FOR SELF-DIFFUSION IN AQUEOUS SOLUTIONS OF SODIUM DIHYDROGEN PHOSPHATE

Concentration (moles/liter)	$-\frac{d \log D}{d(1/T)}$	E_D (kcal./mole.)	$-\frac{d \log (1/\eta)}{d(1/T)}$	E_η (kcal./mole)
0.926	1.178	5.4	0.921	4.8
0.1	1.051	4.8	0.870	4.6
0.01	1.024	4.7	0.870	4.6
0.001	0.996	4.6	0.870	4.6
0.0001	0.974	4.5	0.870	4.6
∞ Dilution	0.946	4.3	0.870	4.6

The plot of activation energy from diffusion data, E_D vs. log C is given in Fig. 5.

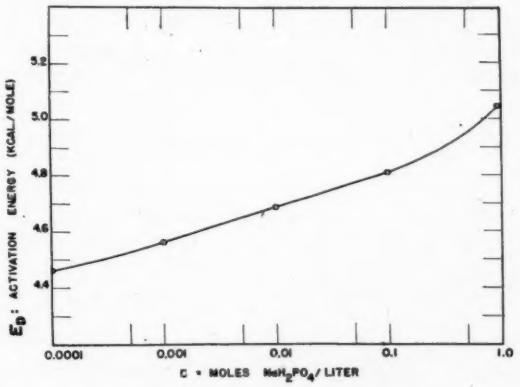

FIG. 5. Plot of E_D vs. log C.

DISCUSSION

From Table III it is seen that, for solutions of moderate concentration, the activation energy of self-diffusion for the $H_2PO_4^-$ ion is about 4.8 kcal./mole and that it decreases somewhat with increasing dilution. The extrapolated value for infinite dilution is 4.3 kcal./mole, not very different from the value for HHO^{18}(4.4 kcal./mole, Table I). The fact that the activation energy for the dilute solution of $H_2PO_4^-$ is close to that for water is not surprising in view of the fact that ions are commonly hydrated in aqueous solution. It has been suggested that the activation energy for the diffusion of water is due

to the breaking of the hydrogen bond for which the approximate energy is 4.5 kcal./mole (5).

ACKNOWLEDGMENTS

We are grateful to the Consolidated Mining and Smelting Company of Canada and to the National Research Council of Canada for financial assistance. One of us (C. J. K.) was holder of a Cominco Fellowship.

REFERENCES

1. ADAMSON, A. W., COBBLE, J. W., and NIELSEN, J. M. J. Chem. Phys. 18: 229. 1949.
2. ANDERSON, J. S. and SADDINGTON, K. J. Chem. Soc. S381. 1949.
3. BURKELL, J. E. Thesis, University of Saskatchewan, Saskatoon. 1951.
4. BURKELL, J. E. and SPINKS, J. W. T. Can. J. Chem. 30: 311. 1952.
5. GLASSTONE, S., LAIDLER, K. J., and EYRING, H. The theory of rate processes. McGraw-Hill Book Company, Inc., New York. 1941.
6. GRAUPNER, K. and WINTER, E. R. S. J. Chem. Soc. 1145. 1952.
7. HOFFMAN, R. E. J. Chem. Phys. 20: 1567. 1952.
8. KRAUSS, C. J. Thesis, University of Saskatchewan, Saskatoon. 1953.
9. MASON, C. M. and CULVERN, J. B. J. Am. Chem. Soc. 71: 2387. 1949.
10. MCBAIN, J. W. and DAWSON, C. R. J. Am. Chem. Soc. 56: 52. 1934.
11. MYSELS, K. J. and STIGTER, D. J. Phys. Chem. 57: 104. 1953.
12. PARTINGTON, J. R., HUDSON, R. F., and BAGNALL, K. W. Nature, 169: 583. 1952.
13. WAHL, A. C. and BONNER, H. A. Radioactivity applied to chemistry. John Wiley & Sons, Inc., New York. 1951. p. 62.
14. WANG, J. H. J. Am. Chem. Soc. 73: 510. 1951.
15. WANG, J. H. J. Am. Chem. Soc. 73: 4181. 1951.
16. WANG, J. H. J. Am. Chem. Soc. 74: 1182. 1952.
17. WANG, J. H. J. Am. Chem. Soc. 74: 1612. 1952.
18. WANG, J. H. and MILLER, S. J. Am. Chem. Soc. 74: 1611. 1952.
19. WANG, J. H., ROBINSON, C. B., and EDELMAN, I. S. J. Am. Chem. Soc. 75: 466. 1953.

METHYL ETHYL KETONE IN THE PHOTOLYSIS OF ACETONE VAPOR[1]

By L. Mandelcorn[2] and E. W. R. Steacie

ABSTRACT

By mass spectrometric analyses, methyl ethyl ketone was determined as a product of the photolysis of acetone between 100 and 284°C. According to the postulated mechanism, methyl ethyl ketone together with methane and ethane accounted for approximately 95% of the methyl radicals produced.

INTRODUCTION

It is now accepted that the mechanism for the photolysis of acetone vapor between 100°C. and 250°C. is (6,7)

$$CH_3COCH_3 + h\nu \rightarrow 2CH_3 + CO \quad [1]$$

$$2CH_3 \rightarrow C_2H_6 \quad [2]$$

$$CH_3 + CH_3COCH_3 \rightarrow CH_4 + CH_3COCH_2 \quad [3]$$

$$CH_3 + CH_3COCH_2 \rightarrow CH_3COC_2H_5 \quad [4]$$

$$2CH_3COCH_2 \rightarrow (CH_3COCH_2)_2 \quad [5]$$

Reaction [1] was shown to proceed with a quantum yield of unity in this temperature range (4). The kinetics of reactions [2] and [3] have been investigated (3,6,7) in some detail. Methyl ethyl ketone was identified as a product but was not studied quantitatively (1). Ketene was also found at temperatures above 200°C., presumably resulting from the decomposition of acetonyl radicals (2)

$$CH_3COCH_2 \rightarrow CH_3 + CH_2CO \quad [6]$$

Considering reaction [1] as the only source of methyl radicals, it can be seen from the results of Trotman-Dickenson and Steacie (7) that reactions [2] and [3] account for from 70 to 100% of the methyl radicals produced, the percentage depending on temperature and concentration. Therefore, the inclusion of reaction [4] should account for all the methyl radicals, and the material balance

$$[2R_{C_2H_6} + R_{CH_4} + R_{CH_3COC_2H_5}]/R_{CO}$$

where $R_{C_2H_6}$ is the rate of production of ethane etc., should be equal to 2 under all conditions in this temperature range. If reaction [6] is significant, then the above ratio should increase with temperature above 200°C.

The purpose of this work was to study the material balances in the acetone photolysis when methyl ethyl ketone is included. It serves as the basis of an investigation of the kinetics of addition of methyl radicals to unsaturated hydrocarbons, the loss of methyl radicals by addition being related to a decrease in the material balance.

[1] *Manuscript received October 15, 1953.*
Contribution from the Division of Pure Chemistry, National Research Council of Canada, Ottawa, Canada. Issued as N.R.C. No. 3149.

[2] *National Research Council of Canada Postdoctorate Fellow 1951-53.*

EXPERIMENTAL

The reaction cell consisted of a cylindrical quartz vessel with plane polished ends and 195 cc. in volume, 10 cm. long, and 5 cm. in diameter. It was kept in an aluminum block furnace which had a quartz window at each end. Three thermocouples were fastened to different points on the cell. Two tubes extended from the cell through the furnace, one serving as a cold finger and the other connected to a stopcock located one inch from the top of the furnace. The total volume of the cell and connecting tube was 205 cc.

The analytical system consisted of two traps, a modified Ward still (5), a small mercury diffusion pump, a combination gas burette and Toepler pump, and a copper oxide tube heated to 240°C., all in series. The cell, analytical system, and reagent reservoirs were suitably connected to a two-stage mercury diffusion pump.

A Hanovia S-100 lamp served as the light source and proved to be fairly constant over long periods of use. The light was collimated by a stop and a series of lenses, thereby filling over 90% of the cell and, for greater efficiency, was reflected back by an aluminum mirror on the rear window of the furnace. The light was filtered with a Corning No. 9863 filter. Different light intensities were obtained by adding neutral density filters. In a few experiments the full arc was used.

The acetone was Merck Reagent Grade. It was dried over "Drierite", degassed by bulb to bulb distillation, and separated from the system by a mercury cutoff.

For an experiment, acetone was introduced into the cell to the desired pressure. After condensing in the cold finger and pumping to remove any traces of noncondensible gases, the acetone was photolysed to about seven per cent decomposition.

The products of main interest were carbon monoxide, methane, ethane, and methyl ethyl ketone. Methane and carbon monoxide were separated at −196°C. and the carbon monoxide was combusted and separated in the copper oxide tube. Ethane was separated at −175°C. and various samples were analyzed with the mass spectrometer. The remainder, consisting mainly of acetone, was collected into 150 cc. sample bulbs and analyzed for methyl ethyl ketone with the mass spectrometer.

The analyses for methyl ethyl ketone were based on the height of peak 72. Two synthetic samples containing amounts of acetone used in most experiments and 2.5 and 1.0% methyl ethyl ketone were subjected to the same procedure as after photolysis. Mass spectroscopic analyses of these gave 2.2 and 0.85% methyl ethyl ketone respectively, and therefore all the results for methyl ethyl ketone, obtained by this method, are reported 15% higher than those obtained in the analyses.

Since it is possible that some of the heavier methyl ethyl ketone was absorbed by the stopcock grease in the apparatus and in the sample bulbs, it was felt necessary to check on the validity of applying the 15% correction factor. The apparatus was altered so that the methyl ethyl ketone would not be in contact with stopcock grease except for a short time when introduced

into the mass spectrometer. Mercury cutoffs were appropriately installed to isolate the cell (volume of connecting tubing = 37 cc.) analytical system and gas burette. The acetone and methyl ethyl ketone mixtures were measured in a known volume which was connected with a mercury cutoff also serving as a manometer, and then collected in sample bulbs equipped with breakseals. Mass spectroscopic analyses of two synthetic samples (prepared under stopcock grease free conditions) containing 0.37 and 0.71% methyl ethyl ketone gave here 0.36 and 0.72% respectively. Obviously, with this procedure the mass spectroscopic results for methyl ethyl ketone may be used unambiguously.

RESULTS

The results of experiments done at three different acetone concentrations and at various temperatures are given in Table I. Included also, at 184°C. is

TABLE I
PRODUCTS OF PHOTOLYSIS OF ACETONE

Temp., °C.	Time, sec.	$R_{C_2H_6}$	R_{CH_4}	$R_{CH_3COC_2H_5}$	R_{CO}	$\frac{2R_{C_2H_6}+R_{CH_4}}{R_{CO}}$	$\frac{2R_{C_2H_6}+R_{CH_4}+R_{CH_3COC_2H_5}}{R_{CO}}$	$\Phi_{CH_3COC_2H_5}$
		$\times 10^5$ cc. N.T.P./sec.						
Mean acetone conc.—1.76 × 10⁻⁶ M./cc.								
105	3600	5.25	0.49	0	5.78	1.90	1.90	....
143*	7200	6.63	1.60	1.1	8.35	1.79	1.92	0.13
144	3600	6.06	1.70	1.2	7.72	1.79	1.95	0.16
159	3600	3.19	1.74	1.3	4.82	1.68	1.95	0.3
184	12600	0.63	1.29	0.6	1.70	1.50	1.86	0.4
183	3600	3.29	2.90	2.2	5.98	1.59	1.95	0.4
184	3600	5.25	4.36	2.3	9.22	1.61	1.86	0.3
184	2700	9.88	5.46	4.5	15.06	1.67	1.96	0.3
207	3600	2.26	4.34	2.2	5.94	1.49	1.86	0.25
240	3600	1.34	6.41	2.6	6.11	1.48	1.91	0.3
242	3090	2.41	10.28	4.0	10.52	1.43	1.82	0.3
242*	3600	0.77	4.59	1.3	4.11	1.49	1.81	0.3
284	3600	0.44	8.47	2.2	6.15	1.55	1.88	0.3
Mean acetone conc.—3.56 × 10⁻⁶ M./cc.								
144	3600	7.72	3.75	3.3	11.66	1.64	1.93	0.3
183	2700	5.33	8.86	5.9	12.77	1.53	2.00	0.5
240	1800	2.06	17.70	7.4	14.45	1.51	2.02	0.5
Mean acetone conc.—.88 × 10⁻⁶ M./cc.								
138	5160	2.66	0.47	0.5	3.29	1.76	1.91	0.15
184	7200	2.10	1.29	0.7	3.39	1.62	1.82	0.2
240	7200	0.90	2.94	1.2	3.18	1.49	1.86	0.3

**Stopcock-grease free system.*

the effect of variation of light intensity, seen from the rates of carbon monoxide production. Quantum yields of methyl ethyl ketone production are calculated on the assumption of a quantum yield of unity for carbon monoxide production.

It can be seen from the material balances obtained in the stopcock grease free system that the application of 15% correction to the rest of the results for methyl ethyl ketone is valid.

Mass spectrometric analyses occasionally showed traces of propane in the ethane fraction. However, after removing the ethane no significant fraction could be obtained at −150°C., i.e., propane. In the experiment at 284°C., about 20% of the ethane fraction consisted of ethylene. No other products could be found by the above method of analysis.

DISCUSSION

The constancy of the material balance

$$(2R_{C_2H_6} + R_{CH_4} + R_{CH_3COC_2H_5})/R_{CO},$$

over the temperature range studied indicates that reaction [6] is relatively insignificant at these conditions. Therefore, it is apparent that reactions [2], [3], and [4] account for 95 ± 3% of the methyl radicals produced, reaction [1] being the main source. The deviation falls within the possible error of 15% in methyl ethyl ketone analysis. Conversely, these results lend support to the postulated mechanism for acetone photolysis at these temperatures.

It is possible to obtain some information on the kinetics of reactions [2], [4], and [5]. If it is assumed that the acetonyl radicals produced in reaction [3] react only to produce methyl ethyl ketone and biacetonyl, then $R_{(CH_3COCH_2)_2}$ would be equal to $(R_{CH_4} - R_{CH_3COC_2H_5})/2$. Hence $(k_2^{\frac{1}{2}}k_5^{\frac{1}{2}})/k_4$ could be calculated as it is equal to $(R^{\frac{1}{2}}_{C_2H_6} R^{\frac{1}{2}}_{(CH_3COCH_2)_2})/R_{CH_3COC_2H_5}$. Such calculations were made and an average value of 0.7 ± 0.3 was found for $(k_2^{\frac{1}{2}}k_5^{\frac{1}{2}})/k_4$. These values, although considerably scattered, are fairly constant with temperature and are also in the range of ~0.5, the magnitude of $(Z_2^{\frac{1}{2}}Z_5^{\frac{1}{2}})/Z_4$, Z being the collision frequency. It seems unlikely that this is due to an accidental equivalence of $P_5^{\frac{1}{2}}$ and P_4 when both are small, and the results strongly support collision efficiencies for reactions [4] and [5] of the order of magnitude of that of [2], i.e., unity.

ACKNOWLEDGMENT

The authors wish to tender their sincere thanks to Dr. F. P. Lossing for his helpful discussions on the methyl ethyl ketone analysis, and to Miss F. Gauthier and Miss J. Fuller for the mass spectrometric analysis.

REFERENCES

1. ALLEN, A. O. J. Am. Chem. Soc. 63: 708. 1941.
2. FERRIS, R. C. and HAYNES, W. S. J. Am. Chem. Soc. 72: 893. 1950.
3. GOMER, R. and KISTIAKOWSKY, G. B. J. Chem. Phys. 19: 85. 1951.
4. HERR, D. S. and NOYES, W. A., JR. J. Am. Chem. Soc. 62: 2052. 1940.
5. LEROY, D. J. Can. J. Research, B, 28: 492. 1950.
6. NOYES, W. A., JR. and DORFMAN, L. M. J. Chem. Phys. 16: 788. 1948.
7. TROTMAN-DICKENSON, A. F. and STEACIE, E. W. R. J. Chem. Phys. 18: 1097. 1950.

THE ALKALOIDS OF PAPAVERACEOUS PLANTS

L. *DICRANOSTIGMA LACTUCOIDES* HOOK. F. ET THOMS. AND *BOCCONIA PEARCEI* HUTCHINSON[1]

By R. H. F. Manske

ABSTRACT

Dicranostigma franchetianum has been renamed *Stylophorum franchetianum* (Prain) comb. nov. because its alkaloids are the same as those of *S. diphyllum*. It is proposed to retain the name *D. lactucoides* because the contained alkaloids, namely protopine, isocorydine, sanguinarine, and chelerythrine present a combination hitherto encountered only in a *Glaucium*. *Bocconia pearcei* was shown to contain, in addition to chelerythrine (and presumably sanguinarine), small amounts of protopine and allocryptopine.

The genus *Dicranostigma* Hook. f. et Thoms. is presently considered to include three species. The uncertainty of the position of these species and of the genus is illustrated by the fact that at one time or another all were referred to *Chelidonium* Tourn. while one (*D. leptopodum*) was referred to *Glaucium* Tourn. and another (*D. lactucoides*) to *Stylophorum* Nutt.

It seemed probable that a chemical examination might aid in solving some of the moot points in the classification of these plants and the examination of one of them, *Dicranostigma franchetianum* (Prain) Fedde (2) has already been reported (4). This plant is the least named in the genus and was originally described as *Chelidonium franchetianum* Prain (5). Inasmuch as the alkaloids that it elaborates are the same as those elaborated by *Stylophorum diphyllum* (Michx.) Nutt. (4) the writer suggests that it should henceforth be known as *Stylophorum franchetianum* (Prain) comb. nov. This transfer out of *Dicranostigma* is specifically warranted because of the results of the chemical examination of *D. lactucoides* Hook. f. et Thoms. which is recorded in this communication. This much named plant was the type upon which the genus was founded but it has also been known as *Chelidonium dicranostigma* Prain (5), *C. lactucoides* (Hook. f. et Thoms.) Prain (6), and *Stylophorum lactucoides* Baill (1). The contained alkaloids, namely protopine, sanguinarine, chelerythrine, and isocorydine, indicate that the plant has affinities with *Sanguinaria* Dill. and *Bocconia* Plum. and with *Glaucium* but the absence of chelidonine definitely precludes any alliance with *Stylophorum* or *Chelidonium*. The taxonomic fate of the remaining species, *D. leptopodum* (Maxim.) Fedde must await its chemical investigation. Unfortunately it has not been available.

The alkaloids of *Bocconia pearcei* had already been examined (3) and a mixture of them from the same source confirmed the presence of chelerythrine and offered indirect proof of the presence of sanguinarine. Protopine and allocryptopine were also present but phenolic alkaloids, as in other species of this genus, were absent.

[1] *Manuscript received July 28, 1953.*
Contribution from the Dominion Rubber Company Limited Research Laboratories, Guelph, Ont.

EXPERIMENTAL*

D. lactucoides is a facultative biennial and the plant material, which was grown locally, was collected at practically all stages of growth. There was available a total of 3.94 kgm. of dried plant material including that from the roots. It was extracted with methanol in Soxhlet apparatus and the solvent was removed from the extract which was boiled with water and enough hydrochloric acid to render it acid to Congo red. The clear but reddish colored filtered extract was extracted with chloroform (extract C), then made alkaline with ammonia and again extracted with chloroform (extract AC).

Isocorydine

The extract C was freed of solvent, the residue extracted with dilute hydrochloric acid, filtered, and exhausted with ether. The aqueous solution was then rendered alkaline with an excess of sodium hydroxide (the small amount of precipitate here formed proved to consist largely of protopine), filtered, and again extracted with ether. The residue from the combined ether extract crystallized readily in contact with methanol and when recrystallized from the same solvent it was obtained in almost colorless stout prisms which, either alone or in admixture with authentic isocorydine, melted at 185°.

Sanguinarine and Chelerythrine

The chloroform extract (AC) was dissolved in hot dilute hydrochloric acid, filtered, and allowed to cool slowly. The deep red salt which then crystallized was decomposed with ammonia in the presence of chloroform. The residue from the chloroform extract was converted to its hydrobromide in acetone solution. The sparingly soluble orange salt thus obtained was decomposed with ammonia in the presence of a large volume of ether. When the washed ether solution was slowly evaporated a colorless base crystallized. This precipitate was washed with ether and then melted at 277° when placed in the melting point bath at 250°. This is the highest melting point ever recorded for sanguinarine but there can be no doubt about the identity of the compound. Analytical results are of no value in the identification because of the tenacity with which this alkaloid retains many solvents in molecular combination. A methoxyl determination gave a value corresponding to somewhat less than one group and this only after prolonged boiling. Since chelerythrine with two methoxyls yields methyl iodide corresponding to three methoxyls it is expected that sanguinarine under the same conditions will show one methoxyl. The ψ-cyanides of these bases are however characteristic and have sharp melting points. A solution of the base in chloroform was treated with a copious volume of methanol and then boiled with an aqueous solution of potassium cyanide, the mixed solvents being allowed to escape. While the somewhat concentrated solution was still hot, crystals of the desired product separated out. The substance was washed with water, with dilute acid, with methanol, and finally recrystallized from chloroform–methanol. Sanguinarine ψ-cyanide as thus obtained consisted of colorless stout prisms which melted at 227°. Found: N, 7.93, 7.97. Calc. for $C_{21}H_{14}O_4N_2$: N, 7.82.

**All melting points are corrected.*

The mother liquors from which the sanguinarine salts had been prepared were digested with an excess of potassium cyanide and the resulting precipitate separated and washed with water. It was then digested with cold dilute hydrochloric acid and the insoluble portion separated by filtration (the acid filtrate yielded protopine). When the dried product was recrystallized several times from acetone, then from chloroform–methanol, and again from acetone–methanol it melted at 258–259° and in admixture with authentic chelerythrine ψ-cyanide it melted at the same temperature.

Protopine

The acid extract obtained from the mixture which was precipitated by potassium cyanide was basified with ammonia and shaken with a large volume of ether. The residue from the ether extract crystallized readily when moistened with methanol and when the base was recrystallized from chloroform–methanol it melted sharply at 211° either alone or in admixture with protopine.

The total yield of alkaloids from this plant was approximately 0.2%. Of this, sanguinarine was the major constituent followed by isocorydine, protopine, and chelerythrine in that order. There were small amounts of alkaloid containing mother liquors, some of them phenolic in nature, which would undoubtedly yield other bases if more material were available.

Bocconia pearcei

The author is sincerely indebted to Mr. Isidoro Macció, Direccion Nacional de Quimica, Buenos Aires, Argentina, who supplied a specimen of total mixed alkaloids from *B. pearcei*. These alkaloids were dissolved in chloroform–methanol and digested with aqueous potassium cyanide. The amorphous resinous mixture that was obtained when the organic solvents had largely been expelled was digested with cold dilute hydrochloric acid. Systematic recrystallization of the insoluble portion from acetone, chloroform–methanol, and acetone–methanol served to yield pure chelerythrine ψ-cyanide melting at 259–260° and a series of fractions of lower melting points which undoubtedly consisted of a mixture of the ψ-cyanides of chelerythrine and sanguinarine.

The acid soluble portion from the above treatment with potassium cyanide was basified with ammonia and shaken with much ether. This residue from the washed ether extract readily yielded a crop of protopine (m.p. and mixed m.p. 210°). The methanolic filtrate from the protopine was neutralized with nitric acid and a further small amount of protopine separated as its sparingly soluble nitrate. The bases in the filtrate from this were again regenerated and in contact with methanol and seeding with allocryptopine this base rapidly separated. When recrystallized from methanol it consisted of colorless fine needles which melted, either alone or in admixture with allocryptopine, at 159°.

There were no fractions soluble in alkali and hence phenolic alkaloids were absent.

REFERENCES

1. Baillon, H. Hist. Plantes. 3: 114.
2. Fedde, F. von. *In* Engler, A. Das Pflanzenreich. Papaveraceae-Hypecoidene. 1909. p. 211.
3. Macció, I. Arch. farm. y bioquim. Tucumán, 3: 27. 1946.
4. Manske, R. H. F. Can. J. Research, B, 20: 53. 1942.
5. Prain, D. Bull. Herb. Boissier 3: 586. 1895.
6. Prain, D. Ann. Roy. Botan. Gardens, Calcutta, 9: 7. 1901.

THE EFFECT OF TEMPERATURE ON SUSPENSIONS OF GLASS BEADS IN TOLUENE CONTAINING VARIOUS PERCENTAGES OF WATER[1]

By A. E. J. Eggleton[2] and I. E. Puddington

ABSTRACT

The influence of temperature on the sedimentation volume and relative yield values of suspensions of spherical glass beads in toluene containing varying percentages of water has been measured. The increased sedimentation volume and yield value, due to the presence of water, found at room temperature virtually disappeared below approximately 0° C. This is in agreement with the theory which ascribes the effect of water to its interfacial tension against toluene. At temperatures above 0° C. there was a gradual fall in the sedimentation volume and yield value from the maximum found at 0° C. This is attributed to the increasing solubility of water in toluene. Suspensions containing no water or only a small quantity showed an unexpected steady increase in sedimentation volume and yield value as the temperature was lowered to −60° C. This effect was also observed with a suspension of glass beads in pentane. The results indicate a close connection between yield value and equilibrium sedimentation volume.

INTRODUCTION

The sedimentation volume of suspensions of inert materials in organic liquids has been a subject of interest for some time. Earlier work is typified by that of Ostwald and Haller (6) who investigated the sedimentation volumes of a number of inorganic oxides, carbonates, and silicates in various organic liquids, both polar and nonpolar. Differences in the sedimentation volumes were ascribed to the binding of differing numbers of layers of liquid to the particles, in other words to lyosorption.

The importance of small quantities of water has only been recognized comparatively recently. Kruyt and van Selms (3) found that the yield value of starch and quartz suspensions in organic liquids depended on the care taken in drying the materials and the amount of water subsequently added. Bloomquist and Shutt (1) related the sedimentation volumes of glass spheres in various organic liquids to their interfacial tension against water. Those with the largest values gave the largest sedimentation volumes. Organic liquids with which water was miscible gave low sedimentation volumes. Gallay and Puddington (2) showed how an attractive force between particles caused an increase in the sedimentation volume by preventing the close packing of the particles. McFarlane and Tabor (5) investigated the adhesion between two glass surfaces and found that it was directly related to the surface tension of a small drop of liquid placed at the point of contact, as predicted theoretically.

The present work is concerned with the effect of temperature on suspensions of glass beads in toluene. Clearly, if the effect of water is due to its interfacial tension against toluene we should expect changes in the properties of the suspensions when the temperature is lowered below 0° C. So that the system

[1] *Manuscript received October 23, 1953.*
Contribution from the Division of Applied Chemistry, National Research Council, Ottawa, Canada. Issued as N.R.C. No. 3157.
[2] *N.R.L. Postdoctorate Fellow, 1951–53, National Research Council, Ottawa.*

should be as simple as possible, spherical glass beads of definite size were chosen and suspended in toluene, which enabled the suspensions to be cooled to −60° C. without solidifying.

EXPERIMENTAL

Glass beads, −275 + 320 mesh, were supplied by the Flexolite Manufacturing Corporation. They were further fractionated by sedimentation against a constant upward current of water in a tube 3 cm. diameter and 100 cm. long. By successively increasing the rate of flow, fractions of increasing size were carried over the top of the tube and collected. Flocculation of the spheres, which would disturb the fractionation process, was prevented by dispersing them in a small quantity of sodium hexametaphosphate solution which, when diluted with the main body of liquid, gave a concentration of sodium hexametaphosphate approximately 0.1% by weight.

In order to conserve the solution a closed system was used, a small circulating pump returning the overflowed solution to a constant head device. Boiled out distilled water was used to prevent variations in the rate of flow caused by the formation of air bubbles in the connecting tubing.

A fraction of average diameter 43 μ was used for all experiments. Fig. 1 shows the distribution of sizes about the mean. The beads were cleaned with

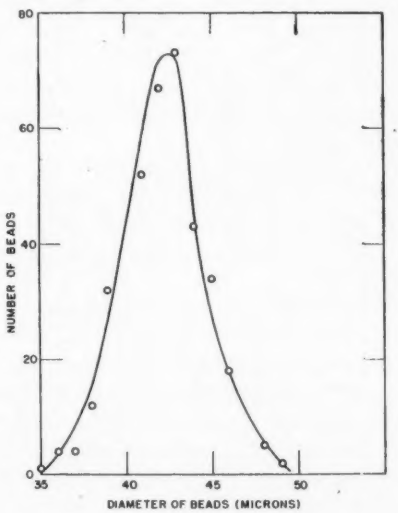

FIG. 1. Size distribution of beads.

boiling nitric acid and aqua regia and finally extracted with hot distilled water in a Soxhlet apparatus for two weeks to remove traces of soluble material.

Reagent grade toluene was freed from water and air by boiling off approximately a quarter of the original material, followed by refluxing under vacuum. For some of the experiments, where complete absence of water was desired,

the toluene was let stand 24 hr. over calcium hydride and again refluxed under vacuum.

Pentane, 99.99% pure, was dried over calcium hydride and refluxed under vacuum.

Distilled water was boiled at atmospheric pressure to about half its original volume to remove as much air as possible and then distilled into a flask which had been baked at 350° C. under vacuum overnight. By repeatedly distilling the water back and forth on to a cold trap under vacuum, a sample was finally obtained which when distilled into a 1 mm. capillary tube formed a continuous thread showing the absence of dissolved air.

Fig. 2 shows the apparatus used for determining sedimentation volumes and relative yield values of suspensions which were contained in the tube *A*.

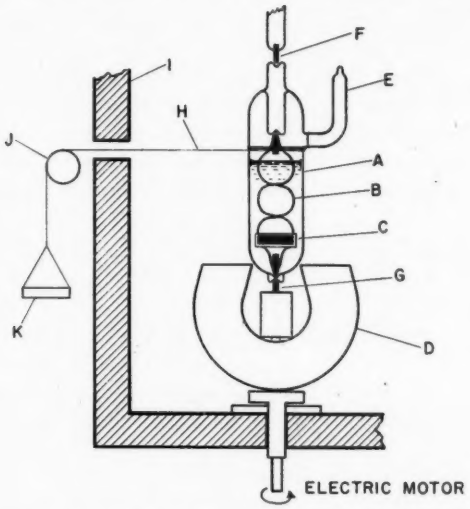

FIG. 2. Apparatus used for determining relative yield values and sedimentation volume of suspensions.

This tube (of pyrex, approximately 40 mm. by 12 mm. diameter) contained a spiral stirrer *B* pivoted at both ends on tungsten points bearing in conical depressions. Sealed in the stirrer, near the bottom, was a small iron slug *C*. This enabled the stirrer to be rotated at speeds up to approximately 3000 r.p.m. by a horseshoe magnet *D* which was attached to the shaft of a small electric motor.

Before filling, the tube was cleaned with chromic cleaning mixture, washed with distilled water, and dried. The required quantity of beads was weighed into the tube which was then sealed by the side-arm *E* to a vacuum apparatus. The glass beads were out-gassed at 350° C. overnight after which the pressure, read on a MacLeod gauge, was less than 10^{-5} mm. A calibrated bulb was filled with water vapor at measured temperature and pressure from the reservoir of de-gassed water, and then by immersing the tube *A* in dry ice the

water contained in the bulb was condensed on the glass beads. The percentage of water by weight of beads could be calculated with sufficient accuracy from the volume, pressure, and temperature of water vapor in the calibrated bulb, using the ideal gas equation. By condensing more than one volume of water vapor on the beads, tubes containing up to 0.62% of water were prepared.

With the tube still immersed in dry ice the required quantity of toluene, which was not critical, was condensed in the tube, after which the side-arm was sealed off. The suspensions contained approximately 45% glass beads by weight.

The tube as shown in Fig. 2 was pivoted between two bearings *F* and *G*. The upper one, *F*, consisted of a tungsten point sealed in a short length of pyrex tube which was free to move vertically. It was kept in place by a small spring which enabled the tube to be inserted in place easily. The lower bearing *G* was attached to the shaft carrying the horseshoe magnet *D* and rotated with it. This bearing consisted of a chromium steel phonograph needle to avoid excessive wear on the glass tube.

A light nylon thread *H* was fastened at one end to side arm *E* of the tube and the other passed through the wall of the thermostat *I* and over the small aluminum pulley *J*, pivoted on steel points, to a small pan *K* on which weights could be placed. The apparatus, with the exception of the pan *K*, was contained in an air thermostat consisting of an insulated box which could be maintained between room temperature and $-60°$ C. within $\pm 0.3°$ C. by circulating air over dry ice contained in a separate compartment. The circulating fan was controlled by a bimetallic element.

In a typical run the tube was placed in the thermostat at room temperature and cooled slowly with the spiral stirrer in operation. Provided the temperature was very gradually lowered while passing through 0° C. the beads did not freeze to a solid mass. Once the temperature was below about $-5°$ C. it was lowered rapidly to $-60°$ C. to prevent the ice on the bead surface from recrystallizing and causing agglomeration. The tube was held at $-60°$ C. for an hour or more with the stirrer rotating at 3000 r.p.m. to break up any agglomerates which may have been formed during the cooling process.

The stirring motor could be stopped suddenly, in about a second, by a brake. This was necessary when measuring sedimentation volumes since a gradual slowing down of the stirrer caused the beads to stick to the walls of the tube, particularly with those suspensions containing larger percentages of water. The tube was tapped lightly by hand until the layer of sedimented beads had reached a constant volume. The height of the sedimented volume was measured with a cathetometer using a scratch mark on the tube as a reference point. The tube had been previously calibrated with weighed quantities of water so that the sedimentation heights could be converted to volumes.

A large weight was placed on the scalepan *K* during these measurements to prevent the tube from rotating. When measuring relative yield values of suspensions, smaller weights were placed on the pan in order that, with the stirring motor in operation, the tube *A* rotated and the nylon thread wound round the tube until the scalepan was held at the top of its travel. The weights

on the pan were then adjusted until they were just sufficient to pull the pan downwards and so rotate the tube when the stirring motor was suddenly stopped with the brake. This method gave more reproducible results than stopping the motor and then increasing the weights on the pan until the tube commenced rotating, since an indeterminate amount of settling occurred each time.

The method of plotting shearing stress against rate of shear and extrapolating to zero rate of shear was not used, since at high rates of shear the stirrer caused turbulence and cavitation in the suspension, while at low rates the beads settled and a two layer system was formed. Measurements of both sedimentation volume and yield value were made at various temperatures, increasing from −60° C. to room temperature.

RESULTS AND DISCUSSION

Fig. 3 shows the sedimentation volume per gram of beads for the various suspensions at different temperatures and Fig. 4 shows the corresponding relative yield values.

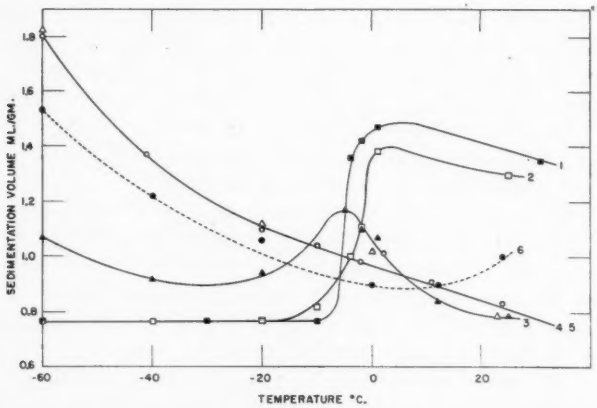

FIG. 3. Sedimentation volumes of suspensions. Curves 1–5 represent behavior of glass spheres in toluene with the following added percentages of water, 0.62, 0.47, 0.28, 0.10, and 0.0. Curve 6 shows behavior in dry pentane.

The suspensions containing 0.62% and 0.47% of water respectively show clearly that the effect due to the water disappears below 0° C. when the water surrounding the beads is frozen. This is in agreement with the hypothesis that the effect of water is due to its interfacial tension against toluene. When the water is frozen no 'necks' can be formed between adjacent particles and the increased viscosity no longer exists, the yield value being similar to that for dry beads at 20° C. The apparent small residual yield value in these two cases is possibly attributable to friction in the bearings. The small depression of the apparent freezing point of the water may be noted. This is not due to supercooling of the water as all measurements were made by cooling the suspension to −60° C. and then raising the temperature to successively

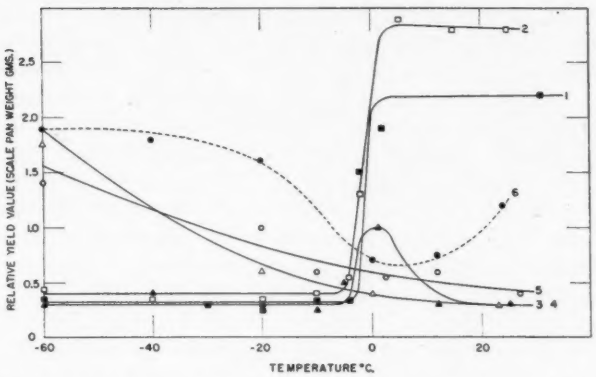

FIG. 4. Relative yield value of suspensions. Curves 1–5 represent behavior of glass spheres in toluene with the following added percentages of water, 0.62, 0.47, 0.28, 0.10, and 0.0. Curve 6 shows behavior in dry pentane.

higher values. The depression is probably due to slight solubility of alkalis present in the glass beads. Some earlier experiments were conducted with beads that had not been subjected to the prolonged extraction with hot distilled water. On cooling, these showed a continuous lowering of the sedimentation volume and yield value, with no sharp break at all. Values corresponding with those for water-free beads at room temperature were only obtained below −40° C.

The slight falling off of the yield value and sedimentation volume above 0° C. is probably the result of two factors. Increasing temperature will lower the interfacial tension between toluene and water and in addition some of the water will dissolve in the toluene, reducing the amount between the beads. This probably accounts for the behavior of the suspension containing 0.28% water which exhibits maximum yield value and sedimentation volume at −5° C., the values falling off rapidly above this temperature till at 25° C. a value similar to that for water-free beads is obtained. We may calculate the effect of solubility in the following manner. From the average diameter of the beads (43 μ) and their density 2.32 gm./ml. we obtain a value of 603 sq. cm./gm. for their geometrical surface area. Thompson *et al.* (8) measured the adsorption of carbon dioxide on similar glass beads. They found a B.E.T. surface area value close to the geometrical area for unetched beads but a value 21 times the geometrical area for beads which had been etched with water for three weeks. Using this figure and a value of 10.5 sq. A for the area of a water molecule (calculated from the liquid density) we calculate that 0.036% water by weight of the beads is required to form a monolayer. The water present in a suspension will be divided between the surface of the glass beads and solution in the toluene. If we assume that the toluene is saturated with water we can calculate from solubility tables (7) the amount remaining on the beads. The values for the suspension containing 0.28% water are 7.0 monolayers at 0° C. and 6.1 monolayers at 30° C.

McFarlane and Tabor (5) measured the adhesion of a small glass bead on a vertical glass plate, the adhesion being due to an adsorbed film of water. When approximately five monolayers had been adsorbed the adhesion increased rapidly from zero reaching the maximum value when about 20 monolayers had been adsorbed. Although the above calculation is only approximate it does show that the solution of water in the toluene changes the number of adsorbed monolayers significantly in the region where a rapid change in adhesion is occurring. Consequently we should expect the decrease in yield value and sedimentation volume which was experimentally observed.

In this connection we may note the paper by Kruyt and van Selms (4) in which the effect of varying percentages of water on the yield value of similar suspensions of glass beads is calculated. They arrived at a relation between the yield value and water content of a suspension by calculating the work required to separate a pair of glass beads with a known quantity of water in the 'neck' joining them. However, the yield value of a suspension would appear to have the dimensions of force rather than those of work. Once the shearing stress has reached the critical value the suspension will yield. Hence the adhesion between the beads is the important factor, as discussed in this work. The agreement between Kruyt and van Selms' calculation and their experimental results may be due to the fact that the calculation contained an adjustable parameter (the number of other beads which touch each bead). They have also taken no account of the fact that the real surface area of their beads may be considerably greater than the geometric area. Using values given in the paper by McFarlane and Tabor, a plot of adhesion against the number of monolayers gives a curve of similar shape to the yield value vs. percentage water graphs given by Kruyt and van Selms. An alternative explanation for their results, making reasonable assumptions about the real surface area of their glass spheres, is therefore possible.

The suspensions containing no water and 0.1% water showed, as expected, no break at 0° C. but exhibited an unexpected steady increase in the yield value and sedimentation volume as the temperature was lowered to −60° C. This indicates an increasing attractive force between the beads at low temperatures. It is suggested that this may be due to the adsorption of toluene molecules on the glass surface. These molecules will have fewer degrees of freedom than those in the liquid and their arrangement will tend towards that of the solid state. When two beads touch, local freezing at the point of contact may occur. The force required to separate the beads will increase at lower temperatures as the area of local freezing increases.

The presence of water already adsorbed on the glass surface will prevent the subsequent adsorption of toluene, so this process will not occur with the suspensions containing considerable amounts of water. However, it is difficult to understand why the suspension containing 0.1% of water has similar properties to the water-free suspension. On the basis of our previous calculation there will be nearly three monolayers of water on the surface of the glass beads and we should not expect toluene to be adsorbed on such a substrate. The anomalous increase of the sedimentation volume and yield value was also

observed with a water-free suspension in pentane (dotted lines in Figs. 3 and 4). Thus the effect is not due to any special properties of the benzene ring and its cause remains uncertain.

ACKNOWLEDGMENT

Preliminary experiments related to this work were carried out by B. A. Dunell. To him and to P. G. Howe, with whom many helpful discussions were held, grateful acknowledgment is made.

REFERENCES

1. BLOOMQUIST, C. R. and SHUTT, R. S. Ind. Eng. Chem. 32: 827. 1940.
2. GALLAY, W. and PUDDINGTON, I. E. Can. J. Research, B, 21: 171. 1943.
3. KRUYT, H. R. and VAN SELMS, F. G. Rec. trav. chim. 62: 407. 1943.
4. KRUYT, H. R. and VAN SELMS, F. G. Rec. trav. chim. 62: 415. 1943.
5. MCFARLANE, J. S. and TABOR, D. Proc. Roy. Soc. (London), A, 202: 224. 1950.
6. OSTWALD, W. and HALLER, W. Kolloid-Beih. 29: 354. 1929.
7. SEIDELL, A. Solubilities of organic compounds. Vol. II. D. van Nostrand Company, Inc., New York. 1941.
8. THOMPSON, J. B., WASHBURN, E. R., and GUILDNER, L. A. J. Phys. Chem. 56: 979. 1952.

THE PRODUCTION OF Na^{22} BY A (H^3, n) REACTION IN A NUCLEAR REACTOR[1]

By L. G. Cook and K. D. Shafer

ABSTRACT

The positron emitting Na^{22} of 2.6 year half-life has been prepared in a nuclear reactor by the double reaction $Li^6(n, \alpha)H^3$, $Ne^{20}(H^3, n)Na^{22}$. The over-all yield was 2.3×10^{-7} atoms of Na^{22} per atom of tritium formed. Eleven grams of lithium as aluminum alloy turnings in a neon atmosphere at 200 p.s.i. was irradiated for 175 days in a neutron flux of about 4×10^{12} n./cm.^{2}/sec. About 380 μc. of Na^{22} was obtained in a sodium extract having a specific activity of 10 mc. Na^{22}/gm. of Na^{23}. A specific activity in the curie/gm. level would be expected from a longer irradiation in the highest flux (6×10^{13} n./cm.^{2}/sec.) in the NRX reactor. The separation and purification of the sodium proved practicable by paper chromatography or ion exchange; the analyses for trace Li and Na^{23} were carried out by radioactivation.

INTRODUCTION

Neutron deficient positron emitting (or *K*-capture) nuclides are usually produced by charged particle reactions in accelerators followed by chemical separation of the product element. In nuclear reactors, however, the only general method of preparation is by the $(n, 2n)$ reaction. This reaction is not too satisfactory. The $(n, 2n)$ effective cross sections are low, thus preventing the attainment of high specific activity; also the product element is the same as the irradiated element, preventing the use of chemical separation to attain high specific activity.

For example, the reaction $Na^{23}(n, 2n)Na^{22}$ has a threshold of 12.2 Mev. (9) and a maximum total neutron cross section of 900 mbarns (2). Since the fraction of neutrons in a reactor with energies >12 Mev. is $\sim 10^{-4}$ (8), in a reactor position with thermal neutron flux of 4×10^{12} n./cm.^{2}/sec., a 175 day irradiation would be expected to produce a specific activity of only $\sim 10^{-5}$ curies/gm.

However, by utilizing a double reaction, an improvement can sometimes be made. For example, if one mixes neon gas with lithium in a suitable way, and irradiates the mixture with thermal neutrons, the Li^6 captures neutrons with 930 barns (1) cross section, and provides a steady supply of 2.75 Mev. tritons (5) which in turn produce Na^{22} by a (H^3, n) reaction on Ne^{20}. (F^{18} and Cl^{34} have also been made by this general method (6).)

The preparation of the carrier free Na^{22} involves in principle a chemical separation of trace sodium from macro amounts of neon, lithium, and aluminum. In practice, the specific activity attainable depends on the neutron flux, the irradiation time, unavoidable traces of Na^{23} contamination, and, of course, the degree of dispersion of the lithium in the neon.

[1] *Manuscript received September 28, 1953.*
Contribution from the Chemistry Branch, Atomic Energy of Canada Limited, Chalk River, Ontario. Issued as A.E.C.L. No. 87.

EXPERIMENTAL

(1) *Irradiation Technique*

A 4% Li (by weight) in "super pure" aluminum alloy was prepared and fine wool-like turnings turned off on a lathe. Two hundred and seventy-six grams of these turnings were packed loosely in aluminum cartridges 1 in. diam. × 4 in. long, which were then slipped into an aluminum pressure tube. The pressure tube was installed in a position in the NRX reactor where the nominal neutron flux was 4×10^{12} n./cm.^{2}/sec., and filled with neon at 200 p.s.i.

After 175 reactor operating days the tube was taken out and the aluminum–lithium alloy wool removed to the laboratory for processing.

(2) *Extraction of Na^{22}*

The lithium–aluminum alloy wool was rinsed four times with distilled water, using 100 cc., 150 cc., 250 cc., and 900 cc. respectively. Twenty cubic centimeters of nitric acid were added to each washing, and the solutions boiled until the suspended material dissolved and the solutions became clear.

The hot acidified solution was then neutralized with aqueous ammonium carbonate to decided cloudiness, then cleared with ammonium oxalate solution. This neutralization and clearing was repeated four times at the boiling point, then finally the solution was made slightly basic with ammonium carbonate. The resultant aluminum oxalate – carbonate precipitate was compact, filtered easily, and in previous tests using Na^{24} tracer had been shown not to carry down trace sodium.

The filtrate contained the Na^{22}, lithium, and any trace accumulation of Na^{23}.

(3) *Purification of Na^{22} by Ion Exchange*

The Na^{22} was to be separated from the substantial amount of Li present, as well as from any other impurities. An ion exchange separation of Na, K, Rb, Cs, on Dowex 50 resin has been described (4). The same technique was found to give a clean separation of the lithium from the sodium. The lithium appeared as a peak between the 9th and 14th column volumes; the Na^{22} peak lay between the 16.5 and 23rd column volumes. To identify the Na^{22} positively, a γ–γ coincidence crystal counter was used to identify the positron annihilation radiation, and the positron energy was checked by determining the absorption curve in aluminum.

(4) *Purification of Na^{22} by Paper Chromatography (Alternative Process)*

A separation of sodium and lithium by paper chromatography has been described (3). The separation was demonstrated by detecting two chloride bands in the paper chromatograph, and not by direct analysis for sodium and lithium.

In the present work, direct analysis for sodium and lithium was used. The sodium was detected by the Na^{22} activity; the lithium was detected using the 0.88 sec. Li^8 activity, produced in a neutron reactor. The samples to be analyzed were placed in iron capsules, sent down a tube into the reactor, then blown through a pneumatic tube directly into a counting position, where the intensity and decay of the 0.88 sec. activity could be measured directly. In this way 10^{-7} gm. of Li can be detected.

Using absolute methyl alcohol as elutant, and placing the alkali salt on the paper as chloride, complete separation was obtained in three and one half hours. The lithium band extended from the 6th to the 10th inch, the solvent front being at 12 in. The sodium band extended from zero to the 5th inch, with its peak at 1.5 in. A 33 hr. creep period placed the sodium peak at 2.0 in., with no greater spreading than before. The lithium was not detectable until the 10th in. and was concentrated at the tip of the paper (12th inch).

(5) *Analysis of Product for Na^{22}/Na^{23} Ratio*

A sample of the unextracted rinse solution was evaporated and irradiated for 10 hr. in the NRX reactor to produce the reaction Na^{23} $(n, \gamma)Na^{24}$. The sample was then extracted and purified by the techniques described and the decay of the Na^{24} activity and the residual Na^{22} activity were observed. The Na^{22}/Na^{23} ratio in the sample was found to be 10 mc. Na^{22}/gm. Na^{23}.

(6) *Determination of Yield*

The over-all yield of Na^{22} was 14×10^6 disintegrations/sec. or $\sim$380 μc., and was obtained in the first three rinses of the alloy turnings. The last rinse had a negligible amount of Na^{22} in it. This confirmed the expectation that the Na^{22} formed in the gas phase would settle on nearby surfaces, and be easily washed off with water.

A straightforward calculation of the number of neutrons consumed in 11.0 gm. of Li in 175 days at a flux of 4×10^{12} n./cm.^{2}/sec. gives a neutron consumption of 4.1×10^{21} neutrons (making no allowance for "blackness" to neutrons; the turnings were spread out over a length of four feet). Thus the yield was 3.5×10^{-15} disintegrations/sec./atom of tritium formed, or 2.3×10^{-7} atoms of Na^{22}/atom of tritium formed.

A sample of sodium chloride which had been irradiated in the same nominal flux (4×10^{12} n./cm.^{2}/sec.) for five years was purified by the ion exchange procedure, and the Na^{22} content of the Na^{23} determined. A specific activity of 1.6×10^{-5} curies Na^{22}/gm. Na^{23} was found, confirming the predicted low yield of the $(n, 2n)$ reaction.

DISCUSSION

The yield of the $Na^{23}(n, 2n)Na^{22}$ reaction in a thermal neutron reactor has been determined. It has been found that the $Li^6(n, \alpha)H^3$, $Ne^{20}(H^3, n)Na^{22}$ reaction will produce Na^{22} with specific activity 10^4 times higher in a neutron flux of 4×10^{12} n./cm.^{2}/sec.

It would be expected that the use of 10 times higher fluxes (available in the interior of the NRX reactor), longer irradiation periods, and a program to reduce sodium pickup could be made to increase the specific activity to the curie/gm. level.

CONCLUSION

The double reaction $Li^6(n, \alpha)H^3$, $Ne^{20}(H^3, n)Na^{22}$ makes possible the preparation of Na^{22} in present thermal neutron reactors with specific activity of the order of one curie Na^{22}/gm. Na^{23}.

REFERENCES

1. AECU-2040. Available from Office of Technical Services, Department of Commerce, Washington, D.C. June 15/53 Supplement.
2. BLATT, J. M. and WEISSKOPF, V. F. Theoretical nuclear physics. John Wiley & Sons, Inc., New York. 1952. pp. 483–484.
3. BURSTALL, F. H. J. Chem. Soc. 516. 1950.
4. COHN, W. E. and KOHN, H. W. J. Am. Chem. Soc. 70: 1986. 1948.
5. FACCHINI, U., GATTI, E., and GERMAGNOLI, E. Phys. Rev. 81: 475. 1951.
6. KNIGHT, J. D., NOVEY, T. B., CANNON, C. V., and TURKEVITCH, A. Paper 326. Radiochemical studies of the fission products, Book 3. McGraw-Hill Book Company, Inc., New York. 1951. p. 1917.
7. PAUL, E. B. A.E.C.L., Chalk River. Private communication.
8. U.S.A.E.C. Technical Release on "Nuclear data for low power research reactors". November, 1950.
9. VAN PATTER, D. M. Measurements of nuclear disintegration energies of light nuclei. M.I.T. Laboratory for Nuclear Science and Engineering, January 15, 1952. Technical Report No. 57.

PVT MEASUREMENTS IN THE CRITICAL REGION OF XENON[1]

By H. W. Habgood[2] and W. G. Schneider

ABSTRACT

Extensive PVT measurements of xenon extending from 1.8° above the critical temperature to the critical temperature, and in a few cases to 4° below the critical temperature, have been carried out at densities ranging from somewhat above the critical density to well below. In order to make the corrections for hydrostatic head small and easily calculable, a bomb having a height of only 1.0 cm. was used in the present measurements. The previously reported value for the critical temperature 16.590° is confirmed. The critical density is estimated to be 1.099 ± 0.002 gm./ml. compared with 1.105 gm./ml. found previously. The critical pressure is found to be 57.636 ± 0.005 atm.

The isotherms at temperatures above the temperatures of meniscus disappearance do not appear to have any flat portions. However, the critical isotherm is considerably flatter and broader over a range of densities than that corresponding to a van der Waals equation, and at the critical point the third and fourth derivatives of pressure with respect to volume appear to be zero.

INTRODUCTION

In order to obtain an improved understanding of critical phenomena a program has been under way in this laboratory to measure with the highest possible precision a number of properties in the critical region of a single substance. Xenon, being monatomic, and having a critical temperature conveniently close to room temperature, was chosen for this work. Previous publications have already described the liquid–vapor coexistence curve (15), density distributions in a vertical tube (16), and the velocity and absorption of ultra sound (2). We now wish to report measurements of the compressibility of xenon in the critical region. These measurements are used in the succeeding paper (5) to calculate thermodynamic properties in this region.

A major difficulty in making accurate measurements near the critical point results from the very high compressibility of the system which causes a partial compression of the medium under its own weight.* Accordingly the density inside the experimental bomb changes considerably with height, while it is only the average density which is directly measured. Also, the pressure is measured at a particular level in the system for which the density is not known; correction to any other level requires a knowledge of the density distribution in the fluid head. These effects were first discussed by Gouy in 1892 (3) but appear to have been ignored by subsequent workers. Their significance in actual measurements was first shown in the determinations by MacCormack and Schneider (6) of the isotherms of sulphur hexafluoride where, using a relatively tall bomb, the corrections for fluid head were several times larger than the uncertainties in the pressure measurements and significantly affected the shapes of the isotherms. The effect was further demonstrated in the

[1] *Manuscript received October 7, 1953.*
Contribution from the Division of Pure Chemistry, National Research Council of Canada, Ottawa, Canada. Issued as N.R.C. No. 3161.
[2] *National Research Laboratories Postdoctorate Fellow.*
* *This question has been discussed at greater length in a recent symposium (13).*

measurements of Weinberger and Schneider (15) on the liquid–vapor coexistence temperatures of xenon where observations in a tall bomb yielded a temperature–density coexistence curve with a flat top, while those in a similar bomb mounted horizontally and only 14 mm. high gave a round-topped coexistence curve and hence pointed to the existence of a unique critical density as postulated originally in classical theory. Recently Whiteway and Mason (18) have completely confirmed these observations.

Since the prediction of a flat-topped coexistence curve and of a region of horizontal isotherms above the temperature of meniscus disappearance was one of the main features of the theory of Mayer and Harrison (8), it is of considerable importance that experimental observations should be properly corrected for the effects of gravity. It was at first not clear whether the flat top observed with xenon in the tall bomb could be explained entirely by the gravitational effect. However, it was later shown (14), using the measured compressibilities given in the present paper, that the calculated density range of the flat top agreed closely with the observations.

In PVT measurements the necessary corrections for the effect of the fluid head may be calculated by successive approximations from the observed isotherms either to give the pressure at the level where the local density equals the average density of the filling, or to give the local density at the level where the pressure was measured. Our present measurements have been carried out using a horizontal glass bomb 10 mm. in diameter (i.e. height) in order to make these corrections very small and easily calculable. However, to illustrate the nature and extent of these gravitational effects we repeated measurements of the critical isotherm in a bomb 25 cm. tall. The details of this work have been reported elsewhere (4). The observations were in complete agreement with the expected pressure and density variations resulting from the gravitational field as calculated for different fillings on the basis of the isotherm obtained from the horizontal bomb. It was apparent, however, that calculation in the opposite direction, i.e. to derive the "true" isotherm from measurements in a tall bomb, would require several steps of approximation and the resulting uncertainty in the corrected isotherm would be much greater than the experimental scatter of the original measurements.

The geometry of the apparatus used by MacCormack and Schneider in the measurements on sulphur hexafluoride was such that calculation of the corrections for fluid head was particularly difficult and some rather rough approximations were used. The isotherms thus corrected did not show any horizontal portions in the immediate supercritical region. Later Wentorf and Boyd (17) using a somewhat shorter bomb* reported measurements also on sulphur hexafluoride which yielded horizontal portions in several isotherms in this region, the most impressive experimental evidence so far in favor of the Mayer–Harrison theory. They supported their results by applying "more realistic corrections" to the measurements of MacCormack and Schneider to

* *Although most of the bomb volume was confined to a height of approximately 5.7 cm. the stirring mechanism fixed to the top of the bomb provided an additional volume and an additional hydrostatic head making the total effective height close to 19 cm. It is not clear from the report of Wentorf and Boyd whether their corrections for hydrostatic head took account of this.*

obtain similar horizontal isotherms. However, these new corrections merely involved correcting the observed pressure to the level at which the meniscus disappeared, and the xenon measurements referred to above (4) showed quite clearly that this procedure automatically gives a horizontal isotherm. Consequently the measurements of MacCormack and Schneider cannot be said to give definite confirmation to the "derby hat" region of horizontal isotherms reported by Wentorf and Boyd. For carbon dioxide, the measurements of Wentorf and Boyd (17) as well as the earlier measurements of Michels *et al.* (9) do not support any appreciable region of horizontal isotherms above the temperature of meniscus disappearance. In the case of xenon the measurements reported in the present paper likewise do not suggest any such "derby hat" region.

Previously published PVT measurements on xenon include isotherms from 16.65° C. (given as the critical temperature) to 300° C. over the density range 1–10 moles/liter reported by Beattie, Barriault, and Brierley (1), and vapor pressure measurements up to 0.56° below the critical temperature reported by Michels and Wassenaar (10). Palmer (11) using a schlieren technique has measured approximate density gradients in xenon near the critical point and from these has estimated P–V isotherms.

METHOD

The method of measurement was closely similar to that used by MacCormack and Schneider (6). The bomb assembly is shown schematically in Fig. 1. The design of the bomb and stirrer has been previously described (15).

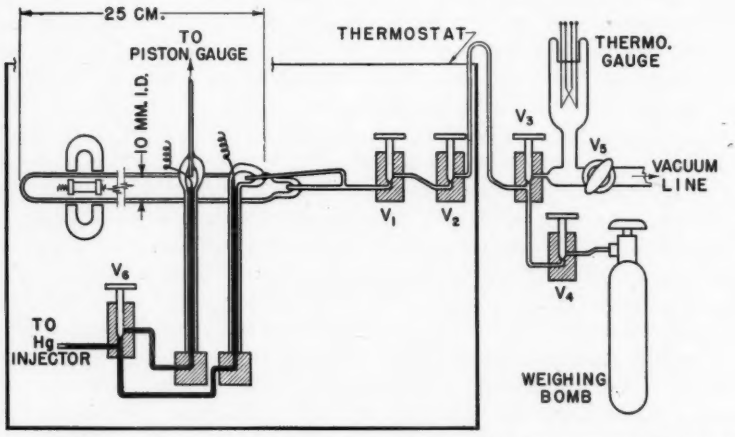

FIG. 1. Schematic diagram of the bomb assembly for PVT measurements in the critical region.

The glass capillary forming the xenon side of the mercury U-tube was bent at right angles just above the tungsten contact wire in order that the connecting tube to the bomb could be kept short and as nearly as possible at the

same height as the bomb itself. The maximum possible head of xenon at any point in the system was 16 mm. The pressure was measured at a level 1 mm. above the center of the bomb, this being the position of the contact wire in the mercury U-tube.

The complete assembly inside the thermostat was mounted as a unit which could be rotated through 45° about a pivot point so that a dewar flask could be raised about the closed end of the bomb to condense in a charge of xenon from the brass weighing bomb. The thermostat bath itself, which has been previously described (15), was mounted on the platform of a hydraulic lift operated by compressed air. When the bomb was being charged, the bath with its stirrers, etc., was lowered and could be quickly raised as soon as the bomb had started to warm up.

The contents of the bomb were stirred before each pressure measurement but the stirrer was turned off during the actual measurement. Pressures measured with continuous stirring were 0.002–0.003 atm. higher than without, probably owing to a slight heating produced by the vigorous stirring. It was found that the slight temperature fluctuations in the heating–cooling cycle of the bath were rapidly transmitted to the bomb yielding noticeable pressure fluctuations lagging by about 30 sec. However, near the critical point it was necessary to wait one hour or longer to be sure that true thermal equilibrium had been attained.

The xenon used in the measurements was part of the same sample used by Weinberger and Schneider supplemented by additional material of equivalent purity obtained from the Linde Air Products. Analysis with the mass spectrometer failed to disclose any detectable impurities. The material was roughly fractionated from time to time between runs.

Errors

The mean temperature of the bath could be controlled to better than ±0.001° C. for short periods and within ±0.002° C. overnight. The temperature oscillations during the heating cycle ripple were about ±0.001°. The sensitivity of the temperature measurements using a resistance thermometer and a Mueller bridge was about 0.0005° C. and the absolute accuracy is estimated to be ±0.002° C.

The sensitivity of the piston gauge was ±0.0003 atm. at 50 atm. and the reproducibility of the pressure measurements at times approached this—indicating a somewhat better degree of temperature control than ±0.001° which would correspond to ±0.001 atm. The absolute accuracy of the pressure measurements, which depends mainly on the calibration of the piston gauge, is estimated to be around ±0.005 atm.

The absolute accuracy of the density measurements is estimated to be ±0.2%, although relative accuracies are much greater.

On some occasions, it was found on repeating a series of measurements that the pressure values were higher or lower by an almost uniform amount of up to 0.002 atm. This is now believed to be due to an uncertainty in the contacts in the U-tube, partly the result of contact not always being estab-

lished at the extreme tip of the tungsten wire and partly due to a change in the curvature of the mercury surface. This contributes a somewhat further uncertainty to the pressure readings but has only a slight effect on the $(\partial P/\partial T)$ values which are used in the following paper.

MEASUREMENTS

The measurements were carried out in two series, (*a*) isotherms and (*b*) isochores. The first series was limited to temperatures in the immediate neighborhood of the critical temperature where it was desired to determine the exact shape of the isotherms as accurately as possible. Each isotherm included measurements of pressure at from 10 to 16 densities achieved by successive expansions from the bomb.

In series (*b*), isochores were determined at three densities above the critical density, at approximately the critical density, 8.4 moles/liter, and at 11 densities below, down to 2.5 moles/liter. Except for the three lowest densities, each covered the temperature interval from the two-phase region to 1.8° above the critical temperature and at the lowest densities measurements were carried to around 2° below the critical temperature, still in the gas region. A sufficient number of measurements were made in the two-phase region to establish the vapor pressure curve to 4° below the critical temperature. A major purpose of this series of measurements was to determine as accurately as possible the slopes of the isochores $(\partial P/\partial T)$ for use in calculating thermodynamic properties, and the experimental densities were chosen with this in view. The weight of the xenon was checked after each isochore to be sure that no leak had occurred which would tend to cause a steady decrease in pressure. Towards the end of the work a small leak did develop, amounting to around 50 mgm. out of a 15–20 gm. charge over the three or four days required for a run. This significantly affected the readings at the three lowest densities and corrections were applied, based on the slopes of the isotherms and assuming a steady rate of leakage.

The measurements are given in Tables I and II. The isochore measurements presented in Table II are given in the order in which they were obtained, determinations having been made with both increasing and decreasing temperatures, and successive measurements were made at the same temperature after the bomb had been allowed to stand overnight.

Fig. 2 is a small-scale plot showing most of the region covered by this work with the data of Table II plotted as isotherms. Individual points have not been shown since on this scale the scatter from the lines cannot be seen. The densities at which measurements were made are indicated by the arrows near the bottom of the figure.

In Fig. 3 the immediate critical region is shown on a larger scale using the data of Table I together with the isotherm at 16.690° from Fig. 2.

The results of Beattie, Barriault, and Brierley (1) at 16.65° are shown in Fig. 2. They reported that the xenon used in their investigation contained 0.14% krypton and this might account for their pressure being somewhat higher, agreeing almost with our 16.79° isotherm.

TABLE I

DENSITY–PRESSURE ISOTHERMS OF XENON NEAR THE CRITICAL POINT
Italicized values refer to two-phase region

16.550° C.		16.585° C.		15.590° C.	
Density, gm./ml.	Pressure, atm.	Density, gm./ml.	Pressure, atm.	Density, gm./ml.	Pressure, atm.
1.28383	57.6360	1.30426	57.7134	1.30705	57.7202
1.25847	57.6114	1.27870	57.6746	1.25890	57.6590
1.23352	57.5991	1.25268	57.6510	1.23305	57.6476
1.20875	57.5946	1.22686	57.6413		57.6505
1.18354	*57.5895*	1.20046	57.6332	1.20744	57.6398
1.15828	*57.5878*	1.17323	57.6318		57.6402
1.13320	*57.5870*	1.14733[a]	57.6319	1.18121	57.6370
1.10811	*57.5877*	*1.12343*	*57.6305*	1.15681	57.6358
1.08396	*57.5899*	*1.09576*	*57.6302*	1.13010	57.6360
1.05936	*57.5885*	1.06940[b]	57.6307		57.6367
1.03593	*57.5893*	1.04316	57.6298	1.10495	57.6358
1.01275	57.5871	1.01754	57.6273	1.07965	57.6361
0.98978	57.5806	0.99172	57.6212	1.05548	57.6353
0.96687	57.5742	0.96659	57.6120	1.03114	57.6347
0.94494	57.5611	0.94157	57.5973		57.6326
		0.91591	57.5744	1.00764	57.6308
		0.89197	57.5343	0.98294	57.6255
				0.96091	57.6131
				0.91503	57.5753

16.590° C.		16.600° C.		16.620° C.	
Density, gm./ml.	Pressure, atm.	Density, gm./ml.	Pressure, atm.	Density, gm./ml.	Pressure, atm.
1.30171	57.7118	1.29780	57.7195	1.27140	57.7077
1.27556	57.6731	1.27366	57.6849	1.24667	57.6899
1.24892	57.6522	1.24912	57.6668	1.22215	57.6788
	57.6554	1.22412	57.6587	1.19793	57.6735
1.22181	57.6436	1.20006	57.6534	1.17260	57.6721
1.19470	57.6380	1.17592	57.6484	1.14784	57.6680
1.16746	57.6361	1.15091	57.6483	1.12321	57.6658
1.13958	57.6356	1.12685	57.6475	1.09844	57.6655
	57.6365	1.10289	57.6473	1.07441	57.6633
1.11185	57.6358	1.07818	57.6466	1.05009	57.6643
1.08557	57.6354	1.05437	57.6469	1.02694	57.6624
1.05939	57.6349	1.03150	57.6446	1.00470	57.6582
1.03310	57.6331	1.00903	57.6423	0.98257	57.6496
1.00750	57.6311	0.98674	57.6384	0.95964	57.6397
	57.6318	0.96522	57.6260	0.93619	57.6234
0.98199	57.6248	0.92303	57.5886	0.91686	57.5984
0.95589	57.6138			0.87630	57.5248

[a] *Trace of gas.* [b] *Trace of liquid.*

TABLE II

TEMPERATURE–PRESSURE ISOCHORES OF XENON
Italicized values refer to two-phase region

1.27167 gm./ml. 9.6852 moles/l.		1.17819 gm./ml. 8.9733 moles/l.		1.14341 gm./ml. 8.7084 moles/l.	
Temp., ° C.	Pressure, atm.	Temp., ° C.	Pressure, atm.	Temp., ° C.	Pressure, atm.
16.378[a]	57.3853	*13.690*	*54.3397*	*16.190*	*57.1689*
16.490	57.5306	*14.290*	*55.0038*	*16.490*	*57.5211*
16.590	57.6646	*14.790*	*55.5674*	16.590	57.6374
16.690	57.7984	*15.290*	*56.1325*	16.690	57.7565
16.790	57.9329	*15.790*	*56.7055*		57.7573
16.890	58.0673	*16.190*	*57.1684*	16.790	57.8761
16.990	58.2050	*16.390*	*57.4023*	16.890	57.9967
17.190	58.4717	16.490	*57.5195*	16.990	58.1171
17.390	58.7414		*57.5201*	17.390	58.6013
17.590	59.0164	16.563[a]	..	18.390	59.8195
17.790	59.2889	16.590	57.6364	17.390	58.6016
17.990	59.5618	16.690	57.7575	16.990	58.1159
17.590	59.0153	16.790	57.8814	16.590	57.6365
17.190	58.4713	16.990	58.1289	*16.190*	*57.1681*
16.790	57.9342	17.190	58.3774		
16.390	57.4036	17.590	58.8753		
		17.990	59.3777		
			59.3773		
		18.390	59.8816		
		16.990	58.1295		
		16.790	57.8822		
		16.590	57.6376		
		16.390	*57.4036*		

1.09947 gm./ml. 8.3738 moles/l.		1.08216 gm./ml. 8.2451 moles/l.		1.07904 gm./ml. 8.2205 moles/l.	
Temp., ° C.	Pressure, atm.	Temp., ° C.	Pressure, atm.	Temp., ° C.	Pressure, atm.
16.190	*57.1697*	*12.721*	*53.2805*	*15.990*	*56.9362*
16.390	*57.4032*	*14.390*	*55.1181*	*16.190*	*57.1675*
16.590[a]	57.6364	*15.385*	*56.2430*	*16.390*	*57.4026*
16.690	57.7540	*15.890*	*56.8256*	*16.490*	*57.5203*
16.790	57.8722	*16.390*	*57.4042*		*57.5210*
16.990	58.1045	16.590	57.6382	16.590	57.6369
17.190	58.3411		57.6390	16.690	57.7542
17.590	58.8109	16.690	57.7542	16.790	57.8701
17.990	59.2815	16.790	57.8704	16.990	58.1030
18.390	59.7523	16.990	58.1034		58.1067
17.590	58.8127	17.190	58.3357	17.190	58.3366
16.990	58.1057		58.3363	17.390	58.5651
16.790	57.8713	17.590	58.7989	17.790	59.0340
16.590[a]	57.6359	17.990	59.2640	17.990	59.2634
16.490	*57.5206*	18.490	59.8437	18.190	59.4945
16.390	*57.4048*	*16.190*	*57.1704*		
		16.390	*57.4034*		
		16.590	57.6365		
			57.6370		
		16.690	57.7547		
		16.790	57.8720		

[a] *Maximum temperature of liquid-vapor coexistence.*

TABLE II–(*Continued*)

1.06706 gm./ml. 8.1269 moles/l.		1.05461 gm./ml. 8.0321 moles/l.		1.00835 gm./ml. 7.6798 moles/l.	
Temp., °C.	Pressure, atm.	Temp., °C.	Pressure, atm.	Temp., °C.	Pressure, atm.
16.290	*57.2845*	*14.890*	*55.6799*	*15.990*	*56.9366*
16.490	*57.5170*	*15.990*	*56.9407*	*16.190*	*57.1688*
	57.5188	*16.390*	*57.4021*	*16.390*	*57.4035*
16.590	57.6349	16.590	57.6368	16.506[a]	57.5370
16.690	57.7523	16.690	57.7525	16.690	57.7435
16.790	57.8674	16.790	57.8677	16.790	57.8519
16.990	58.0956	16.990	58.0961	16.990	58.0754
17.190	58.3280		58.0983		58.0745
17.590	58.7870	17.190	58.3279	17.390	58.5138
17.990	59.2474	17.590	58.7792	17.590	58.7326
18.390	59.7031	18.190	59.4606	17.790	58.9519
16.990	58.0975	18.390	59.6868	17.990	59.1677
16.790	57.8675	17.990	59.2333		59.1681
16.690	57.7517	16.990	58.0975	18.390	59.6056
16.590	57.6347	16.790	57.8700	17.990	59.1676
16.390	*57.4028*	16.690	57.7551	18.390	59.6047
		16.590	57.6408	17.190	58.2964
				17.390	58.5145
				16.790	57.8538
				16.690	57.7442
				16.590	57.6325
				16.513[a]	57.5449

0.96356 gm./ml. 7.3386 moles/l.		0.96048 gm./ml. 7.3151 moles/l.		0.86446 gm./ml. 6.5839 moles/l.	
Temp., °C.	Pressure, atm.	Temp., °C.	Pressure, atm.	Temp., °C.	Pressure, atm.
15.390	*56.2438*	*15.390*	*56.2480*	*15.190*	*56.0114*
15.790	*56.7018*	16.390[a]	57.4001	*15.390*	*56.2416*
15.990	*56.9351*	16.590	57.6178	*15.590*	*56.4704*
16.190	*57.1660*	16.790	57.8297	*15.690*	*56.5838*
16.372	*57.3788*	16.990	58.0395	15.740[a]	..
16.506	57.5271	17.190	58.2499	15.990	56.9003
16.590	57.6172	17.690	58.7739	16.290	57.1836
16.690	57.7235	18.390	59.4990	16.490	57.3715
16.790	57.8359	16.890	57.9358	16.590	57.4682
16.990	58.0458	16.690	57.7224	16.690	57.5594
17.190	58.2579	16.590	57.6176	16.790	57.6565
17.590	58.6760	16.490	57.5119	16.990	57.8405
17.990	59.0929	16.390[a]	57.3997	17.390	58.2150
18.390	59.5085	*16.290*	*57.2861*	17.890	58.6777
18.790	59.9269			18.390	59.1406
19.190	60.3410			16.790	57.6524
16.790	57.8318			16.090	56.9920
16.690	57.7256			15.890	56.8008
16.590	57.6192				56.7993
16.490	57.5122			15.790	56.6943
16.590	57.6193			*15.690*	*56.5858*

[a] *Maximum temperature of liquid-vapor coexistence.*

TABLE II–(*Concluded*)

0.74938 gm./ml. 5.7074 moles/l.		0.61835 gm./ml. 4.7094 moles/l.		0.33003 gm./ml. 2.5145 moles/l.	
Temp., ° C.	Pressure, atm.	Temp., ° C.	Pressure, atm.	Temp., ° C.	Pressure, atm.
14.790	55.3803	12.755	52.4665	14.046	40.7519
15.290	55.7823	14.690	53.6729	14.990	41.0089
15.790	56.1804		53.6738		41.0078
16.190	56.4945	15.373	54.0964	15.990	41.2805
16.490	56.7310	15.890	54.4101	16.990	41.5530
16.690	56.8864	16.790	54.9645		41.5550
16.990	57.1219	17.290	55.2661	17.990	41.8273
17.390	57.4343		55.2639	14.990	41.0074
17.790	57.7447	17.890	55.6289		
18.390	58.2099	18.390	55.9317		
16.190	56.5003	16.790	54.9564		
15.990	56.3434	16.390	54.7136		

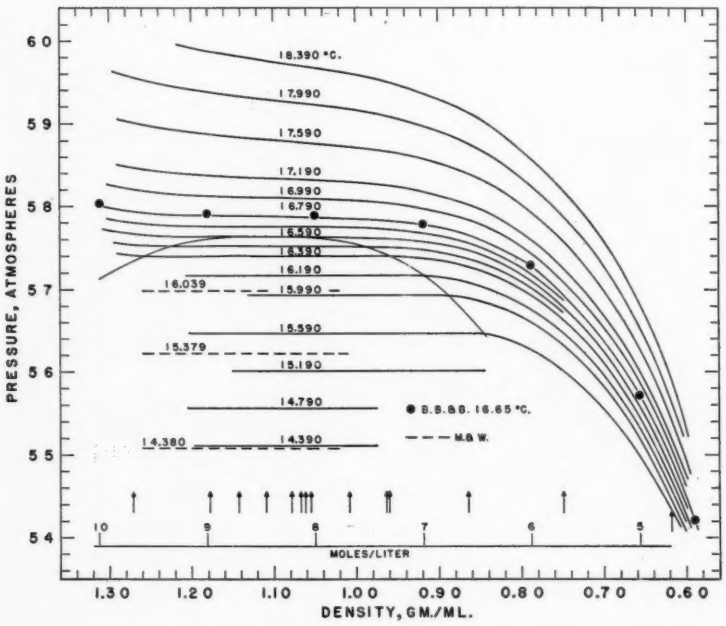

FIG. 2. Pressure–density isotherms of xenon plotted from isochore measurements. Densities at which measurements were made are indicated by arrows at the bottom of the figure.

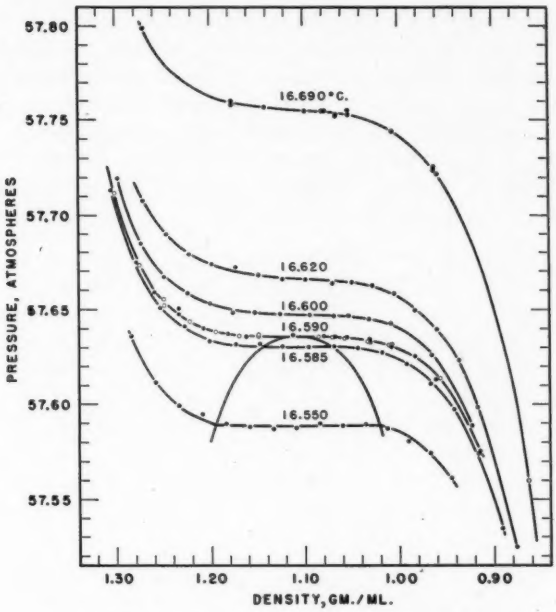

FIG. 3. Pressure–density isotherms of xenon in the immediate neighborhood of the critical point.

Vapor Pressure

Our pressure measurements in the two-phase region may be compared with the vapor pressure measurements of Michels and Wassenaar (10). Four of their values between 12.86° C. and 16.04° may be compared with a smoothed curve through our values and this is shown in Table III. The difference

TABLE III
VAPOR PRESSURE MEASUREMENTS
COMPARISON WITH MICHELS AND WASSENAAR (9)

Temp., °C.	Pressure, M. and W., atm.	Pressure, N.R.C. (smoothed), atm.	Δ M. and W. − N.R.C.
16.039	56.9917	56.9915	+0.0002
15.379	56.2289	56.2324	−0.0035
14.380	55.0868	55.1036	−0.0168
12.863	53.3871	53.4346	−0.0475

appears to increase more or less regularly with decreasing temperature but since we have only one measurement near the lowest value, it is difficult to tell whether this represents a significant trend.

Coexistence Curve

The liquid–vapor coexistence curve shown in Figs. 2 and 3 is that determined by Weinberger and Schneider (15). Our measurements were made

less precisely than theirs which bracketed the coexistence temperatures within one or two thousandths of a degree by repeated heating and cooling. Within about 0.04° of the critical temperature we agree approximately with their curve but beyond that on the low density side our observations correspond to a shift of the coexistence curve by about 1% towards higher density. Not enough measurements were made on the high density side to decide whether this corresponded to a shifting of the whole curve to higher densities or just a slight narrowing of the two-phase region.

Corrections for Nonuniform Density

The isotherms at 16.590°, 16.600°, and 16.620° in Fig. 3 have been corrected for the effect of the density gradient set up across the bomb due to gravitational effects. This results in a difference between the average filling density and the density at the level of pressure measurement. Using the method described previously (15), a curve of density *vs.* height was calculated from the uncorrected isotherm (drawn from the data in Table I). The bomb was then imagined to be divided into horizontal layers each 1 mm. thick. Assuming a given density at the level where the pressure was measured, 1 mm. above the center, the corresponding densities in the various layers were obtained from the curve and the approximate average density of the bomb contents calculated. The differences between these average densities and the densities 1 mm. above the center represented the corrections to be applied to the observed average densities. These corrections amounted to a maximum of 0.03 gm./ml. and resulted in a shifting of the experimental points away from the flattest part of the isotherms making the isotherms somewhat flatter still. In terms of pressure the maximum corrections, using the horizontal bomb, are only 0.0002 atm. and so may be neglected for most of the measurements. They would probably be significant for the isotherm at 16.585° but the calculations were a little more uncertain here and were not carried out.

DISCUSSION

Critical Temperature

We have taken the critical temperature to be 16.590° as found by Weinberger and Schneider. From our observations we believe that this represents within ±(0.002–0.003°) the temperature of meniscus disappearance. When a critical filling of xenon at this temperature is allowed to settle after it has been thoroughly stirred, it separates after about one hour into two layers of rather light opalescence separated by a band of dark brown opalescence. After 12–24 hr. this band has become very dark and narrowed to about 1 mm. in thickness. It is not possible, however, to see a sharp surface. Lowering the temperature 0.002° to 0.003° produces a definite dividing line in the middle of the opalescent band. During the measurements at 16.585° an unmistakable surface was present and the observed density range of the two-phase region was in good agreement with the coexistence curve of Weinberger and Schneider. At 16.600° and even at 16.620° there was slow stratification on standing, with a middle layer of heavier opalescence which, however, did not become so concentrated as at 16.590°.

The critical temperature may also be estimated as the highest temperature at which $(\partial P/\partial \rho)_T = 0$ by plotting the minimum slopes of the P–ρ isotherms against temperature. The slopes were determined from large-scale plots and the minimum values are shown in Fig. 4. The three isotherms nearest the

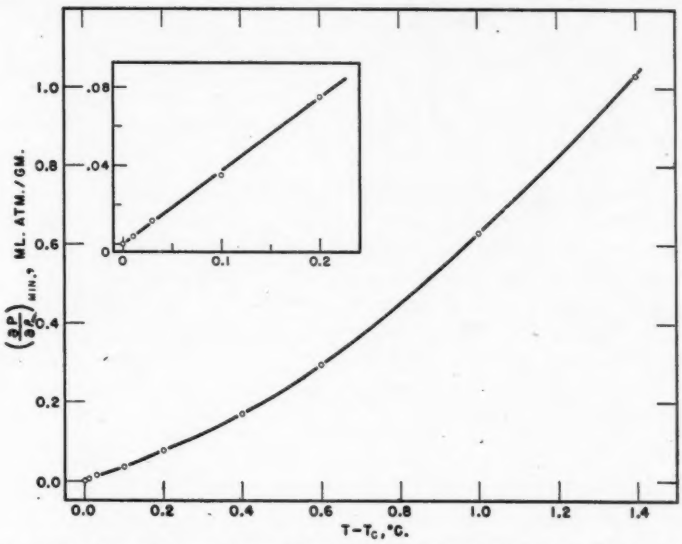

FIG. 4. Plot of the minimum slopes of the isotherms at and above the critical temperature. The immediate critical region is shown in the insert.

critical temperature can be drawn more accurately than the others which were taken from the isochore measurements and hence only included three densities above the critical density. However, the graph gives no reason for believing that the maximum temperature of zero slope differs from the temperature of meniscus disappearance.

For carbon dioxide Michels *et al.* (9) found that $(\partial P/\partial \rho)_{\min}$ was linear in temperature up to 0.5° above the critical temperature. MacCormack and Schneider (6) for sulphur hexafluoride over a range of 1.5° found a curve somewhat similar in shape to ours.

Critical Density

The critical density may be estimated, in a manner similar to that used for the critical temperature, by plotting the densities of minimum slope of the isotherms against temperature. This has been done in Fig. 5. A straight line through the points indicates a critical density of 1.099 gm./ml. but it is doubtful from the scatter of the points whether the assumption of such a linear relationship is justified. The rectilinear diameter for the liquid–vapor coexistence curve found by Weinberger and Schneider is also shown in Fig. 5 and this gives a critical density of 1.105 gm./ml. As stated earlier, our coexistence observations would indicate, if anything, a still higher critical

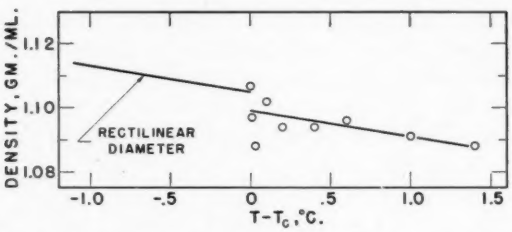

FIG. 5. Densities of minimum slopes of the isotherms at and above the critical temperature. The rectilinear diameter of the liquid–vapor coexistence curve is also shown.

density. Thus, it appears unlikely that a linear continuation of the rectilinear diameter above the critical temperature would include the densities of minimum slope of the isotherms. The coexistence curve reported by Whiteway and Mason gave a critical density of 1.110 ± 0.002 gm./ml.

An alternative method of estimating the critical density from the PVT measurements is to plot $(\partial^2 P/\partial T^2)$ at the critical temperature against density, the critical density then being the density where this quantity becomes zero. Such a plot is shown in the following paper and it also gives a value for the critical density of 1.099 gm./ml.

Critical Pressure

The critical pressure is obtained directly from the critical isotherm as 57.636 ± 0.005 atm.

Relationship to Theories of the Critical State

Mayer has recently discussed (7) the status of three of the current theories which predict the nature of the critical isotherms. The simple "derby hat" picture of Mayer and Harrison (8) predicts flat, horizontal isotherms at temperatures above the temperature of meniscus disappearance; the modified "derby hat" theory of Rice (12) predicts a flat, horizontal critical isotherm with linear but sloping isotherms immediately above the critical temperature; and the singular point theory of Zimm (19) describes the critical point as a singularity in the critical isotherm where all derivatives of P with respect to ρ are zero.

Our critical isotherm is significantly flatter and broader than that corresponding to the van der Waals equation and, indeed, over a short density range and within the experimental uncertainty could be fitted as well to a horizontal line as to a curve. It was shown in a previous publication (16) that the observed density distributions resulting from the gravitational field in a vertical tube at the critical point are not in good agreement with a van der Waals isotherm but can be quantitatively accounted for by the present isotherm.

Our measurements offer no support for the Mayer–Harrison theory since there is no obvious region of flat, horizontal isotherms above the critical temperature. The isotherms could be easily reconciled with either the second or third theory although Rice's theory would predict a flattopped coexistence

curve whereas the observed coexistence curve (15) appeared to be definitely rounded at the apex.

In connection with the third picture we have calculated $(\partial^2 P/\partial \rho^2)$ by numerical differentiation from our smoothed critical isotherm. These values are plotted in Fig. 6 together with the corresponding values calculated for a van

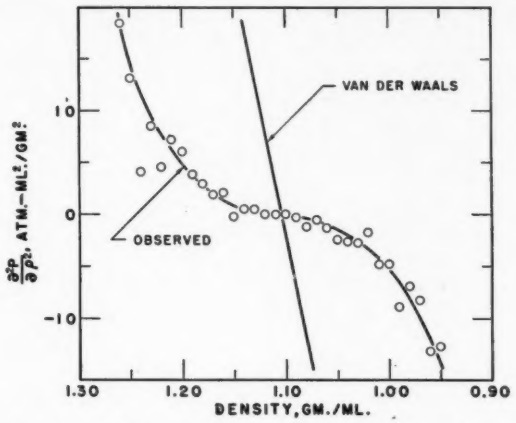

FIG. 6. $\partial^2 P/\partial \rho^2$ for the critical isotherm and for a van der Waals isotherm.

der Waals critical isotherm using the experimentally determined critical constants. The degree to which the experimental isotherm is flatter than the van der Waals isotherm is clearly seen. The curve from the experimental isotherm, while having a considerable degree of uncertainty, suggests that at the critical point the third derivative of P with respect to ρ is very close to zero and the fourth derivative is identically so, since this is a point of inflection.

ACKNOWLEDGMENT

The authors wish to express their thanks to Mr. A. Stevenson for help in the design and construction of the apparatus, to Mr. G. Ensell for making the glass bombs and the glass capillaries in the U-tube, and to Dr. F. P. Lossing and his associates for the mass spectrometer analysis.

REFERENCES

1. BEATTIE, J. A., BARRIAULT, R. J., and BRIERLEY, J. S. J. Chem. Phys. 19: 1219. 1951.
2. CHYNOWETH, A. G. and SCHNEIDER, W. G. J. Chem. Phys. 20: 1777. 1952.
3. GOUY, G. Compt. rend. 115: 720. 1892.
4. HABGOOD, H. W. and SCHNEIDER, W. G. J. Chem. Phys. 21: 2080. 1953.
5. HABGOOD, H. W. and SCHNEIDER, W. G. Can. J. Chem. 32: 164. 1954.
6. MACCORMACK, K. E. and SCHNEIDER, W. G. Can. J. Chem. 29: 699. 1951.
7. MAYER, J. E. Changement de phases. Compte rendu de la deuxième réunion annuelle de la société de chimie physique, Paris. 1952. p. 35.
8. MAYER, J. E. and HARRISON, S. F. J. Chem. Phys. 6: 87. 101. 1938.
9. MICHELS, A., BLAISSE, B., and MICHELS, C. Proc. Roy Soc. (London), A, 160: 358. 1937.
10. MICHELS, A. and WASSENAAR, T. Physica, 16: 253. 1950.
11. PALMER, H. B. Schlieren optical studies in the critical region. University of Wisconsin, Department of Chemistry Publication CM-740, Madison, 1952.
12. RICE, O. K. J. Chem. Phys. 15: 314. 1947.

13. SCHNEIDER, W. G. Changement de phases. Compte rendu de la deuxième réunion annuelle de la société de chimie physique, Paris. 1952. p. 69.
14. WEINBERGER, M. A., HABGOOD, H. W., and SCHNEIDER, W. G. Can. J. Chem. 30: 815. 1952.
15. WEINBERGER, M. A. and SCHNEIDER, W. G. Can. J. Chem. 30: 422. 1952.
16. WEINBERGER, M. A. and SCHNEIDER, W. G. Can. J. Chem. 30: 847. 1952.
17. WENTORF, R. H. and BOYD, C. A. Isotherms in the critical regions of carbon dioxide and sulfur hexafluoride. University of Wisconsin, Department of Chemistry, Publication CM-724, Madison. 1952.
18. WHITEWAY, S. G. and MASON, S. G. Can. J. Chem. 31: 569. 1953.
19. ZIMM, B. H. J. Chem. Phys. 19: 1019. 1951.

THE PHOTOLYSIS OF MERCURY DIMETHYL WITH DEUTERIUM[1]

By Richard E. Rebbert[2] and E. W. R. Steacie

ABSTRACT

Mercury dimethyl was photolyzed in the presence of deuterium in the temperature range from 27°C. to 253°C. The activation energy for the reaction

$$CH_3 + D_2 \rightarrow CH_3D + D$$

was found to be 12.7 ± 0.5 kcal./mole. This is in satisfactory agreement with the work done with acetone and deuterium.

INTRODUCTION

Recently a very extensive investigation was carried out in this laboratory of the reaction of methyl and deuterated methyl radicals with hydrogen, deuterium, and deuterium hydride (2, 7). However, in all this work the methyl radicals were obtained from the photolysis of acetone and the temperature was kept above 135°C. It was thought profitable to reinvestigate some of these reactions using mercury dimethyl as the source of methyl radicals.

Earlier work using the photolysis of mercury dimethyl to investigate the reaction

$$CH_3 + H_2 \rightarrow CH_4 + H$$

gave a very definite curvature in the Arrhenius plot below 100°C. (4). This has been interpreted by some as evidence of "hot" radicals. However, above 100°C. the activation energy obtained agrees very well with the results from the photolysis of acetone with hydrogen. Unfortunately the amount of methane obtained at very low temperatures is too small to measure accurately. Phibbs and Darwent decomposed about 30 per cent of their mercury dimethyl at low temperatures in order to get enough methane to measure accurately. However, if deuterium is used in place of hydrogen, one needs only to measure the ratio CH_3D/CH_4 which can be done fairly accurately on a mass spectrometer even at low temperatures and low percentage conversions. This was our reason for choosing deuterium. In the present work the CH_3D/CH_4 ratio was in the range 1.00 to 3.00. In this range the ratio can be determined with an accuracy of from 2 to 4%.

EXPERIMENTAL

Apparatus

The apparatus was the same as that used in the previous work on the photolysis of mercury dimethyl (6) with the exception that a palladium thimble was used to get rid of the excess deuterium after photolysis and also to purify the deuterium before the reaction.

The quartz reaction cell had a volume of 179.5 cc. and since the light beam almost completely filled the cell, the volume of the cell was considered to be the

[1] *Manuscript received September 17, 1953.*
Contribution from the Division of Pure Chemistry, National Research Council, Ottawa, Canada. Issued as N.R.C. No. 3159.

[2] *National Research Council of Canada Postdoctorate Fellow 1951-53.*

reaction volume. Neutral density filters were used at low temperatures to reduce the intensity in the hope of increasing the amount of methane formed relative to the ethane formation.

Material

The mercury dimethyl was obtained from the Delta Chemical Works and fractionated. It was better than 99 per cent pure. Commercial cylinder deuterium was used and this was purified by passing it through a palladium thimble at approximately 350°C. This was analyzed on the mass spectrometer and contained 3% HD and a very small amount of H_2. A small correction was applied for the presence of deuterium hydride.

Method of Calculation

When mercury dimethyl is photolyzed alone methane and ethane are produced by the reactions

$$CH_3 + Hg(CH_3)_2 \rightarrow CH_4 + CH_3HgCH_2 \qquad [1']$$

and

$$2CH_3 \rightarrow C_2H_6. \qquad [2]$$

In the presence of deuterium we also have the reaction

$$CH_3 + D_2 \rightarrow CH_3D + D. \qquad [1]$$

Also, owing to the 3% HD, we will have the following reactions occurring to a small extent—

$$CH_3 + HD \rightarrow CH_4 + D \qquad [3]$$

$$CH_3 + DH \rightarrow CH_3D + H. \qquad [4]$$

Thus the total rate of formation of deuterated methanes will be

$$R^T_{CH_3D} = R^1{}_{H_3D} + R^4{}_{H_3D} = k_1[CH_3][D_2] + k_4[CH_3][HD]$$

and the total rate of formation of methane will be

$$R^T_{CH_4} = R^{1'}_{CH_4} + R^3_{CH_4} = k_1'[CH_3][Hg(CH_3)_2] + k_3[CH_3][HD].$$

Therefore, we have

$$\frac{R^T_{CH_3D}}{R^T_{CH_4}} = \frac{\dfrac{k_1}{k_{1'}}\dfrac{[D_2]}{[Hg(CH_3)_2]} + \dfrac{k_4}{k_{1'}}\dfrac{[HD]}{[Hg(CH_3)_2]}}{1 + \dfrac{k_3}{k_{1'}}\dfrac{[HD]}{[Hg(CH_3)_2]}}$$

or

$$\frac{k_1}{k_2^{\frac{1}{2}}} = \frac{k_1'}{k_2^{\frac{1}{2}}}\left\{\frac{R^T_{CH_3D}}{R^T_{CH_4}}\frac{[Hg(CH_3)_2]}{[D_2]} + \frac{R^T_{CH_3D}}{R^T_{CH_4}}\cdot\frac{k_3}{k_{1'}}\frac{[HD]}{[D_2]} - \frac{k_4}{k_{1'}}\frac{[HD]}{[D_2]}\right\}.$$

We can measure the ratio $R^T_{CH_3D}/R^T_{CH_4}$ on the mass spectrometer. We know the concentration of mercury dimethyl, deuterium, and deuterium hydride. $k_1'/k_2^{\frac{1}{2}}$ was previously measured (5), and $k_3/k_2^{\frac{1}{2}}$ and $k_4/k_2^{\frac{1}{2}}$ have been determined by Whittle and Steacie (7). The second and third terms in the above equation are the correction terms needed because of the presence of deuterium hydride in

the deuterium sample. Together they amount to about 10 per cent of the uncorrected term.

There is no doubt that the above mechanism is incomplete and that there are some complications (1, 3). However, a recent investigation (5) has shown that *under the conditions used here* the simple mechanism is adequate.

The intensities employed in the present investigation were varied at different temperatures in order to obtain sufficient methane to permit accurate analysis. In all cases, however, the intensities were in the range in which we have previously shown (5) that the ratio $k_1/k_2^{\frac{1}{2}}$ is independent of intensity. The experiments in the temperature range 378–526°C. were at the same intensities as the highest intensity runs in the previous work. The run at 347°C. was at an intensity one-half as great, and those at the lowest temperatures were at intensities 1/15th as great.

Results

The results are given in Table I and they are plotted in Fig. 1. Also in Fig. 1 the results from the photolysis of acetone with deuterium (2) are plotted. The agreement between the two sources of methyl radicals is seen to be very good. The best line through the points has been found by the method of least squares to be

$$13 + \log k_1/k_2^{\frac{1}{2}} = 6.70 - (2778/T).$$

The slope of this line gives a value of 12.7 kcal. per mole for $E_1 - \frac{1}{2}E_2$. The results from acetone give 11.7 kcal. per mole for this activation energy. Usually

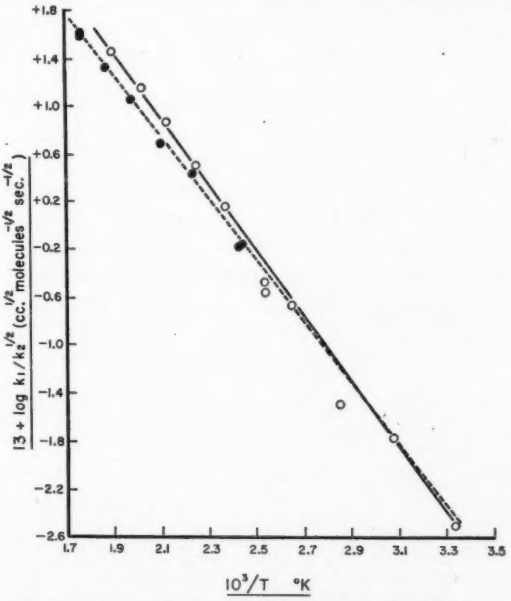

FIG. 1. Reaction of methyl radicals with deuterium.
Open circles—mercury dimethyl photolysis.
Filled circles—acetone photolysis.

TABLE I

THE PHOTOLYSIS OF MERCURY DIMETHYL WITH DEUTERIUM

Temp., °K.	Pressure of $Hg(CH_3)_2$, mm.	Pressure of D_2, mm.	CH_3D/CH_4	$k_1/k_2^{\frac{1}{2}} \times 10^{13}$
300	29.8	116.0	1.00	0.0033
324	31.6	129.0	1.46	0.0182
347	34.7	153.7	1.00	0.0339
378	37.9	136.7	1.55	0.229
395	39.4	159.7	1.42	0.339
395	41.0	134.9	0.98	0.282
422	43.0	153.7	2.32	1.52
446	46.7	159.4	2.40	3.24
472	47.1	174.6	3.03	7.41
496	49.6	148.1	2.55	13.5
526	51.6	113.8	2.08	27.5

about 5 per cent of the mercury dimethyl was decomposed and in no case was more than 10 per cent of the mercury dimethyl photolyzed.

DISCUSSION

The present work gives added proof in support of the lower value for the activation energy, namely about 12 kcal. per mole, for the reaction of a methyl radical with deuterium. Thus we have the following situation for this reaction—

	E_1 in kcal. per mole
Majury and Steacie (source: acetone)	11.7
Whittle and Steacie (source: acetone)	11.8
Davison and Burton (source: acetone)	12.2—12.7*
Rebbert and Steacie (source: mercury dimethyl)	12.7

**Corrected by Wijnen and Steacie, Faraday Soc. Discussions, 14: 118. 1953.*

In view of this agreement we consider the low value for this reaction to be established.

The agreement between results with acetone and mercury dimethyl indicates that the results are not affected by "hot" radical effects, under the conditions employed. Even at room temperature, under our conditions, there are no indications of any deviation from the Arrhenius plot on this account. This does not, of course, preclude the occurrence of hot radical effects with mercury dimethyl under certain special conditions (3).

ACKNOWLEDGMENT

We are indebted to Miss Frances Gauthier of these laboratories for the mass spectrometric analyses used in this work.

REFERENCES

1. GOMER, R. and NOYES, W. A., JR. J. Am. Chem. Soc. 71: 3390. 1949.
2. MAJURY, T. G. and STEACIE, E. W. R. Can. J. Chem. 30: 800. 1952.
3. MARTIN, R. B. and NOYES, W. A., JR. J. Am. Chem. Soc. 75: 4183. 1953.
4. PHIBBS, M. K. and DARWENT, B. DEB. Trans. Faraday Soc. 45: 541. 1949.
5. REBBERT, R. E. and STEACIE, E. W. R. Can. J. Chem. 31: 631. 1953.
6. REBBERT, R. E. and STEACIE, E. W. R. J. Chem. Phys. 21: 1723. 1953.
7. WHITTLE, E. and STEACIE, E. W. R. J. Chem. Phys. 21: 993. 1953.

HYDROGEN PEROXIDE: THE LOW TEMPERATURE HEAT CAPACITY OF THE SOLID AND THE THIRD LAW ENTROPY[1]

By Paul A. Giguère[2], I. D. Liu[2,3], J. S. Dugdale[4], and J. A. Morrison[5]

ABSTRACT

The heat capacity of crystalline hydrogen peroxide between 12° K. and the melting point has been determined with a low temperature adiabatic calorimeter. The heat of fusion was also measured and found to be 2987 ± 3 cal./mole. The two samples of hydrogen peroxide used were 99.97 mole % pure as deduced from behavior on melting and from premelting heat capacities; the triple point was estimated to be 272.74° K.

The only anomaly observed in the heat capacity measurements was the absorption of 1.3 cal./mole at 216.8 ± 0.15° K., the lower eutectic temperature of H_2O–H_2O_2 solutions. Such an effect is to be expected if the only significant impurity is water. The entropy of hydrogen peroxide as an ideal gas at 1 atm. pressure and 25° C. computed from the thermal measurements is 55.76 ± 0.12 cal./mole deg. Comparison of this datum with the recalculated statistical entropy leads to a value of 3.5 kcal./mole for the height of a hypothetical single barrier hindering internal rotation in the molecule. From these results it is concluded that hydrogen peroxide does not consist of two tautomeric modifications.

INTRODUCTION

Knowledge of the thermal properties of solid hydrogen peroxide has hitherto been fragmentary and uncertain (15, 5). The accurate determination of the heat capacity of the compound in the solid state down to low temperatures was considered to be of special interest, primarily because it would make possible a calculation of the third law entropy. An X-ray investigation of the crystal structure of hydrogen peroxide (1) has shown that it should not retain any appreciable residual entropy at the absolute zero. On the other hand, evaluation of the statistical entropy of the ideal gas from structural and spectroscopic data (7) is hampered by the lack of sufficient information on the internal rotation of the two OH groups in the molecule. The potential barrier restricting that motion is expected to have two unequal maxima (22) which makes difficult a rigorous calculation of the contribution of that internal degree of freedom to the various thermodynamic functions. Another important point is the question of whether transitions (18) and tautomeric forms (6) of hydrogen peroxide exist in the solid state (cf. Discussions of the Faraday Society, 14: 140–142. 1953).

Because of the tendency of hydrogen peroxide to decompose spontaneously in contact with most materials, the project held certain experimental difficulties. For convenience, the work was divided between two laboratories, one

[1] *Manuscript received November 13, 1953.*
Joint contribution from the Department of Chemistry, Laval University, Quebec, Quebec, and the Division of Pure Chemistry, National Research Council, Ottawa, Canada. Issued as N.R.C. No. 3158.
[2] *Laval University.*
[3] *Holder of a Fellowship from the Bureau of Scientific Research of the Province of Quebec.*
[4] *National Research Laboratories Postdoctorate Fellow.*
[5] *National Research Laboratories.*

at Laval University where facilities existed for preparing the samples of pure hydrogen peroxide and for sealing them in suitable containers, and the other at the National Research Council where the calorimetric measurements could be made.

EXPERIMENTAL

The Preparation of the Samples

The starting material for preparing the pure hydrogen peroxide was the very stable 90% solution supplied by the Buffalo Electro-Chemical Company. Some six liters of this solution was concentrated to about 99.6% hydrogen peroxide by distillation at reduced pressure through a 1 meter fractionating column filled with small glass helices and heated electrically to prevent flooding. Extensive precautions were taken to avoid contamination of the solution. All glassware was treated with fuming sulphuric acid following the procedure recommended by Huckaba and Keyes (11). The still was assembled through ground glass-joints on which only a trace of silicone grease was used. A fritted glass disc was placed on the vacuum line to filter off all dust particles from the air let in after a distillation.

Further concentration of the peroxide was achieved by fractional crystallization as described elsewhere (4). The apparatus was made simpler by using a straight filtering tube with the two flasks connected at each end. For separating the solid from the mother liquor the whole assembly was merely turned upside down and then suction was applied at the outlet tube. The entire operation was rendered still more effective by growing a single large crystal instead of a mass of tiny ones. To this end the flask filled with some 700 gm. of concentrated peroxide solution was wrapped in a thick glass-wool lagging before it was placed in an ice machine at $-10°$ C. Crystallization was initiated by seeding and it proceeded very slowly (two days for solidification of about 90% of the sample). The progress of purification was followed by measuring the freezing point (4) which did not change further after three or four operations.

The Calorimeter Vessels

Having once prepared the pure hydrogen peroxide it was important that it should not come in contact with anything except very inert materials such as specially treated glass or pure aluminum. For this reason and because glass-to-aluminum seals are not available, the calorimeter vessels were made entirely of pure (1S) aluminum. As will be seen from Fig. 1, the construction was such that no soldering or brazing was used. The tapered re-entrant well in the base of the calorimeter receives the thermometer–heater assembly. With this design the thermometer may be attached after the filling of the calorimeter is completed. The resistance thermometer and calorimeter heater were cast with Wood's metal into a tapered brass tube which fitted closely the tapered re-entrant well. The brass tube was held firmly in place with a threaded collar which screwed into the bottom of each vessel. Thermal contact between the brass tube and the well was enhanced by a light film of silicone grease.

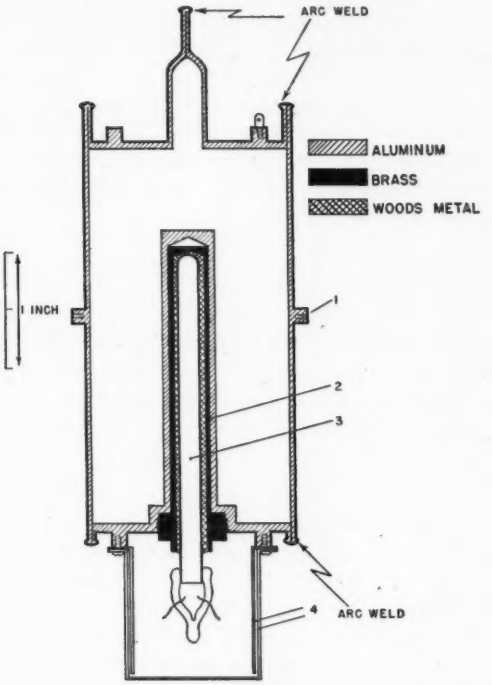

FIG. 1. Aluminum calorimeter vessel. 1. Point of attachment of difference thermocouple. 2. Tapered brass tube. 3. Platinum resistance thermometer. 4. Anchoring ring for lead wires and radiation shield.

The Filling of the Calorimeter Vessels

Although special precautions were taken in assembling the calorimeter vessels, their inside surfaces needed extensive passivation treatment before use. This long and tedious operation involved the following steps. The metal was first degreased by rinsing with acetone and then treated for a few minutes with a 3% solution of sodium hydroxide followed by numerous rinsings with distilled water. Thereafter each vessel was filled with 25% nitric acid, allowed to stand for several hours, and washed again thoroughly with distilled water. Finally, repeated fillings with solutions of hydrogen peroxide of increasing concentration from 30% to 99% over a period of a few weeks brought the surfaces to a satisfactory level of inertness in the case of three out of the six vessels originally made. The rate of decomposition of 99% hydrogen peroxide in these was of the order of 0.001% in 24 hr. at room temperature and less than one tenth of this at 0°, which was deemed entirely safe.

After prolonged evacuation for drying, the vessels were filled with helium gas at atmospheric pressure for better thermal conductivity, and the pure liquid peroxide was poured in directly. A temporary closure was effected at once by pinching off the thin filling tubes, and after the vessels were accurately

weighed, the tubes were welded in an argon arc with the containers immersed in ice water to prevent decomposition of the peroxide. They were then cooled gradually to the temperature of dry ice and were kept at this temperature during transport to the National Research Laboratories in Ottawa. It was assumed that the rate of decomposition of the frozen peroxide would be negligible, and this was confirmed by the subsequent experiments. At no time during the experiments was there any sign of thermal effects due to decomposition of the hydrogen peroxide.

The Cryostat

The cryostat used for this work was similar to one already described in a previous publication (20). Adiabatic operation was possible over the entire temperature range from 11° K. The design of the cryostat proved to be particularly convenient for mounting the calorimeter vessel without melting the sample of hydrogen peroxide. By careful arrangement of the procedure it was possible to assemble the cryostat in about an hour, during which time the temperature of the calorimeter vessel rose from that of dry ice to about −5° C.

The Measurements

The resistance of the platinum thermometer and the energy supplied to the calorimeter were measured after the methods which have become standard for this type of work (26). All of the measurements were made with a White double potentiometer. The standard resistors and standard cells have been checked periodically against standards maintained by the Division of Physics of the National Research Laboratories. Time of input of energy to the calorimeter was determined with a synchronous clock operated from a constant frequency power supply through a switch coupled directly to that controlling the heater current. The indications of the clock have been checked many times by comparison with the time signals from the Dominion Observatory. The error in the clock has never exceeded 0.02 seconds. Platinum resistance thermometer T-3 was used for this work. The calibration of this thermometer has been described elsewhere (14).

RESULTS

The Heat Capacity

Of the three different samples of hydrogen peroxide prepared in separate calorimeter vessels only two were used for the measurements (containing 3.3706 and 2.9175 moles respectively). Since it was not known beforehand whether or not the peroxide would decompose appreciably on melting (8), it seemed preferable to measure the heat capacity with one sample and the heat of fusion with the other.

The results are given in Table I as smoothed values of the heat capacity at rounded values of the temperature. (In all the calculations the calorie was taken equal to 4.184 absolute joules). The difference plot in Fig. 2 shows the deviations of the experimental results from a smooth curve. It will be noted that over most of the temperature range the mean precision was better than 0.1%; below 30° K. the uncertainty was greater (of the order of 0.3%).

TABLE I
THE HEAT CAPACITY OF SOLID HYDROGEN PEROXIDE

T, ° K.	C_p, cal./mole deg.	T, ° K.	C_p, cal./mole deg.
12	0.062	70	4.188
13	0.079	75	4.545
14	0.099	80	4.895
15	0.124	85	5.243
16	0.151	90	5.568
17	0.181	95	5.865
18	0.215	100	6.144
19	0.253	110	6.676
20	0.295	120	7.164
22	0.387	130	7.614
24	0.494	140	8.039
26	0.611	150	8.438
28	0.735	160	8.822
30	0.872	170	9.191
32	1.015	180	9.556
34	1.165	190	9.917
36	1.325	200	10.283
38	1.484	210	10.657
40	1.648	220	11.044
42	1.815	230	11.437
44	1.985	240	11.857
46	2.157	250	12.30*
48	2.328	255	12.57*
50	2.505	260	12.98*
55	2.941	265	13.83*
60	3.372	268	15.70*
65	3.794		

* *Marked premelting.*

Premelting of the solid became evident around 250° K. as illustrated in Fig. 3. A few measurements of the heat capacity of the second sample made in the region above 250° K. yielded results indistinguishable from those obtained with the first sample. The dotted line in Fig. 3 represents the heat capacity of pure solid hydrogen peroxide estimated as described below. Calculations showed that the correction to be applied for evaporation into the dead space of the calorimeter was negligible.

During the heat capacity measurements on the first sample a small absorption of energy was detected around 217° K. The amount of heat involved seemed to depend upon the extent to which the calorimeter had been cooled previously. After cooling to temperatures below 77° K., the energy amounted to 3.4 cal. while with cooling to around 200° K. it was only 1.9 cal. An attempt was made to determine the temperature region over which this energy was absorbed by following the temperature of the calorimeter while it received energy at a constant rate from its surroundings. From this experiment it appeared that the heat was absorbed between 216.78° and 216.94° K. That this effect was due to the melting of an eutectic mixture of hydrogen peroxide and the addition compound $H_2O_2 \cdot 2H_2O$ is suggested by two facts. First, the temperature region is very close to the eutectic temperature reported by Foley and Giguère (216.7° K. (4)). Second, assuming the eutectic mixture to be an ideal one and the impurity present (0.032 mole %—see below) to be

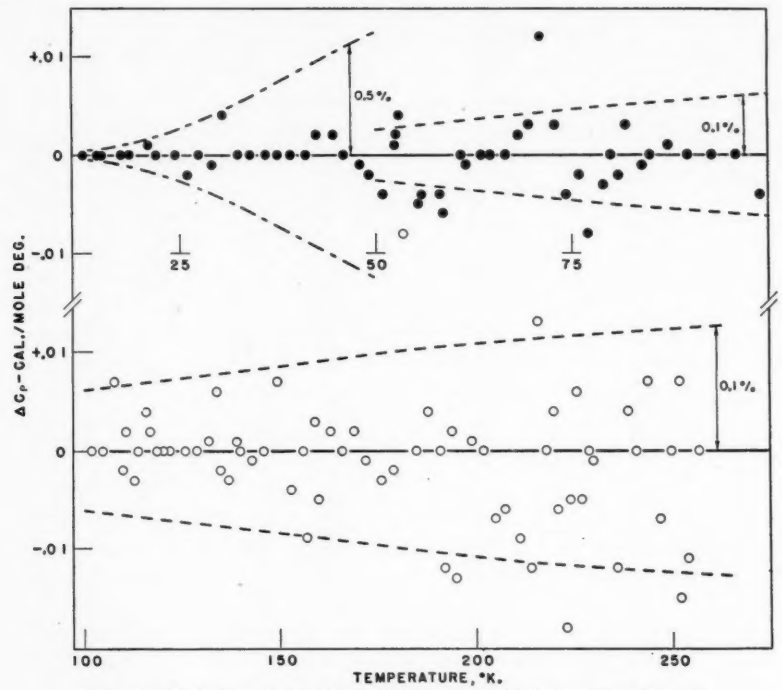

FIG. 2. Deviations of experimental heat capacities from a smooth curve.

entirely water, the calculated energy to be expected at the eutectic temperature is 3.9 cal., which agrees very well with the maximum amount found experimentally.

Apart from this absorption of energy, no other anomalies were observed. It is estimated that at the higher temperatures any transition involving an energy greater than 0.1 cal./mole concentrated in a temperature interval of 4° or less would be detected in these measurements; at the lower temperatures even smaller quantities are detectable.

The Heat of Fusion

The heat of fusion of hydrogen peroxide was determined by measuring the energy required to heat the calorimeter and the second sample over a temperature interval which included the triple point. From this quantity was subtracted the energy required to heat (*a*) the pure solid up to the triple point, (*b*) the liquid from the triple point to the final temperature, and (*c*) the calorimeter vessel from the initial to the final temperature. The premelting energy is then included in the heat of fusion. The value so obtained was 2987 ± 3 cal./mole which may be compared with 2920 cal./mole determined by Foley and Giguère (5) using an ice calorimeter. The latter value is based upon a rather uncertain estimate of the heat capacity of the solid just below the melting point. However, using the corrected heat capacity of the solid does not remove the discrepancy.

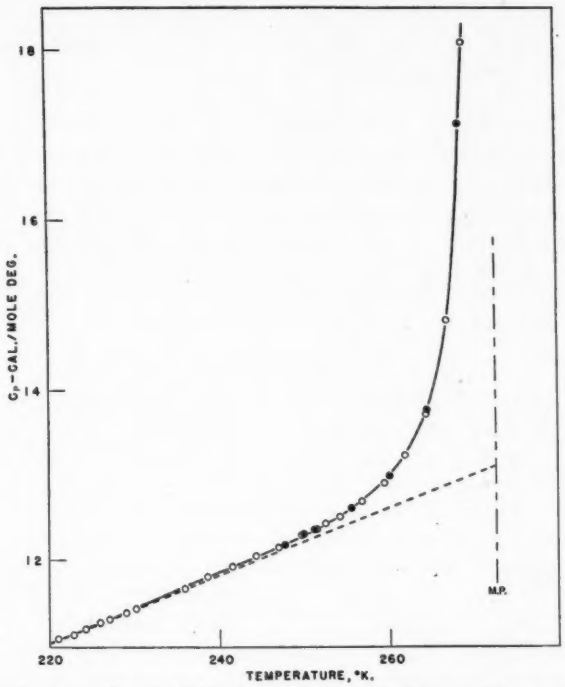

FIG. 3. The heat capacity of solid hydrogen peroxide in the premelting region. ○ — Sample 1. ● — Sample 2. ----- Pure solid (equation [1]).

The Purity of the Samples

The melting temperatures as a function of the fraction melted are given in Table II. From these results the calculated triple point of hydrogen peroxide is 272.74° K. and the estimated impurity content 0.032 mole %.

TABLE II
THE MELTING POINT OF H_2O_2
(0° C. = 273.16° K.)

% Melted	T, ° K.
49.9	272.708
65.2	272.714
98.8	272.725
100	272.725

Impurity: 0.032 mole %.
Triple point: 272.74° K.

The degree of purity of the hydrogen peroxide used could also be estimated from the heat capacity in the premelting region. The excess heat capacity was calculated using (*a*) the phase diagram for the system H_2O–H_2O_2 (4) and (*b*) a constant value for the heat of fusion (2987 cal./mole). The amount of impurity was then so chosen that the derived heat capacity of the pure solid

was a linear function of the temperature. A calculated impurity of 0.038 mole % together with the expression for the heat capacity of the pure solid (plotted in Fig. 3)

$$[1] \qquad C_p = 2.31 + 0.03967\ T \text{ cal./mole deg.}$$

suffice to represent the experimental results very closely between 220° and 271° K. The good agreement between the estimates of impurity from the melting temperatures and from the premelting heat capacities, as well as the shape of the heat capacity curve in the premelting region (2) provide definite evidence that the impurity (water) does not form solid solutions with hydrogen peroxide. This confirms the results of two independent investigations of phase equilibria in this binary system (4, 18).

DISCUSSION

The first important conclusion to be drawn from the above results is that there are no transitions either of the first or the second order in solid hydrogen peroxide, notwithstanding assertions to the contrary (18). This provides further evidence that ordinary hydrogen peroxide contains no measurable proportion of a tautomeric form, H_2O–O, as has been suggested (29). Numerous structural studies as well as recent measurements of the magnetic susceptibility of the solid (21) and of the ionization potential of the molecule (25) may be cited in support of this conclusion. On the other hand the possibility is not ruled out that an unstable isomer, such as proposed by Geib and Harteck (6), could be formed under special conditions (low temperature reaction between oxygen and atomic hydrogen, etc.). But this hypothetical isomer should not be reversibly convertible into normal hydrogen peroxide.

The present results for the heat of fusion and the triple point of hydrogen peroxide lie outside the limits of error assigned by Foley and Giguère for their determinations (4, 5). Because the experimental method used this time was much more accurate there is no question that the new values are to be preferred. The limitations of the freezing point method for measuring melting points are well known (3). That thermodynamic equilibrium was not perfectly realized in the determinations by the above authors was indicated by the uncertainty of their calculated melting point at zero impurity. More recent measurements made with an improved type of apparatus (9) have yielded a melting temperature of −0.43° C. for the pure compound (28) in agreement with the present value after correction for the pressure effect (5) ($dt/dp = 0.007°$ atm.$^{-1}$).

It is perhaps worth emphasizing that the present calorimetric determination of impurities in hydrogen peroxide is the most precise reported so far. The usual procedures based upon chemical analysis are not capable of an accuracy much greater than 0.1%. Because of this, previous workers have often assumed erroneously that they had succeeded in preparing 100% pure hydrogen peroxide.

The Entropy of Hydrogen Peroxide

The computation of the entropy of hydrogen peroxide from the thermal data

is outlined in Table III. The contribution of the solid between 12° K. and the triple point was deduced by integrating values of C_p/T using Simpson's rule. Up to 250° K. the values of C_p were taken from Table I and thereafter from equation [1].

TABLE III
THE ENTROPY OF H_2O_2

	Cal./mole deg.	
ΔS (0° to 12° K.) Debye extrapolation	0.02	
ΔS (12° to 272.74 ° K.) Solid	13.30 ± 0.01	
$\Delta S_{272.74°}$ (2987/272.74) Fusion	10.95 ± 0.01	
Entropy of the liquid at 272.74° K.		24.27 ± 0.02
*ΔS (272.74° to 298.16° K.) Liquid	1.90 ± 0.01	
*$\Delta S_{298.16}$ (12330/298.16) Vaporization	41.34 ± 0.07	
**$\Delta S_{\text{compression}}$ R ln (1.95/760)	−11.85 ± 0.02	
Correction for ideal gas	0.10	
Entropy of the ideal gas at 298.16° K. and 1 atm. pressure		55.76 ± 0.12

* *Reference (19).* ** *Reference (27).*

An alternative calculation of the entropy of the liquid at the triple point was also made using only experimentally measured quantities. Up to 250° K. the procedure was as above. From 250° K. to the point where melting was complete, the total entropy was computed by means of the expression

$$[2] \qquad \Delta S = \sum_n \frac{\Delta Q_n}{T_n}$$

where ΔQ_n is the energy supplied in the nth heat capacity measurement and T_n is its mean temperature. From this was subtracted the increase in entropy of the calorimeter vessel. The result of this calculation was within 0.01 cal./mole deg. of that given in Table III. Thus, to this degree of precision the entropy of the liquid is independent of any assumption concerning the behavior of the heat capacity of the pure solid in the premelting region.

The specific heat of the liquid was taken as 21.35 cal./mole deg. and the latent heat of vaporization as 12.33 kcal./mole at 25° C. from the results of recent redeterminations to be published soon (19). For the entropy of compression to one atmosphere the equilibrium vapor pressure of hydrogen peroxide at 25° C. (1.95 mm. Hg) was obtained by extrapolation of the equation of Scatchard and co-workers (27). Finally, the Berthelot equation of state with the approximate critical constants T_c = 459° C. (16), P_c = 240 atm. (13), was used to evaluate the small correction for gas imperfection.

The value thus obtained for the third law entropy at 25° C. is significantly higher than the entropy calculated previously by the statistical method (54.18 cal./mole deg. (7)). Since the various structural and vibrational data of the molecule are known with fair accuracy, except those pertaining to the internal rotational mode, it was obvious that the discrepancy was to be traced

to the latter. On reviewing the statistical calculations, it was discovered that an error had been made in selecting a value for n in the expression for the rotational partition function (10)

[3] $$Q_f = (8\pi^3 I\gamma kT)^{\frac{1}{2}}/hn\,.$$

Although the potential energy restricting free rotation about the O–O bond exhibits two maxima, these are unequal and therefore distinguishable. Consequently, n in equation [3] must be taken as 1 and not 2 as was chosen previously. After correcting this term, the statistical entropy is only 0.45 units smaller than the third law entropy, and the two can be made equal by using a barrier height of about 3.5 kcal./mole (instead of 5 kcal./mole as in the earlier calculations (7)). Hitherto, values ranging from a few hundred calories (17) up to 12 kcal./mole (12) have been proposed for the potential barriers in hydrogen peroxide. The various thermodynamic functions for gaseous hydrogen peroxide have been recalculated up to 1500° K. (Table IV),

TABLE IV
REVISED VALUES OF THE THERMODYNAMIC FUNCTIONS FOR HYDROGEN PEROXIDE GAS AT 1 ATM. PRESSURE

T, °K.	$-\frac{F^\circ - H_0^\circ}{T}$, cal./mole deg.	$\frac{H^\circ - H_0^\circ}{T}$, cal./mole deg.	S°, cal./mole deg.	C°, cal./mole deg.	$H^\circ - H_0^\circ$, cal./mole deg.
298.16	46.33	9.42	55.76	11.00	2810
300	46.39	9.43	55.82	11.02	2830
350	47.87	9.69	57.54	11.47	3391
400	49.17	9.94	59.11	11.93	3976
500	51.44	10.42	61.84	12.68	5210
600	53.38	10.85	64.23	13.28	6511
700	55.09	11.21	66.31	13.76	7848
800	56.61	11.58	68.17	14.15	9263
900	57.99	11.89	69.86	14.51	10702
1000	59.26	12.15	71.40	14.84	12153
1100	60.43	12.41	72.83	15.15	13656
1200	61.56	12.65	74.17	15.45	15186
1300	62.52	12.87	75.41	15.72	16737
1400	63.50	13.09	76.58	15.97	18322
1500	64.41	13.29	77.69	16.20	19935

the contribution of internal rotation being estimated after the method of Pitzer and Gwinn (24) with a barrier height $V_0 = 3.5$ kcal./mole and the simple sinusoidal potential function

[4] $$V = \tfrac{1}{2}V_0\,(1 - \cos n\theta)\,.$$

Because of this approximation there still remains some uncertainty in the revised thermodynamic quantities, especially at the higher temperatures.

The internal rotational mode may be treated differently, namely as a double minimum oscillator such as the ammonia molecule. Then a satisfactory approximation consists of taking the energy levels for an equivalent single minimum oscillator with each level being doubly degenerate (23). This is tantamount to adding an R ln 2 term to the entropy and free energy functions. However, here again the calculated functions will be less accurate at higher

temperatures because then the molecules change gradually from pure oscillation towards free internal rotation. It turns out that the values of the entropy calculated by the two methods agree fairly well even at 1500° K.* but the enthalpy and heat capacity functions are appreciably different. More exact calculations of these various quantities must await further spectroscopic data and an adequate theoretical treatment of the molecule.

ACKNOWLEDGMENT

The success of these experiments depended to a large extent upon careful fabrication of the calorimeter vessels. For this work the authors are indebted to Messrs. A. Dubois, A. Lavergne, and F. C. Mason of the National Research Laboratories. They also wish to thank Dr. A. Cholette of Laval University for valuable assistance with the sealing of the vessels.

RÉSUMÉ

La capacité calorifique du peroxyde d'hydrogène à l'état solide a été mesurée entre 12° K. et le point de fusion au moyen d'un calorimètre adiabatique. La chaleur latente de fusion a également été déterminée et trouvée égale à 2987 ± 3 cal./mole. Les deux échantillons de peroxyde d'hydrogène qui ont servi pour ces mesures étaient d'un haut degré de pureté, soit 99.97 mole %, ainsi qu'il ressort des variations de la capacité calorifique qui ont précédé fusion. De ces mêmes données on a déduit que le point triple du peroxyde d'hydrogène se trouve à 272.74° K.

La seule anomalie que l'on ait remarquée au cours des mesures fut l'absorption d'une faible quantité de chaleur, 1.3 cal./mole, à 216.8° K., le point eutectique des solutions concentrées du peroxyde d'hydrogène. Cette observation conduit au même résultat que celui déjà mentionné pour la pureté des échantillons employés.

A partir de ces données on peut calculer l'entropie calorimétrique du peroxyde d'hydrogène considéré comme gaz parfait à 25° C. et à 1 atm. En comparant cette valeur, (55.76 ± 0.12 cal./mole deg.) avec celle que donne la méthode statistique il appert que la rotation interne des deux groupes OH dans la molécule est gênée par une énergie potentielle équivalente à un seuil unique d'environ 3.5 kcal./mole.

REFERENCES

1. ABRAHAMS, S. C., COLLIN, R. L., and LIPSCOMB, W. N. Acta Cryst. 4: 15. 1951.
2. ASTON, J. G., CINES, M. R., and FINK, H. L. J. Am. Chem. Soc. 69: 1532. 1947.
3. CINES, M. R. The physical properties of hydrocarbons. Vol. I. Academic Press Inc., New York. 1950. p. 346.
4. FOLEY, W. T. and GIGUÈRE, P. A. Can. J. Chem. 29: 123. 1951.
5. FOLEY, W. T. and GIGUÈRE, P. A. Can. J. Chem. 29: 895. 1951.
6. GEIB, K. H. and HARTECK, P. Ber. 65: 1551. 1932.
7. GIGUÈRE, P. A. Can. J. Research, B, 28: 485. 1950.
8. GIGUÈRE, P. A. and GEOFFRION, P. Can. J. Research, B, 28: 599. 1950.
9. HERINGTON, E. F. G. and HANDLEY, R. J. J. Chem. Soc. 199. 1950.
10. HERZBERG, G. Infrared and raman spectra of polyatomic molecules. D. Van Nostrand Company Inc., New York. 1945. p. 511.

* *A hypothetical frequency of 400 cm.$^{-1}$ (based on the calorimetric entropy) was assumed for the oscillator.*

11. HUCKABA, C. E. and KEYES, F. G. J. Am. Chem. Soc. 70: 1640. 1948.
12. LASSETTRE, E. N. and DEAN, L. B. J. Chem. Phys. 17: 317. 1949.
13. LORENZ, R. Z. anorg. Chem. 94: 240. 1916.
14. LOS, J. M. and MORRISON, J. A. Can. J. Phys. 29: 142. 1951.
15. MAASS, O. and HATCHER, W. H. J. Am. Chem. Soc. 42: 2548. 1920.
16. MAASS, O. and HIEBERT, P. G. J. Am. Chem. Soc. 46: 2693. 1924.
17. MASSEY, J. T. and BIANCO, D. R. J. Chem. Phys. In press.
18. MIRONOV, K. E. and BERGMAN, A. G. Doklady Akad. Nauk. U.S.S.R. 81: 1081. 1951.
19. MORISSETTE, B. G. M. Sc. Thesis, Laval University, Quebec. 1952.
20. MORRISON, J. A. and LOS, J. M. Discussions Faraday Soc. 8: 321. 1950.
21. NEIDING, A. B. and KAZARNOVSKII, I. A. Doklady Akad. Nauk. U.S.S.R. 74: 735. 1950.
22. PENNEY, W. G. and SUTHERLAND, G. B. B. M. J. Chem. Phys. 2: 492. 1934.
23. PITZER, K. S. Quantum chemistry. Prentice-Hall, Inc., New York. 1953. p. 246.
24. PITZER, K. S. and GWINN, W. D. J. Chem. Phys. 10: 428. 1942.
25. ROBERTSON, A. J. B. Trans. Faraday Soc. 48: 228. 1952.
26. RUEHRWEIN, R. A. and HUFFMAN, H. M. J. Am. Chem. Soc. 65: 1620. 1943.
27. SCATCHARD, G., KAVANAGH, G. M., and TICKNOR, L. B. J. Am. Chem. Soc. 74: 3715. 1952.
28. SECCO, E. A. Ph.D. Thesis, Laval University, Quebec. 1953.
29. SIDGWICK, N. V. The chemical elements and their compounds. Vol. II. The Clarendon Press, Oxford. 1950. p. 869.

THE MECHANISM OF THE HYDRATION OF TRICALCIUM SILICATE AND β-DICALCIUM SILICATE[1]

By W. A. G. Graham, J. W. T. Spinks, and T. Thorvaldson

ABSTRACT

Labelled tricalcium silicate, prepared by heating together inactive dicalcium silicate and lime labelled with Ca^{45}, has been hydrated in saturated solutions of calcium hydroxide at 21°C. Parallel studies of the rate of liberation of lime due to hydrolysis and the coincident appearance of Ca^{45} in the solution indicate that the $CaO:SiO_2$ ratio in the precipitated hydrated silicate is 3:2. A similar result is obtained when inactive tricalcium silicate is hydrated in an active lime solution. Comparable studies on the hydrolysis of labelled β-dicalcium silicate indicate the formation of a product with the same $CaO:SiO_2$ ratio. The method appears to have rather general application.

INTRODUCTION

In the well known "crystallization theory" of the hydration of Portland cement, it is assumed that the anhydrous compounds pass into solution, with or without hydrolysis, forming hydrated products of lower solubility which separate from the supersaturated solution. The condition of supersaturation is maintained as long as any of the more soluble anhydrous substances remain in contact with the solution. Thus, during complete hydration, the hydraulic compounds "pass through" the liquid phase although the amount dissolved at any given moment may be very small.

Many studies have been made on the hydration of the calcium silicates, considered to be present in Portland cement, and on the composition of the products obtained. Using silica sol and solutions of calcium hydroxide Le Chatelier (3, pp. 59–62) obtained hydration products with $CaO:SiO_2$ ratios varying between 1 and 1.7, depending on the concentration of lime in the solution at the end of the precipitation. He found that the only product to which the properties of a definite chemical compound could be attributed had the composition, $CaO.SiO_2.2\frac{1}{2}H_2O$, and considered that the lime present in excess of this ratio was "fixed by a phenomenon of superficial attraction well known for finely divided chemical precipitates."

Le Chatelier (3, p. 84) assigned this formula to the chemical compound obtained on hydration of the silicates present in Portland cement. Many later investigators have arrived at similar conclusions while others have considered that, under the conditions existing in mortars and concrete, compounds with $CaO:SiO_2$ ratios of 3:2 or 2:1 are formed. A summary of the literature on the hydration of Portland cement and of the pure cement compounds at ordinary temperatures has been compiled by Steinour (6). It is interesting to note that in the latest studies on hydrated calcium silicates at ordinary temperatures, Taylor (4, 5) has concluded that the product formed at concentrations of calcium hydroxide somewhat below saturation has a $CaO:SiO_2$ ratio varying from 1 to 1.5 and states that his X-ray data are consistent with the view that the lime in excess of a ratio of 1:1 is held

[1] *Manuscript received September 23, 1953.*
Contribution from the Department of Chemistry, University of Saskatchewan, Saskatoon, Sask., with financial support from the National Research Council of Canada.

either in the adsorbed state or in solid solution in a zeolite type of crystal. He found, however, that on hydration of tricalcium silicate at 17°C. in a solution approaching saturation with lime (>1.13 gm. calcium oxide per liter), a product with a $CaO:SiO_2$ ratio of 2:1 was formed, giving an X-ray pattern differing slightly from that of the product obtained at the lower concentrations of lime.

It is evident that a quantitative chemical study of the hydration products of Portland cement during the course of the hydration presents great difficulties on account of the intimate mixture of several compounds and of the lack of effective methods for separating the hydration products from each other and from the unhydrated material. Even when the pure silicates are used, the latter difficulty applies. Furthermore, complete hydration and uniform hydration products are not easily obtained.

The availability of radioactive calcium-45 as a tracer has opened up new methods for the study of the mechanism of the hydration, both of cements and of the pure cement compounds. For instance, in the study of the hydration of the silicates one may incorporate Ca^{45} in the anhydrous silicate and hydrate the product in water or in a solution of calcium hydroxide. As an alternative, the inactive* silicate may be hydrated in a solution of calcium hydroxide labelled with the isotope, Ca^{45}. By following the rate of liberation of lime due to hydrolysis and the coincident appearance of Ca^{45} in the solution, or in the second case by determining the simultaneous rate of removal of Ca^{45} from the solution by the precipitation of the hydration product, one obtains experimental data which appear to distinguish decisively between postulated $CaO:SiO_2$ ratios for the composition of the precipitated hydrated silicate under the experimental conditions used.

The data reported in the present paper deal with the hydration of tricalcium silicate and β-dicalcium silicate at 21°C. in slightly supersatured solutions of lime, thus approximating the condition of lime saturation present for the most part during the hydration of the silicates in rich mortars and concrete.

MATERIALS

The chemicals used in the preparation of the silicates and the solutions of calcium hydroxide were of very high purity. 'Reagent' calcium carbonate, reprecipitated from dilute solution, contained negligible amounts of impurities. The silica gel (16% H_2O) had initially a nonvolatile residue with hydrofluoric and sulphuric acids of 0.16% and passed a 325-mesh sieve (<44 microns). After extracting with hydrochloric acid and washing free from chlorides, the nonvolatile residue was <0.06%. Determination by flame photometer gave 0.004% sodium oxide and <0.001% potassium oxide.

Preparation of the Silicates

Carefully proportioned mixtures of calcium carbonate and silica gel in the $CaO:SiO_2$ ratio of 2:1 were given a preliminary ignition in platinum crucibles in a muffle furnace, the temperature being raised gradually to about

**Unless otherwise indicated the terms "active" and "inactive" will refer only to the radioactivity of the materials under discussion and not to chemical activity.*

950°C. to avoid mechanical loss. Two ignitions in the temperature range, 1400 to 1700°C. in an induction furnace followed. The product "dusted" and passed a 200-mesh sieve (<74 microns) without grinding. A sample of γ-dicalcium silicate labelled with Ca^{45} was thus prepared and converted to β-dicalcium silicate by heating at 950 to 1000°C. and cooling rapidly. After several prolonged heatings microscopic examination indicated that less than 1% remained in the γ form. Tests for free lime were negative.

A second sample of γ-dicalcium silicate which was not labelled with Ca^{45} was prepared for use as the starting material for the preparation of tricalcium silicate. The product was mixed in stoichiometric proportions with Ca^{45} labelled calcium carbonate and, after a preliminary ignition to 950°C., was heated repeatedly in the induction furnace in the 1400 to 1700°C. range with rapid cooling and intermediate grinding to pass a 325-mesh sieve (in dry air, using a dust-tight safety chamber) until tests for free lime were negative, or only a small quantity was found by the alcohol–glycerol method. Four labelled samples of tricalcium silicate (and a fifth unlabelled) were prepared in the course of the present work.

Calcium Hydroxide

The solutions of calcium hydroxide were prepared from freshly ignited calcium oxide which was shaken in stoppered bottles of glass or polyethylene in a room thermostated at 21.0 ± 0.1°C. Supersaturated solutions were quickly formed and the shaking was continued until saturation was approached. The concentration of the solutions was determined by titration with 0.06 molar hydrochloric acid which was standardized against a very pure sample of calcium carbonate as well as against calcium hydroxide solution, the concentration of which had been determined by precipitation of the calcium as oxalate. Special precautions were taken against access of carbon dioxide to the lime and to the solutions of calcium hydroxide, and the water used was carbon-dioxide-free. The hydroxide solutions used at various times contained from 1.135 to 1.244 gm. calcium oxide per liter at 21°C.

THE HYDROLYSIS OF THE SILICATES

All the work, except the counting of the radioactive samples, was done in a room at 21.0 ± 0.1°C. The silicates, ground to pass a 325-mesh sieve, were shaken in a rotary shaker with the 'saturated' solution of calcium hydroxide in steel tubes completely lined with pure silver or gold foil. A thin film of silicone stopcock grease was used at the ground cap joint. A blank using a silver-lined tube and saturated solution, shaken for 116 days, showed a loss in titer of less than 3 parts in 1000 which may be considered to be close to the experimental variation for duplicate determinations. The saturated solution of calcium hydroxide was used in the hydrolysis experiments to prevent the formation of a hydrosilicate low in lime, in the initial stages of the hydration, and in the case of tricalcium silicate to attempt to produce the hydrosilicate of $CaO:SiO_2$ ratio of 2:1 for the existence of which Taylor (4) found evidence.

A supersaturated solution of lime was formed on the hydrolysis of the silicate but no precipitation of lime could be detected until the solution reached a high degree of supersaturation. Thus, when 0.1 gm. portions of tricalcium silicate were shaken with 100 ml. of the saturated lime solution on a rapidly revolving rotary shaker, the supersaturation usually reached about 20% before there was any evidence of precipitation of calcium hydroxide. This corresponds to the liberation of 1 mole calcium oxide per mole of the silicate. For greater extent of hydrolysis, 0.05 gm. portions of the silicate were used with 100 ml. of the saturated lime solution. When β-dicalcium silicate was used, precipitation of lime occurred at a lower degree of supersaturation thus limiting the degree to which hydrolysis of this compound could be carried under the conditions of our experiments. All the experimental work described in this paper was carried on in the metastable range of supersaturation.

The amount of lime liberated in a given time interval was determined as the difference between the titer of 25 ml. portions of the original saturated lime solution and the hydrolyzate after centrifuging. The small solubility of the silicate caused no appreciable error. The activity of the calcium in the hydrolyzate was determined on 0.500 ml. portions by a Geiger counter after precipitation of the calcium as oxalate (window thickness 1.6 mgm. per sq. cm; scale of 64 scaler). Care was taken to keep the geometry constant. Before and after the counting of the unknown a standard sample of radioactive calcium and a preparation of the silicate being hydrolyzed was counted. The latter was prepared by decomposing (with hydrochloric acid) the same weight of the silicate as that used in 100 ml. in the hydrolysis experiment, removing the silica by dehydration, and making the solution up to 100 ml. A 0.500 ml. portion was then counted in exactly the same manner as the hydrolyzate. It was found that the additional calcium in the hydrolyzate did not affect the count appreciably. The ratio of the activity of the hydrolyzate to the activity of the solution from the silicate (after correction for background) was thus independent of the decay of the calcium-45, and the counting of the 'standard sample' of radioactive calcium served as an additional check.

Effect of Variation in the Method of Preparation of Tricalcium Silicate

Five samples of tricalcium silicate were prepared in a similar manner except for the time of ignition in the 1400 to 1700°C. range. The number of ignitions, the total time, and the free lime content were as follows:

Sample No.	Total time at 1400–1700°C., min.	Number of ignitions	Free lime, % CaO
1–52	25	1	5.4
2–52	85	2	0.13
1–53	200	3	0.30
1–51	250	3	0.57
2–53	360	5	0.00

The rates of liberation of lime of three of the samples at 21°C. on hydrolysis of 0.1 gm. portions in 100 ml. of saturated calcium hydroxide are plotted in Fig. 1. It shows that the rate is in the inverse order to the time of ignition, suggesting that progressive recrystallization of the silicate had occurred during the heating. No data are, however, available on the relative particle size, except that all the samples were ground to pass a 325-mesh sieve. Lime liberated by the hydrolysis of the dicalcium silicate present in the samples (which was small except in the case of sample 1–52) was considered to be negligible in the time involved. This is supported by the experimental data of Fig. 4. A correction was made for the free lime contained in sample 1–52 on the assumption that all the free lime passes quickly into solution. This

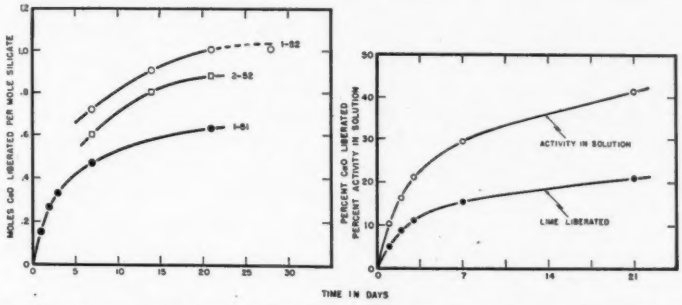

FIG. 1. The effect of the time of heating at 1400-1700°C. on the rate of hydrolysis of tricalcium silicate. (No. 1–52, 25 min., No. 2–52, 85 min., No. 1–51, 250 min.)

FIG. 2. Relative rates of increase with time of activity and alkalinity of the liquid phase during the hydration of labelled tricalcium silicate.

represents an over-correction so that the actual rate of hydrolysis of sample 1–52 was greater than that shown in Fig. 1. Precipitation of calcium hydroxide had begun in the case of sample 1–52 at the 28 day point. The corresponding curves (not shown) for the other two samples of tricalcium silicate were in agreement. The rate of hydrolysis of sample 1–53 was slightly higher and that for sample 2–53 slightly lower than for sample 1–51.

The Hydrolysis of Labelled Tricalcium Silicate and β-Dicalcium Silicate in a Saturated Solution of Calcium Hydroxide: The Relative Rates of the Appearance of Activity and of Alkalinity in the Liquid Phase

Fig. 2 gives the percentage of the total lime in the silicate liberated on hydrolysis as determined by titration, and the corresponding percentage of the total calcium activity found in the solution plotted against time for tricalcium silicate sample 1–51. It is evident that at any given time the percentage of the total activity in the solution is much greater than the percentage of the total lime of the silicate found in the solution. A similar relationship was found in the case of samples 1–52, 2–52, and 2–53.

In the preparation of tricalcium silicate the Ca^{45} was, in all cases, introduced in the third molecule of lime which was added to the already prepared inactive γ-dicalcium silicate. Considering the relationship between the

activity and lime in the hydrolyzate, it might be thought that this indicates that the last molecule introduced into the crystal lattice was the first to be liberated on hydrolysis, thus supporting the view that the three molecules of calcium oxide in tricalcium silicate are not chemically equivalent — a conclusion which would be of great interest on account of the uncertainty as to the structure of this substance (1, 2).

There are, however, some obvious objections to this explanation of the experimental data. Fig. 1 shows the great variation in the relative rates of liberation of lime on hydrolysis of different samples of tricalcium silicate, but when time is eliminated as a parameter as in Fig. 3, which is a plot of the percentages of the total activity found in the solution against the lime liberated by hydrolysis as determined by titration, the experimental results for all the labelled samples, 1–51, 2–52, and 2–53, fall on the same curve. (The values for sample 1–52 are not included on account of the difficulty in correcting for the large amount of free lime in the sample.) If one assumes the existence of two types of lattice positions for Ca^{++} in the crystals of the silicate, one would expect some interchange between them to occur during the heating at 1400 to 1700°C. Such exchange should cause the samples of tricalcium silicate heated for the longer periods of time to give curves (Fig. 3) approaching a slope of 45°, corresponding to the uniform distribution of the Ca^{45} throughout the crystals. As the results for all the samples fall on the same curve, it appears probable that the Ca^{45} was uniformly distributed throughout the lattice of sample 2–52 as well as those heated for longer time, and that these hydrolysis experiments, therefore, cannot give any evidence for or against the equivalence of the three lime molecules in tricalcium silicate. Fig. 3, however, indicates that the mechanism of the hydrolysis of tricalcium silicate is independent of the rate.

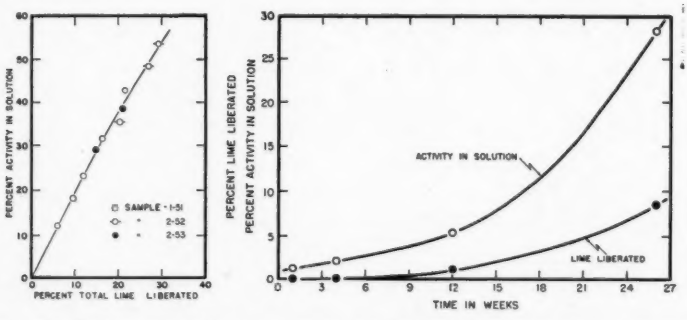

FIG. 3. The hydration of tricalcium silicate labelled with Ca^{45} in a saturated solution of calcium hydroxide. The relative increase in calcium hydroxide content and in the activity of the solution.

FIG. 4. The hydration of radioactive β-dicalcium silicate labelled with Ca^{45} in a saturated solution of calcium hydroxide. The relative increase with time of the activity and alkalinity of the liquid phase.

Data for the hydrolysis of a sample of labelled β-dicalcium silicate in a saturated solution of calcium hydroxide plotted in Fig. 4 are also of interest.

Here, too, the percentage of total activity found in the hydrolyzate is far in excess of the percentage of total lime liberated as calculated from the increase in the titer.

THEORETICAL CALCULATIONS

The theoretical curve for the activity of the calcium in the hydrolyzate plotted against the lime liberated, as determined by titration, can be calculated for any postulated lime: silica ratio of the hydrosilicate on the basis of the assumption that the anhydrous silicate (labelled with Ca^{45}) passes into solution in the form of ions and that the 'life' of the Ca ions is long enough to allow uniform distribution throughout the hydrolyzate, under the conditions of agitation used, before precipitation of the calcium in the form of calcium hydrosilicate occurs. The presence of calcium in undissociated molecules in the solution would not change the conclusion reached, provided the interval of time before precipitation is long enough for attainment of exchange equilibrium. The activity present in the solution at any moment will be a function of the amount of anhydrous silicate which has entered the solution, the specific activity of the anhydrous silicate, the amount of calcium hydroxide in the original solution, and the ratio of lime to silica in the precipitated calcium hydrosilicate. The problem is simplified somewhat for a given series of experimental determinations where the specific activity of the sample of anhydrous silicate (corrected for the rate of decay) is a constant and the volume and concentration of the original solution of calcium hydroxide is fixed.

The Hydration of Labelled Tricalcium Silicate in Inactive Calcium Hydroxide Solution

A mathematical expression for the percentage activity in the solution during the hydrolysis and hydration of tricalcium silicate according to the over-all equation

$$2(3CaO.SiO_2) + (n + 3)\ H_2O \rightarrow 3CaO.2SiO_2.nH_2O + 3Ca(OH)_2,$$

may be developed as follows:

Let a represent the number of moles of lime in the original solution and b the specific activity of the labelled silicate defined in terms of the activity per mole of lime present in the silicate. Let x be the amount of anhydrous silicate which has passed into the solution expressed in terms of moles CaO and $f(x)$ be the specific activity of CaO in solution in units of activity per mole of CaO. Consider the hydrolysis of $\frac{1}{3}\ dx$ moles of tricalcium silicate, which in the first step of this mechanism liberates dx moles of calcium oxide to the solution. We take dx sufficiently small that it does not appreciably change the specific activity of calcium oxide in the solution, $f(x)$. In the second step of this mechanism calcium oxide to the extent of one-half of the amount of calcium oxide liberated, or $\frac{1}{2}\ dx$, of specific activity $f(x)$, is removed to form the hydration product. It is clear that the calcium radioactivity liberated to the solution is bdx while that removed is $\frac{1}{2}\ f(x)dx$, so that the net increase in the total calcium radioactivity in solution is $bdx - \frac{1}{2}\ f(x)dx$. When x moles have been liberated, the increase is

[1] $$\int_0^x (b - \tfrac{1}{2} f(x))\, dx.$$

To find $f(x)$,we consider the liberation of Δx moles of calcium oxide by tricalcium silicate which has already liberated x moles. There has been an increase of only $\frac{1}{2} x$ moles of calcium oxide in the solution, in which the specific activity of calcium oxide is $f(x)$. After x moles have been liberated, the total calcium radioactivity in solution is

$$(a + \tfrac{1}{2}x)f(x).$$

If we permit Δx moles to be liberated with no precipitation, the resulting total calcium radioactivity in solution will be

$$(a + \tfrac{1}{2}x)f(x) + b\Delta x,$$

and the new specific activity will be

$$f(x + \Delta x) = \frac{(a + \frac{1}{2}x)\, f(x) + b\Delta x}{a + \frac{1}{2} x + \Delta x}.$$

We now form

$$\frac{f(x + \Delta x) - f(x)}{\Delta x} = \left[\frac{(a + \frac{1}{2} x)\, f(x) + b\Delta x}{a + \frac{1}{2} x + \Delta x} - f(x) \right] \Big/ \Delta x$$
$$= \frac{b - f(x)}{a + \frac{1}{2} x + \Delta x}.$$

In the limit as $x \to 0$, this expression becomes

$$\frac{d\, f(x)}{dx} = \frac{b - f(x)}{a + \frac{1}{2} x}.$$

If we solve this differential equation under the conditions that $f(x) = 0$, when $x = 0$, we get

[2] $$f(x) = b - [4a^2b/(2a + x)^2].$$

Now substitute [2] in [1] and obtain for the total calcium radioactivity in solution

$$\int_0^x \left(\tfrac{1}{2} b + \frac{2a^2 b}{(2a + x)^2} \right) dx = \tfrac{1}{2} bx + 2a^2 b \int_0^x \frac{dx}{(2a + x)^2}$$
$$= b \left[\tfrac{1}{2} (2a + x) - \frac{2a^2}{(2a + x)} \right]$$

on integration.

For convenience, we convert this into percentage activity in solution by dividing by the total calcium activity in the tricalcium silicate used, namely b times moles of calcium oxide in the solid, and multiplying by 100; whence,

[3] $$\%\ \text{activity in solution} = \frac{\frac{1}{2} (2a + x) - [2a^2/(2a + x)]}{(\text{moles CaO originally in solid})} \times 100.$$

On the basis of the over-all process postulated above, for each mole of tricalcium silicate which "passes through" the liquid phase three moles

of lime pass into solution and 1.5 moles pass out of the solution in the hydrated silicate. The value of x in equation [3] is therefore twice the number of moles of lime liberated as determined by titration.

An expression for the percentage activity in the solution if the over-all reaction for the hydrolysis and hydration is represented by the equation

$$3CaO.SiO_2 + (n + 1)\ H_2O \rightarrow 2CaO.SiO_2.nH_2O + Ca(OH)_2,$$

may be developed in analogous fashion.

In this process of hydration defining a, b, x, and $f(x)$ as before, when $\frac{1}{3}dx$ moles of tricalcium silicate pass through the liquid phase dx moles of labelled calcium oxide pass into solution carrying bdx units of radioactivity and $\frac{2}{3}dx$ moles are removed from solution carrying $\frac{2}{3}f(x)dx$ units of radioactivity as defined above. As in equation [1] above, we express the increase in total calcium radioactivity in solution as

$$[4] \qquad \int_0^x (b - \tfrac{2}{3}f(x))\, dx.$$

If, after x moles of calcium oxide from the silicate have passed into the solution with the concurrent precipitation of hydrated silicate, we consider the liberation of Δx moles of calcium oxide to the solution we may obtain by the same process as before the expression

$$\frac{d\,f(x)}{dx} = \frac{b - f(x)}{a + \frac{1}{3}x},$$

which on integration and simplification yields

$$[5] \qquad f(x) = b - [27a^3b/(3a + x)^3],$$

where as before $f(x) = 0$ when $x = 0$.

Substitution of [5] in [4] yields, on integration,

$$b[\tfrac{1}{3}(x + 3a) - \{9a^3/(3a + x)^2\}]$$

for the total radioactivity in the solution, whence,

$$[6] \quad \%\ \text{activity in solution} = \frac{\frac{1}{3}(x + 3a) - [9a^3/(3a + x)^2]}{(\text{moles CaO originally in solid})} \times 100.$$

The value of x in equation [6] is three times the number of moles of lime which have been liberated as determined by titration.

A general expression for the activity in the solution for any postulated lime:silica ratio in the hydration product may be developed for the hydrolysis of tricalcium silicate in the same manner. If a and x are defined as before and r is the $CaO:SiO_2$ ratio in the hydrate, the final expression for the percentage of the total activity in the solution becomes,

$$[7] \quad \frac{x - \frac{1}{3}rx - \frac{r-3}{3}\left\{\frac{3a}{3-r}\right\} + \frac{r-3}{3}\left\{\frac{3a}{3-r}\right\}^{3/(3-r)}\left\{\frac{3a}{3-r} + x\right\}^{r/(r-3)}}{(\text{moles CaO in original silicate})} \times 100$$

where $x = 3/(3 - r)$ times the number of moles of lime which have been liberated as determined by the increase in the titer of the solution.

The Hydration of Labelled Dicalcium Silicate in Inactive Calcium Hydroxide Solution

An expression for the hydrolysis of dicalcium silicate labelled with Ca^{45} with the formation of the 3:2 calcium hydrosilicate may be derived in a similar manner.

In this case, with the same definitions for a, b, x, and $f(x)$ as before, when $\frac{1}{2}dx$ moles of the silicate pass through the solution, dx moles of labelled calcium oxide pass into solution carrying bdx units of activity, but $\frac{3}{4}\ dx$ moles are removed from the solution carrying $\frac{3}{4}\ f(x)dx$ units of activity. After x moles of lime (from the silicate) have entered the solution with the concurrent precipitation of the hydrosilicate, the activity of the solution is given by

$$[8] \qquad \int_0^x (b - \tfrac{3}{4} f(x))\ dx.$$

Evaluating $f(x)$ as before, we obtain

$$[9] \qquad f(x) = b - \frac{256a^4b}{(4a + x)^4},$$

taking $f(x) = 0$ when $x = 0$. Substituting [9] in [8], integrating and simplifying, we obtain, upon dividing by the total initial calcium activity in the solid and multiplying by 100,

$$[10] \quad \%\ \text{activity in solution} = \frac{\frac{1}{4}\ (4a + x) - [64a^4/(4a + x)^3]}{(\text{moles CaO originally in solid})} \times 100.$$

The value of x in equation [10] is four times the number of moles of lime which have been liberated as determined from the increase in the titer of the solution.

Fig. 5 shows the theoretical curves for the hydrolysis of tricalcium silicate with the formation of a 3:2 calcium hydrosilicate (Curve A), the formation of a 2:1 calcium hydrosilicate (Curve B), and also the hydrolysis of dicalcium silicate with the formation of a 3:2 calcium hydrosilicate (Curve C), for 0.1 gm. portions of the silicate in 100 ml. of a calcium hydroxide solution containing initially 1.2 gm. calcium oxide per liter. There is a wide divergence between the theoretical curves for the two hydrosilicates.

The Hydrolysis of Inactive Tricalcium Silicate in a Saturated Calcium Hydroxide Solution Labelled with Ca^{45}

An expression for the change in the activity of a solution of labelled calcium hydroxide during the hydrolysis of a sample of inactive tricalcium silicate can also be developed. On the assumption that a hydrated 3:2 calcium hydrosilicate is formed, the fraction of the initial activity which remains in the solution after x moles of the calcium oxide of the silicate have passed into the solution with the consequent precipitation of hydrosilicate is given by the expression:

[11] $$2a/(2a + x)$$

where a = moles of calcium oxide originally present in the solution, and x, the number of moles of lime which have passed from the solid into the liquid phase, is equal to twice the increase in the concentration of calcium oxide in the solution.

The corresponding expression for the activity in the solution for the formation of a hydrated silicate with a $CaO:SiO_2$ ratio of 2:1 is:

[12] Per cent activity remaining in solution $= [9a^2/(3a + x)^2] \times 100.$

In this case x has a value three times the number of moles of lime liberated as determined by titration.

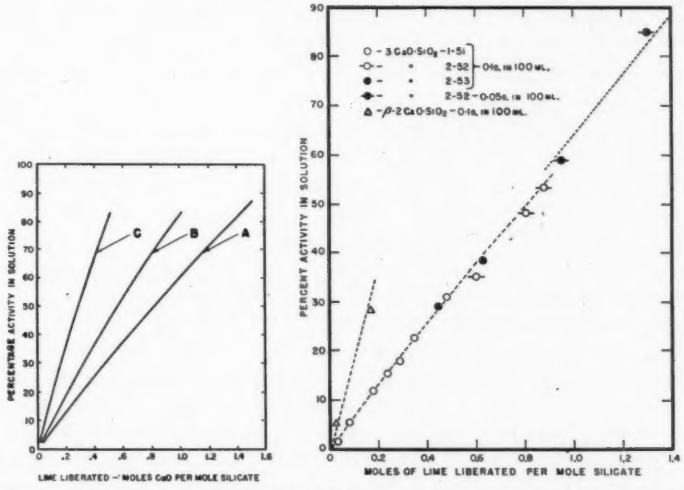

FIG. 5. Theoretical curves for the hydration of tricalcium silicate and dicalcium silicate labelled with Ca^{45} in a solution of calcium hydroxide (0.1 gm. portions of the silicate in 100 ml. of solution containing 1.2 gm. calcium oxide per liter).

A. Tricalcium silicate to give a 3:2 calcium hydrosilicate.
B. Tricalcium silicate to give a 2:1 calcium hydrosilicate.
C. Dicalcium silicate to give 3:2 calcium hydrosilicate.

FIG. 6. Experimentally determined points for the hydration of labelled tricalcium silicate and β-dicalcium silicate at 21°C., in saturated solutions of calcium hydroxide, showing the theoretical curves for the formation of a product with a $CaO:SiO_2$ ratio of 3:2.

EXPERIMENTAL RESULTS

Table I gives the experimental and calculated data for the hydrolysis and hydration of three samples of labelled tricalcium silicate and one sample of labelled β-dicalcium silicate at 21°C. Fig. 6 shows plots of the data together with the theoretical curves for the formation of a hydrate of the composition $3CaO.2SiO_2.nH_2O$. No corrections were applied to the experimental data for the small amount of free lime present in some of the samples, as the validity of such corrections is doubtful and would be only of the order of magnitude of the experimental error in counting (probable error about

TABLE I

THE HYDRATION OF TRICALCIUM SILICATE AND β-DICALCIUM SILICATE (LABELLED WITH Ca^{45}) IN SOLUTIONS OF CALCIUM HYDROXIDE AT 21°C.

Silicate Sample No.	Initial conc. of lime sol'n., millimoles/ 100 ml.	Time of shaking	Lime liberated as determined by titration, mole CaO/mole silicate	Percent of activity in the hydrolyzate	
				Exp.	Calc.
$3CaO.SiO_2$					Basis $3CaO.2SiO_2.nH_2O$
1–51	2.194	6 hr.	0.030	1.7	2.0
1–51	2.125	12 hr.	0.079	5.5	5.3
1–51	2.125	24 hr.	0.178	11.9	11.6
1–51	2.125	36 hr.	0.238	15.3	15.5
1–51	2.125	48 hr.	0.287	17.9	18.6
1–51	2.189	72 hr.	0.348	22.6	22.4
1–51	2.189	1 wk.	0.479	31.0	30.6
2–52	2.195	1 wk.	0.602	35.1	38.0
2–52	2.195	2 wk.	0.806	48.2	49.9
2–52	2.201	3 wk.	0.879	53.4	54.2
2–52*	2.184	4 wk.	0.950	59.1	60.4
2–52*	2.184	11 wk.	1.31	84.9	82.3
2–53	2.184	1 wk.	0.446	29.1	28.5
2–53	2.184	2 wk.	0.627	38.4	39.5
β-$2CaO.SiO_2$	2.200	12 wk.	0.023	5.4	4.5
β-$2CaO.SiO_2$	2.200	26 wk.	0.170	28.3	31.8

*0.05 gm. $3CaO.SiO_2$ in 100 ml. solution.
Weight of silicate in 100 ml. solution 0.1 gm.

one per cent). The experimental results are in agreement with the assumption that the product formed during the hydrolysis and hydration of both silicates at 21°C. is the 3:2 calcium hydrosilicate.

It should be noted that the dotted curve in the upper right hand corner of Fig. 6 is the calculated curve for the hydrolysis of 0.05 gm. portions of active tricalcium silicate in 100 ml. of the lime solution used in the experiments, while the other curves are calculated for the hydrolysis of 0.1 gm. portions of the silicates in 100 ml. of lime solution, the formation of a hydrosilicate of $CaO:SiO_2$ ratio of 3:2 being postulated in all cases.

When the experimental results with active tricalcium silicate are plotted as in Fig. 6, precipitation of calcium hydroxide from the super-saturated solution gives abnormally high values for the percentage of total activity found in the hydrolyzate. This is due to the fact that such precipitation reduces the value for lime liberated per mole of silicate, as determined from the increase in titer, proportionally more than the activity count. Such divergence from consistent values for the activity is probably a more sensitive means than microscopic examination for detecting the beginning of precipitation of hydrated lime.

Fig. 7* is a plot of the calculated theoretical curves for the hydration of inactive tricalcium silicate in a solution of calcium hydroxide (0.1135 gm. calcium oxide per 100 ml.) labelled with Ca^{45} for the formation of the 3:2 calcium hydrosilicate (Curve A) and of the 2:1 calcium hydrosilicate (Curve

*The authors are indebted to Mr. F. W. Birss for making some of the determinations recorded in Fig. 7.

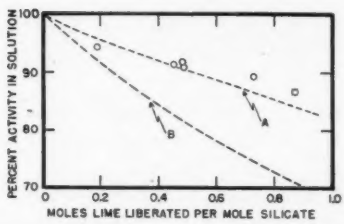

FIG. 7. Theoretical curves for the hydration of inactive tricalcium silicate in labelled calcium hydroxide solution together with experimental points at 21°C. (0.1 gm. portions of silicate in 100 ml. calcium hydroxide solution containing 1.13 gm. calcium oxide per liter).

B), respectively. The points are the experimental values obtained when tricalcium silicate 1–53 was shaken with calcium hydroxide solution of the above concentration. The experimental results are in general agreement with the assumption that a hydration product of the composition $3CaO.2SiO_2.nH_2O$ is formed. It may be noted that in this series the total amount of tricalcium silicate used in an experiment does not enter into the calculation of the expected percentage activity in the solution, only the amount of the silicate passing through the solution being significant. Also, since the solution is at the maximum of activity at the beginning of the runs when the rate of hydrolysis is very high (see Fig. 1), the results are particularly sensitive to any interruptions in shaking. Such interruptions and any lack of attainment of complete homogeneity of the hydrolyzate at all stages would tend to give low values for the removal of activity from the solution or high values for the activity as plotted in Fig. 7.

The question of the effect of exchange of calcium between the solution and the hydrated silicate has to be considered. In the experiments with labelled tricalcium silicate such exchange, if it occurs, would tend to lower the values for the activity found in the hydrolyzate while in the case of the hydrolysis of inactive tricalcium silicate in active calcium hydroxide solution the values would tend to increase. Considering the hydration of labelled tricalcium silicate to form the 3:2 hydrosilicate and assuming that complete exchange equilibrium between the calcium of the hydrolyzate and the hydrated portion of the silicate occurs, the expression for the per cent activity in the hydrolyzate becomes

$$x(2a + x) \times 100/[2(a + x)(\text{moles CaO in original silicate})].$$

For similar conditions with the formation of the 2:1 calcium hydrosilicate the expression would be

$$x(3a + x) \times 100/[3(a + x)(\text{moles CaO in original silicate})],$$

x and a being defined as above.

If these expressions are plotted as in Fig. 5, the curves have a slightly lower slope than the corresponding curves 'A' and 'B'. Under the conditions of our experiments, the change in the activity of the hydrolyzate which would be caused by complete exchange equilibrium of the calcium between the

solution and the hydrated solid is, however, only a small fraction of the difference in percentage activity for corresponding points on curves 'A' and 'B' of Fig. 5.

Similar considerations apply to the experiments with inactive tricalcium silicate in the labelled solution of calcium hydroxide. Here the per cent activity in the solution for complete exchange equilibrium is given by $(2a + x)\ 100/[2(a + x)]$ for the formation of the 3:2 hydrosilicate and by $(3a + x)\ 100/[3(a + x)]$ for the formation of the 2:1 product. The calculated curves differ slightly from curves 'A' and 'B' of Fig. 7. Again the change in the activity of the solution caused by complete exchange equilibrium under the conditions of our experiments is only a small fraction of the calculated difference in percentage activity for the formation of the two hydrosilicates.

Such exchange of calcium between the hydrolyzate and the hydration product could, therefore, not affect the conclusions arrived at above as to the composition of the hydrated silicate. The extent to which exchange occurs is being further studied.

While our experiments give no indication of the formation of a hydrated dicalcium silicate when tricalcium silicate is hydrated in a saturated solution of calcium hydroxide at 21°C., our results do not necessarily contradict those of Taylor (4) since his work was done at 17°C.

The results of our experiments are in fact in accord with the conclusions of Jeffery (2) that tricalcium silicate is composed of discrete ions of calcium, oxygen, and (SiO_4) and of Bernal, Jeffery, and Taylor (1) that in the initial stage of hydration the anhydrous silicates act only as a source of calcium and silicate ions from which the hydration products can be formed. From our experiments it would seem that in a saturated solution of calcium hydroxide at 21°C. the $(SiO_4)^{4-}$ ions undergo chemical change before, or incidental to, the formation of the hydrated silicate.

The work described in this paper illustrates a new approach to the study of the mechanism of the hydrolysis and hydration of slightly soluble solids by the use of radioactive tracers. It appears that the method could be extended to the study of the mechanism of many other chemical reactions especially when the progress of the reaction can be followed independently by both chemical and radiochemical methods.

REFERENCES

1. Bernal, J. D., Jeffery, J. W., and Taylor, H. F. W. Mag. of Concrete Research, October, 1952.
2. Jeffery, J. W. Third international symposium on the chemistry of cement, London. 1952. Paper 2.
3. Le Chatelier, H. Experimental researches on the constitution of hydraulic mortars. *Translated by* J. L. Mack. McGraw Publishing Co., New York. 1905.
4. Taylor, H. F. W. J. Chem. Soc. 3682: 1950.
5. Taylor, H. F. W. J. Chem. Soc. 163: 1953.
6. Steinour, H. H. Third international symposium on the chemistry of cement, London. September, 1952. Paper 10.

PREPARATION OF ION-EXCHANGE RESINS[1]

By I. H. Spinner,[2] J. Ciric, and W. F. Graydon

ABSTRACT

Ion-exchange resins as membranes and in granular form have been prepared by the copolymerization of divinylbenzene with various esters of *p*-styrenesulphonic acid and subsequent hydrolysis. The synthesis of the sulphonated styrene monomers is described. Equilibrium data for the sodium–hydrogen ion exchange on a resin prepared in this manner are discussed in terms of postulated variations of sulphonate group environment.

INTRODUCTION

Polystyrenesulphonic acid ion-exchange resins have been prepared previously by the sulphonation of cross-linked polystyrene (5, 7, 10). It is evident that this process yields an ion-exchange resin in which the environment of some sulphonate groups may differ markedly from that of other sulphonate groups. Sulphonate groups may exist in regions which on a micro scale are more or less highly cross-linked, or more or less highly sulphonated than the average for the resin bead. There is, in addition, the possibility of producing benzene nuclei bearing two sulphonate groups. A capacity of 1.2 sulphonate groups per benzene nucleus has been reported (7). Even resins with an over-all capacity of less than one sulphonate group per benzene nucleus may contain disubstituted nuclei near the surface of the bead. Also it is probable that sulphonation of divinylbenzene nuclei occurs.

Observed variations in the mass law "relative affinity coefficients" or equilibrium quotients of ion-exchange resins prepared by the sulphonation of polystyrene have been considered on the implicit assumption that all of the sulphonate groups are identical (2, 4, 6). Thus the exchange groups on a resin have been considered as a fraction of a mole of exchange groups and have been assigned in effect a standard free energy.

Alternatively, if the assumption is made that the variations in the sulphonate group environments are not negligible, the sulphonate groups may be considered as a mixture of exchange groups with various standard free energies. The exchange process is then considered as a number of simultaneous equilibrium reactions. It is apparent that such a process if treated as a single equilibrium reaction would not yield a constant value for the equilibrium quotient, even if resin activity coefficients were unity and swelling pressure variations were negligible. Walton in 1943 (11) recognized that ion-exchangers bearing more than one type of exchange group, such as phenolic, carboxylic, or sulphonic, would give rise to an equilibrium quotient which would be a function of the mole fraction of exchanging ions on the resin. Boyd (3) has mentioned the

[1] *Manuscript received October 5, 1953.*
Contribution from the Department of Chemical Engineering, University of Toronto, Toronto, Ontario, with financial assistance through the School of Engineering Research of the University of Toronto.

[2] *Part of the work described herein was included in a thesis submitted by I. H. Spinner to the Department of Chemical Engineering, University of Toronto, in partial fulfillment of the requirements for the degree of Master of Applied Science in January, 1953.*

possible significance of chemical or structural nonuniformities in monofunctional ion exchange resins. Thus it seems that the possibility of a significant departure from sulphonate group identity ought to be eliminated before variations in the mass law equilibrium quotients are attributed to other causes.

In order to test this hypothesis, it would be of interest to prepare a polystyrenesulphonic acid resin by the copolymerization of monomers which differ in reactivity ratios from the styrene–divinylbenzene system. In addition it would be desirable to use ionogenic monomers which could be converted after polymerization to sulphonic exchange groups without polymer sulphonation. Thus the possibility of disubstitution or divinylbenzene substitution could be eliminated. The esters of *p*-styrenesulphonic acid have been chosen as a group of compounds fulfilling these desiderata.

EXPERIMENTAL

Preparation of Monomers

p-(β-Bromoethyl)-benzenesulphonylchloride

β-Phenylethylbromide (180 gm.) was reacted with 500 ml. of chlorosulphonic acid essentially in accordance with the procedure of Inskeep and Deanin (8), except that the temperature was maintained at 3–5°C. The product was extracted with ether, crystallized at dry ice temperature, and recrystallized rapidly from dry methanol. The yield was 160 gm. (56%), m.p. 54–55°C.

Anal. calc. for $C_8H_8BrSO_2Cl$: C, 33.91%; H, 2.85%; S, 11.31%.

Found:* C, 34.16%; H, 2.89, 2.90%; S, 11.46, 11.50%.

Inskeep and Deanin did not separate the para isomer but they established the presence of the para compound by the preparation and oxidation of *p*-vinylbenzene-N,N′-dimethylsulphonamide. The derivative *p*-(β-bromoethyl)-benzene-N,N′-dimethylsulphonamide was prepared, m.p. 98.5–99°C. Inskeep and Deanin (8) reported m.p. 99–100°C. The derivative *p*-vinylbenzene-N,N′-dimethylsulphonamide was prepared, m.p. 62–63°C. Reported m.p. 63–63.5°C. The derivative *p*-(β-bromoethyl)-benzenesulphonamide was prepared m.p. 184.5–185.5°C. Reported m.p. was 185.5–186°C. The derivative *p*-vinylbenzenesulphonamide was prepared, m.p. 139–140°C.

n-Propyl-p-(β-bromoethyl)-benzenesulphonate

One hundred grams of *p*-(β-bromoethyl)-benzenesulphonylchloride were suspended in 200 gm. of *n*-propanol and allowed to stand until the solid had dissolved. The solution was neutralized slowly at 10°C. with 6 *N* aqueous sodium hydroxide solution. The propyl ester separated as an oil. The suspension was diluted to 500 cc. with cold water. The aqueous layer was saturated with sodium chloride and the oil was extracted with ether. The ether solution was washed with cold water, dried, concentrated in vacuum in the cold, and the ester distilled at 1μ in a Hickman still. The yield was 85.5 gm. (80%), m.p. 6–8°C., n_D^{25} 1.5442, d_{25}^{25} 1.385.

Anal. calc. for $C_{11}H_{15}O_3BrS$: C, 43.00%; H, 4.92%; S, 10.44%; Br, 26.01%.

Found:* C, 43.63%, 43.48%; H, 5.17%, 5.01%; S, 10.30%, 10.57; Br, 25.97%, 25.80%.

**All analyses done by Micro-Tech Laboratories, Skokie, Illinois.*

n-Propyl-p-vinylbenzenesulphonate

Fifty-five grams of *n*-propyl-*p*-(β-bromoethyl)-benzenesulphonate were dissolved in 120 cc. of ethanol and heated to 50°C., 11.5 gm. of potassium hydroxide dissolved in 140 cc. of ethanol at 50°C. were added. The reaction mixture was diluted to 500 cc. with cold water and the ester was extracted with ether. A trace of tertiary butyl catechol was added to the solution, which was then dried. The ether was removed in vacuum in the cold and the ester distilled at 1μ in a Hickman still. A yield of 23.7 gm. (55%) of the colorless liquid product was obtained, n_D^{25} 1.5374, d_{25}^{25} 1.165. Attempts to cause crystallization were unsuccessful.

Anal. calc. for $C_{11}H_{14}O_3S$: C, 58.37%; H, 6.23%; S, 14.17%.
Found:* C, 58.10%, 58.04%; H, 6.26%, 6.40%; S, 14.15%, 14.27%.

A number of similar esters, which are listed below, were prepared by the method given above. Purification was found to be difficult because of decomposition and polymerization. In general the crude product was used for the preparation of the resins.

Methyl-p-(β-bromoethyl)-benzenesulphonate

Using 85 gm. of *p*-(β-bromoethyl)-benzenesulphonyl chloride, 45.0 gm. (75%) of white solid was obtained. After recrystallization from petroleum ether (b.p. 80–100°C.) the solid melted at 66–66.5°C.

Anal. calc. for $C_9H_{11}O_3BrS$: C, 38.72%; H, 3.97%; S, 11.48%; Br, 28.62%.
Found:* C, 38.74%, 38.83%; H, 4.04%, 4.20%; S, 11.65%, 11.75%; Br, 28.64%, 28.38%.

The ethyl and butyl esters of *p*-vinylbenzenesulphonic acid were also prepared. These products were both oils which were difficult to purify. In both cases traces of bromine were found in the final product and in both cases this impure product was used for polymerization. The major impurity was expected to be the bromide which would not interfere with the polymerization.

Polymerization and Hydrolysis

p-Vinylbenzenesulphonamide could not be copolymerized successfully with styrene and divinylbenzene by suspension techniques owing to its water solubility. Solution polymerization in methanol gave a polymer which was hydrolyzed for 72 hr. with 25% hydrochloric acid.

Suspension copolymers of styrene, divinylbenzene, and the other monomers were prepared according to the following recipe based on monomer mixtures totalling 100 gm. The monomers containing 1 gm. of benzoyl peroxide were added to 1000 ml. of the stabilizing solution, in a three-necked standard taper flask fitted with a reflux condenser and stirrer. The stabilizing solution contained 0.1% hydroxyethyl cellulose (Cellosize WPL_H). The speed of the stirrer was adjusted to give beads of the desired size (1 mm. or larger) and the temperature was maintained at 90°C. When the beads had hardened, agitation was stopped and heating continued for an additional 40 hr. The copolymer of *p*-vinylbenzene-N,N′-dimethylsulphonamide was hydrolyzed for 120 hr. with 25% hydrochloric acid under reflux. The ester copolymers were hydrolyzed with 5% sodium

**All analyses done by Micro-Tech Laboratories, Skokie, Illinois.*

hydroxide. The copolymers were then conditioned with 2 *N* sodium chloride and 2 *N* hydrochloric acid, thoroughly rinsed, and the capacities determined by the addition of 2 *N* sodium chloride to a known weight of exchanger and titration with 0.1 *N* sodium hydroxide.

Polymerization charge	Yield, gm.	Maximum capacity, mgm. equiv./gm. dry H resin
20.0 gm. *p*-vinylbenzenesulphonamide 60 gm. divinylbenzene solution (21%)	16.0	1.80
20.2 gm. *p*-vinylbenzene-N,N′-dimethylsulphonamide 20.7 gm. divinylbenzene solution (21%)	30.8	0.94
8.3 gm. *n*-butyl-*p*-vinylbenzenesulphonate 8.3 gm. divinylbenzene solution (21%)	15.3	2.91
8.0 gm. *n*-propyl-*p*-vinylbenzenesulphonate 2.0 gm. divinylbenzene solution (55.4%)	8.0	1.94
21.4 gm. ethyl-*p*-vinylbenzenesulphonate 8.5 gm. divinylbenzene solution (55.4%)	23.6	3.12

One of the difficulties encountered in the preparation of the polymers was the loss resulting from the hydrolysis of the esters in the suspension polymerization. This hydrolysis during polymerization is indicated by the intercept at zero time in the polymer hydrolysis curves of Fig. 1. Thus the nominal cross-linking is

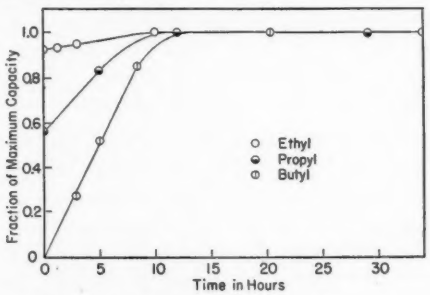

FIG. 1. Hydrolysis of ester copolymers.

somewhat higher than the composition of the polymerization charge would indicate. The polymer prepared from the butyl ester was obtained with greatest yield and was used for the equilibrium determinations. This hydrolyzed resin prepared from the butyl ester is called for conveneince, ester resin.

Equilibrium Quotient Determinations

A sample of about 2 mgm. equiv. of the hydrogen form of the resin was placed in a flask and the capacity determined by the addition of 2 *N* sodium chloride solution and titration with 0.1 *N* sodium hydroxide solution using bromcresol

green as the indicator. The same sample after complete conversion to either the hydrogen or sodium form was equilibrated with solutions containing 0.1 *N* sodium chloride and 0.1 *N* hydrochloric acid solutions in various proportions. After equilibrium had been attained, the solution was analyzed for sodium chloride by evaporation and for hydrochloric acid by titration. The resin sample was drained by suction, thoroughly rinsed, and the hydrogen ion on the resin determined as in the capacity determinations. The sodium ion on the resin was calculated from the difference between the hydrogen ion on the resin and the capacity. In all cases equilibrium quotient values were obtained using resin initially in the hydrogen form and also using resin initially in the sodium form. Equilibrium quotients were also determined in a similar way on a sample of this butyl ester resin which had been sulphonated by treatment with sulphuric acid to a capacity of 4.87 mgm. equiv. per gm.

Ion-exchange Membranes

One of the major difficulties encountered in the preparation of unsupported "homogeneous" ion-exchange membranes by the sulphonation of polystyrene films is the low tensile strengths which the products possess. The copolymerization of ester monomers with divinylbenzene permits the preparation of resins which because of low capacity have much less tendency to swell. For example, such films prepared by the copolymerization of *n*-propyl-*p*-vinylbenzenesulphonate with divinylbenzene had the following characteristics:

TABLE I
ION-EXCHANGE MEMBRANES

Capacity, mgm. equiv./gm. dry hydrogen form	Yield strength, lb. per sq. in.
1.22	2010
1.92	1670
2.72	1270

The detailed properties of films of this sort will be discussed in a subsequent contribution.

DISCUSSION

One of the features of the equilibrium data obtained for the ester resin, as given in Fig. 2, Plot 1, is that the equilibrium quotients are more nearly constant than those reported in the literature for sulphonated polystyrene resins of comparable cross-linking.

The postulate has been made that the constancy of the ion-exchange equilibrium quotient may be a function of the detailed structure of the resin. Hence it is of interest to consider the variations which would be obtained for the equilibrium quotient of a hypothetical ion-exchange resin in which the sulphonate groups are of two types. The environment of type 1 sulphonate groups is assumed to be significantly different from the environment of type 2 sulphonate

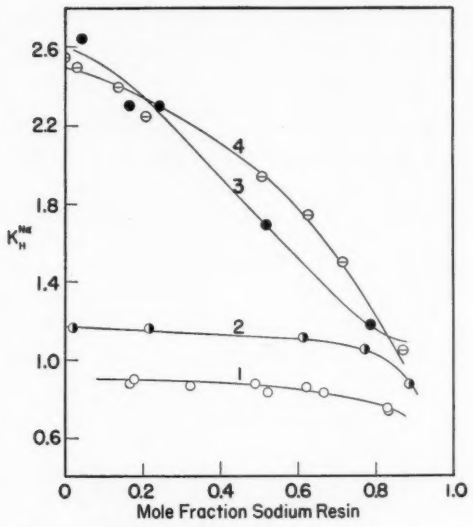

FIG. 2. Equilibrium data:
○ Butyl ester copolymer:—2.91 mgm. equiv./gm. 14–15 mole % divinylbenzene.
◑ Above resin sulphonated:— 4.87 mgm. equiv./gm. 14–15 mole % divinylbenzene.
● Data of Reichenberg (10):— 5.00 mgm. equiv./gm. 15 mole % divinylbenzene.
⊖ Data of Bonner (2):— 5.10 mgm. equiv./gm. 14 mole % divinylbenzene.
Solid lines are results for hypothetical exchanger with parameters as shown in Table II.

groups. All sulphonate groups within a type are assumed to be identical. Activity coefficients are assumed to be unity and swelling pressure variations are assumed to be negligible. For this hypothetical resin the following equations can be written for the uni-univalent exchange of the ionic species A and B:

$$\left(\frac{A}{B}\right)_{R_1} = K_1\left(\frac{A}{B}\right)_s \qquad \left(\frac{A}{B}\right)_{R_2} = K_2\left(\frac{A}{B}\right)_s$$

where: $\left(\frac{A}{B}\right)_{R_1}$ represents the mole ratio of A to B on the type 1 sulphonate groups,
subscript $_{R_2}$ represents type 2 sulphonate groups,
subscript $_s$ represents solution.

These two equations may be combined to give the following expression for the over-all exchange on the resin:

$$\left(\frac{A}{B}\right)_R = \frac{\left[C_1K_1 + (1 - C_1)K_2\right]\left(\frac{A}{B}\right)_s + K_1K_2\left(\frac{A}{B}\right)_s^2}{1 + \left[(1 - C_1)K_1 + C_1K_2\right]\left(\frac{A}{B}\right)_s}$$

where: subscript $_R$ represents the resin as a whole,
C_1 represents the fraction of the whole resin capacity which is type 1 capacity.

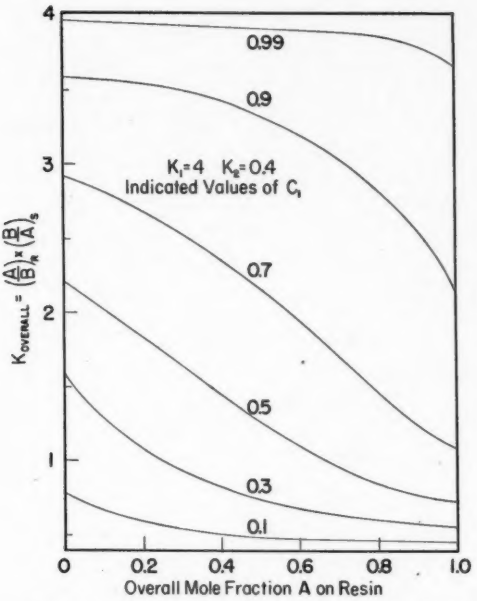

FIG. 3. Equilibrium plots for hypothetical exchanger. Effect of variation in C_1 parameter.

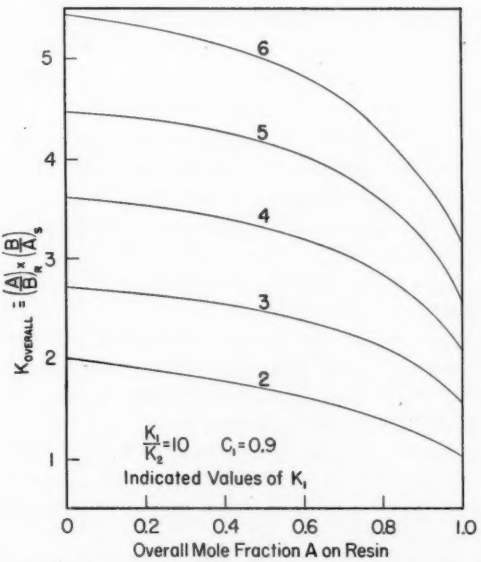

FIG. 4. Equilibrium plots for hypothetical exchanger. Effect of variation in K_1, K_2, parameters.

This equation has been evaluated for various values of the parameter C_1 and the equilibrium quotient versus mole fraction on the resin plots are given in Fig. 3. The effect of variations in the parameters K_1 and K_2 with constant C_1 are illustrated by Fig. 4. These figures illustrate that for the hypothetical resin, variations of C_1 determine the general shape of the equilibrium coefficient plot. Variations in the K_1 and K_2 parameters change the position of the curve on the equilibrium coefficient scale but have only a secondary effect on the form of the curve. This sensitivity to the C_1 parameter is, of course, diminished as the values of K_1 and K_2 approach each other. Thus for the hypothetical resin, the equilibrium plot could be regarded as an indication of the relative amounts of type 1 and type 2 exchange groups. Numerically, C_1 values which approach zero or unity are indicative of uniformity of sulphonate group environment in the resin.

The model described above is considered only as a first approximation to the polystyrenesulphonic ion-exchange resins. However, even this simple assumption permits the correlation of the experimental data. Equilibrium quotients reported (2, 10), can be fitted closely by the equation for the hypothetical resin with the following parameters:

TABLE II
PARAMETER VALUES FOR FIG. 2 PLOTS

Resin type	Curve	C_1	K_1	K_2
Ester resin	1	0.966	0.946	0.00485
Sulphonated ester resin	2	0.966	1.210	0.0275
Sulphonated polystyrene (10)	3	0.873	2.837	0.183
Sulphonated polystyrene (2)	4	0.620	3.950	0.410

Considering only the experimental values of the equilibrium quotients in Fig. 2, curves 1 and 2, and without regard to the hypothetical model, certain conclusions may be drawn. The process of increasing the capacity of the ester resin by sulphonation did not produce any marked increase in the variation of the equilibrium quotient. Hence, the disubstitution of benzene nuclei, and the substitution of divinylbenzene nuclei, if they occur at all, have only a small effect on the constancy of the equilibrium quotient of the ester resin.

The sulphonation of the ester resin also indicated that the value of the equilibrium quotient for an ion-exchange is a function of the capacity of the resin. It is of some interest to note that the equilibrium quotients for the ester resin given in Fig. 2, Curve 1, lie significantly below unity while the values obtained for the same resin after sulphonation are all above 1. These data if correlated on the basis of variations in swelling pressure (6) would require a reversal of sign in the pressure–volume term.

The ester resin prior to sulphonation differed nominally from the sulphonated polystyrene resins only in capacity. All were nominally 14–15 mole % divinyl-

benzene copolymers. After sulphonation the ester resin was nominally similar to the two sulphonated polystyrene resins with respect to capacity and cross-linking. However, the equilibrium quotient data for the sulphonated ester resin was very different from those reported for sulphonated polystyrene resins. This leads to the conclusion that nominal cross-linking and capacity are not sufficient to characterize a polystyrenesulphonic ion-exchange resin.

If the hypothetical model is accepted as a representation of the polystyrene-sulphonic ion-exchange resins, the equilibrium quotient data as given in Fig. 2 may be considered in terms of the relative amounts of sulphonate groups in two different environments. The parameter C_1 in Table II is the fraction of the total groups which are in type 1 environment. This fraction is not changed by the sulphonation of the ester resin. Hence the detailed structure of the polymer is assumed to be the major factor determining the C_1 parameter.

The fraction (C_1) for the ester resin is very different from the C_1 parameter for the sulphonated polystyrene resins. Thus the detailed structure of the ester copolymer is assumed to be very different from that of the styrene–divinylbenzene copolymer.

The detailed structure of a resin is dependent on the reactivity ratios of the monomers used in the polymerization. The data at present available do not permit a prediction of the detailed structure of divinylbenzene copolymers. However, following the methods discussed by Alfrey, Bohrer, and Mark (1) and using the reported data for butyl vinyl sulphonate (9), it has been estimated that monomer reactivity ratios similar to those for *p*-cyanostyrene could be expected for the ester monomer. This indicates that the polymer detail structure for the ester resin could be considerably different from the detail structure of a styrene–divinylbenzene copolymer.

CONCLUSIONS

1. A method of preparation of cross-linked polystyrene–sulphonic ion-exchange resins is described. The resin products have properties which differ considerably from the properties of resins which are prepared by the sulphonation of cross-linked polymers. The method permits the preparation of low capacity ion-exchange resins in which the sulphonate groups are distributed throughout the resin. Unsupported ion-exchange films of high tensile strength may be prepared by this method.

2. The equilibrium quotients for the sodium–hydrogen exchange on resins prepared from the ester monomer are lower and more constant than values reported for similar resins prepared by the sulphonation of cross-linked polystyrene.

3. The nominal cross-linking and capacity are not sufficient to characterize a resin of the polystyrenesulphonic type.

4. Variations in the detailed structure of the resins are postulated as a possible explanation.

5. An equation is developed with parameters which may be interpreted in terms of variations of detailed structure.

ACKNOWLEDGMENT

The authors gratefully acknowledge the financial aid which was received through the School of Engineering Research of the University of Toronto.

REFERENCES

1. ALFREY, T., JR., BOHRER, J. J., and MARK, H. High polymers. Vol. VIII. Copolymerization. Interscience Publishers, Inc., New York. pp. 79–104.
2. BONNER, O. D. and RHETT, V. J. Phys. chem. 57: 254. 1953.
3. BOYD, G. E. Ann. Rev. Phys. Chem. 2: 309. 1951.
4. BOYD, G. E., SCHUBERT, J., and ADAMSON, A. W. J. Am. Chem. Soc. 69: 2818. 1947.
5. D'ALELIO, G. F. U.S. Patent No. 2,366,007. Dec. 26, 1945.
6. GREGOR, H. P. J. Am. Chem. Soc. 73: 643. 1951.
7. GREGOR, H. P., BREGMAN, J. I., GUTOFF, F., BROADLEY, R. D., BALDWIN, D. E., and OVERBERGER, C. G. J. Colloid Sci. 6: 21. 1951.
8. INSKEEP, G. E. and DEANIN, R. J. Am. Chem. Soc. 69: 2237. 1947.
9. OVERBERGER, C. G., BALDWIN, D. E., and GREGOR, H. P. J. Am. Chem. Soc. 72: 4864. 1950.
10. REICHENBERG, D., PEPPER, K. W., and MCCAULEY, D. J. J. Chem. Soc. 493. 1951.
11. WALTON, H. F. J. Phys. Chem. 47: 371. 1943.

THE RATE OF DISSOLUTION OF COPPER[1]

By Benjamin C.-Y. Lu[2] and W. F. Graydon

ABSTRACT

The rate of dissolution of polycrystalline metallic copper in sulphuric acid solutions has been determined as a function of temperature, oxygen pressure, rotation speed, hydrogen ion concentration, sample area, and corroding solution volume. A typical set of conditions would involve a volume of 500 ml. of air-saturated sulphuric acid solution at room temperature and a cylindrical sample of copper of 11 sq. cm. area rotated at 1000 r.p.m. An empirical rate equation has been given which represents the data with an average deviation of ±5%. The rate equation is discussed in terms of a mechanism in which it is postulated that the rate controlling step in the dissolution of copper is the oxidation of cuprous ion at the solution–copper interface.

INTRODUCTION

Although a number of publications have appeared concerning the corrosion of copper, only a few have presented data which are subject to direct interpretation in terms of a mechanism. Many of the rates of corrosion of copper data are based on the metal weight loss divided by the time of the corrosion run. Often no attempt is made to determine the effect of time as a variable. Thus the rate "constants" so obtained may be time dependent. Such rate constants are very difficult to correlate and the prediction of copper corrosion rates is therefore uncertain. In addition, other variables which may be important are often neglected, as, for example, the volume of the corroding medium.

In this work we have attempted to choose and control conditions so that the data obtained may be subject to interpretation on the basis of a mechanism for the dissolution of copper. We have tried to avoid the more complex and more practical situations. It is anticipated that the data so obtained may serve as a basis for further work by providing some indication of the dissolution mechanism under relatively simple conditions.

EXPERIMENTAL

Materials

The copper samples used in this investigation were machined from refinery copper rod and bar stock.* A typical analysis for this material is given below.

Copper	99.95+%	Selenium	0.001%
Nickel	0.0002%	Tellurium	0.0004%
Iron	0.0004%	Bismuth	<0.0001%
Arsenic	0.0004%	Gold	0.003 oz. per ton
Antimony	0.0001%	Silver	0.30 oz. per ton
Lead	0.0002%		

[1] *Manuscript received October 15, 1953.*

Contribution from the Department of Chemical Engineering, University of Toronto, Toronto, Ontario.

Financial assistance was received through the School of Engineering Research of the University of Toronto and the Corrosion Subcommittee of the National Research Council.

[2] *Cominco Research Fellow, 1952-53.*

**We are indebted to Anaconda American Brass Limited of Toronto who supplied the copper stock and the analysis.*

Metallographic examinations of the samples used were obtained.* The photomicrographs are shown in Fig. 1.

All reagents used were "Analar" reagent grade and all solutions were prepared using redistilled water.

Apparatus

The rates of dissolution were determined for a cylinder of copper which was rotated on a lucite rod. The dissolving medium was contained in a pyrex beaker fitted with a lucite baffle plate and cover. The ends of the copper cylinder were protected from the dissolving medium by lucite washers. The beaker was surrounded by a thermostat. An inlet tube for gas bubbling was provided. The baffle plate was adjusted to prevent gas from impinging on the sample.

Procedure

The cylindrical copper sample about three quarters of an inch in length and diameter was polished with 3/0 emery paper, washed with water, and dried with absolute alcohol. The corroding solution was saturated with the oxygen–nitrogen mixture. The sample was rotated on the lucite rod in the corroding medium with the gas bubbling continuously at a rate of about one liter per minute.

Three milliliter samples of the corroding solution were withdrawn from time to time and analyzed for copper using the polarograph (5). Because of the possibility of hydrogen peroxide formation (1) the samples were evaporated to dryness at 110°C. prior to the diffusion current measurements.

RESULTS AND DISCUSSION

The stoichiometry for the dissolution of copper is as follows:

$$Cu + 2H^+ + \tfrac{1}{2}O_2 \rightarrow Cu^{++} + H_2O.$$

All of the data reported here have been obtained under such conditions that hydrogen ion and oxygen were in great excess. The copper flux was of the order of 5×10^{-5} moles per liter per hour. The oxygen concentration in the bulk of the solution was of the order of 2×10^{-4} moles per liter and it was continuously replenished by bubbling. The hydrogen ion concentration in the bulk of the solution was at least 10^{-3} moles per liter and it remained unchanged during each rate determination.

All of the rate data obtained under these conditions are of the typical form shown in Fig. 2. The data have been plotted in subsequent diagrams as the square root of the cupric ion concentration versus the time, since this plot was found to be linear in all cases.

It will be noted that all of the plots in Figs. 3 to 8 show an ordinate intercept implying a copper concentration of about 2×10^{-5} molar at zero time. The data plotted in Fig. 7 show that this intercept may be reduced to a value corresponding to about 2×10^{-6} molar cupric solution at zero time by leaching the dissolution apparatus with hydrochloric acid for considerable periods of time. Thus the intercept is considered to result from the adsorption of copper ions

**Metallographic examinations were done by Dr. W. C. Winegard, Department of Metallurgy, University of Toronto.*

PLATE I

FIG. 1, A. Photomicrograph ×100 typical of samples 1, 2, and 3 cut from bar stock.
FIG. 1, B. Photomicrograph ×100 of sample cut from rod stock.

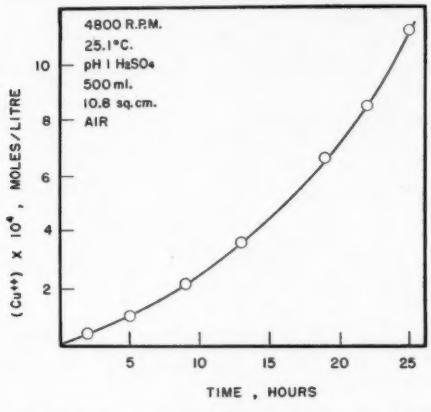

FIG. 2. Rate of dissolution of copper. The figures in the upper left hand corner refer to the sample rotation speed, temperature, acidity, and the acid species in the corroding medium, the volume of the corroding medium, the area of the copper sample, and the composition of the gas in equilibrium with the corroding medium.

on the glass and lucite rod. All of the data given were determined in apparatus which was cleaned and rinsed in the normal way only. Thus each plot shows an intercept which is somewhat variable and which may be regarded as dependent on the history of the dissolution apparatus. In addition it is possible that a portion of the intercept may result from the dissolution of an oxide layer on the metal sample. From the data of Miley and Evans (6) we estimate that this possibility might account for an intercept corresponding to about 2×10^{-6} moles per liter of copper.

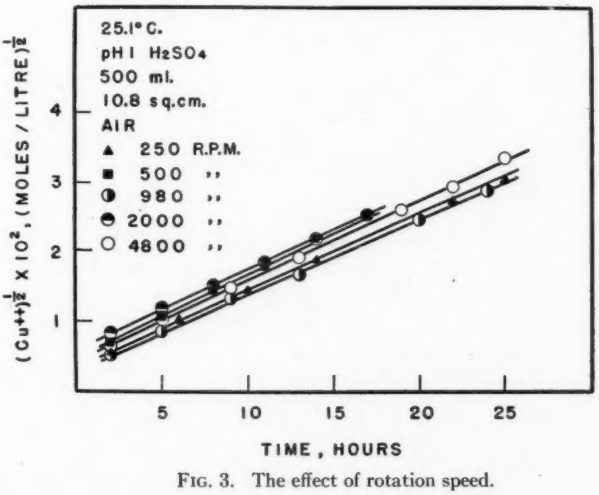

FIG. 3. The effect of rotation speed.

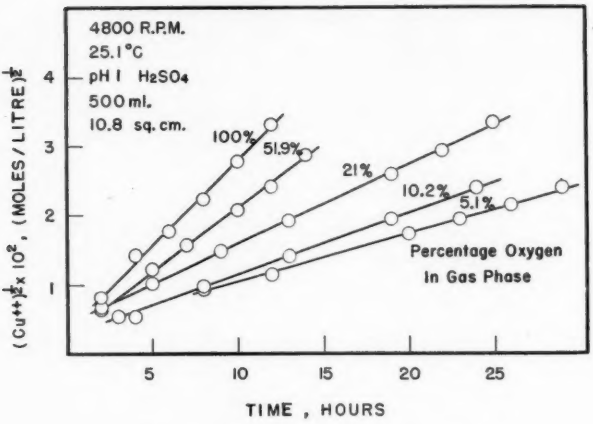

FIG. 4. The effect of oxygen concentration.

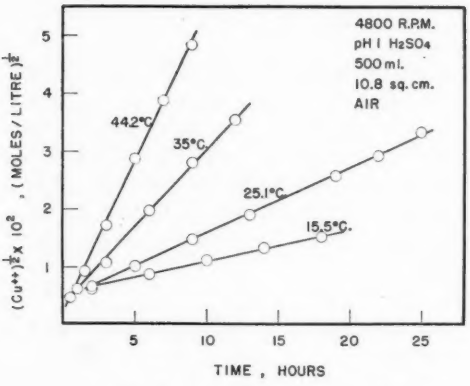

FIG. 5. The effect of temperature.

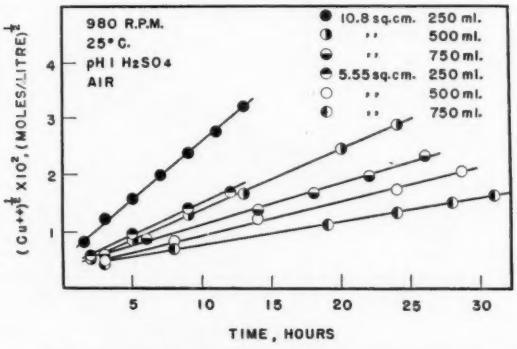

FIG. 6. The effect of sample area and solution volume.

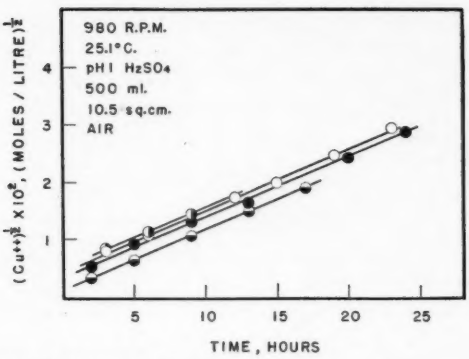

FIG. 7. Variation in the intercept at zero time.
◑ and ○ Apparatus was washed and allowed to stand overnight in redistilled water after each run.
● Apparatus was washed and allowed to stand overnight in 6 *N* hydrochloric acid then rinsed with redistilled water.
◒ Apparatus was washed with five portions of 6 *N* hydrochloric acid. The total time of contact being 48 hr. Rinsed and allowed to stand in pH 1 sulphuric acid overnight.

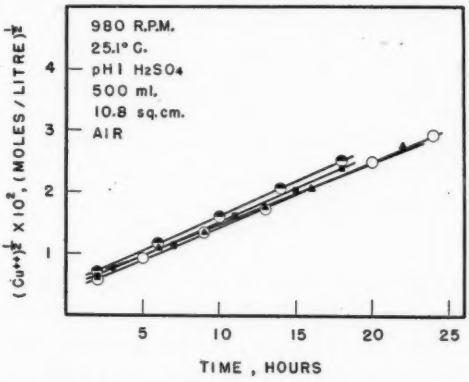

FIG. 8. Rates for various copper samples.
◓ Sample from bar 1. ■ Sample from bar 2. ▲ Sample from bar 3. ○ Sample from rod 4. Three samples from rod 4 were used in obtaining data in Figs. 2–7.

Rate Dependence on Cupric Ion Concentration

The data shown in Figs. 3 to 8 illustrate clearly the linearity of the plot of the square root of the cupric ion concentration against time.

Thus for the conditions used in this work we may write,

$$d[Cu^{++}]/dt = k[Cu^{++}]^{\frac{1}{2}}.$$

This rate dependence has been considered on the basis of the following assumptions.

(1) The cupric-ion concentration in the bulk of the solution is assumed to be essentially the same as the cupric-ion concentration at the copper–solution interface.

(2) The cuprous-ion, cupric-ion equilibrium, $Cu + Cu^{++} \rightleftharpoons 2Cu^{+}$, is assumed to be established at the interface.

(3) The rate of dissolution of copper is assumed to be controlled by the removal of cuprous ions from the interface by a reaction which is first order with respect to cuprous ion.

$$-d[Cu_i^{+}]/dt = K[Cu_i^{+}],$$

where subscript i refers to copper–solution interface, or

$$d[Cu^{++}]/dt = K[Cu_i^{+}].$$

By assumption (2) $$d[Cu^{++}]/dt = KK'[Cu_i^{++}]^{\frac{1}{2}},$$

where $$K' = [Cu^{+}]/[Cu^{++}]^{\frac{1}{2}}.$$

By assumption (1) $$d[Cu^{++}]/dt = KK'[Cu^{++}]^{\frac{1}{2}}.$$

Rate Dependence on Revolutions Per Minute

The possibility that this first order removal of cuprous ion might be by diffusion seems to be eliminated by the very small effect of rotation speed on the rate of dissolution of copper. As may be seen from Table I the variation in rate is less than 8% between 250 and 4800 r.p.m.

TABLE I
SLOPES FROM FIGURE 3

R.p.m.	$(d[Cu^{++}]^{\frac{1}{2}}/dt) \times 10^{3}$
250	1.08
500	1.15
980	1.11
2000	1.09
4800	1.15

These observations confirm and extend the data of Glauner (2) who found little variation between 150 and 350 r.p.m. The possibility that this small effect of r.p.m. might result from diffusion in the pores of an oxide layer seems unlikely because of the low pH of the corroding media. Although some elevation of pH at the interface is to be expected, a hydrogen ion flux of about 10^{-4} gram-ions per liter per hour from a bulk concentration of 10^{-1} gram-ions per liter could have only a negligibly small effect. On the basis of the small effect of sample r.p.m. on the dissolution rate, it is assumed that cuprous ion is removed from the interface by a chemical reaction.

Rate Dependence on Oxygen Pressure

The data plotted in Fig. 9 show that the rate of dissolution of copper is proportional to the square root of the oxygen pressure in the gas phase with which the dissolving solution is equilibrated. Russell and White (7) reported that the corrosion of copper was directly proportional to the concentration of dissolved oxygen. However, in their work the corrosion of copper was measured in terms of weight loss over a 24 hr. period.

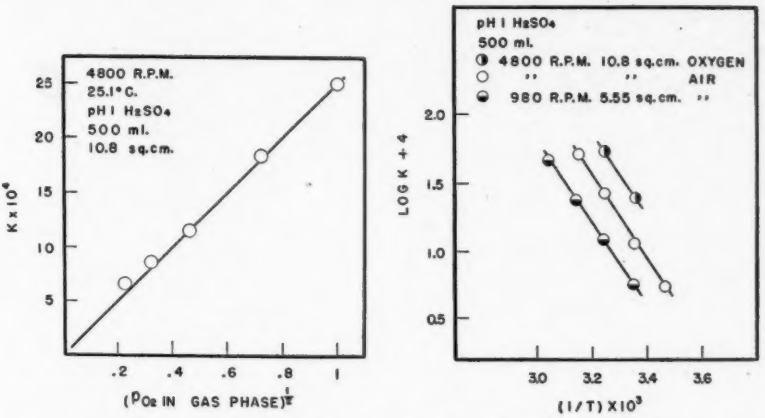

FIG. 9. Rate of dissolution as a function of oxygen concentration. K is slope of plot from Fig. 4.
FIG. 10. Rate of dissolution as a function of temperature. K is slope of plot from Fig. 5.

This method of calculating "rate constants" gives values which are dependent on the time. If the data of Russell and White are recalculated on the basis of the square root of cupric ion concentration versus time, the rate constant obtained is a function of the square root of the oxygen concentration.

To interpret the above we assume that the rate determining reaction in the dissolution of copper under the conditions of these experiments is of the following nature:

$$Cu_i^+ + O_i \rightarrow Cu_i^{++} + O_i^-.$$

This oxygen dependence implies either a surface adsorption isotherm which is linear over the range of oxygen concentrations used or alternatively that the oxygen dissociation occurs in the liquid phase.

Rate Dependence on Temperature

High temperature coefficients for the rate of dissolution of copper have been reported (4). It has been implied that chemical reaction control rather than diffusion control is thereby indicated. As shown in Fig. 10 we find a temperature coefficient corresponding to an activation energy for the dissolution of copper of 14 kilocalories per mole. In order to compute the activation energy for the controlling reaction on the basis of the mechanism postulated above, the activation energy for dissolution must be corrected for the temperature variations of the assumed equilibria.

$$Cu_i^{++} + Cu \rightleftharpoons 2\,Cu_i^+$$
$$O_2 \text{ gas} \rightleftharpoons O_2 \text{ solution}$$
$$O_2 \text{ solution} \rightleftharpoons 2\,O_i.$$

Thermodynamic data are available for the first two of these equilibria but not for the third. The value of 14 kilocalories does not in itself confirm the chemical

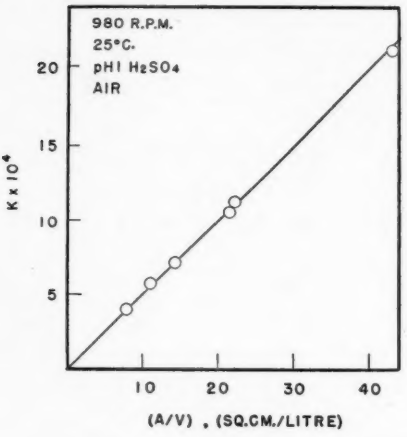

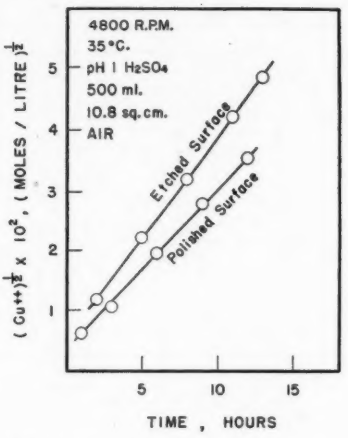

FIG. 11. Rate of dissolution as a function of sample area and solution volume. K is slope of plot from Fig. 8.
FIG. 12. Effect of surface roughness.

reaction control of dissolution. The chemical reaction mechanism which is assumed above is thus based, at present, on the r.p.m. and oxygen concentration dependence data.

From Fig. 10 it may be seen that the activation energy of dissolution is not affected by the variations in the conditions used. These data thus indicate that there is no change in the controlling mechanism.

Rate Dependence on Sample Area and Corroding Solution Volume

The rate of dissolution of copper has been found to be directly proportional to the area of the sample used and inversely proportional to the volume of the corroding medium as shown in Fig. 11. Some dependence on the volume of the solution is required whether the mole rate of dissolution or the concentration rate is considered.

$$d[\mathrm{Cu}^{++}]/dt = K[\mathrm{Cu}^{++}]^{\frac{1}{2}}/v$$

or

$$-d|\mathrm{Cu}|/dt = K[\mathrm{Cu}^{++}]^{\frac{1}{2}}$$

where $|\ |$ represents number of moles.

The area of the sample used in the above correlation was the gross apparent surface area obtained by micrometer measurement. The precision of the data indicates either that the method of polishing produces a true surface area which is proportional to the gross surface area or that the rate of dissolution of copper is not sensitive to minor variations in surface roughness. Large variations in surface roughness, produced by etching in sulphuric acid solution for about 70 hr., did change the rate of dissolution as shown in Fig. 12. This effect of surface roughness was also observed as an increase of rate constant for polished samples which were allowed to dissolve for periods up to 48 hr.

The Effect of Hydrogen Ion Concentration

The data discussed above were obtained in solutions at pH 1. As shown in Fig. 13 there is only a small variation in the rate of dissolution for solutions of lower

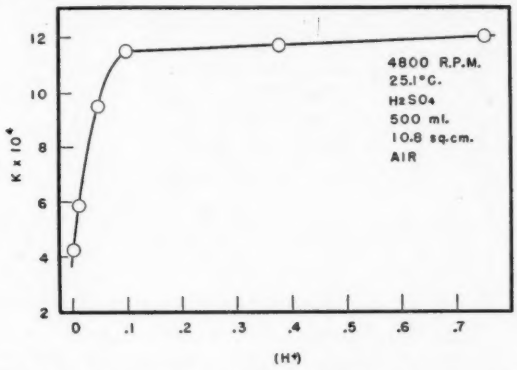

FIG. 13. Rate of dissolution as a function of hydrogen ion concentration. K represents $d[Cu^{++}]^{\frac{1}{2}}/dt$ and $[H^+]$ represents hydrogen ion concentration in gram-ions per liter.

pH than this value. However, the rate decreases sharply for solutions more dilute with respect to hydrogen ion. The reduction in the rate may result from film formation on the metal at higher pH values. Alternatively the rate dependence may result from the adsorption of hydrogen ion at the interface. This latter possibility could be interpreted in terms of a rate controlling reaction of the following nature.

$$Cu_i^+ + H_i^+ + O_i \rightarrow Cu_i^{++} + OH_i$$

Although the data at present do not permit a conclusive choice of reactions for the rate of dissolution of copper, the following set of reactions is presented as a suggestion.

$$\begin{array}{lll} Cu_i^{++} + Cu & \rightleftharpoons 2\,Cu_i^+ & \text{Equilibrium} \\ Cu_i^+ + H_i^+ + O_i & \rightarrow Cu_i^{++} + OH_i & \text{Slow} \\ Cu_i^+ + OH_i & \rightarrow Cu_i^{++} + OH_i^- & \end{array}$$

$$Cu + 2H^+ + \tfrac{1}{2}O_2 \rightarrow Cu^{++} + H_2O$$

This mechanism satisfies the rate dependence on cupric ion and oxygen concentrations and also the stoichiometry.

Empirical Equation and Range of Application

The data discussed above may be summarized in the form of the following equation

$$-d|\overline{Cu}|/dt = K\, e^{-(14.1/RT)}\, [Cu^{++}]^{\frac{1}{2}}\, (p_{O_2})^{\frac{1}{2}},$$

where $|\overline{Cu}|$ represents moles of copper per unit area

or $$d[Cu^{++}]/dt = 4.92 \times 10^6 \, e^{-(14.1/RT)} \, [Cu^{++}]^{\frac{1}{2}} \, (p_{O_2})^{\frac{1}{2}} \, \frac{A}{V}$$

where

$$[Cu^{++}] = 0\text{–}2.5 \times 10^{-3} \text{ moles/liter}$$
$$T = 288\text{–}328°K.$$
$$A = 5.47\text{–}11.10 \text{ sq. cm.}$$
$$V = 0.25\text{–}0.75 \text{ liter}$$
$$t = 3\text{–}30 \text{ hr.}$$
$$(p_{O_2}) = 0.051\text{–}1.00 \text{ atm.}$$
$$[H^+] = 0.1\text{–}0.75 \text{ gm. ions per liter.}$$

The value 4.92×10^6 is an average of 40 plots. The average deviation from this value was $\pm 0.24 \times 10^6$ absolute or about 5%.

The major portion of this work was done with three samples cut from a single copper rod. In order to eliminate the possibility that the data obtained might be applicable to that rod only, the data given in Fig. 8 were obtained. As shown in Table II below the data obtained for four samples, each refined at a different time were found to be within the average deviation stated above.

TABLE II
RATE CONSTANTS FROM FIGURE 8

Sample	$K \times 10^{-6}$	Deviation from average	Deviation from 4.92×10^6
1	4.94	.22	.02
2	4.78	.06	.14
3	4.39	.33	.53
4	4.78	.06	.14
Average	4.72	±.17	±.21

Very little data have been published for the dissolution of copper with time as a variable. Data of this sort have been presented by Katz (3) for nearly neutral or slightly acidified corroding media.

From our own data on hydrogen ion concentration dependence it is apparent that no correlation of rate constant values is to be expected. However, the data of Katz when replotted as the square root of the weight loss against time gave linear plots for time up to 30 days at 16.3°C. This would indicate that the equilibrium reaction assumed in our mechanism is a valid assumption for the conditions used by Katz.

Glauner (2) has also published data for the dissolution of copper as a function of time. Three of his experiments were conducted in sulphuric acid media. Although the experimental conditions were different from those described in this paper, Glauner's data when replotted on the square root basis gave linear plots up to 50 hr. as illustrated in Fig. 14. In addition the rate constants calculated from Glauner's replotted data were in good agreement with the constant determined above as shown in Table III.

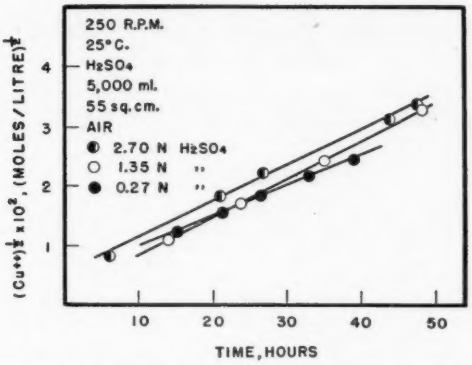

FIG. 14. Replotted data of Glauner (2) for polycrystalline copper of random orientation in sulphuric acid.

TABLE III
RATE CONSTANTS FROM DATA OF GLAUNER (2)

Sulphuric acid normality	Rate constant for Glauner's data	Rate constant predicted	Deviation
0.27	4.36×10^6	4.92×10^6	0.56
1.35	5.31×10^6	4.92×10^6	0.39
2.70	5.13×10^6	4.92×10^6	0.21
Average	4.93×10^6	4.92×10^6	± 0.39

CONCLUSIONS

An empirical equation has been established for the rate of dissolution of metallic copper in oxygenated sulphuric acid solutions.

It is suggested that the rate of dissolution of copper is controlled by the rate of oxidation of cuprous ion at the copper–solution interface.

ACKNOWLEDGMENTS

The authors gratefully acknowledge the financial aid which was received through the School of Engineering Research of the University of Toronto and the Corrosion Subcommittee of the National Research Council.

We are also indebted to the Consolidated Mining and Smelting Company for providing the Cominco Research Fellowship for one of us (B.C.–Y.Lu) for the session 1952–1953.

REFERENCES

1. DUNSTAN, W. R., JOWETT, H. A. D., and GOULDING, E. J. Chem. Soc. 87: 1548. 1905.
2. GLAUNER, R. Z. physik. Chem. A, 142: 67. 1929.
3. KATZ, W. Metalloberfläche, Ausgabe A, 4: 101. 1950.
4. KING, C. V. and WEIDENHAMMER, L. J. Am. Chem. Soc. 58: 602. 1936.
5. KOLTHOFF, I. M. and LINGANE, J. J. Polarography. Revised reprint. Interscience Publishers, Inc., New York, N.Y. 1946. pp. 215–20, 278–80.
6. MILEY, H. A. and EVANS, U. R. Nature, 139: 283. 1937.
7. RUSSELL, R. P. and WHITE, A. Ind. Eng. Chem. 19: 116. 1927.

THERMODYNAMIC PROPERTIES OF XENON IN THE CRITICAL REGION[1]

By H. W. Habgood[2] and W. G. Schneider

ABSTRACT

Using the detailed compressibility data in the critical region of xenon given in the preceding paper, supplemented by measurements of Beattie, Barriault, and Brierley over a wider range of temperatures and densities, thermodynamic properties have been calculated for the critical region—extending from the critical temperature to 50° above it and from low densities to somewhat above the critical density. The values of C_v at the critical density are in good agreement with those calculated from acoustical data at temperatures higher than $T_c + 1°$; closer to the critical temperature however, the C_v values derived from the equation of state data become much greater than those derived from the acoustic data. This difference can be accounted for by dispersion effects in the high frequency acoustic data near the critical point.

INTRODUCTION

The compressibility data for xenon in the region of the critical point presented in the preceding paper (4) have been used to derive the thermodynamic properties in this region. By supplementing our data with those of Beattie, Barriault, and Brierley (1), we have been able to extend these calculations down to low densities and to a temperature 50° above the critical in order to show the variations in the various properties near the critical point. Of the various thermodynamic properties, the specific heat is of particular interest. C_v has a finite maximum at the critical point and C_p becomes infinite.

Somewhat similar calculations have previously been carried out for carbon dioxide by Michels, Bijl, and Michels (5). They found an increase in C_v at the critical point of about 10 cal./mole deg. over the low density value, but their measurements (6) in this region were not very detailed. A recent calorimetric study, also on carbon dioxide, by Michels and Strijland (7) indicated values in excess of 20 cal./mole deg. for the increase in C_v. These authors give references to earlier workers who have attempted to determine C_p or C_v at the critical point calorimetrically.

From our measurements $(\partial P/\partial T)_V$ can be evaluated more accurately than $(\partial V/\partial T)_P$ or $(\partial P/\partial V)_T$. We have therefore used the following relationships in calculating thermodynamic properties:

$$[1] \qquad C_{V_{T,\rho}} - C_{V_{T,0}} = \lim_{\rho_1 \to 0} \left[-T \int_{\rho_1}^{\rho} \frac{1}{\rho^2} \left(\frac{\partial^2 P}{\partial T^2} \right)_\rho d\rho \right],$$

$$[2] \qquad (C_p - C_v)_{T,\rho} = \frac{T}{\rho^2} \frac{(\partial P/\partial T)_\rho^2}{(\partial P/\partial \rho)_T},$$

$$[3] \qquad (S^* - S)_{T,\rho} = \lim_{\rho_1 \to 0} \int_{\rho_1}^{\rho} \left[\frac{1}{\rho^2} \left(\frac{\partial P}{\partial T} \right)_\rho - \frac{R}{\rho} \right] d\rho,$$

[1] *Manuscript received October 7, 1953.*
Contribution from the Division of Pure Chemistry, National Research Council, Ottawa, Canada. Issued as N.R.C. No. 3164.
[2] *National Research Council of Canada Postdoctorate Fellow.*

$$[4] \qquad (A^* - A)_{T,\rho} = \lim_{\rho_1 \to 0} \int_{\rho_1}^{\rho} \left(\frac{RT}{\rho} - \frac{P}{\rho^2} \right) d\rho,$$

where the starred quantities refer to an ideal gas. From these quantities the differences from the ideal gas values for E, H, and F may be readily calculated as:

$$[5] \qquad (E^* - E)_{T,\rho} = (A^* - A) + T(S^* - S),$$

$$[6] \qquad (F^* - F)_{T,\rho} = (A^* - A) + (RT - [P/\rho]),$$

$$[7] \qquad (H^* - H)_{T,\rho} = (E^* - E) + (RT - [P/\rho]).$$

CALCULATIONS AND DISCUSSION

Evaluation of $(\partial P/\partial T)$ *and* $(\partial^2 P/\partial T^2)$

It was necessary to determine $(\partial P/\partial T)$ and $(\partial^2 P/\partial T^2)$ over the temperature range of interest and at all densities down to zero density. From our measurements we first determined $(\partial P/\partial T)$ and $(\partial^2 P/\partial T^2)$ as functions of temperature for each isochore. Some attempts were made to fit analytical functions to the data but none of these were very promising and graphical methods were used.

Large-scale plots of P against T were made for each density. For convenience, the difference between the measured pressure and that corresponding to an arbitrary isochore of constant slope was plotted. The various isochores formed a family of gently curved lines, each branching from the vapor pressure curve at the maximum temperature of liquid–vapor coexistence. For most of the isochores sufficient measurements had been taken to establish independently the vapor pressure curve for each. These curves were in good agreement except for two which seemed obviously displaced to slightly lower pressures, presumably by small constant errors, and which were so drawn in order to minimize the effect on the slopes.

The temperature of branching for each isochore taken as the temperature of apparent intersection of the two arms of the curve was in good agreement with the observed maximum coexistence temperature. Within 0.01° of the critical temperature, the maximum coexistence temperature was not always determined but was sometimes taken from the coexistence curve of Weinberger and Schneider (9) which appeared to agree with our observations in this region.

The average deviation of the measured pressures from the curves was less than 0.001 atm. and a few deviations were as high as 0.004 atm. The greatest scatter occurred in the neighborhood of the branching point where the high specific heat and slow approach to equilibrium made determinations more difficult. This was partly compensated by the greater number of measurements taken in this region.

From these curves pressures were read off at intervals of 0.01° to 0.05° and from the differences were constructed curves of $(\partial P/\partial T)$ vs. $T - T_c$ where T_c is the critical temperature, 16.590°C. These curves are shown in

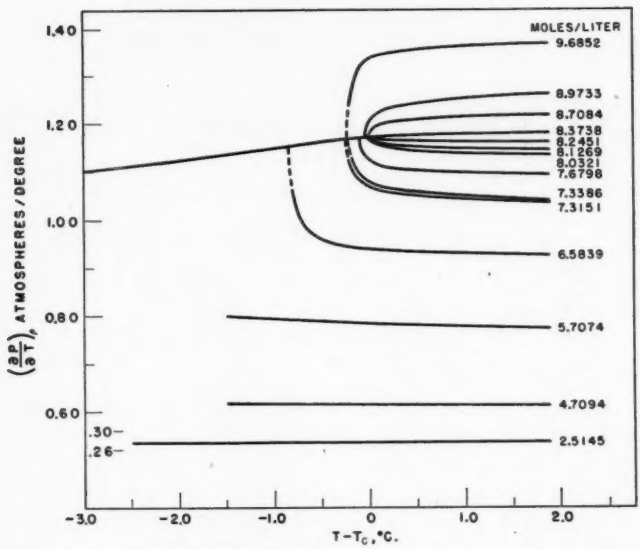

FIG. 1. $(\partial P/\partial T)_\rho$ from smoothed isochores.

Fig. 1. From them, curves of $(\partial^2 P/\partial T^2)$ vs. $T - T_c$ were obtained by a similar process.

Qualitatively, the general shape of the curves in Fig. 1 appears to be clearly established, particularly at densities away from the critical where the slope, i.e. $(\partial^2 P/\partial T^2)$, increases regularly in absolute value with decreasing temperature towards the condensation point, presumably becoming infinite when a second phase appears. Near the critical density we have assumed that the curves have the same general nature although the value of the slope very close to the branch point can be little more than a rough estimate. To some extent, the uncertainty can be reduced by smoothing $(\partial P/\partial T)$ against ρ for various temperatures.

The degree of uncertainty in the curves of $(\partial P/\partial T)$ may be illustrated by plotting directly the values of $\Delta P/\Delta T$ obtained from the differences between successive measurements. This is done in Fig. 2 for the isochore at 7.68 moles/liter where the measured pressures exhibit an average degree of scatter from a smooth curve. On this plot of the observed $(\Delta P/\Delta T)$'s we have superimposed $(\partial P/\partial T)$ obtained from the smoothed P–T curve as described above. It can be seen that while $(\partial P/\partial T)$ is fairly well established over most of the range, a relatively small shifting near the steep portion of the curve could cause a considerable change in the value of $(\partial^2 P/\partial T^2)$ at a particular temperature.

At low densities $(\partial^2 P/\partial T^2)$ is very small and the data of Beattie *et al.* (1) covering a wide temperature range were more satisfactory than measurements restricted to just a few degrees. Their data were also used to cover the complete density range at higher temperatures so that C_v could be calculated at

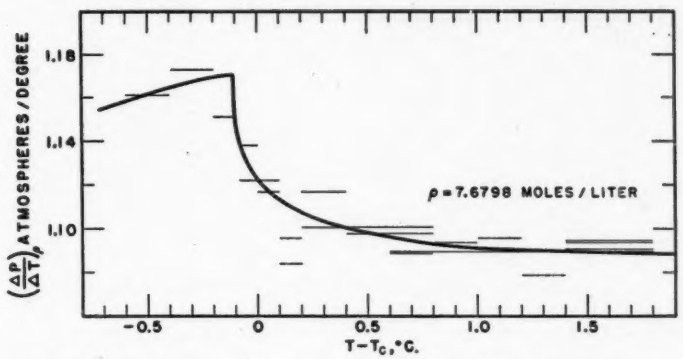

FIG. 2. Experimental values of $(\Delta P/\Delta T)$ at 7.68 moles/liter. Solid curve taken from Fig. 1 obtained from smoothed isochore.

temperatures up to 50° above the critical. Unfortunately, their measurements did not extend below 16.65° so there is added uncertainty in the derivatives at the lowest temperatures.

While the required derivatives could be calculated from the Beattie–Bridgeman equation of state [1] or the virial equation [2] to which their data were fitted, these values, particularly $(\partial^2 P/\partial T^2)$, would require correction by a graphical analysis of the relatively large and systematic deviations. It was therefore more convenient and almost equally accurate to apply graphical methods directly to their data. This was done by drawing smooth curves through plots of $\Delta P/\Delta T$ vs. T obtained from readings at successive temperatures for each density. The first interval was 8.35° and succeeding intervals were 25°. Away from the critical point the curves could be drawn with but slight uncertainty and near the critical point, values of $(\partial P/\partial T)$ from our measurements could be fitted smoothly to these plots. Values of $(\partial^2 P/\partial T^2)$ were then obtained as the slopes of these curves.

Heat Capacities at Constant Volume and Constant Pressure, C_v and C_p

To determine C_v according to Equation 1 values of $-(1/\rho^2)\ \partial^2 P/\partial T^2$ were plotted against density for various temperatures. The limiting value at zero density is $(\partial^2 B/\partial T^2)$ where B is the second virial coefficient in the virial equation

$$[8] \qquad PV = RT + \frac{B(T)}{V} + \ldots .$$

This was estimated from the virial coefficients given by Beattie *et al.* (2). These curves are shown in Fig. 3, the points for some temperatures being omitted for clarity. C_v was then determined by graphical integration of the area under the appropriate curve from 0 to the desired density.

The values for C_v are given in Table I, the zero density value for an inert gas being 2.98 cal./mole deg. These values are plotted as functions of density in Fig. 4. For the three temperatures nearest the critical the values appear to

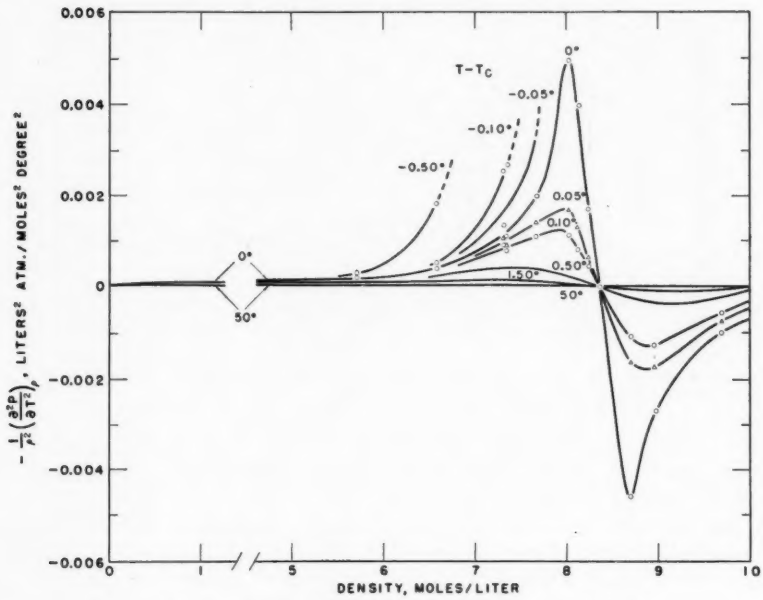

FIG. 3. Curves of $-(1/\rho^2)\ (\partial^2 P/\partial T^2)$ vs. ρ for evaluation of C_v.

TABLE I

HEAT CAPACITY AT CONSTANT VOLUME, C_v (CAL./MOLE DEG.)

$T-T_c$, °C. \ Density, moles/l.	0	3	6	7	8	8.37	9	10
0.00	2.98	4.56	7.12	9.92	23.1	30.1	16.4	(6.5)
0.05	2.98		7.07	9.66	18.1	20.4	14.6	(7.4)
0.10	2.98		7.03	9.33	16.0	17.5	13.5	(8.1)
0.20	2.98		6.94	8.92	13.8	14.6	11.9	8.3
0.50	2.98		6.66	8.22	10.80	11.11	10.08	8.01
1.50	2.98	4.48	6.47	7.39	8.04	8.01	7.65	6.79
5.00	2.98	4.23	5.78	6.29	6.50	6.47	6.30	5.81
10.00	2.98	4.02	5.25	5.58	5.71	5.68	5.56	5.23
50.00	2.98	3.58	4.06	4.14	4.16	4.15	4.12	4.01

be obviously in error at the highest densities. This is believed to be mainly the result of fewer measurements having been made at densities greater than the critical. For the vapor region below the critical temperature it was possible from the curves of Fig. 3 to estimate C_v at densities approaching the condensation point but these values are considerably more uncertain.

The density of maximum C_v is 8.37 moles/liter which is somewhat lower than the critical density found by Weinberger and Schneider, 8.42 moles/liter. As mentioned in the preceding paper, our observations of coexistence temperatures and densities would support the critical density found by Weinberger

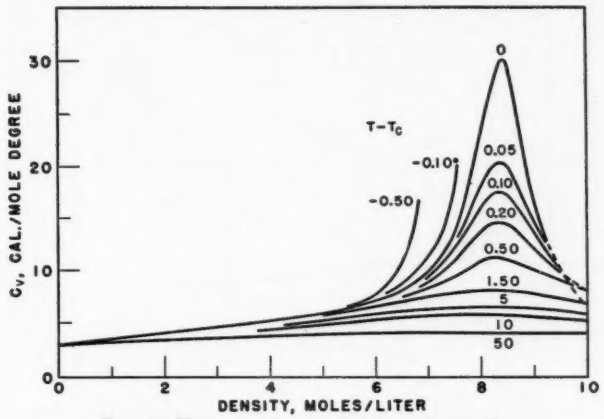

FIG. 4. Heat capacity at constant volume, C_v.

and Schneider or even a slightly higher value. It would thus appear that the density of maximum C_v is slightly lower than the critical density as determined from the coexistence curve, but the evidence is rather incomplete. It is difficult to give a reliable estimate of the probable accuracy of these C_v values. The principal source of uncertainty is in the determination of $(\partial^2 P/\partial T^2)$ and the nature of this uncertainty is such as to favor somewhat lower values of C_v.

The values of C_v determined in this manner may be compared with C_v calculated from the measured velocity of sound, c, using the relationship

$$[9] \qquad c^2 = \frac{Tv^2}{C_v}\left(\frac{\partial P}{\partial T}\right)^2 - v^2\left(\frac{\partial P}{\partial v}\right).$$

Chynoweth and Schneider (3) measured ultrasonic velocities at the critical density at frequencies of 250 kc. and 1250 kc. Using these velocities and the values of $(\partial P/\partial T)$ and $(\partial P/\partial v)$ found in the present work we have calculated C_v from Equation 9 from 0.4° below the critical temperature to 2.0° above. These values together with the values for the critical density from Table I are presented in Fig. 5. There is seen to be an apparent frequency dependence in C_v near the critical point, the value from PVT data, which may be considered to represent a low frequency limit, being much greater than the high frequency values. Such behavior has been noted previously by Schneider and Chynoweth (8) and explained in terms of structural relaxation processes near the critical point. It was also pointed out that the variation with frequency should more properly be considered to be not in C_v but in the quantities $(\partial P/\partial T)$ and $(\partial P/\partial v)$, i.e., the critical system is very highly compressible to a slowly applied force but only slightly compressible to very rapidly varying pressure changes. The region of this dispersion is confined to within less than 1° of the critical temperature. This is also the region of maximum ultrasonic absorption and of visible opalescence. Above $T_c + 1°$ the C_v's obtained from the two

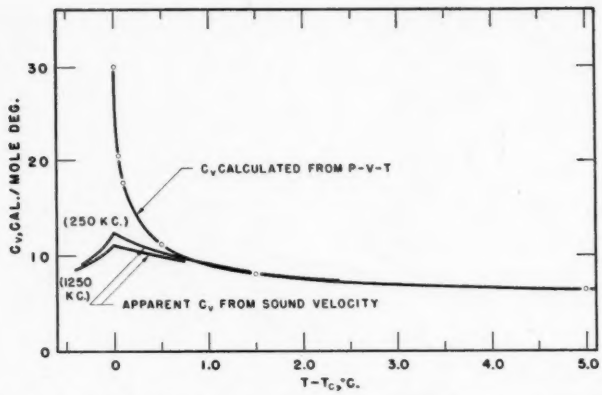

FIG. 5. C_v at the critical density compared with C_v calculated from acoustical measurements.

sources agree within 3% which may be regarded as a very satisfactory check. It is perhaps worth pointing out that to determine C_v using Equation 9 and the velocity of sound, one need know only the first derivatives at the point in question rather than second derivatives at all densities down to zero.

To calculate $C_p - C_v$ according to Equation 2, $(\partial P/\partial \rho)_T$ was required. For our data this was estimated from large-scale plots of the $P - \rho$ isotherms and for the data of Beattie *et al.* it was determined from the Beattie–Bridgeman equation supplemented by a graphical analysis of the deviations. $(\partial P/\partial T)$ had already been obtained in determining $(\partial^2 P/\partial T^2)$ for the evaluation of C_v. The resulting values of $C_p - C_v$ are given in Table II and plotted in Fig. 6.

TABLE II
$C_p - C_v$ (CAL./MOLE DEG.)

$T - T_c$, °C. \ Density, moles/l.	0	3	6	7	7.5	8	8.37	9	10
0	1.99	11.08	160	818	2700	23,400		13,600	200
0.10	1.99				2200	12,300	30,600	9,500	
0.20	1.99				1800	7,300	13,800	4,200	
0.50	1.99				1300	2,700	4,600	1,600	
1.50	1.99	10.76			610	900	955	640	
5.00	1.99	10.20	75	146	198	206	196	177	94.3
10.00	1.99	9.50	51.4	79.9	91.2	98.2	99.7	88.7	66.2
50.00	1.99	6.34	14.7	17.0	17.7	18.0	18.0	17.7	16.8

The very large values are determined almost entirely by the $(\partial P/\partial \rho)$ term in the denominator which becomes very small near the critical point. The uncertainty in this region is consequently much greater than elsewhere. Fig. 6 shows the rather wide range of densities over which C_p is very large.

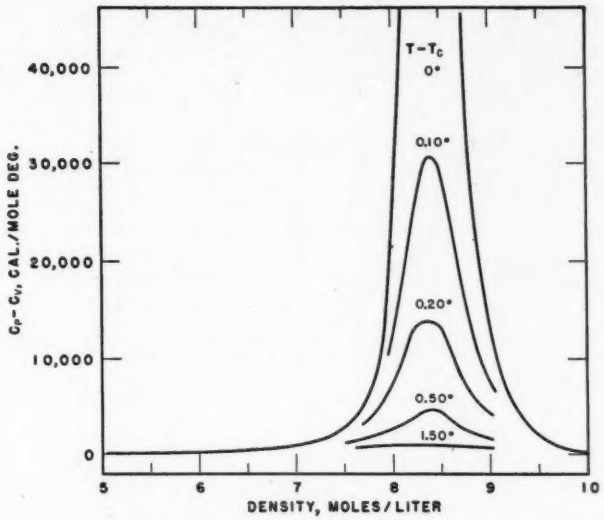

FIG. 6. Difference in heat capacities at constant volume and at constant pressure, $C_p - C_v$.

This explains, in part, the difficulty in achieving a true temperature equilibrium in a system near the critical point.

Entropy

Evaluation of the entropy in excess of the ideal gas value was straightforward once $(\partial P/\partial T)$ had been determined. The quantity $[(1/\rho^2)(\partial P/\partial T) - R/\rho]$ was found to be approximately constant over the whole density range. It was plotted against density and the area under the curve determined graphically. The limiting value at zero density is (dB/dT), B being the second virial coefficient in Equation 8. The probable errors are estimated to be 1% or less.

TABLE III

ENTROPY, $S^* - S$ (CAL./MOLE DEG.)

Density, moles/l. / $T - T_c$, °C.	3	6	7	8	8.37	9	10
0	0.771	1.498	1.722	1.928	1.999	2.089	2.228
0.05		1.497	1.720	1.924	1.995	2.087	2.228
0.10		1.496	1.719	1.922	1.992	2.085	2.227
0.20		1.495	1.716	1.917	1.987	2.081	2.224
0.50	0.768	1.490	1.710	1.908	1.977	2.073	2.219
1.50	0.761	1.477	1.693	1.886	1.955	2.052	2.202
5.00	0.747	1.443	1.651	1.841	1.911	2.010	2.170
10.00	0.726	1.401	1.603	1.789	1.860	1.962	2.128
50.00	0.627	1.205	1.388	1.569	1.641	1.751	1.938

Table III lists the values of $(S^* - S)$ where S^* is the value for an ideal gas. The entropy considered as a function of density and temperature shows only a slight abnormality near the critical point.

Other Properties

To calculate the differences from the ideal gas values of A, the Helmholtz free energy, the quantity $[RT/\rho - P/\rho^2]$ was found to give an almost linear plot against density and differences from linearity could be plotted on a large scale and evaluated graphically. A small constant correction was applied to make the measurements of Beattie *et al.* consistent with ours since their pressures were slightly higher. $A^* - A$ is tabulated in Table IV.

TABLE IV
HELMHOLTZ FREE ENERGY, $A^* - A$ (CAL./MOLE)

$T - T_c$, °C. \ Density, moles/l.	3	6	7	8	8.37	9	10
0.00	221.03	410.57	466.22	518.15	536.96	566.56	611.66
1.50	219.91	408.36	463.69	515.33	534.03	563.49	608.37
5.00	217.32	403.04	457.58	508.54	528.03	556.07	600.38
10.00	213.66	395.94	449.45	499.47	518.59	546.15	589.64
50.00	186.84	344.44	390.42	433.15	449.31	472.67	508.98

The differences from the ideal gas values of E, the internal energy, F, the Gibbs free energy, and H, the enthalpy, were calculated directly according to Equations 5 to 7 and are given in Tables V, VI, and VII.

TABLE V
INTERNAL ENERGY, $E^* - E$ (CAL./MOLE)

$T - T_c$, °C. \ Density, moles/l.	3	6	7	8	8.37	9	10
0	444.46	844.73	965.14	1076.67	1116.20	1171.88	1257.37
1.50	441.61	838.48	956.75	1064.57	1103.57	1161.14	1249.67
5.00	437.56	828.28	944.30	1051.20	1091.24	1148.64	1240.05
10.00	431.34	815.83	929.83	1035.84	1076.07	1134.17	1227.60
50.00	399.86	753.77	861.96	966.15	1006.91	1067.47	1167.28

TABLE VI
GIBBS FREE ENERGY, $F^* - F$ (CAL./MOLE)

$T - T_c$, °C. \ Density, moles/l.	7	8	8.37	9	10
0.00	842.73	919.54	946.66	987.33	
1.50	838.32	914.57	941.63	982.20	
5.00	827.26	902.79	930.59	969.61	1028.65
10.00	812.23	886.60	913.93	952.33	1009.68
50.00	698.16	757.78	777.39	805.27	843.69

TABLE VII
ENTHALPY, $H^* - H$ (CAL./MOLE)

$T - T_c$, °C. \ Density, moles/l.	7	8	8.37	9	10
0.00	1341.65	1478.06	1525.90	1592.65	
1.50	1331.38	1463.81	1511.17	1579.85	
5.00	1313.98	1445.45	1493.80	1562.18	1668.32
10.00	1292.61	1422.97	1471.41	1540.35	1647.64
50.00	1169.70	1290.78	1334.99	1400.07	1501.99

These properties likewise, considered as functions of density and temperature, do not show any pronounced effect at the critical point. If they are considered as functions of pressure and temperature as is often done, the behavior at the critical point becomes more extreme reflecting the P–ρ relationship here.

ACKNOWLEDGMENT

We wish to thank Mr. W. A. Evans for assistance with the calculations.

REFERENCES

1. BEATTIE, J. A., BARRIAULT, R. J., and BRIERLEY, J. S. J. Chem. Phys. 19: 1219. 1951.
2. BEATTIE, J. A., BARRIAULT, R. J., and BRIERLEY, J. S. J. Chem. Phys. 19: 1222. 1951.
3. CHYNOWETH, A. G. and SCHNEIDER, W. G. J. Chem. Phys. 20: 1777. 1952.
4. HABGOOD, H. W. and SCHNEIDER, W. G. Can. J. Chem. 32: 000. 1954.
5. MICHELS, A., BIJL, A., and MICHELS, C. Proc. Roy. Soc. (London), A, 160: 376. 1937.
6. MICHELS, A., BLAISSE, B., and MICHELS, C. Proc. Roy. Soc. (London), A, 160: 358. 1937.
7. MICHELS, A. and STRIJLAND, J. Physica, 18: 613. 1952.
8. SCHNEIDER, W. G. and CHYNOWETH, A. J. Chem. Phys. 19: 1607. 1951.
9. WEINBERGER, M. A. and SCHNEIDER, W. G. Can. J. Chem. 30: 422. 1952.

THE HYDROLYSIS OF THE CONDENSED PHOSPHATES[1]

II (A). THE ROLE OF THE HYDROGEN ION IN THE HYDROLYSIS OF SODIUM PYROPHOSPHATE

II (B). THE DISSOCIATION CONSTANTS OF PYROPHOSPHORIC ACID

By J. D. McGilvery and Joan Pedley Crowther

ABSTRACT

The general rate equations for the hydrolysis of pyrophosphate anion proposed by Muus have been proved to be inapplicable over the pH range 2.0 to 11.0. A general rate equation is proposed which is based on the assumption that each anionic species of pyrophosphoric acid hydrolyzes at a rate which depends on its concentration, and that the only role of the hydrogen ion concentration is to determine the proportion of each species present in the solution. A mechanism for the hydrolysis of pyrophosphate anion is suggested.

The dissociation constants of pyrophosphoric acid have been determined at 65.5°C. for the concentration range 0.08 to 0.18 molar.

II (A). THE ROLE OF THE HYDROGEN ION IN THE HYDROLYSIS OF SODIUM PYROPHOSPHATE

Introduction

In the first paper (9) on this subject, it was established that the rate of hydrolysis of sodium pyrophosphate in solution depended on the hydrogen ion concentration but that this hydrolysis was a first order reaction when a constant hydrogen ion concentration was maintained. Fig. 1 is the curve obtained by

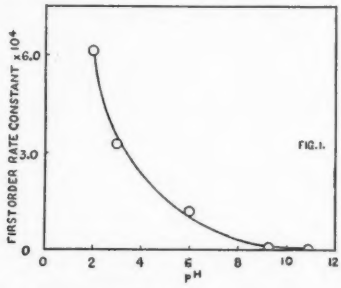

Fig. 1. Effect of pH on rate of hydrolysis of sodium pyrophosphate in solution.

plotting the first order rate constants against the pH of the pyrophosphate solutions.

Although there was no evidence of a base-catalyzed hydrolysis over the entire pH range investigated, Fig. 1 shows that hydrogen ion is an effective catalyst. It is also evident that the relationship between the rate of hydrolysis and the hydrogen ion concentration is not a simple one. If, for example, we assume a rate equation of the form:

$$[1] \qquad dC/dt = -k[H^+]^n C$$

[1] *Manuscript received September 28, 1953.*
Contribution from the Department of Chemistry and the Electric Reduction Company Fellowship, Ontario Research Foundation, Toronto, Ontario.

where C is the concentration of pyrophosphate at time t (this includes all the various forms of pyrophosphate which may be present in the solution, as e.g. $H_4P_2O_7$, $H_3P_2O_7^-$, etc.), it is found that the data are best satisfied by a value of about 1/4 for n.

It is difficult to conceive of a mechanism which would satisfactorily explain the fractional power of the hydrogen ion concentration. Furthermore, this rate equation implies that all the pyrophosphate forms in the solution are equivalent in so far as hydrolysis is concerned. Although this might be true, it seems likely that the reactivity of a pyrophosphate anion is influenced by its degree of ionization. Since pyrophosphoric acid is polybasic, pyrophosphate solutions contain a variety of partially dissociated anionic species, the relative amounts of which are determined by the pH of the solution and the dissociation constants. Thus, in a pyrophosphate solution, the following ions would be present: $H_3P_2O_7^{1-}$, $H_2P_2O_7^{2-}$, $HP_2O_7^{3-}$, and $P_2O_7^{4-}$. In addition some undissociated acid $H_4P_2O_7$ would occur. For convenience in what follows, references to the anionic species present in pyrophosphate solutions will include the undissociated $H_4P_2O_7$.

Rate Equations for Hydrolysis of Sodium Pyrophosphate Solution

If the ease of hydrolysis of sodium pyrophosphate solutions depends on the anionic species, i.e. $H_3P_2O_7^{1-}$, $H_2P_2O_7^{2-}$, $HP_2O_7^{3-}$, $P_2O_7^{4-}$, and $H_4P_2O_7$, it is doubtful whether any simple rate equation which takes the form of equation [1] will fit the observational data over a wide range of hydrogen ion concentrations.

A general rate equation for the acid-catalyzed hydrolysis of pyrophosphate solutions is:

$$[2] \qquad -dC/dt = f_0[H^+][H_0] + f_1[H^+][H_1] + f_2[H^+][H_2] + f_3[H^+][H_3] + f_4[H^+][H_4],$$

where C is the concentration of pyrophosphate at time t;

t is the reaction time;

$[H^+]$ is the hydrogen ion concentration;

$[H_0]$, $[H_1]$, $[H_2]$, $[H_3]$, and $[H_4]$ are the concentrations of $P_2O_7^{4-}$, $HP_2O_7^{3-}$, $H_2P_2O_7^{2-}$, $H_3P_2O_7^{1-}$, and $H_4P_2O_7$, respectively;

$f_0[H^+]$, $f_1[H^+]$, $f_2[H^+]$, $f_3[H^+]$, and $f_4[H^+]$ are the hydrogen ion concentration functions associated with the rate of hydrolysis of H_0, H_1, H_2, H_3, and H_4, respectively;

and $[H_0]$, $[H_1]$, $[H_2]$, $[H_3]$, and $[H_4]$ are interrelated in accordance with the dissociation constants of pyrophosphoric acid.

In order to find a rate equation for the hydrolysis of pyrophosphate solutions which fitted the experimental data, simple forms of equation [2] were investigated.

Muus (7) considered that the different anionic species of pyrophosphoric acid reverted at different rates, and the rate equation which he proposed assumed that:

$$f_i[H^+] = k_i[H^+]$$

where the k_i's are the hydrolysis rate constants associated with the various anionic species and $i = 0, 1, 2, 3, 4$. Thus Muus' (7) rate equation took the form:

$$[3] \qquad -dC/dt = [H^+]\{k_0[H_0] + k_1[H_1] + k_2[H_2] + k_3[H_3] + k_4[H_4]\},$$

where the symbols represent the same factors as above. Muus (7), however, only investigated the hydrolysis of pyrophosphate solutions over the pH range 0.91 to 1.4, and hence could not verify equation [3] outside this range. Within this pH range, Muus (7) believed that the anion $H_3P_2O_7^-$ (H_3) was the only species of pyrophosphate that played a significant rate determining role, and hence equation [3] reduced to the form:

$$[3a] \qquad -dC/dt = k_3[H^+][H_3].$$

Another simple assumption from a kinetic point of view is that each anionic species hydrolyzes at its own specific rate which is quite independent of the hydrogen ion concentration. In such a picture, the only role of the hydrogen ion is to determine the proportion of each species present in the pyrophosphate solution, and thus

$$f_i[H^+] = k_i, \text{ where } i = 0, 1, 2, 3, 4.$$

The rate equation would then be:

$$[4] \qquad -dC/dt = k_0[H_0] + k_1[H_1] + k_2[H_2] + k_3[H_3] + k_4[H_4],$$

where the symbols represent the same factors as above.

The above rate equations cannot be tested for applicability without a knowledge of the relationship between the proportions of each anionic species and the pH of the solution. To obtain such information the dissociation constants of a pyrophosphoric acid solution of suitable concentration were determined at 65.5°C. (II(B)) and the following values obtained:

$$[5] \quad K_1 = [H^+][H_3]/[H_4] = 0.107 \ (\sigma = 0.009 \text{ where } n = 4),$$

$$[6] \quad K_2 = [H^+][H_2]/[H_3] = 7.58 \times 10^{-3} \ (\sigma = 0.20 \times 10^{-3} \text{ where } n = 6),$$

$$[7] \quad K_3 = [H^+][H_1]/[H_2] = 1.45 \times 10^{-6} \ (\sigma = 0.04 \times 10^{-6} \text{ where } n = 7),$$

$$[8] \quad K_4 = [H^+][H_0]/[H_1] = 9.81 \times 10^{-9} \ (\sigma = 0.13 \times 10^{-9} \text{ where } n = 12),$$

where σ is the standard deviation (3) and equations 5, 6, 7, and 8 are simultaneous. The following equations relate the concentration of the various pyrophosphate anionic species to the dissociation constants, the hydrogen ion concentration, and the total pyrophosphate concentration:

$$[9] \qquad [H_0] = K_1K_2K_3K_4\,C\,R,$$

$$[10] \qquad [H_1] = K_1K_2K_3[H^+]\,C\,R,$$

$$[11] \qquad [H_2] = K_1K_2[H^+]^2\,C\,R,$$

$$[12] \qquad [H_3] = K_1[H^+]^3\,C\,R,$$

$$[13] \qquad [H_4] = [H^+]^4\,C\,R,$$

where $R = 1/(K_1K_2K_3K_4 + K_1K_2K_3[H^+] + K_1K_2[H^+]^2 + K_1[H^+]^3 + [H^+]^4)$. Fig. 2, which shows the effect of the pH of the solution on the proportions of the various anionic species of pyrophosphate present, was constructed with the aid of equations [9] to [13], and the dissociation constants.

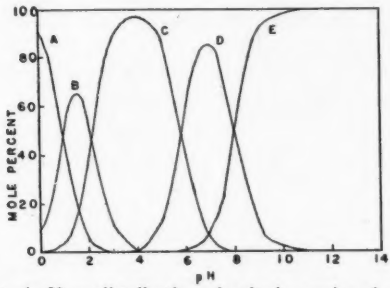

FIG. 2. Effect of pH on distribution of anionic species of pyrophosphate.
A, $H_4P_2O_7$; B, $H_3P_2O_7^{1-}$; C, $H_2P_2O_7^{2-}$; D, $HP_2O_7^{3-}$; E, $P_2O_7^{4-}$.

The necessary data to solve equations [3] and [4] for the rate constants k_0, $k_1 \ldots k_4$ have now been obtained, and are summarized in Table I. It will be noted that Abbott's (1) rate data have been included in Table I. Since our studies only covered the pH range 2.0–11.0, no rate data were obtained in the pH region where the concentration of $H_4P_2O_7$ was comparatively large. Therefore Abbott's (1) data, at pH 0.91 where 53% $H_4P_2O_7$ was present, were used to obtain a rough approximation of the rate constant, k_4. It should be noted that values of k_4, based on this data, are a very rough estimate since Abbott's (1) data were obtained for a 0.05 *M* pyrophosphate solution at 75°C. and our data were obtained for a 0.12 *M* solution at 65.5°C. Furthermore, Abbott (1) did not measure the rate at a constant hydrogen ion concentration.

Evaluation of k_i's Assuming Muus' (7) Rate Equation

$$[3] \qquad -dC/dt = [H^+]\{k_0[H_0] + k_1[H_1] + k_2[H_2] + k_3[H_3] + k_4[H_4]\}.$$

Since the hydrolysis of sodium pyrophosphate is a first order reaction at constant hydrogen ion concentration:

$$[14] \qquad kC = [H^+]\{k_0[H_0] + k_1[H_1] + k_2[H_2] + k_3[H_3] + k_4[H_4]\},$$

where k is the over-all first order rate constant.

Using the data in Table I, equation [14] was solved and the following values obtained for the various rate constants:

$$k_0 = 3.9 \times 10^5 \text{ min.}^{-1},$$
$$k_1 = -7.2 \times 10^6 \text{ min.}^{-1},$$
$$k_2 = 0.40 \text{ min.}^{-1},$$
$$k_3 = -0.21 \text{ min.}^{-1},$$
$$k_4 = 9.4 \times 10^{-2} \text{ min.}^{-1}$$

Since k_1 and k_3 are negative values implying that orthophosphate anion was forming pyrophosphate anion (against which there is experimental evidence (4, 5)), equation [14] and hence equation [3] is inapplicable. If equation [3*a*] were applicable, the values for k_0, k_1, k_2, and k_4 would have been insignificant or zero, and k_3 would have been positive. Since neither condition was satisfied on solving, equation [3*a*] is not applicable. Thus Muus' (7) rate equations are not applicable over the pH range 2.0–11.0.

TABLE I

CONCENTRATION OF INDIVIDUAL PYROPHOSPHATE ANIONS IN MOLES PYROPHOSPHATE PER LITER AT VARIOUS HYDROGEN ION CONCENTRATIONS

pH	Hydrogen ion concentration	First order rate constant (k in min.$^{-1}$)	$P_2O_7^{4-}$ $[H_0]$	$HP_2O_7^{3-}$ $[H_1]$	$H_2P_2O_7^{2-}$ $[H_2]$	$H_3P_2O_7^{1-}$ $[H_3]$	$H_4P_2O_7$ $[H_4]$
10.9	1.26×10^{-11}	4.8×10^{-6}	1.22×10^{-1}	1.57×10^{-4}	—	—	—
9.3	5.01×10^{-10}	1.0×10^{-5}	1.17×10^{-1}	5.95×10^{-3}	2.06×10^{-6}	—	—
7.34	4.57×10^{-8}	5.0×10^{-5}*	2.11×10^{-2}	9.83×10^{-2}	3.10×10^{-3}	—	—
6.0	1.0×10^{-6}	1.25×10^{-4}	7.07×10^{-4}	7.21×10^{-2}	4.97×10^{-2}	—	—
3.0	1.0×10^{-3}	3.31×10^{-4}	—	1.56×10^{-4}	1.08×10^{-1}	1.42×10^{-2}	1.33×10^{-4}
2.5	3.16×10^{-3}	4.35×10^{-4}*	—	—	8.57×10^{-2}	3.57×10^{-2}	1.06×10^{-3}
2.0	1.0×10^{-2}	5.42×10^{-4}	—	—	5.01×10^{-2}	6.62×10^{-2}	6.18×10^{-3}
0.91	1.23×10^{-1}	2.22×10^{-3}**	—	—	3.41×10^{-3}	5.54×10^{-2}	6.37×10^{-2}

Rate constant source: Fig. 1.
**Rate constant source: Abbott (1).*

Evaluation of k_i's Assuming Alternate Rate Equation

$$[4] \qquad -dC/dt = k_0[H_0] + k_1[H_1] + k_2[H_2] + k_3[H_3] + k_4[H_4],$$

where the symbols represent the same factors as above.

Using data from Table I, equation [4] was solved, and the following approximate values for the rate constants were obtained:

$$k_0 = 4.7 \times 10^{-6} \text{ min.}^{-1},$$
$$k_1 = 5.25 \times 10^{-5} \text{ min.}^{-1},$$
$$k_2 = 2.8 \times 10^{-4} \text{ min.}^{-1},$$
$$k_3 = 7.3 \times 10^{-4} \text{ min.}^{-1},$$
$$k_4 = 3.9 \times 10^{-3} \text{ min.}^{-1}.$$

These rate constants satisfy two necessary conditions for the applicability of equation [4] in that they are positive numbers and approximately satisfy all the data in Table I. However, the equation is not necessarily acceptable. This equation (developed by following the reasoning outlined earlier) contains sufficient constants that even if the reaction mechanism were not as pictured, a good fit might conceivably be obtained. However, since equation [4] permits a reasonable explanation of the role of the hydrogen ion and since our data approximately fit this equation, it is proposed as the general rate equation for the hydrolysis of pyrophosphate anion pending evidence to the contrary.

Order of Reaction

At constant hydrogen ion concentration equation [4] reduces to an equation for a first order reaction as demanded by the experimental data. Rewriting equation [4]:

$$[4a] \qquad -\frac{dC}{dt} = C \text{ times the expression}$$
$$\left\{\frac{K_1K_2K_3K_4k_0 + K_1K_2K_3[H^+]\,k_1 + K_1K_2[H^+]^2\,k_2 + K_1[H^+]^3\,k_3 + [H^+]^4\,k_4}{K_1K_2K_3K_4 + K_1K_2K_3[H^+] + K_1K_2[H^+]^2 + K_1[H^+]^3 + [H^+]^4}\right\}$$

where C is the pyrophosphate concentration at time t.

The bracketed expression is a constant when the hydrogen ion concentration is constant, and equation [4a] becomes:

$$[15] \qquad -dC/dt = kC,$$

where k is the over-all first order rate constant.

Mechanism of Reaction

The magnitude of the rate constants evaluated for equation [4] indicate that the order of stability of the pyrophosphate anionic species is: $P_2O_7^{4-} > HP_2O_7^{3-} > H_2P_2O_7^{2-} > H_3P_2O_7^{1-} > H_4P_2O_7$. In addition the rate equation formulated implies that the hydrolysis is a simple reaction between water molecules and these various pyrophosphate anions. The question now arises as to why there should be such profound differences in the ease of hydrolysis of the various species.

A possible explanation might be based on the assumption that the primary steps in the hydrolysis are the formation of loose bonds between a phosphorus

atom and the oxygen atom of a water molecule, and between the oxygen atom of the P–O–P linkage and the hydrogen atom of the water molecule:

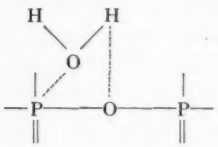

It follows that the orientation of a water molecule approaching a pyrophosphate anion will be of considerable importance. As is well known, water is a polar molecule—the fractional negative charge being located on the oxygen atom, and the fractional positive charge being located on the hydrogen atoms. It seems reasonable to suppose that, as the phosphorus atom becomes less negative, the possibility of a water molecule approaching in the required orientation for hydrolysis increases. Since the negativity of the phosphorus atoms in the various pyrophosphate anionic species decreases in the order: $P_2O_7^{4-}$, $HP_2O_7^{3-}$, $H_2P_2O_7^{2-}$, $H_3P_2O_7^{1-}$, $H_4P_2O_7$, it follows that the rate of hydrolysis of these various species will increase in the same order.

II (B). THE DISSOCIATION CONSTANTS OF PYROPHOSPHORIC ACID

Introduction

The dissociation constants of pyrophosphoric acid have been determined by Abbott and Bray (2) at 18°C. Muus (7) has also determined the second and third dissociation constants at 40°C., but he based his calculations on the assumption that the first dissociation constant was greater than two. As Abbott and Bray (2) found the value 0.14 for the first dissociation constant, Muus' (7) values seem unlikely. Since insufficient thermodynamic data were available to accurately extrapolate Abbott and Bray's (2) values, these dissociation constants were determined at 65.5°C.

Experimental

Procedure and Results

An electrometric titration method was employed for the determination of the dissociation constants. A mechanically stirred solution of sodium pyrophosphate, maintained at 65.5 ± 0.1°C., was titrated with 3 *N* hydrochloric acid. The changes in the pH of the solution were plotted against the volume of acid added. The inflection points occurred at pH 10.0, 6.8, and 4.0. In the light of considerations which will be discussed shortly, regions between these inflection points were selected for further investigation.

Having thus delineated the critical pH regions, accurate measurements of the acid increments and the resulting pH values were made. Fifty milliliter portions of a 0.179 molar sodium pyrophosphate solution were titrated with 1 *N* hydrochloric acid. The experimental conditions were as described above, but particular care was taken to minimize the time required in obtaining the measurements. None of the samples were subjected to acid conditions for more than five minutes. This procedure was followed on three separate portions of the sodium pyro-

phosphate solution, and the averages of the results are recorded in Table II. For the same volume of acid added, the pH readings checked within ±0.02 units. In the present experiments, the accuracy of the pH measurements is the limiting factor in calculating the dissociation constants.

TABLE II

Volume *N* HCl added (ml.)	Average pH*	Average hydrogen ion concentration (gew/l.)
0	9.52	3.020×10^{-10}
2.00	8.48	3.311×10^{-9}
3.00	8.26	5.495×10^{-9}
4.00	8.05	8.913×10^{-9}
6.00	7.66	2.188×10^{-8}
12.00	6.06	8.710×10^{-7}
12.50	5.95	1.122×10^{-6}
13.00	5.87	1.349×10^{-6}
14.00	5.65	2.239×10^{-6}
19.00	2.88	1.318×10^{-3}
19.50	2.72	1.905×10^{-3}
20.00	2.57	2.692×10^{-3}
24.00	1.90	1.259×10^{-2}
25.00	1.78	1.660×10^{-2}

**These figures are the averages of three separate determinations.*

Theory of the Method

It is possible to estimate the dissociation constants of a polybasic acid such as pyrophosphoric by a method of successive approximations utilizing the data obtained from an electrometric titration of the material. Although theoretically all of the anionic species will be present at a given pH, the concentrations of one or more of the species will always be small enough at that pH to be neglected in making approximate calculations of the dissociation constants (6). These values of the dissociation constants may then be used to estimate the concentrations of the components which were neglected in the first approximation. The appropriate corrections may then be made, and the dissociation constants estimated for a second time. This process may, of course, be continued indefinitely, but it was found that the second approximation was satisfactory in every case.

As stated earlier the inflection points in the electrometric titration curve of sodium pyrophosphate at 65.5°C. occur at the pH values: 10.0, 6.8, and 4.0, and at these points the concentration of $P_2O_7^{4-}$, $HP_2O_7^{3-}$, and $H_2P_2O_7^{2-}$ respectively, predominate. At intermediate points two of the species predominate, and it is in these regions that the most accurate estimations of the dissociation constants may be obtained. The method of calculation also permits the inclusion of one minor component in obtaining the first approximation of K_1, K_2, and K_3. The pH regions chosen and the anionic species assumed to be present in calculating the first approximations to the various dissociation constants are shown in Table III. The predominating species in each pH range are underlined.

TABLE III

Dissociation constant	Anionic species assumed present	pH Range
K_1	$\underline{H_4P_2O_7}$, $\underline{H_3P_2O_7^{1-}}$, $\underline{H_2P_2O_7^{2-}}$	< 2
K_2*	$\underline{H_3P_2O_7^{1-}}$, $\underline{H_2P_2O_7^{2-}}$, $HP_2O_7^{3-}$	2.5–3.0
K_3	$\underline{H_2P_2O_7^{2-}}$, $\underline{HP_2O_7^{3-}}$, $P_2O_7^{4-}$	5.6–6.2
K_4	$\underline{HP_2O_7^{3-}}$, $\underline{P_2O_7^{4-}}$	8.0–9.5

**In the pH region below pH 4, $H_4P_2O_7$, $H_3P_2O_7^{1-}$, and $H_2P_2O_7^{2-}$ predominate, but little $H_4P_2O_7$ would be present in the region 2.5 – 3.0. At 18°C., Abbott and Bray's (2) dissociation constants indicate that approximately three per cent $H_4P_2O_7$ is present at pH 3. Furthermore, Thomsen's (8) heat of ionization data for the reaction:*

$$H_4P_2O_7 \rightleftharpoons H^+ + H_3P_2O_7^-,$$

show that increasing the temperature will shift the equilibrium to the right. Thus the first approximation to the second dissociation constant was calculated assuming that no $H_4P_2O_7$ was present in the pH range 2.5–3.0.

Calculation of the Fourth Dissociation Constant (K_4)

The initial solution of sodium pyrophosphate is in the pH range where $P_2O_7^{4-}$ and $HP_2O_7^{3-}$ are the only anionic species present in significant amounts. Therefore to a first approximation:

[1] $$H_0 + H_1 = P_T,$$

where H_0 and H_1 are the amounts of $P_2O_7^{4-}$ and $HP_2O_7^{3-}$ respectively, and P_T is the total amount of pyrophosphate present.

A quantity of acid is now added which lowers the pH of the solution but does not take it out of the range where $P_2O_7^{4-}$ and $HP_2O_7^{3-}$ are the only major components. However, the acid does convert an equivalent amount of $P_2O_7^{4-}$ to $HP_2O_7^{3-}$ as indicated by the equation:

[2] $$P_2O_7^{4-} + H^+ \rightleftharpoons HP_2O_7^{3-}.$$

The amounts of $P_2O_7^{4-}$ and $HP_2O_7^{3-}$ present become $(H_0 - H_a^+)$ and $(H_1 + H_a^+)$ respectively, when H_a^+ is the equivalent amount of acid added.

The dissociation constant K_4 is defined by the expression:

[3] $$K_4 = [H^+]\,[P_2O_7^{4-}]/[HP_2O_7^{3-}].$$

Since a ratio of anionic species is involved, it is immaterial which units are employed to express the amounts of $P_2O_7^{4-}$ and $HP_2O_7^{3-}$ so long as they are identical for both species. Therefore, before adding acid:

[4] $$K_4 = [H^+]_i\, H_0/H_1.$$

After adding acid:

[5] $$K_4 = [H^+]_f\,(H_0 - H_a^+)/(H_1 + H_a^+),$$

where $[H^+]_i$ and $[H^+]_f$ are the initial and final hydrogen ion concentrations. Equating [4] and [5] and substituting $(P_T - H_1)$ for H_0, a quadratic in H_1 is obtained which may be solved. Although two positive solutions are obtained,

only one solution gives reasonable results in the calculation of K_4. The latter calculation is made by simply substituting values for H_1, H_0 (which is $P_T - H_1$), and $[H^+]_f$ in equation [4].

Calculation of the Third Dissociation Constant (K_3)

Having now obtained a value for K_4 it is possible to determine K_3 using much the same procedure as in estimating K_4.

A quantity of acid is added to the initial solution of sodium pyrophosphate such that the resulting pH of the solution lies in the range 5.6–6.2 where $HP_2O_7^{3-}$ and $H_2P_2O_7^{2-}$ are the major components and $P_2O_7^{4-}$ is the largest minor component. The acid added is consumed in two reactions:

[2] $$P_2O_7^{4-} + H^+ \rightleftharpoons HP_2O_7^{3-}$$

and

[6] $$HP_2O_7^{3-} + H^+ \rightleftharpoons H_2P_2O_7^{2-}.$$

If the total amount of acid added is H_b^+ and an amount B is consumed in reaction [2], then $(H_b^+ - B)$ is consumed in reaction [6]. Consequently the amounts of the various species after the addition of the acid are as follows:

$$\begin{array}{lll} P_2O_7^{4-} & = H_0 - B & = P_T - H_1 - B, \\ HP_2O_7^{3-} & = H_1 + B - (H_b^+ - B) & = H_1 - H_b^+ + 2B, \\ H_2P_2O_7^{2-} & = & H_b^+ - B. \end{array}$$

If the hydrogen ion concentration at this point is designated by $[H^+]_f$ then by substituting in equation [3], the following equation is obtained:

[7] $$K_4 = [H^+]_f (P_T - H_1 - B)/(H_1 + H_b^+ + 2B).$$

Since B is the only unknown it may be evaluated.

The third dissociation constant K_3 is defined by the expression:

[8] $$K_3 = [H^+] [HP_2O_7^{3-}]/[H_2P_2O_7^{2-}].$$

Therefore:

[9] $$K_3 = [H^+]_f (H_1 - H_b^+ + 2B)/(H_b^+ - B).$$

Since all the factors on the right-hand side of equation [9] are known, K_3 may be evaluated.

Calculation of the Second (K_2) *and First* (K_1) *Dissociation Constants*

The second and first dissociation constants are determined in a similar manner making the appropriate assumptions with regard to the anionic species present.

Table IV illustrates the distribution of the various anionic species in each pH range used in the calculation of dissociation constants.

H_c^+ and H_d^+ are the amounts of acid added to the pyrophosphate solution to change from the initial pH to pH values in the ranges 2.5–3.0 and <2.0 respectively.

C is the amount of acid consumed in the reaction:

[6] $$HP_2O_7^{3-} + H^+ \rightleftharpoons H_2P_2O_7^{2-},$$

when H_c^+ is the amount of acid added.

TABLE IV
DISTRIBUTION OF ANIONIC SPECIES ASSUMED IN CALCULATION OF DISSOCIATION CONSTANTS

Amounts ionic species assumed present	Dissociation constant			
	K_1	K_2	K_3	K_4
	pH range			
	8.0–9.5	5.6–6.2	2.5–3.0	< 2.0
H_0	$P_T - H_1 - H_a^+$	$P_T - B$	—	—
H_1	$H_1 + H_a^+$	$H_1^+ + 2B - H_b^+$	$P_T - C$	—
H_2	—	$H_b^+ - B$	$P_T + 2C - H_c^+ - H_1$	$P_T - D$
H_3	—	—	$H_c^+ - C - P_T + H_1$	$2P_T + 2D - H_d^+ - H_1$
H_4	—	—	—	$H_d^+ - D - 2P_T + H_1$

Similarly D is the amount of acid consumed in the reaction:

[10] $$H_2P_2O_7^{2-} + H^+ \rightleftharpoons H_3P_2O_7^{1-},$$

when H_d^+ is the amount of acid added.

On substituting the data in Table II into the approximate equations developed in this manner, the following average values for the dissociation constants of pyrophosphoric acid were obtained:

$$K_1 = 0.122 \quad (\sigma = 0.014 \text{ where } n = 4),$$
$$K_2 = 7.29 \times 10^{-3} \quad (\sigma = 0.37 \times 10^{-3} \text{ where } n = 6),$$
$$K_3 = 1.45 \times 10^{-6} \quad (\sigma = 0.04 \times 10^{-6} \text{ where } n = 7),$$
$$K_4 = 9.72 \times 10^{-9} \quad (\sigma = 0.12 \times 10^{-9} \text{ where } n = 12),$$

where σ is the standard deviation (3).

Using the above dissociation constants and the method of calculation outlined, the following set of values were obtained as a second approximation to the dissociation constants. Further approximations did not alter the values appreciably.

$$K_1 = 0.107 \quad (\sigma = 0.009 \text{ where } n = 4),$$
$$K_2 = 7.58 \times 10^{-3} \quad (\sigma = 0.20 \times 10^{-3} \text{ where } n = 6),$$
$$K_3 = 1.45 \times 10^{-6} \quad (\sigma = 0.04 \times 10^{-6} \text{ where } n = 7),$$
$$K_4 = 9.81 \times 10^{-9} \quad (\sigma = 0.13 \times 10^{-9} \text{ where } n = 12),$$

where σ is the standard deviation (3).

The standard deviations indicate the precision of the experiment but not the accuracy.

Since no attempt was made to distinguish between the concentration and the activity of these anionic species, the concentration range in which the dissociation constants are applicable must be specified. Abbott and Bray (2) found that the values of the dissociation constants changed very little with the molarity of the pyrophosphate solution if that concentration were higher than 0.08 molar. Thus the dissociation constants, determined above, are considered to be applicable at least over the concentration range 0.08 to 0.18 molar.

ACKNOWLEDGMENT

The authors are indebted to Dr. A. E. R. Westman and Dr. D. B. De Lury for their guidance and assistance during the progress of this work.

REFERENCES

1. ABBOTT, G. A. J. Am. Chem. Soc. 31: 763. 1909.
2. ABBOTT, G. A. and BRAY, W. C. J. Am. Chem. Soc. 31: 729. 1909.
3. A. S. T. M. Manual on Quality Control of Materials, Special Technical Publication 15 C. Prepared by A. S. T. M. Committee E-11.
4. BELL, R. N. Ind. Eng. Chem. 39: 136. 1947.
5. KIEHL, J. and COATS, H. P. J. Am. Chem. Soc. 49: 2180. 1927.
6. KOLTHOFF, I. M. and SANDELL, E. B. Textbook of quantitative inorganic analysis. Macmillan Co., New York. 1938.
7. MUUS, J. Z. physik. Chem. A, 159: 268. 1932.
8. THOMSEN, J. *In* Thermochemistry. Ramsay Series.
9. WESTMAN, A. E. R. and CROWTHER, J. P. Can. J. Chem. 32: 42. 1954.

CONSTITUTION OF A POLYURONIDE HEMICELLULOSE FROM WHEAT LEAF[1]

By G. A. Adams[2]

ABSTRACT

Crude hemicellulose of mature wheat leaves has been prepared by alkaline extraction of leaf holocellulose. Purification by repeated complexing with Fehling's solution yielded a polyuronide hemicellulose ($[\alpha]_D^{25}$ − 93°) composed of D-xylose (88.5%), L-arabinose (6.90%), and uronic acid anhydride (5.27%). Methylation studies indicated a molecular structure comprising a main xylan chain of 30 anhydro-D-xylose residues to which three L-arabinose residues and one D-glucuronic acid unit were attached as side chains by glycosidic linkages. Periodate oxidation data supported the proposed structure and the yield of formic acid indicated a molecule containing approximately 32 sugar residues. Estimations of the degree of polymerization of the molecule by measurements of viscosity and reducing power agreed with the foregoing values. The structure of the hemicellulose closely resembled that of one isolated previously from wheat straw.

Although fructosans (3, 13) and galactans (6) have been found in leaves of annual plants, little information is available on the occurrence and nature of hemicelluloses of the "xylan" type in similar materials. In the wheat plant, "xylans" have been reported in the straw and bran although these hemicelluloses may not have consisted exclusively of anhydro-D-xylose units. The presence of L-arabinose and D-glucuronic acid in the crude hemicelluloses indicated a more complex molecule, and a hemicellulose fraction of wheat straw has been shown to consist of D-xylose, L-arabinose, and D-glucuronic acid (1). From wheat flour an araboxylan or xyloaraban molecule has recently been isolated by Perlin (11). Since preliminary experiments indicated the presence of hemicelluloses of the "xylan" type in mature wheat leaves, a further investigation was made to determine whether these hemicelluloses were of the same type as found in the straw and bran.

Hemicelluloses, extracted from wheat leaf chlorite holocellulose by dilute potassium hydroxide in 27% yield, contained pentosan (90.9%), uronic acid anhydride (6.08%), and lignin (2.1%). On hydrolysis, xylose and arabinose were released in a ratio of 4.3 : 1 along with traces of glucose and galactose. The crude pentosan was subjected to further purification by repeated precipitation as a copper complex with Fehling's solution as described by Chanda *et al.* (7). Although this treatment reduced the arabinose content markedly, there remained a xyloaraban containing a xylose to arabinose ratio of 12.8 : 1 beyond which no further reduction was possible. The constant composition of the hemicellulose indicated strongly that the pentoses were combined in the same molecule. Ready removal of the hexoses showed that they were not an integral part of the pentosan molecule.

Graded hydrolysis of the hemicellulose with 0.02 *N* oxalic acid readily released the arabinose without appreciably affecting the xylose. This observation indicated that the arabinose units were on the periphery of the molecule

[1] *Manuscript received October 30, 1953.*
Contribution from the Division of Applied Biology, National Research Laboratories, Ottawa. Issued as Paper No. 165 of the Uses of Plant Products and as N.R.C. No. 3162.
With the technical assistance of A. E. Castagne.

and were readily attacked. In addition, the acid lability suggested that the arabinose was in the furanoside configuration while the xylose was in the more stable pyranoside form. Recovery of at least a portion of the xylose units in polymer form after removal of the arabinose units suggested a molecular structure consisting of a chain of xylose units to which the arabinose units were attached as side groups. The uronic acid groups were probably attached to the xylan chain as the recovered portion retained almost its original uronic acid content.

The purified hemicellulose was methylated initially with dimethyl sulphate and strong alkali and finally to constant methoxyl content with Purdie's reagent. Fractionation with chloroform – petroleum ether solution yielded a fully methylated fraction having $[\alpha]_D^{25} - 88°$ (*c*, 1.0% in chloroform) and OCH_3 content 38.6%, (calculated for $C_7H_{12}O_4 : OCH_3$, 38.8%). Hydrolysis of the methylated product yielded the following products which were identified as described in the experimental section: (I) 2-methyl-D-xylose; (II) 2,3-dimethyl-D-xylose; (III) 2,3,4-trimethyl-D-xylose; (IV) 2,3,5-trimethyl-L-arabinose; (V) 2-methyl-3[2,3,4-trimethyl-D-glucuronosido]D-xylose.

Identification of almost all of the arabinose in the original hemicellulose as 2,3,5-trimethyl-L-arabinose provided proof that the arabinose residues existed as side chains attached by glycosidic linkages to a main structure. The absence of monomethyl and dimethyl arabinose units precluded the existence of a separate araban structure and provided additional evidence that the arabinose units were an integral part of the hemicellulose molecule.

The 2,3,4-trimethyl-D-xylose which appeared in the methanolysis mixture originated from the nonreducing end of the xylan chain and the amount (3.0% molar) corresponded to 33 residues per nonreducing end group.

The presence of 2,3-dimethyl-D-xylose as the main component of the free methylated sugar mixture indicated that the xylose units were linked 1,4; the pyranose form required for this linkage was reasonably established by stability to acid. The change in specific rotation of the methylated polysaccharide from $-88°$ to $+58°$ on hydrolysis indicated that the xylose units were joined in the β-configuration.

Branch points in the main xylan chain were indicated by the presence of 2-methyl-D-xylose (11.6% molar). Since 2-methyl xylose was the only monomethyl xylose found, it was apparent that $C_{(3)}$ must be the site of side group attachment in the 1,4-linked xylan chain. The presence of one monomethyl residue was obscured in the hydrolysis mixture by its attachment to a glucuronic acid residue as an aldobiuronic acid unit. The number of branch points as indicated by 2-methyl xylose (11.6%) exceeded the number of side groups as represented by 2,3,5-trimethyl arabinose (9.1%). The excess monomethyl xylose may be explained by incomplete methylation of the original hemicellulose and/or by demethylation of 2,3-dimethyl xylose (8). The possibility that other types of branching exist in the molecule cannot be rejected although no direct evidence for them was found.

The methylated aldobiuronic acid ester was reduced with sodium borohydride and the product hydrolyzed with dilute acid. The trimethyl glucose

derived from the uronic acid could only be 2,3,4-trimethyl glucose because reduction of a methylated uronic acid could not yield a 2,3,6-trimethyl derivative. The monomethyl xylose corresponded chromatographically to 2-methyl xylose; the possibility that it was another monomethyl derivative was unlikely unless this xylose residue was substituted differently from those in the rest of the molecule. Therefore the methylated aldobiuronic acid was 2-methyl-3[2,3,4-trimethyl glucuronosido]D-xylose; the high positive rotation (+78°) indicated an α linkage. The uronic acid unit occupied the position of a nonreducing end group and was linked glycosidically to a xylose unit. From analysis of the original hemicellulose, the amount of uronic acid was calculated to be one mole. The structure of the aldobiuronic acid residue in the wheat leaf appears to be identical with that found in wheat straw hemicellulose (1, 5) and in pear cell wall xylan (8).

Methylated sugars I, II, III, and IV occurred in a molar ratio of 4 : 25 : 1 : 3. In addition, one mole of glucuronic acid was present in the hemicellulose molecule. From the foregoing data a possible structure for the molecule is proposed as follows: a straight chain of approximately 29 D-xylopyranose units joined by 1,4-β-glycosidic linkages and terminated by one reducing and one nonreducing end group. Three L-arabinose units and one D-glucuronic acid unit are attached as side groups to the main chain by 1,3-glycosidic bonds. With one xylose residue bound into the aldobiuronic unit, a total of 30 xylose units are present in the main chain which along with the arabinose and glucuronic acid units make up a total of 34 units in the molecule.

Periodate oxidation of the hemicellulose provided additional evidence for the proposed structure which theoretically should consume 0.97 moles of periodate per mole ($C_5H_8O_4$). Actual consumption was 0.94 moles of periodate after 168 hr. when the oxidation appeared complete. The calculated yield of formic acid from the proposed molecule was 0.118 moles per sugar unit. Although the formation of formic acid continued slowly after 168 hr. oxidation, it was considered complete at that time, when 0.128 moles had been formed. For the molecular structure proposed, this value corresponds to a molecule containing approximately 32 sugar units since two moles of formic acid originate from the reducing end and one mole each from the nonreducing end and glucuronic acid respectively. The xylose residues which were branch points in the molecule were not oxidized by periodate and on hydrolysis yielded small amounts of free sugar.

Estimates of the number of sugar units from the reducing power measured by three different methods were in reasonable agreement and indicated one reducing group per approximately 30–35 sugar residues.

Viscosity measurements on the acetylated and methylated hemicellulose gave degree of polymerization values of 46 and 37 respectively. While these results are somewhat higher than those given by chemical methods, they are, nevertheless, of the same general order of magnitude.

One of the main features of the wheat leaf polyuronide hemicellulose is its close similarity to the hemicellulose of wheat straw (1). The general structure of the molecule is almost identical except that the proportion of L-arabinose

and D-glucuronic acid is less. The glucuronic acid of wheat straw appeared to consist entirely of the monomethoxyl derivative but less than 50% of the wheat leaf glucuronic acid was in this form. The molecular dimensions of the two molecules are of the same general order and both appear to be small short chain structures with side groups of L-arabinose and D-glucuronic acid. Concepts of "xylan" in plant tissues have undergone modification in recent years and now permit inclusion of arabinose (11, 4) and D-glucuronic acid (8, 9) in the molecule. Wheat straw (1) and wheat leaf hemicelluloses appear to have all three components joined in a single molecule.

EXPERIMENTAL

Preparation of Wheat Leaf Holocellulose

The blades of wheat leaves were harvested by hand from wheat plants which had been cut two to three weeks previously and stored out-of-doors. The leaf material was then ground in a Wiley mill and screened to give a fraction which passed 40 mesh and was retained on 60 mesh. Extraction with ethanol–benzene (1 : 2) for 16 hr. and subsequently with ethanol for five hours removed pigments, lipoids, and waxy substances. Water soluble material was removed by two four-hour extractions at 85°C. The residue was then thoroughly washed with cold water and dried in air. Holocellulose was prepared from this residue in 76% yield by the acid chlorite method (2).

Isolation of Leaf Hemicellulose from Holocellulose

Air-dry holocellulose (350 gm.) was extracted by stirring for 20 hr. at room temperature with 12 liters of 4% potassium hydroxide in an atmosphere of nitrogen. The residue was recovered by filtration on cloth and subjected to two further extractions. The combined extracts were clarified in a Sharples supercentrifuge and brought to pH 7.0 with acetic acid. The white precipitate which formed was recovered and washed thoroughly with water (Hemicellulose I). Further reduction of the pH to 5.0 and addition of four volumes of ethanol brought a further precipitate (Hemicellulose 2). The total yield of hemicellulosic material was 27%. Acid hydrolysis of both fractions yielded xylose and arabinose and a small amount of glucose and galactose. Since these analyses, as well as the optical rotations of the two fractions, were very similar, the fractions were combined.

Purification of the Leaf Hemicellulose

Crude hemicellulose (40 gm.) was purified by repeated complexing with Fehlings' solution (7). Table I shows that the xylose : arabinose ratio of the

TABLE I

EFFECT OF COPPER COMPLEXING TREATMENTS ON XYLOSE : ARABINOSE RATIO IN WHEAT LEAF HEMICELLULOSE

Number of treatments	Xylose : arabinose
None	4.3 : 1
3	11.6 : 1
6	12.8 : 1
9	12.8 : 1

hemicellulose remained constant after six treatments. No glucose or galactose was detected in the purified product.

The composition of the purified hemicellulose was as follows: ash, 0.34%; nitrogen, nil; methoxyl, 0.5%; uronic acid anhydride, 5.27%; D-xylose, 88.5%; L-arabinose, 6.9%; and $[\alpha]_D^{25} - 93°$ (*c*, 1% in sodium hydroxide (2%)).

Graded Hydrolysis

In a preliminary experiment, hemicellulose (50 mgm.) was heated under reflux in a boiling water bath with oxalic acid (5 ml., 0.02 *N*). Chromatographic examination of the hydrolyzate at regular time intervals showed that at the end of three hours only a trace of xylose had appeared although arabinose was present in large amounts. Repetition of this experiment on a quantitative basis permitted measurement of the maximum yield of arabinose with minimal removal of xylose. The results given in Table II show that at the end of a one-

TABLE II
GRADED HYDROLYSIS OF WHEAT LEAF HEMICELLULOSE WITH 0.02 *N* OXALIC ACID

Hydrolysis time, hr.	Percentage individual sugar released	
	Arabinose	Xylose
1	100	0.8
2	100	1.2
3	100	2.4
4	100	4.4

hour heating period, 100% of the arabinose and only 0.8% of the xylose had been released. Addition of five volumes of ethanol to the hydrolyzate yielded a precipitate which on hydrolysis gave only xylose. Uronic acid anhydride estimation on this precipitate gave a value of 5.06%.

Methylation

Hemicellulose (15.0 gm.) was methylated with dimethyl sulphate and sodium hydroxide (40%) by a procedure previously described (1). The partially methylated product was recovered after each two methylation treatments by dialysis and evaporation. After 10 treatments the product was recovered as a friable yellowish solid (OCH_3, 36.4%) soluble in methanol, acetone, and methyl iodide. The partially methylated product (15.7 gm.) was dissolved in methyl iodide (200 ml.) and refluxed at 45°C. during the addition of silver oxide (50 gm.) over a period of four hours. The methylated hemicellulose was recovered by chloroform extraction and subjected to two similar treatments. The final product was a porous yellow solid; yield 16.0 gm.; OCH_3, 38.3% (theoretical value for dimethyl xylan 38.8%); $[\alpha]_D^{25} - 84.5$ (*c*, 0.49% in chloroform). Two further methylations by the Purdie method failed to increase the methoxyl content.

Fractionation of Methylated Hemicellulose

The methylated hemicellulose (16.0 gm.) was extracted under gentle reflux with solvent mixtures of chloroform – petroleum ether (b.p. 30–60°C.). After

filtration through a glass filter ("C" porosity) the solvent was removed under reduced pressure and the product dried *in vacuo* at 50°C. The results of the fractionation are given in Table III. Fraction 5 comprised 75% of the product and was fully methylated; this material was used in subsequent studies.

TABLE III
FRACTIONATION OF METHYLATED WHEAT LEAF HEMICELLULOSE

Fraction No.	Chloroform – petroleum ether solvent mixture	Yield, %	OCH_3, %	$[\alpha]_D^{25}$
1	0 : 100	0.2	—	—
2	10 : 90	0.9	—	—
3	20 : 80	2.3	33.8	−69
4	30 : 70	19.8	38.3	−84
5	40 : 60	75.7	38.6	−88

Hydrolysis Products of Methylated Hemicellulose

Fraction 5 (100 mgm.) was heated with methanolic hydrogen chloride (10 ml.; 8%) in a sealed tube at 100°C. for 18 hr. After removal of the solvent, the sirupy methyl glycosides were hydrolyzed with hydrochloric acid (10 ml.; 0.5 *N*) for eight hours at 100°C. The hydrolyzate was worked up in the usual way and the free methylated sugars separated chromatographically on filter paper using the solvent system *N*-butanol–ethanol–water–ammonia (40 : 10 : 49 : 1). Sugar spots were developed with aniline phthalate spray and authentic samples of methylated sugars were used as reference compounds. The following sugars were detected: (1) 2,3,5-trimethyl arabinose (R_f 0.81–83); (2) 2,3-dimethyl xylose (R_f 0.66–0.69); (3) 2-methyl xylose (R_f 0.43–0.47); (4) a pink spot (R_f 0.15–0.17) indicative of uronic acids. Repetition of the foregoing experiment using a methyl ethyl ketone – water (2 : 1) solvent system showed the presence of the same sugars. The free methylated sugars were extracted from a quantitative chromatogram and analyzed by the alkaline hypoiodite method (7). The results are given in Table IV.

TABLE IV
COMPOSITION OF HYDROLYZATE FROM METHYLATED HEMICELLULOSE

Component sugar	Molar composition, %
Monomethyl pentose	11.6
Dimethyl pentose	76.4
Trimethyl pentose	12.1

Separation of Methylated Pentoses

For separation and confirmation of the identity of the free methylated sugars, larger quantities were prepared in the following way. Methylated hemicellulose (Fraction 5; 7.7 gm.) was heated under reflux with methanolic hydrogen chloride (300 ml.: 8%) until the rotation became constant ($[\alpha]_D^{25}$ +59°).

After removal of the chloride ions with silver carbonate, and excess silver ions as silver sulphide, the solution was concentrated to a brown sirup (8.05 gm.). The methyl glycosides were hydrolyzed to free sugars with hydrochloric acid (300 ml.; 0.5 *N*) until the rotation became constant (+22.5°). Yield of free methylated sugars was 7.80 gm.

The mixture of methylated sugars was separated on a column of powdered cellulose (8) and the following fractions were obtained: (I) trimethyl pentose (0.87 gm.); (II) dimethyl xylose (4.76 gm.); (III) monomethyl pentose (0.71 gm.); (IV) uronic acid fraction (0.35 gm.).

Examination of the Fractions

Fraction I.—This sirup did not crystallize on standing. The specific rotation value of −11° suggested the product was a mixture of 2,3,5-trimethyl arabinose ($[\alpha]_D^{25}$ −39.5°) and 2,3,4-trimethyl xylose ($[\alpha]_D^{25}$ +24.2°). Demethylation of the sirup (25 mgm.) with hydrobromic acid (48%) at 100°C. for 12 min. showed on chromatographing that arabinose and xylose were both present. Use of authentic samples of 2,3,5-trimethyl arabinose and 2,3,4-trimethyl xylose indicated that complete separation could be achieved readily on paper chromatograms using the solvent system ethanol–benzene–water (47 : 170 : 15). Therefore, the trimethyl pentose fraction (460 mgm.) was separated chromatographically into fraction I*a* (120 mgm.) and fraction I*b* (315 mgm.). The composition of the trimethyl pentose fraction (12.1% of the methylated sugars) was therefore trimethyl xylose (I*a*) (3.0% molar) and trimethyl arabinose (I*b*) (9.1% molar).

Fraction Ia.—This material was clarified by filtration through charcoal and then dissolved in ethyl ether to which a few drops of petroleum ether (b.p. 35–60°C.) had been added. On seeding with 2,3,4-trimethyl-D-xylose crystallization occurred. Recrystallization from the same solvent yielded 2,3,4-trimethyl-D-xylopyranose, m.p. 89–90° (undepressed on admixture with an authentic sample) and $[\alpha]_D^{25}$ +19.8 (*c*, 1.0% in water).

Analysis: calculated for $C_8H_{16}O_5$: OCH_3 48.4%; found; OCH_3, 48.1%.

Fraction Ib.—Clarification with charcoal yielded a sirup having η_D^{20} 1.4525; $[\alpha]_D^{25}$ −35.2°; OCH_3, 47.9% (calculated for $C_8H_{16}O_5$, 48.4%). Oxidation of this sugar with bromine yielded a lactone which was converted to the corresponding amide by methanolic ammonia. Recrystallization of the amide yielded pure 2,3,5-trimethyl-L-arabonamide, m.p. 138°C. and $[\alpha]_D^{25}$ −17.9° (*c*, 1.10 in water).

Analysis: calculated for $C_8H_{17}O_5N$: OCH_3, 44.9; found: OCH_3, 44.8.

Fraction II.—Chromatographic examination of the clarified sirup indicated that only 2,3-dimethyl-D-xylose was present, and the physical constants $[\alpha]_D^{25}$ +24° (*c*, 1% in water) and η_D^{25} 1.4733 provided further evidence of its identity.

Analysis: calculated for $C_7H_{14}O_5$: OCH_3, 34.8%; found: OCH_3, 34.8%.

A crystalline anilide was prepared having m.p. 123–124°C.; (reported value 124°C.). An X-ray powder photograph of this anilide showed it to be identical with 2,3-dimethyl-D-xylose anilide.

Fraction III.—This fraction partially crystallized on standing. After clarification of the alcoholic solution with charcoal, it was readily recrystallized from methanol, m.p. 133°C. and $[\alpha]_D^{25}$ +37° (*c*, 1% in water).

Analysis: calculated for $C_6H_{12}O_5$: OCH_3, 18.9%; found: OCH_3, 18.7%.
A crystalline anilide had a m.p. 123° alone or admixed with an authentic sample of 2-methyl-D-xylose anilide.

Fraction IV.—Chromatographic examination of this fraction (320 mgm.) on filter paper showed two spots characteristic of uronic acids, a spot due to methylated xylose and two spots presumably due to unhydrolyzed hemicellulose. Further chromatographing on a small cellulose column failed to separate the uronic acids satisfactorily. The components of the fraction were converted to their glycoside form by heating with methanolic hydrogen chloride (25 ml.; 5%) for six hours. The methanolysis mixture after the usual neutralization treatment with silver carbonate was heated with saturated barium hydroxide solution (25 ml.) for three hours at 60°C. to convert the uronic acid ester into the barium salt. After removal of the excess barium ions with carbon dioxide, the aqueous solution was extracted for 24 hr. with ethyl ether. This solvent dissolved the methyl pentosides but only a small amount of the barium salt of the uronic acid; the latter was then recovered by evaporation. The barium salt (480 mgm.) was taken up in hydrochloric acid (20 ml., 0.5 *N*) and heated at 100°C. for three hours. After neutralization with silver carbonate, the solution was concentrated to a sirup (336 mgm.) which was taken up in methanol. The sirup was heavily spotted on filter paper and chromatographed in methyl ethyl ketone – water (2 : 1) solvent system. The portion of the paper containing the methylated uronic acid was cut out and extracted thoroughly with hot ethanol. Evaporation of the extract yielded the free methylated aldobiuronic acid which was reconverted to its glycoside methyl ester form (290 mgm.) with $[\alpha]_D^{20}$ +78°.

Reduction with Sodium Borohydride

Alcoholic solution of the uronic acid sirup was treated with sodium borohydride (150 mgm.) dissolved in ethanol (5 ml.). After the solution had been allowed to stand overnight, acetic acid was added and the pH reduced to 7.0. The solution was evaporated to dryness, extracted with hot ethyl ether, and a sirup (39 mgm.) recovered. Hydrolysis of the sirup (15 mgm.) yielded the free sugars which were separated on a filter paper chromatogram with the methyl ethyl ketone – water solvent. Four spots on the paper were identified as 2-methyl xylose, 2,3,4-trimethyl-D-glucose, 2,3-dimethyl xylose, and unreduced uronic acid, the latter two substances being present in only small amounts. Appropriate reference compounds were run on the same chromatogram. The identity of the methylated uronic acid was established as 2,3,4-trimethyl-D-glucuronic acid by the presence of 2,3,4-trimethyl-D-glucose.

Periodate Oxidation

In a typical oxidation experiment, leaf hemicellulose (100 mgm.) was suspended in periodic acid solution (4.6 gm. periodic acid in 100 ml. of water) and neutralized with sodium hydroxide to methyl red end point. All oxidations

were carried out in the dark on a shaking apparatus at 16°C. Analyses were performed at various time intervals for periodate consumption and formic acid production (7). The results were as follows:

	Time, hr.				
	48	72	120	168	216
Periodate consumed,*moles per $C_5H_8O_4$	0.61	0.76	0.82	0.94	0.96
Formic acid produced, moles per $C_5H_8O_4$	0.110	0.119	0.126	0.128	0.129

**Corrected for periodate consumed in formic acid production.*

Reducing Power of Hemicellulose

Three methods of determining reducing power were used. The hypoiodite oxidation method of Chanda *et al.* (7), modified by substitution of a sodium hydroxide – disodium hydrogen phosphate buffer (pH 11.40), indicated one reducing group per 30–35 pentose residues. Somogyi's copper reduction method (12) gave a result of one reducing group per 34–36 sugar units. Approximately 32 sugar units per reducing group were indicated by Meyer's dinitrosalicylic acid method as modified by Chanda *et al.* (7).

Viscosity Measurements on Hemicellulose Derivatives

Viscosity measurements were made using an Oswald-Cannon-Fenske viscometer in a water bath at 25°C. ± 0.02°. The derivatives used were the fully acetylated hemicellulose dissolved in *m*-cresol and fully methylated hemicellulose in chloroform solution. The plots of η_{sp}/c versus c were straight lines and, when extrapolated to zero concentration, gave intrinsic viscosity $[\eta]$. Using a K_m factor of 11×10^{-4} (10) for the acetyl derivative and 12×10^{-4} (7) for the methyl derivative, substitution in Staudinger's equation $[\eta] = K_m P$ gave degree of polymerization (P) values of 46 for the former and 37 for the latter derivative respectively.

REFERENCES

1. Adams, G. A. Can. J. Chem. 30: 698. 1952.
2. Adams, G. A. and Castagne, A. E. Can. J. Research, B, 26: 325. 1948.
3. Archbold, A. K. and Barter, A. M. Biochem. J. 29: 2689. 1935.
4. Aspinall, G. O., Hirst, E. L., Moody, R. W., and Percival, E. G. V. J. Chem. Soc. 1631. 1953.
5. Bishop, C. T. Can. J. Chem. 31: 134. 1953.
6. Buston, H. W. Biochem. J. 29: 196. 1935.
7. Chanda, S. K., Hirst, E. L., Jones, J. K. N., and Percival, E. G. V. J. Chem. Soc. 1289. 1950.
8. Chanda, S. K., Hirst, E. L., and Percival, E. G. V. J. Chem. Soc. 1240. 1951.
9. McIlroy, R. J. J. Chem. Soc. 121. 1949.
10. Millet, M. A. and Stamm, A. T. J. Phys. and Colloid Chem. 51: 134. 1947.
11. Perlin, A. S. Cereal Chem. 28: 382. 1951.
12. Somogyi, M. J. Biol. Chem. 160: 61. 1945.
13. Whistler, R. L. and Deszyck, E. J. Arch. Biochem. Biophys. 44: 484. 1953.

LYCOCTONINE: PERIODATE OXIDATION STUDIES[1]

By O. E. Edwards and Léo Marion

ABSTRACT

The periodate oxidation of lycoctonam and des(oxymethylene)-lycoctonam gives rise to diketones, showing that lycoctonine contains a ditertiary vicinal glycol. Evidence is presented relating two of the methoxyl groups to this glycol system. The properties and reactions of isomeric compounds formed by the action of weak base or activated alumina on the diketones are discussed and possible explanations of the isomerization considered. The unusual spectra of the various compounds are discussed.

INTRODUCTION

Evidence has been presented for the presence in lycoctonine ($C_{19}H_{21}(OH)_3(OCH_3)_4(NC_2H_5)$) of the partial structure:

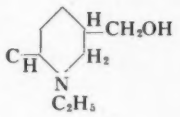

and for the presence of a vicinal glycol system (11), thus accounting for the three hydroxyls in the base. A study of the periodic acid cleavage of lycoctonam (the lactam obtained on oxidation of the methylene next to the nitrogen in lycoctonine) and of des(oxymethylene)-lycoctonam (lycoctonam in which the hydroxymethyl group has been replaced by hydrogen) has confirmed the presence of the vicinal glycol and given information about two of the methoxyls in the compounds. The well-characterized compounds which have now been obtained are indicated in the flowsheet below.

Since the carbonyls formed by the oxidation of the glycol system in these lactams are resistant to oxidation by moist silver oxide, potassium permanganate in acetone, and chromic anhydride in glacial acetic acid, they must be ketonic (a hindered aldehyde like strophanthidin is oxidized readily by potassium permanganate in acetone (20)). Hence the vicinal hydroxyls in lycoctonine are both tertiary.

The infrared absorption maxima (Table I) indicate that one carbonyl (carbonyl 1) (1765 cm.$^{-1}$) is in a five membered ring and that the other (carbonyl 2) (1708 cm.$^{-1}$) is in a six membered or larger ring, or in a chain. Carbonyl 1 is readily reduced catalytically or by sodium borohydride, although in the des(oxymethylene) series it appears to be more hindered than in the lycoctonam series. Carbonyl 2 is resistant to both sodium borohydride and to catalytic reduction in acid.

The diketones rapidly reduce Tollens' reagent at room temperature and Fehling's solution at 100°, and since the ketols (in which carbonyl 1 is reduced)

[1] *Manuscript received August 25, 1953.*
Contribution from the Division of Pure Chemistry, National Research Council, Ottawa, Canada. Issued as N.R.C. No. 3166.

FLOWSHEET

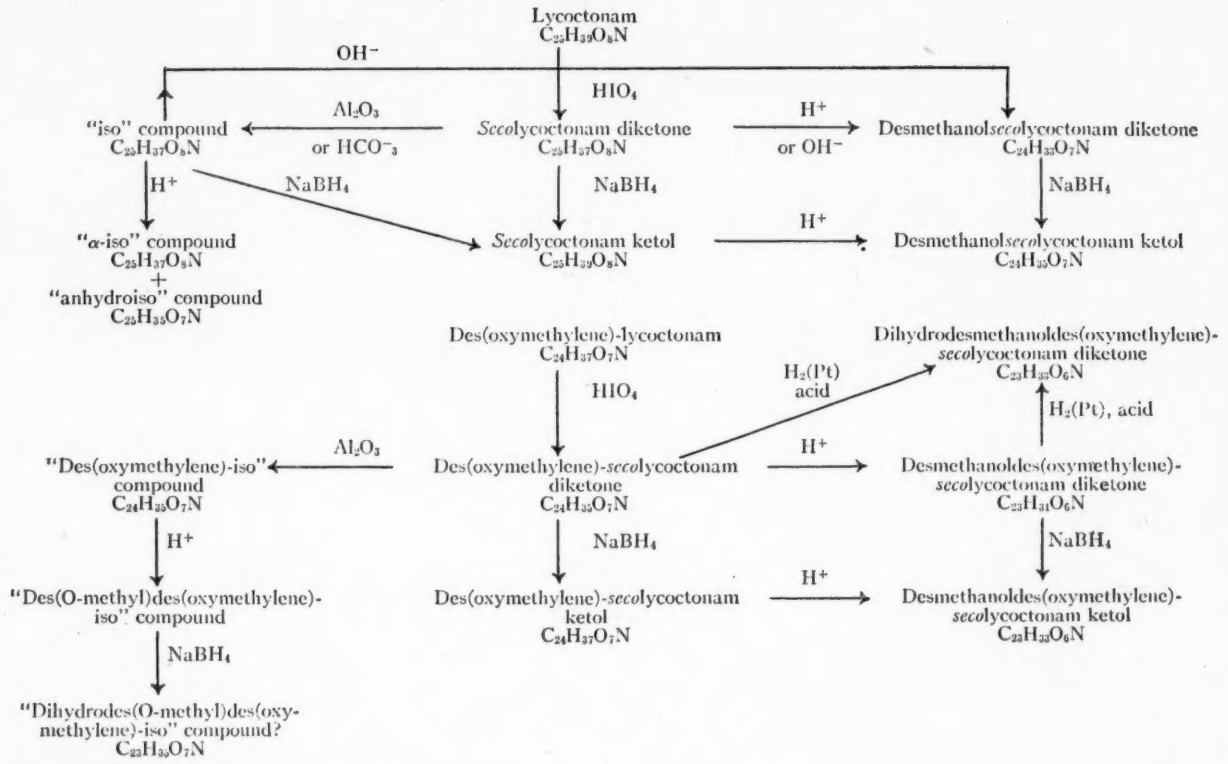
Lycoctonam
$C_{25}H_{39}O_8N$
OH^-
HIO_4
"iso" compound
$C_{25}H_{37}O_8N$
Al_2O_3
or HCO^-_3
*Seco*lycoctonam diketone
$C_{25}H_{37}O_8N$
H^+
or OH^-
Desmethanol*seco*lycoctonam diketone
$C_{24}H_{33}O_7N$
H^+
$NaBH_4$
$NaBH_4$
$NaBH_4$
"α-iso" compound
$C_{25}H_{37}O_8N$
+
"anhydroiso" compound
$C_{25}H_{35}O_7N$
*Seco*lycoctonam ketol
$C_{25}H_{39}O_8N$
H^+
Desmethanol*seco*lycoctonam ketol
$C_{24}H_{35}O_7N$
Des(oxymethylene)-lycoctonam
$C_{24}H_{37}O_7N$
Dihydrodesmethanoldes(oxymethylene)-
*seco*lycoctonam diketone
$C_{23}H_{35}O_6N$
HIO_4
H_2(Pt)
acid
H_2(Pt), acid
Al_2O_3
"Des(oxymethylene)-iso"
compound
$C_{24}H_{35}O_7N$
Des(oxymethylene)-*seco*lycoctonam
diketone
$C_{24}H_{35}O_7N$
H^+
Desmethanoldes(oxymethylene)-
*seco*lycoctonam diketone
$C_{23}H_{31}O_6N$
H^+
$NaBH_4$
$NaBH_4$
$NaBH_4$
"Des(O-methyl)des(oxymethylene)-
iso" compound
Des(oxymethylene)-*seco*lycoctonam
ketol
$C_{24}H_{37}O_7N$
H^+
Desmethanoldes(oxymethylene)-
*seco*lycoctonam ketol
$C_{23}H_{33}O_6N$
"Dihydrodes(O-methyl)des(oxy-
methylene)-iso" compound?
$C_{23}H_{35}O_7N$

are inert to these reagents it must be carbonyl 1 which is involved in the positive tests. Since α-methoxy ketones show this ease of oxidation (14) it is reasonable to postulate the presence of a methoxyl α to carbonyl 1. Since α-methoxy ketones are also readily hydrolyzed by mineral acids (5,25) attempts were made to hydrolyze a methoxyl in various derivatives containing carbonyl 1. In all of these derivatives except one, however, no hydrolysis took place with hot 6 *N* acid. Thus the α-methoxyl (if present) is generally inert. In the case of the "des(oxymethylene)-iso" compound (see flowsheet) hot 6 *N* sulphuric acid did hydrolyze one methoxyl. The resulting product did not react with diazomethane (27) but it did react with periodic acid to give products which have not been characterized. Thus the presence of an α-methoxyl, although indicated, will require further proof.

Both diketones are sensitive to acid and alkali, losing the elements of methyl alcohol to give α-β unsaturated ketones. The fact that the elimination takes place with the ketols, and that it is the infrared absorption peak due to carbonyl 2 that shifts when the conjugated system is formed (Table I), indicates that it is this carbonyl that is involved in the reaction. Since β methoxy and β hydroxy ketones show a parallel ease of elimination, catalyzed by acid or base (8,32), it can be concluded that there is a methoxyl β to carbonyl 2. The ultraviolet spectra (λ_{max} 223 mμ) indicate a low degree of substitution of the double bond (13,34). Thus a tentative formulation of the glycol group and its transformation products (11) is:

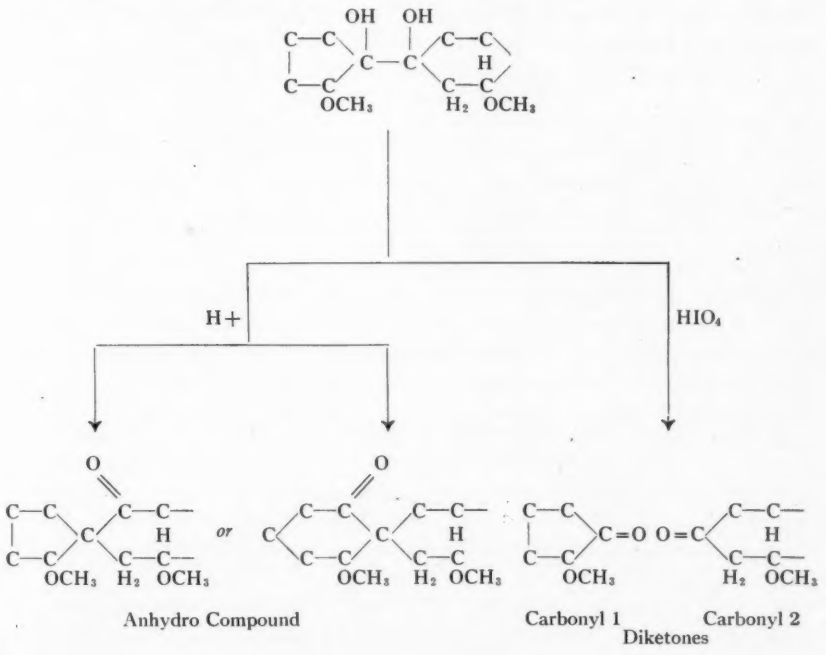

Anhydro Compound

Carbonyl 1 Carbonyl 2
Diketones

TABLE I
INFRARED SPECTRA IN CHLOROFORM

Compound	Frequency in cm.$^{-1}$		
	Carbonyl 1	Carbonyl 2	Lactam
*Seco*lycoctonam diketone	1766	1707	1631
*Seco*lycoctonam diketone monoacetate	1764	1708	1649
Des(oxymethylene)-*seco*lycoctonam diketone	1765	1707	1644
Desmethanol*seco*lycoctonam diketone	1766	1679	1628
Desmethanoldes(oxymethylene)-*seco*lycoctonam diketone	1765	1679	1642
Dihydrodesmethanoldes(oxymethylene)-*seco*-lycoctonam diketone	1761	1705	1646
"Iso" compound	1743		1632
"Iso" compound monoacetate	1740		1650
"Des(oxymethylene)-iso" compound	1742		1645 (Broad)
"Anhydroiso" compound	1736		1652
"Des(O-methyl)des(oxymethylene)-iso" compound	1755	1712 (Weak)	1644

The choice of the migrating group in the pinacolic rearrangement is determined by the fact that the anhydro compounds (11) do not behave like α-methoxy ketones, or like β-methoxy ketones with hydrogen on the α-carbon.

Since the glycol system is ditertiary and hindered, the rate of periodate cleavage does not permit a decision in regard to the orientation of the two hydroxyls relative to each other (33). However, the ready pinacolic dehydration in what is probably a rigid molecule must mean that the hydroxyls have a "gauche" orientation as shown in order that the coplanarity of centers necessary for easy elimination and migration (3,4) exist.

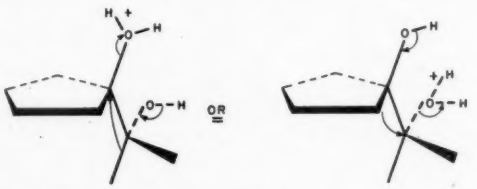

The formation of the "iso" compounds is of great significance. The reaction involves the base-catalyzed conversion of carbonyl 2 to a hydroxyl group (the "iso" compound and "des(oxymethylene)-iso" compound contain a new hydroxyl which is difficult to acetylate). The spectra of these two compounds are characterized by the appearance of a maximum at 219 mμ in the ultraviolet and a shift of the infrared peak due to carbonyl 1 to near 1740 cm.$^{-1}$ (Table I). The reaction is reversible, as shown by the formation of the ketols on catalytic reduction or reduction by sodium borohydride and by the formation of the desmethanol diketone on treatment with strong alkali. However, the reaction is not brought about or reversed in refluxing acetone or methanol or in hot 6 *N* acid.

Hot 6 *N* acid converts the "iso" compound to a mixture consisting mainly of two products. One, the "α-iso" compound is isomeric with the "iso" com-

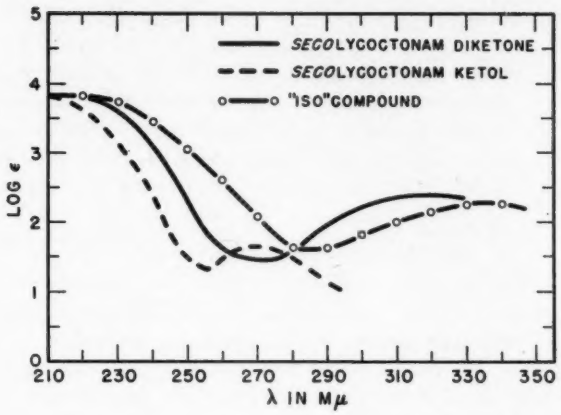

pound. It is no longer a ketone, and is not readily acetylated (i.e., the primary hydroxyl is no longer free to react) although it has two active hydrogens. The other product, "anhydroiso" compound corresponds to "iso" compound less a molecule of water. It has no hydroxyls, but still contains carbonyl 1. Both products have uneventful ultraviolet spectra compared to the "iso" compound.

The formation of the "iso" compounds can be interpreted as involving either (*a*) the conversion of carbonyl 2 to a stable enol, (*b*) a reversible shift from a ketone to an unsaturated alcohol form, or (*c*) a readily reversible internal aldol condensation. A consideration of these possibilities follows:

(*a*) The iso compound does not react with diazomethane. However, it is reported (29) that stable enols are quite inert to the reagent. Although the shift of the band due to carbonyl 1 from 1765 cm.$^{-1}$ to 1740 cm.$^{-1}$ on conversion from the diketone to the iso compound could be due to strong hydrogen bonding as occurs in chelated enols (15,19,23) this is unlikely since the new hydroxyl is not involved in such bonding (the OH stretching peak is at 3530 cm.$^{-1}$ in chloroform which indicates only weak bonding). A stable enol could arise from a β-diketone or β-keto lactam system. The first possibility is unlikely since such systems have ultraviolet maxima near 255 mμ (6). If the "iso" compound was the enol of a β-keto lactam such as is illustrated, it would be expected to have an ultraviolet absorption maximum near 240 mμ (24) in contrast to the actual maximum at 219 mμ. Such a structure should also dehydrate to an α-β unsaturated ketone or eliminate formaldehyde on treat-

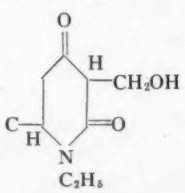

ment with hot mineral acid, neither of which takes place. Thus it seems unlikely that the iso compounds are enols of β-dicarbonyl systems.

(*b*) The ultraviolet maxima at 219 mμ suggests the presence of unsaturation. In addition the "des(oxymethylene)-iso" compound has a band at 3010 cm.$^{-1}$ (mull) which can be attributed to hydrogen attached to doubly bound carbon. A double bond could arise from the following kind of transformation, involving either the two ketone carbonyls or the lactam carbonyl and carbonyl 2

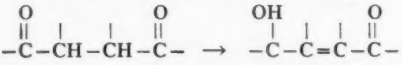

The reverse of this reaction is well known (12,17,28) but the only analogy for the forward reaction known to the authors is the conversion of levulinic acid to β-angelica lactone. It is conceivable, however, (assuming the ketone carbonyls to be close in space), that steric hindrance of carbonyl 2 and some hydrogen bonding stabilization of the hydroxyl form might promote the conversion. A possible mechanism for the base catalyzed reaction is shown:

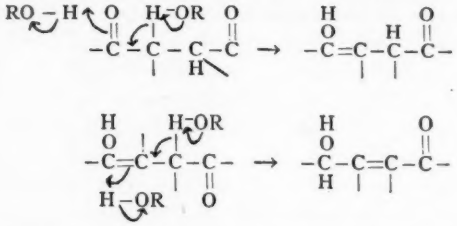

The reversal of the reaction on reduction of carbonyl 1 could be due to lessening of the hindrance due to the rigid carbonyl (carbonyl 1), the greater intrinsic stability of the diketone system, and the stabilizing influence of hydrogen bonding between carbonyl 2 and the hydroxyl derived from carbonyl 1.

It seems unlikely that the two ketone carbonyls are involved in such a change. The ultraviolet maximum is very weak (log ϵ 3.8) and at very short wave length for an α-β unsaturated ketone. In addition, this postulate would require that the two tertiary hydroxyls in lycoctonine be on a cyclobutane ring. This is unlikely since then the anhydro compounds should be cyclobutanones (I.R. evidence indicates a carbonyl on a five or six membered ring) or cyclopropyl ketones (a very unlikely type of product).

The alternative is that carbonyl 2 is γ to the lactam carbonyl as shown.

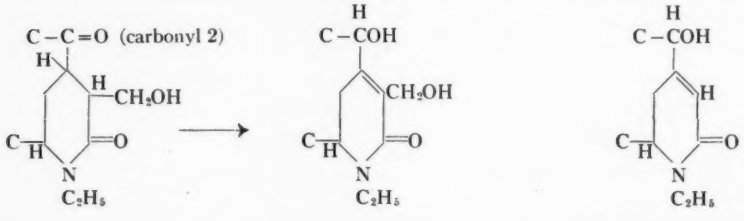

The absence of the 3010 cm.$^{-1}$ band in the "iso" compound is in agreement with this formulation.

Carbonyl 2 cannot be in the nitrogen ring, since hydroxylycoctonine (11) would then contain the partial structure

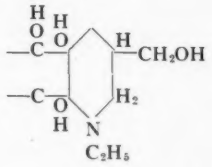

This should react with two moles of periodic acid. Actually hydroxylycoctonine consumes only one mole of the reagent in 68 hr.

The maximum at 219 mμ seems reasonable for an α-β unsaturated lactam, since α-β unsaturated lactones (16) and α-β unsaturated acids (31) have maxima in this region. However, seven membered α-β unsaturated lactams with an NH have maxima in the 240 mμ region (18,26). No spectra of simpleN-alkyl α-β unsaturated lactams have been reported. Thus the above possibility cannot be ruled out on spectral grounds.

The "anhydroiso" compound can be explained on this basis as the product of dehydration to the five-membered ether with the double bond moving out of conjugation (weak ultraviolet absorption). The "α-iso" compound could arise from hemiacetal formation between carbonyl 1 and the primary hydroxyl,

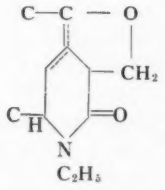

again with the double bond moving out of conjugation. Attempts to demonstrate the presence of an allyl alcohol system in the "iso" compounds by manganese dioxide oxidation (1,30) has been fruitless. The "des(oxymethylene)-iso" compound was inert and the "iso" compound gave a mixture of products, none of which had their main absorption maximum above 220 mμ.

(*c*) An aldol condensation of carbonyl 2 with one of the positions α to carbonyl 1, with the resulting aldol being unable to dehydrate, is a possible explanation of the formation of the iso compounds. However, with such an explanation the spectra cannot be accounted for on classical grounds. (See the discussion of spectra.)

Hypothesis (*b*) is attractive as regards establishing a relation between the glycol system and the nitrogen ring. However, no clear decision can be reached between it and hypothesis (*c*) with the evidence in hand.

When the "iso" compound was hydrogenated over Adams' catalyst in ethanol, desmethanol*seco*lycoctonam ketol was obtained. This means that either before or after reduction of carbonyl 1 the "iso" reaction was reversed and under unusually mild conditions the methoxyl β to carbonyl 2 was eliminated to give the α-β unsaturated ketone. Less surprising is the elimination of the same methoxyl in the reduction of des(oxymethylene)-*seco*lycoctonam diketone in ethanol containing hydrochloric acid. Here, however, the resulting double bond is rapidly reduced giving the dihydrodesmethanol diketone.

Spectra

The position of the C=O stretching frequency of carbonyl 1 in the diketones (Table I) is very unusual for a cyclopentanone. Interaction across space between carbonyls has been shown to shift their maxima as much as 10 wave numbers toward higher frequencies (23), and this effect probably accounts for the anomalies in the diketone spectra. The shift of the peak for carbonyl 1 on formation of the "iso" compounds (Table I) could be due to conjugation or strong hydrogen bonding, or to the disappearance of the above-mentioned interaction. The first two are unlikely, as discussed earlier, hence the last explanation is favored. However, if the "iso" compounds are α-β unsaturated lactams, a shift of the C=O stretching bond for the lactam to smaller frequencies is to be expected. The examination of the spectra of suitbale models may clarify the absence of such a shift in this case.

The presence of the primary hydroxyl produces a decided lowering of the lactam carbonyl frequency (Table I and Table I, reference 1) even in dilute chloroform solution, thus indicating intramolecular hydrogen bonding between the two functions.

Bands in a region generally associated with CH_2CO groups (21,22) appear in the spectra (1410–1430 $cm.^{-1}$) of most of the compounds. However, some of these may be due to hydroxyl groups, since the band at 1418 $cm.^{-1}$ in the "iso" compound disappears when the monoacetate is made. From an examination of the compounds without hydroxyls, it appears that there is no methylene flanking carbonyl 1, but that one or two are next to carbonyl 2. The integrated absorption intensities (10,000 units) of the bands ($CHCl_3$ solution) are much larger than those cited in the literature (2), hence no conclusion can be drawn from this information as to the number of such methylenes.

The ultraviolet spectra of the diketones are most unusual, the high intensity end absorption and the position of the carbonyl maxima being similar to those of conjugated ketones. However, carbonyl 2 when alone (ketols) has a very normal spectrum, and several compounds containing no keto group but carbonyl 1 ("anhydroiso" compound and "des(O-methyl)des(oxymethylene)-iso" compound) have quite normal spectra for compounds with isolated carbonyls. In the spectra of the "iso" compounds the carbonyl maxima are at extremely long wave lengths (337 mμ), a fact which cannot readily be reconciled with the partial structures considered above. There is some possibility that there is no conjugation in the "iso" compounds and that their

ultraviolet spectra are exaggerations of the abnormal diketone spectra. An interaction across space between the two ketone carbonyls or between carbonyl 1 and the lactam carbonyl might be the cause of the abnormal absorption.[2] There is some evidence for similar interaction effects in the literature (7,10). However, 21-acetoxy-pregnene-3-ol-20-one and etiocholan-3-α-ol-11,17-dione which show interaction effects in the infrared (23) have normal ultraviolet spectra, and cyclodecane-1,6-dione has both normal ultraviolet and infrared spectra[3]. Such an effect, if it exists, would be expected to be very dependent on the angle and extent of overlap of the carbonyls, and the diketones from lycoctonine might be quite unique in that regard. If such an effect is present, then the aldol condensation explanation (*c*) of the "iso" compounds is plausible.

Another abnormality in the ultraviolet spectra is the absence of the short wave length maxima in the desmethanol ketols, although they are definitely α-β unsaturated ketones.

Further work to confirm or disprove the postulates put forward in this paper is underway.

EXPERIMENTAL

All melting points are corrected to within $\pm 1°$. The rotations were taken in absolute ethanol at $25 \pm 2°$ C. The alumina used in chromatography was acid washed, and the cited activity is according to Brockmann (9). Ultraviolet spectra were determined on a Beckmann DU spectrophotometer. The log ϵ value for the maximum or minimum is placed in parentheses after the wave length.

The infrared spectra were determined on a Perkin-Elmer single beam model 12B spectrophotometer or on a Perkin-Elmer double beam instrument, model 21. The peaks are indicated by a wave number and the percentage absorption (in parentheses). Shoulders are indicated by an S after the wave number. The compounds were dispersed as mulls in nujol unless otherwise stated.

Secolycoctonam Diketone

Lycoctonam hydrate (11) in solution in four to five molar equivalents of 0.05 molar periodic acid, adjusted to pH 5 using sodium acetate in the dark at room temperature, consumed 0.5 mole of reagent in 24 hr. and one mole in 70 hr. After 115 hr. the molar consumption was 1.2. The product could be extracted nearly quantitatively with methylene dichloride, from which it was obtained as a froth which has not crystallized. A sample of the product (0.94 gm.) was chromatographed on 15 gm. of alumina of activity 3. Six 35 cc. eluate fractions of 50% benzene–chloroform, and five of chloroform contained 679 mgm. This yielded 581 mgm. of crystalline *seco*lycoctonam diketone monoacetate (see below). Methanol in chloroform eluted 272 mgm., of which 175 mgm. (m.p. 217°) crystallized from acetone solution (see "iso" compound).

[2] *This possibility was originally put forward in discussion by Dr. R. A. McIvor.*

[3] *The authors wish to thank Dr. R. N. Jones for providing samples of the two steroids, and Dr. A. G. Anderson Jr. for a generous gift of cyclodecane-1,6-dione.*

The amorphous *seco*lycoctonam diketone rapidly gave a silver mirror with Tollen's reagent and reduced hot Fehling's solution.

Ultraviolet spectrum: λ_{min} 272 mμ (2.14); λ_{max} 318 mμ (2.45); log ϵ 3.92 at 2.10 mμ; and 3.77 at 220 mμ.

Infrared spectrum (30 mgm. per ml. in $CHCl_3$; 0.1 mm. cell): 3465 (5), 3010 (28), 2950 (29), 2900 (20), 2835 (16), 1766 (37), 1713 (32), 1635 (50), 1467 (28), 1420 (19), 1385 (18), 1358 (16), 1328 (13), 1306 (14), 1055S (18), 1028S (36), 1100 (60), 1070S (25), 1045 (20), 1025 (19), 978 (17).

Secolycoctonam Diketone Monoacetate

A solution of 293 mgm. of *seco*lycoctonam diketone in 5 cc. of pyridine and 5 cc. of acetic anhydride was left at room temperature for 24 hr. The reagents were removed under reduced pressure, the product taken up in chloroform, and washed with acid and base. The product recovered from the chloroform crystallized from ether solution. The 269 mgm. of crystals after recrystallization from acetone–ether melted at 178–181°. Chromatography on alumina did not raise the melting point. The compound did not react with potassium permanganate in acetone containing a little acetic acid in three hours at room temperature. $[\alpha]_D$ 62 ± 1° (c = 2.56). Found: C, 61.98; H, 7.71; N, 2.45. Calc. for $C_{27}H_{39}O_9N$: C, 62.17; H, 7.54; N, 2.69.

Ultraviolet spectrum (Fig. 1): λ_{min} 270 mμ (1.44); λ_{max} 320 (2.41).

Infrared spectrum (29 mgm. per ml. in $CHCl_3$, 0.1 mm. cell): 3010 (26), 2960 (26), 2910 (18), 2835 (16), 1763 (40), 1746 (46), 1712 (37), 1650 (51), 1468 (27), 1430 (16), 1386 (23), 1370 (21), 1325 (10), 1303 (11), 1375S (14), 1130S (29), 1100 (60), 1042 (30), 975 (14).

Saponification of Secolycoctonam Diketone Monoacetate

(*a*) To a solution of 200 mgm. of the monoacetate in 2 cc. of methanol was added 200 mgm. of sodium bicarbonate and 2 cc. of water. The mixture was heated to boiling on the steam bath to effect complete solution. After the solution had stood at room temperature for 20 min. a further 1 cc. of water was added, the solution heated for a few minutes, then left at room temperature for 100 min. The faintly yellow solution was extracted with chloroform, giving 195 mgm. of froth. This was dissolved in a minimum volume of acetone, then ether added. Twenty-eight milligrams of "iso" compound, m.p. 214° (see below) deposited. No desmethanol*seco*lycoctonam diketone was obtained, and the residual material when freed from solvent had absorption in the ultraviolet nearly identical to that of the original acetate.

(*b*) A solution of 34 mgm. of the monoacetate in 1 cc. of methanol and 1 cc. of 5% sodium hydroxide solution was left at room temperature for 10 min., diluted with 3 cc. of water, and left for a further 35 min. Extraction with chloroform gave 39 mgm. of froth which crystallized from ether giving 20 mgm., m.p. 204°. When 59 mgm. of similar material was recrystallized three times from acetone–ether, 29 mgm. were obtained, m.p. 203–205.5° (imm. at 185°), identical with desmethanol*seco*lycoctonam diketone (see below).

Desmethanolsecolycoctonam Diketone

(*a*) Potassium hydroxide (0.164 gm.) was added to 26 mgm. of *seco*lycocto-

nam diketone in 3 cc. of water, and the solution left at room temperature for one hour. It was then neutralized and extracted with chloroform. The 25 mgm. of product crystallized readily from ether giving 20 mgm., m.p. 196°. One recrystallization raised the melting point to 201°. This material gave no mixed melting point depression with the product from hydrolysis of the monoacetate with sodium hydroxide in aqueous methanol.

(*b*) A solution of 116 mgm. of *seco*lycoctonam diketone in 6 cc. of 6 *N* sulphuric acid was heated on the steam bath for 40 min. The solution was cooled, neutralized, and extracted with methylene dichloride. The 105 mgm. of product crystallized from acetone–ether, giving 92 mgm., m.p. 203°. The melting point was raised to 203–205.5° by recrystallization from a very concentrated acetone solution. $[\alpha]_D$ 88 ± 1° (c = 2.40). Found: C, 64.30, 64.71, 64.57; H, 7.72, 7.93, 7.65; OCH_3, 20.55, 20.23. Calc. for $C_{24}H_{33}O_7N$: C, 64.41; H, 7.43; 3 OCH_3, 20.80.

Ultraviolet spectrum: λ_{max} 221 mμ (4.04); λ_{min} 275 (1.82); λ_{max} 322 (2.49).

Infrared spectrum: 3394 (46), 1753 (56), 1670S (64), 1655 (75), 1412 (53), 1327 (39), 1304 (32), 1296 (31), 1279 (24), 1267 (24), 1245 (33), 1234 (35), 1220 (48), 1203 (50), 1178 (28), 1163 (33), 1155 (38), 1132 (46), 1116 (67), 1094 (66), 1082S (61), 1056 (42), 1033 (30), 1020 (33), 1009 (37), 981 (31), 968 (43), 956S (31), 903 (26), 870 (20), 853 (23), 822 (17), 793 (12), 756 (29), 728 (31), 686 (27).

When 51 mgm. of the compound was refluxed for 1.5 hr. with 2 cc. of 6 *N* sulphuric acid, the 51 mgm. extracted by chloroform gave 39 mgm. of unchanged material. The remainder did not crystallize.

Secolycoctonam Ketol

Sodium borohydride (25 mgm.) was added to a solution of 56 mgm. of *seco*lycoctonam diketone in 2 cc. of water. After 0.5 hr. the solution was acidified and extracted with chloroform. The 52 mgm. of froth crystallized from acetone–ether, giving 41 mgm., m.p. 206–214°. After two recrystallizations this melted at 210–215° (dec.) then resolidified and melted over a range up to 280°. $[\alpha]_D$ −50 ± 1° (c = 2.20). Found: C, 62.29, 61.79, 62.19; H, 8.53, 8.30, 8.04; OCH_3, 25.91. Calc. for $C_{25}H_{39}O_8N$: C, 62.36; H, 8.16; 4 OCH_3, 25.78.

Ultraviolet spectrum (Fig. 1): λ_{min} 255 mμ (1.31); λ_{max} 270 mμ (1.60).

Infrared spectrum: 3485 (57), 3390 (68), 1710 (73), 1616 (92), 1510 (19), 1494 (24), 1413 (29), 1357 (27), 1344 (26), 1333 (29), 1324 (27), 1296 (31), 1276 (52), 1252 (31), 1236 (59), 1209 (69), 1184 (42), 1166 (48), 1140 (42), 1117S (71), 1105S (86), 1098 (87), 1081 (73), 1065 (59), 1053 (55), 1045S (47), 1025 (32), 997 (38), 974 (29), 957 (37), 894 (18), 867 (15), 805 (22), 782 (19), 754 (18), 705 (17).

Desmethanolsecolycoctonam Ketol

(*a*) Eleven milligrams of *seco*lycoctonam ketol in an evacuated tube was heated to around 240° until decomposition stopped and the product solidified. The product was extracted and recrystallized from acetone, giving 5 mgm.,

m.p. 291° and 2 mgm. m.p. 289°. Neither crop depressed the melting point of the products from (*b*) and (*c*).

(*b*) To a solution of 63 mgm. of desmethanol*seco*lycoctonam diketone in a mixture of 1 cc. of methanol and 3 cc. of water was added 30 mgm. of sodium borohydride. After 0.5 hr. the solution was acidified and extracted with chloroform. The 60 mgm. of crystals obtained on evaporation of the chloroform melted at 279°. After two recrystallizations from methanol 29 mgm. m.p. 291° was obtained.

(*c*) A solution of 52 mgm. of *seco*lycoctonam ketol in 2 cc. of 6 *N* sulphuric acid was heated on the steam bath for 0.5 hr. Chloroform extracted 50 mgm. of product. When recrystallized twice from methanol–acetone this melted at 294–299°. $[\alpha]_D$ $-76 \pm 10°$ ($c = 0.85$) (sparingly soluble in ethanol). Found: C, 64.06; H, 7.65; OCH_3, 20.59. Calc. for $C_{24}H_{35}O_7N$: C, 64.12; H, 7.85; 3 OCH_3, 20.7.

Ultraviolet spectrum: λ_{min} 285 mμ (1.97); λ_{max} 305 mμ (2.03).

Infrared spectrum: 3345 (53), 3215 (53), 1683 (29), 1662 (76), 1640 (88), 1430 (38), 1400 (19), 1356 (28), 1336 (25), 1320 (19), 1287 (18), 1270 (14), 1242S (28), 1221 (57), 1205 (44), 1196 (45), 1170 (33), 1140 (44), 1115 (74), 1096 (80), 1062 (54), 1046 (38), 1025S (15), 1010S (17), 995 (29), 975 (22), 959 (22), 905 (12), 864 (16), 845 (11), 831 (26), 800 (6), 767 (13), 753 (11), 710 (12), 695 (16).

"Iso" Compound

*Seco*lycoctonam diketone (152 mgm.) was adsorbed from benzene on 5 gm. of alumina, activity 3–4, and left on the column for $15\frac{1}{2}$ hr. Thirty cubic centimeters of benzene, 100 cc. of 50% C_6H_6–$CHCl_3$, and 50 cc. of chloroform eluted 71 mgm., from which some desmethanol*seco*lycoctonam diketone was obtained. Chloroform containing 0.25% of methanol eluted 77 mgm. which crystallized from acetone giving 53 mgm. m.p. 216°. After two recrystallizations from acetone the compound melted at 218° after softening at 213° (immersed at 195°). This proved identical with the product from the original chromatogram of the periodate cleavage products. $[\alpha]_D$ $58 \pm 2°$ ($c = 0.72$). Found: C, 62.25; H, 7.82; N, 3.07; OCH_3, 24.4, 26.89. Calc. for $C_{25}H_{37}O_8N$: C, 62.61; H, 7.78; N, 2.92; 4 OCH_3, 25.88.

Ultraviolet spectrum (Fig. 1): λ_{max} 218 mμ (3.82), λ_{min} 285 mμ (1.62), λ_{max} 335 mμ (2.26).

Infrared spectrum: 3430 (54), 3325 (43), 1734 (74), 1632 (92), 1418 (70), 1398 (44), 1345 (49), 1325 (39), 1295 (54), 1269 (59), 1226 (62), 1217 (58), 1197 (53), 1161 (56), 1148S (67), 1138 (79), 1133 (79), 1107 (87), 1099 (86), 1091 (82), 1077 (60), 1063 (70), 1055 (71), 1030 (68), 1016 (49), 1002 (57), 981 (61), 944 (40), 934S (29), 923S (24), 902 (16), 875 (12), 831 (13), 803 (13), 760 (21), 725 (21), 700 (14), 685 (20), 663 (13), 648 (21).

When 25 mgm. of "iso" compound was treated for one hour with diazomethane in methanol–ether, 21 mgm. of unchanged compound was recovered.

A solution of 20 mgm. of "iso" compound and 90 mgm. of potassium hydroxide in 1.5 cc. of methanol was diluted with 1.5 cc. of water and left at

room temperature for one hour. The solution was concentrated to half volume under reduced pressure and extracted with chloroform. The 12 mgm. of neutral product crystallized from acetone–ether when seeded with desmethanol*seco*lycoctonam diketone. The 8 mgm. of crystals after one recrystallization melted at 205° (hot stage) and showed no depression with desmethanol-*seco*lycoctonam diketone. A comparison of infrared spectra confirmed the identity.

A solution of 76 mgm. of "iso" compound and 40 mgm. of sodium borohydride in 4 cc. of 50% aqueous methanol was left at room temperature. After acidification the solution was extracted with chloroform. The 76 mgm. of product crystallized from concentrated acetone solution giving 8 mgm., m.p. 275°, and 52 mgm., m.p. 204–211°. The former proved to be desmethanol-*seco*lycoctonam ketol, while the latter, after one recrystallization, was shown by mixed melting point and comparison of infrared spectra to be *seco*lycoctonam ketol.

The "iso" compound was inert to hydrogen over Adams' catalyst in ethanol containing hydrochloric acid (3 cc. alcohol, two drops concentrated acid).

"Iso" compound (19.7 mgm.) in 3 cc. of ethanol in the presence of platinum from 10 mgm. Adams' catalyst absorbed 1.03 cc. (N.T.P.) of hydrogen (1.1 moles) in 40 min., after which the reaction was stopped. (Another experiment showed that the hydrogenation proceeded at a reduced rate until over two moles were absorbed.) The product crystallized completely. One recrystallization from methanol–acetone gave 10 mgm. m.p. 283–288° (hot stage). Mixed m.p. with a sample of desmethanol*seco*lycoctonam ketol was 283–293° (hot stage).

A mixture of 82 mgm. of "iso" compound and 1.2 gm. of active (1) manganese dioxide in 6 cc. of dry benzene was shaken for two hours. The manganese dioxide was removed by filtration and washed with benzene. The benzene solution contained 56 mgm. of product. A solution of this material in ether containing a little acetone deposited a few milligrams of crystals, after addition of petroleum ether. After recrystallization from acetone–ether this melted at 152° and had λ_{max} 219 mμ (3.7), λ_{min} 285 mμ (1.7), and λ_{max} 340 mμ (2.2) (assumed mol. wt. 480). Methanol extraction of the manganese dioxide gave 27 mgm. of ether-insoluble product. This was combined with the noncrystalline material and chromatographed on 2.5 gm. of alumina (activity 3–4). Fifty per cent chloroform–benzene eluted 18 mgm. which did not crystallize. The main fraction had no short-wave-length maximum, log ϵ 3.76 (215 mμ), λ_{min} 312 mμ (2.1), λ_{max} 330 mμ (2.15) (assumed mol. wt. 480). Chloroform eluted 7 mgm. of amorphous material. Methanol (0.5%) in chloroform eluted 25 mgm. which deposited 6 mgm. of crystals from acetone–ether. After recrystallization these melted at 182° and had λ_{max} 219 mμ (3.66), λ_{min} 285 mμ (1.61), and λ_{max} 335 mμ (2.10) (assumed mol. wt. 480).

"Iso" Compound Monoacetate

Thirty milligrams of "iso" compound was warmed gently with a mixture of 1 cc. of pyridine and 1 cc. of acetic anhydride until it dissolved. The solution

was left at room temperature for 22 hr., the reagents distilled under reduced pressure, and a chloroform solution of the residue washed with dilute acid and base. The product crystallized from ether–petroleum ether, giving 24 mgm. m.p. 176°. One recrystallization raised the m.p. to 177° (immersed at 150°) (21 mgm.). Found: C, 62.87, 62.75; H, 7.24, 7.63; OCH_3, 24.66. Calc. for $C_{27}H_{39}O_9N$: C, 62.17; H, 7.54; 4 OCH_3, 23.79.
Ultraviolet spectrum: λ_{max} 218 mμ (3.82); λ_{min} 285 mμ (1.62); λ_{max} 337 mμ (2.25).
Infrared spectrum: 3500 (30), 1738 (82), 1651 (80), 1335 (43), 1325 (38), 1300 (45), 1291 (49), 1275 (47), 1266 (47), 1248 (75), 1232 (80), 1211 (61), 1195 (41), 1180 (35), 1167 (49), 1145 (52), 1125 (78), 1115 (75), 1094 (79), 1072 (52), 1045 (70), 1026 (50), 990 (50).

"Anhydroiso" and "α-iso" Compounds

A suspension of 77 mgm. of "iso" compound in 3 cc. of 6 *N* sulphuric acid was heated for 45 min. on the steam bath. Solution was complete in 20 min. The 77 mgm. of neutral product extracted by chloroform was adsorbed from benzene on 2.5 gm. of alumina, activity 2.

Eluant (30 cc. portions)	Weight eluted, mgm.
1. Benzene	2
2. 50% Benzene–chloroform	35
3. 50% Benzene–chloroform	9
4. 50% Benzene–chloroform	2
5. ½% Methanol in chloroform	30
6. ½% Methanol in chloroform	4

Fraction 2 crystallized readily from ether, giving 13 mgm., m.p. 204°. This could be readily sublimed at 175°, 5×10^{-4} mm. pressure, without changing the melting point. $[\alpha]_D$ 81 ± 2° (*c* = 0.56). Found: C, 64.89; H, 7.70; OCH_3, 26.78, 26.66. Calc. for $C_{25}H_{37}O_7N$: C, 65.06; H, 7.64; 4 OCH_3, 26.78.
Ultraviolet spectrum: λ_{min} 270 (0.89); λ_{max} 300 (1.9).
Infrared spectrum: 1732 (79), 1646 (88), 1550 (14), 1485 (58), 1450 (62), 1437S (43), 1382 (51), 1365 (52), 1345 (36), 1326 (35), 1306 (30), 1288 (32), 1273 (45), 1257 (53), 1216 (59), 1205S (43), 1185 (45), 1168 (51), 1135 (77), 1100 (90), 1086 (86), 1070 (50), 1048 (47), 1025 (36), 1004 (72), 991 (45), 975 (35), 950 (32), 940 (29), 920 (21), 910 (20), 895 (34), 885 (51), 850 (48), 810 (15), 775 (32), 725 (9), 649 (4).

Fraction 5 crystallized from ether after prolonged scratching, giving 21 mgm., m.p. 167–176°. After two recrystallizations from acetone-ether this melted at 171–175°. $[\alpha]_D$ 66 ± 1° (*c* = 2.18). Found: C, 63.04; H, 7.64; N, 3.19; OCH_3, 25.59; active hydrogen, 0.41, 0.39. Calc. for $C_{25}H_{37}O_8N$: C, 62.61; H, 7.78; N, 2.92; 4 OCH_3, 25.88; 2 active hydrogens 0.42.
Ultraviolet spectrum: log ε 3.22 (225 mμ) and 1.11 (250 mμ) – no features.
Infrared spectrum: 3505 (52), 3450 (32), 1643 (89), 1560 (13), 1486 (61), 1400 (44), 1362 (40), 1327 (42), 1311 (60), 1295 (40), 1267S (38), 1260 (49), 1225 (67), 1205 (50), 1200S (47), 1174 (36), 1158 (40), 1141S (54), 1129 (72),

1110 (80), 1082 (78), 1050 (62), 1030 (59), 1016 (54), 993 (45), 975 (48), 951 (49), 925 (26), 912S (20), 895 (23), 855 (25), 835 (26), 805 (10), 782S (13), 775 (30), 750 (11), 735 (12), 718 (9), 700 (6), 665 (15), 646 (12).

When 20 mgm. of "α-iso" compound was treated at room temperature for five hours with acetic anhydride and pyridine, 19 mgm. of crystalline material m.p. 175° was recovered. This proved identical with starting material (mixed m.p. and infrared spectrum).

Des(oxymethylene)-secolycoctonam Diketone

A solution of 0.5 gm. of des(oxymethylene)-lycoctonam, 0.5 gm. of paraperiodic acid, and 0.8 gm. of hydrated sodium acetate was left for six days at room temperature in the dark (molar uptake of periodate 0.61 in 72 hr., 1.0 in six days). The solution was made nearly neutral with sodium bicarbonate and extracted with chloroform. The 488 mgm. extracted crystallized readily from ether, giving 320 mgm., m.p. 159° and 40 mgm., m.p. 156°. One recrystallization raised the melting point to 160°. An eight funnel countercurrent distribution between benzene and water gave material from funnels three to six melting at 160 to 162°. $[\alpha]_D$ 85 ± 1° (c = 2.39). This reduced Tollen's reagent at room temperature and Fehling's solution on the steam bath, but was unchanged by permanganate in acetone in 1.5 hr. An aqueous solution of the compound was unaffected by two hours contact with fresh silver oxide. Found: C, 64.29, 64.59, 63.80; H, 7.47, 7.56, 7.91; N, 3.40; OCH_3, 27.39. Calc. for $C_{24}H_{35}O_7N$: C, 64.12; H, 7.85; N, 3.12; 4 OCH_3, 27.61.

Ultraviolet spectrum: log ε 3.79 (215 mμ); λ_{min} 265 mμ (1.67); λ_{max} 322 mμ (2.42).

Infrared spectrum (30 mgm. per ml. of chloroform, 0.1 mm. cell): 3010 (42), 2960 (39), 2900 (27), 2840 (26), 1765 (48), 1711 (48), 1646 (68), 1468 (36), 1432 (28), 1385 (22), 1360 (20), 1327 (17), 1294 (18), 1110 (60), 1095 (68), 1028 (16), 1002 (19), 966 (15), 942 (10), 904 (8).

(5 mgm. per ml. in carbon disulphide, 1 mm. cell): 2940 (58), 2880 (45), 2820 (44), 1758 (71), 1713 (68), 1663 (93), 1378 (42), 1358 (39), 1347 (29), 1295 (32), 1268 (33), 1250 (34), 1235 (49), 1210 (61), 1100 (87), 1038 (27), 1004 (32), 967 (28).

Desmethanoldes(oxymethylene)-secolycoctonam Diketone

Ninety milligrams of des(oxymethylene)-*seco*lycoctonam diketone in 4 cc. of 6 *N* sulphuric acid was heated on the steam bath for 30 min. The cooled solution was neutralized and extracted with chloroform. The 86 mgm. of product crystallized from acetone–ether giving 71 mgm. m.p. 229° and 11 mgm. m.p. 225°. After three recrystallizations from acetone the compound melted at 228–230° (immersed at 205°) $[\alpha]_D$ 86 ± 1° (c = 1.88). Found: C, 66.15, 66.44; H, 8.03, 7.71; N, 3.62; OCH_3, 21.4. Calc. for $C_{23}H_{31}O_6N$: C, 66.16; H, 7.49; N, 3.36; 3 OCH_3, 22.30.

Ultraviolet spectrum: λ_{max} 223 mμ (4.04); λ_{min} 275 mμ (1.82); λ_{max} 321 mμ (2.50).

Infrared spectrum (29.8 mgm. per ml. of chloroform, 0.1 mm. cell): 3000 (32), 2940 (33), 2890S (20), 2825 (16), 1762 (44), 1678 (49), 1465 (33), 1433 (23),

1386 (21), 1359 (20), 1332 (14), 1296 (13), 1270 (18), 1155 (18), 1115 (58), 1095 (58), 1052 (18), 1000 (19), 961 (15), 861 (12), 845 (14).

The compound was recovered unchanged after two hours refluxing with 6 *N* sulphuric acid. It reduced Tollen's reagent rapidly at room temperature.

Des(oxymethylene)-secolycoctonam Ketol

A solution of 73 mgm. of des(oxymethylene)-*seco*lycoctonam diketone and 30 mgm. of sodium borohydride in 2 cc. of 50% aqueous methanol was left at room temperature for 30 min. The solution was acidified and the product extracted quantitatively with chloroform. This crystallized, on addition of ether to a very concentrated acetone solution, yielding 56 mgm., m.p. 180–183°. After two recrystallizations from the same solvents, the compound melted at 182–185°. $[\alpha]_D$ $-69 \pm 1°$. Found: C, 63.88; H, 8.07. Calc. for $C_{24}H_{37}O_7N$:C, 63.83; H, 8.26.

Ultraviolet spectrum: log ϵ 3.83 at 212 mμ; shoulder at 265–280 mμ, log ϵ 1.9.

Infrared spectrum: 3365 (86), 1713 (86), 1626 (97), 1355 (74), 1293 (70), 1281 (70), 1253S (49), 1230 (86), 1211 (85), 1180S (62), 1140 (88), 1105 (94), 1089 (79), 1060 (70), 1006 (67), 966 (58), 929 (34), 916 (34), 905 (35), 886 (29), 851 (39), 805 (37), 773 (25), 720 (41), 684 (34), 642 (48).

Desmethanoldes(oxymethylene)-secolycoctonam Ketol

Twenty-eight milligrams of des(oxymethylene)-*seco*lycoctonam ketol in 2 cc. of 6 *N* sulphuric acid was heated for 0.5 hr. The solution was neutralized and extracted with chloroform. An acetone–ether solution of the product deposited 26 mgm. of crystals, m.p. 217°. After recrystallization the compound melted at 214–217° (immersed at 190°). $[\alpha]_D$ $-97 \pm 1°$. Found: C, 66.33, 66.03; H, 8.12, 8.02; N, 3.44; OCH_3, 22.85. Calc. for $C_{23}H_{33}O_6N$: C, 65.84; H, 7.93; N, 3.34; 3 OCH_3, 22.19.

Ultraviolet spectrum: log ϵ 4.04 (212 mμ); log ϵ 4.00 (220 mμ); log ϵ 3.96 (225 mμ); λ_{min} 280 mμ (1.89); λ_{max} 305 mμ (1.99).

Infrared spectrum: 3320 (63), 1670 (77), 1624 (89), 1335 (36), 1290 (27), 1250 (32), 1230 (53), 1210 (50), 1197 (48), 1140 (57), 1114 (77), 1092 (77), 1075 (45), 1055 (46), 1000 (46), 970 (26), 951 (28); 895 (15), 856 (21), 834 (23), 755 (21), 720 (12), 695 (11).

"Des(oxymethylene)-iso" Compound

Des(oxymethylene)-*seco*lycoctonam diketone (162 mgm.) was adsorbed from benzene onto 5 gm. of alumina (activity 2) and left on the column for 15 hr. Benzene eluted a mixture of desmethanoldes(oxymethylene) diketone and starting material; 25% chloroform in benzene gave starting material; then 50% chloroform–benzene, chloroform, and 0.5% methanol in chloroform eluted 105 mgm. An ether solution of this deposited 76 mgm. of crystals. This was best purified by chromatography on alumina (activity 2). The product then was obtained melting at 220–230°. After three recrystallizations from acetone it melted at 222–232°. $[\alpha]_D$ 31 $\pm$ 1° (c = 1.99). Found: C, 63.69, 64.39; H, 7.43, 8.15; N, 3.28; OCH_3, 27.43. Calc. for $C_{24}H_{35}O_7N$: C, 64.12; H, 7.85; N, 3.12; 4 OCH_3, 27.61.

Ultraviolet spectrum: λ_{max} 219 mμ (3.82); λ_{min} 285 mμ (1.71); λ_{max} 340 mμ (2.27).
Infrared spectrum: 3520 (33), 3010 (27), 1742 (74), 1652 (92), 1480 (46), 1429 (50), 1394 (37), 1360 (55), 1335S (31), 1329 (34), 1322S (30), 1308 (34), 1298 (49), 1293 (50), 1282 (41), 1269S (30), 1255 (39), 1224 (58), 1209 (53), 1185 (40), 1174 (44), 1155 (60), 1127 (89), 1117 (85), 1096 (78), 1080S (58), 1065S (53), 1056 (64), 1045 (49), 1011 (42), 1000 (54), 990 (50), 972 (32), 964 (32), 935 (37), 894 (14), 871 (14), 845 (21), 800S (23), 795 (26), 788S (14), 742 (14), 691 (20), 648 (29), 608 (25).

The compound was inert to hydrogen in the presence of Adams' catalyst in acetic acid or in ethanol containing a little concentrated hydrochloric acid. The compound was recovered unchanged after it was shaken in benzene solution with active manganese dioxide (1) for two hours.

"Des(O-methyl)des(oxymethylene)-iso" Compound

Thirty-six milligrams of "des(oxymethylene)-iso" compound in 2 cc. of 6 *N* sulphuric acid was heated on the steam bath for 45 min. Methylene dichloride extracted 36 mgm. which crystallized from acetone–ether giving 30 mgm. m.p. 162° and 3 mgm. of less pure crystals. Recrystallization from the same solvents raised the melting point to 162–164° (preliminary loss of solvent of crystallization). $[\alpha]_D$ $-97 \pm 2°$ (c = 1.25). Found: C, 63.77; H, 7.60; OCH_3, 20.85; active hydrogen 0.41. Calc. for $C_{23}H_{33}O_7N$: C, 63.43; H, 7.64; 3 OCH_3, 21.38; two active hydrogens, 0.46.
Ultraviolet spectrum: log ε 3.6 (215 mμ); log ε 3.3 (220 mμ); log ε 3.1 (250 mμ); λ_{min} 270 mμ (1.29); λ_{max} 312 mμ (1.73).
Infrared spectrum: 3530 (47), 3465 (45), 3380 (42), 1755 (81), 1710 (33), 1657 (92), 1427 (61), 1360 (60), 1321 (46), 1278 (49), 1210 (80), 1187 (63), 1151S (41), 1098 (94), 1075 (68), 1035 (51), 1002 (57), 990 (50), 965 (34), 950 (33), 903 (25), 854 (19), 841 (18), 805 (22), 780 (16), 750S (18), 741 (23), 710 (19), 700 (21), 666 (12), 643 (13).

The compound proved inert to hydrogen over Adams' catalyst in ethanol containing hydrochloric acid.

When 14 mgm. of the compound and 38 mgm. of paraperiodic acid in 2 cc. of water were left at room temperature for 24 hr., only traces of product could be extracted from neutral, acidic, or basic medium.

"Dihydrodes(O-methyl)des(oxymethylene)-iso" Compound

A solution of 55 mgm. of "des(O-methyl)des(oxymethylene)-iso" compound and 43 mgm. of sodium borohydride in 2 cc. of methanol and 0.5 cc. of water stood for one hour at room temperature. Dilute sulphuric acid was added slowly until gas evolution ceased (pH still near 8), water was added, and the solution extracted with chloroform. The 62 mgm. of product was insoluble in ether. It crystallized in part from wet acetone giving 25 mgm., m.p. above 330°. The acetone soluble part crystallized from concentrated aqueous solution, giving 8 mgm. m.p. 82–86°. The high melting solid appeared to be the salt of a borate complex. It was dissolved in 1 cc. of methanol, and 1 cc. of 6 *N* sulphuric acid and 0.5 cc. of water added. After two hours at room temperature

the solution was extracted with chloroform. The product crystallized from chloroform–ether, giving 17 mgm. m.p. 161° and 4 mgm. m.p. 157°. The crystals melting at 86° proved to be a higher hydrate of this compound (infrared and mixed m.p. comparisons of dried samples). One recrystallization raised the melting point to 162°. The compound was dried *in vacuo* at 100° over phosphoric anhydride for 3.5 hr. Found: C, 60.07; H, 7.77; OCH_3, 18.84. Calc. for $C_{23}H_{35}O_7N.H_2O$: C, 60.64; H, 8.19; 3 OCH_3 20.44.
Ultraviolet spectrum: Only end absorption.
Infrared spectrum: (30 mgm. per ml. in chloroform, 0.1 mm. cell): 3425 broad, 3000 (38), 2945 (39), 2900S (29), 2825 (22), 1631 (61), 1465 (29), 1450S (28), 1385 (26), 1359 (25), 1328 (21), 1315 (22), 1298 (20), 1137S (29), 1120 (53), 1095 (63), 1037 (25), 1000 (24), 958 (13).

Dihydrodesmethanoldes(oxymethylene)-secolycoctonam Diketone

(*a*) A solution of 31.5 mgm. of des(oxymethylene)-*seco*lycoctonam diketone in 4 cc. of absolute ethanol containing three drops of concentrated hydrochloric acid was hydrogenated under one atmosphere pressure using Adams' catalyst (prereduced from 25 mgm. of oxide). In three hours 1.0 mole of hydrogen was taken up. The solution was filtered, concentrated to small volume under reduced pressure, and the residue taken up in sodium carbonate solution. Methylene dichloride extracted 31 mgm. which crystallized spontaneously on standing overnight. After three recrystallizations from ether the product melted at 177°. $[\alpha]_D$ 38 ± 1° (c = 1.85). Found: C, 65.19, 66.18; H, 8.02, 7.99; OCH_3, 22.27. Calc. for $C_{23}H_{33}O_6N$: C, 65.84; H, 7.93; 3 OCH_3, 22.19.
Ultraviolet spectrum: log ϵ 3.81 (212 mμ); log ϵ 3.80 (220 mμ); λ_{min} 267 (1.96); λ_{max} 320 (2.40).
Infrared spectrum: 1756 (74), 1701 (73), 1663 (90), 1423 (58), 1358 (42), 1345S (33), 1324 (34), 1292 (27), 1271 (37), 1215S (31), 1241 (48), 1210 (70), 1180S (34), 1173 (35), 1151 (35), 1139 (43), 1120S (72), 1107 (81), 1095 (74), 1088S (72), 1050 (26), 1040 (32), 1013 (38), 998 (41), 963 (33), 925 (20), 903 (18), 858 (16), 843 (16), 800 (13), 725 (25), 675 (5).

(*b*) A suspension of platinum from 12.8 mgm. of platinum oxide (Adams') in a solution of 51 mgm. of desmethanoldes(oxymethylene)-*seco*lycoctonam diketone in 3 cc. of ethanol and three drops of concentrated hydrochloric acid took up 1.07 moles of hydrogen in 40 min. The product crystallized readily from ether, giving 42 mgm., m.p. 169°. After purification by chromatography on alumina the product melted at 171°, and proved identical with the product from (*a*) (mixed m.p. and comparison of infrared spectra).

Periodate Oxidation of Hydroxylcoctonine

Hydroxylcoctonine (41 mgm.) in 5.0 cc. of 0.05 molar periodic acid solution buffered to pH 5 using sodium acetate consumed 0.74×10^{-4} mole (mole ratio 0.87) of the reagent in five hours at room temperature. After addition of sodium carbonate, thorough extraction with chloroform removed only 6 mgm. from the aqueous layer. This crystallized from ether, m.p. 140°, mixed m.p. with hydroxylcoctonine 143–148°. Under similar conditions in 21 hr. 1.07 moles

of periodic acid was consumed per mole of base (only 1 mgm. of base could be extracted (36 mgm. used)), and in 68 hr. the molar uptake of reagent was 1.13.

21-Acetoxypregnene-3-ol-20-one

Recrystallized from ether m.p. 180–183°.

Ultraviolet spectrum: log ϵ 2.62 (215 mμ); λ_{min} 240 mμ (1.81); λ_{max} 280 mμ (2.11).

Etiocholan-3 α-ol-11,17-dione

Ultraviolet spectrum: log ϵ 2.23 (215 mμ); λ_{min} 240 mμ (near 0); λ_{max} 295 mμ (1.83).

Cyclodecane-1,6-dione

Recrystallized from ether m.p. 99–100°.

Ultraviolet spectrum: log ϵ 0.45 (230 mμ); λ_{max} 285 mμ (1.59).

Infrared spectrum (15 mgm. per ml. in chloroform, 0.1 mm. cell): 2940 (26), 2890 (15), 1707 (66), 1443 (28), 1420 (29), 1372 (22), 1345 (19), 1146 (35), 1112 (25), 1042 (12), 980 (11).

ACKNOWLEDGMENT

The authors wish to thank Dr. R. N. Jones and Mr. R. Lauzon for taking the infrared absorption spectra and for advice on their interpretation.

REFERENCES

1. ATTENBURROW, J., CAMERON, A. F. B., CHAPMAN, J. H., EVANS, R. M., HEMS, B. A., JANSEN, A. B. A., and WALKER, T. J. Chem. Soc. 1094. 1952.
2. BARNES, C. S., BARTON, D. H. R., COLE, A. R. H., FAWCETT, J. S., and THOMAS, B. R. J. Chem. Soc. 571. 1953.
3. BARTLETT, P. D. and POECKEL, I. J. Am. Chem. Soc. 59: 820. 1937.
4. BARTON, D. H. R. J. Chem. Soc. 1027. 1953.
5. BERGMANN, M. and GIERTH, M. Ann. 448: 48. 1926.
6. BLOUT, E. R., EAGER, V. W., and SILVERMAN, D. C. J. Am. Chem. Soc. 68: 566. 1946.
7. BRAUDE, E. A., JONES, E. R. H., SONDHEIMER, F., and TOOGOOD, J. B. J. Chem. Soc. 607. 1949.
8. BRAUN, J. v., HAENSEL, W., and ZOBEL, F. Ann. 462: 283. 1928.
9. BROCKMANN, H. and SCHODDER, H. Ber. 74: 73. 1941.
10. CRAM, D. J. and STEINBERG, H. J. Am. Chem. Soc. 73: 5691. 1951.
11. EDWARDS, O. E. and MARION, L. Can. J. Chem. 30: 627. 1952.
12. ELLIS, B. and PETROW, V. A. J. Chem. Soc. 1078. 1939.
13. EVANS, L. K. and GILLAM, A. E. J. Chem. Soc. 815. 1941.
14. GAUTHIER, M. D. Ann. chim. et phys. [8], 16: 289. 1909.
15. GROVE, J. F. and WILLIS, H. A. J. Chem. Soc. 877. 1951.
16. HAYNES, L. J. and JONES, E. R. H. J. Chem. Soc. 954. 1946.
17. HEILBRON, I. M., JONES, E. R. H., and SPRING, F. S. J. Chem. Soc. 801. 1937.
18. HORNING, E. C., STROMBERG, V. L., and LLOYD, H. A. J. Am. Chem. Soc. 74: 5153. 1952.
19. HUNSBERGER, I. M. J. Am. Chem. Soc. 72: 5626. 1950.
20. JACOBS, W. A. J. Biol. Chem. 57: 553. 1923.
21. JONES, R. N. and COLE, A. R. H. J. Am. Chem. Soc. 74: 5648. 1952.
22. JONES, R. N., COLE, A. R. H., and NOLIN, B. J. Am. Chem. Soc. 74: 5662. 1952.
23. JONES, R. N., HUMPHRIES, P., HERLING, F., and DOBRINER, K. J. Am. Chem. Soc. 74: 2820. 1952.
24. JONES, E. R. H. and WHITING, M. C. J. Chem. Soc. 1423. 1949.
25. MANASSE, M. Ber. 35: 3811. 1902.
26. MONTGOMERY, R. S. and DOUGHERTY, G. J. Org. Chem. 17: 823. 1952.
27. MOUSSERON, M. and MANON, G. Bull. soc. chim. 392. 1949.
28. ROMO, J., STORK, G., ROSENKRANZ, G., and DJERASSI, C. J. Am. Chem. Soc. 74: 2918. 1952.
29. SMITH, H. J. Chem. Soc. 803. 1953.
30. SONDHEIMER, F. and ROSENKRANZ, G. Experientia, 9: 62. 1953.
31. UNGNADE, H. E. and ORTEGA, I. J. Am. Chem. Soc. 73: 1564. 1951.
32. WILLIMANN, L. and SCHINZ, H. Helv. Chim. Acta, 32: 2151. 1949.
33. WINTERSTEINER, O. and MOORE, M. J. Am. Chem. Soc. 72: 1923. 1950.
34. WOODWARD, R. B. J. Am. Chem. Soc. 63: 1123. 1941.

NOTES

CALCULATION OF ELECTRON TRAP DEPTHS FROM THERMOLUMINESCENCE MAXIMA*

By A. H. Booth

The thermoluminescence curve, obtained by plotting the intensity of light emission against temperature for a constant rate of heating, is valuable for finding the distribution of electron traps in a phosphor. Each maximum in the light intensity corresponds to the emptying of a trap whose energy level is a function of the temperature at the maximum. This temperature is an easily measured experimental quantity but it has hitherto not been possible to evaluate the trap depth from this alone. Accessory data were required, such as the decay rate or the light sum stored at the peak (4), which might be difficult to obtain or imprecise. It will be shown here how the trap depth can be calculated using only the positions of the maxima at two different rates of heating.

Randall and Wilkins (3) derived the equation for the thermoluminescence or "glow" curve for a single trap depth, assuming first order kinetics and no re-trapping, in the form

$$[1] \qquad I = C\, n_0 s \exp\left[- \int^{T} (s/B) \exp(-E/kT)\, dT \right] \exp(-E/kT),$$

where I is the brightness, C and n_0 are arbitrary constants, E is the trap depth, s is an atomic frequency factor, and B is the rate of heating. From this they did not solve for the conditions for the maximum (the glow peak) directly, but wrote

$$E = T^* [1 + f(s, B)]\ k \log_e s$$

where T^* is the temperature at the maximum; and showed by plotting a numerical example of equation [1], using Bünger and Flechsig's (1) values for s and E in KCl(Tl) phosphor, that $f(s, B)$ is small compared with unity when B is in the range 0.5 to 2.5 degrees/sec. This linear relationship becomes, with the same value of $s(2.9 \times 10^9$ sec.$^{-1})$

$$E = 25\, k\, T^* \text{ (for } B \text{ in the range given).}$$

This last result has been widely quoted as a general rule of thumb; but the numerical constant depends on s, and this will be different for each trap, even in the same substance. In very simple cases where s can be obtained from the intercept on the plot of $1/T$ against the logarithm of the phosphorescence decay constant, E will be known from the slope, so that the glow curve data are then redundant.

It may have escaped attention that, even though the integral in the first exponential bracket cannot be expressed in closed form, an *exact* solution for the maximum in equation [1] can be had by setting the derivative equal to

*Issued as A.E.C.L. No. 89.

zero in the usual way. For we can write

$$u \,.\, dv/dT + v \,.\, du/dz \,.\, dz/dT = 0,$$

where u and v are the two exponentials (in the order written) and $u = e^z = du/dz$. Whence, directly,

$$[2] \qquad \frac{E}{k(T^*)^2} = \frac{s}{B} \exp\,(-E/kT^*).$$

This equation gives a curve which differs very little from a straight line, $E = a\,k\,T^*$. It is 6% below it at 100°K., 6% above it at 900°K. Thus, Randall and Wilkin's linear approximation will be excellent in most cases. The effect of heating rate on the maximum can now be given in explicit form:

$$\log_e B_0/B_1 = (2 \log_e T_0^* + E/kT_1^*) - (2 \log_e T_1^* + E/kT_0^*)$$

$$\sim a_1 - a_0 \text{ (using the linear approximation).}$$

Similarly,

$$\log_e s_0/s_1 \sim a_0 - a_1.$$

A more useful application of equation [2] follows. If the maxima are determined for two different rates of heating we have simultaneous equations in the unknowns E and s. Hence,

$$E = \frac{k\,T_1^*\,T_0^*}{T_0^* - T_1^*} \,.\, (\log_e B_0/B_1 + 2 \log_e T_1^*/T_0^*).$$

If needed, s can be found by substituting E back into [2].

Experimentally, such an approach appears attractive. Easily measured shifts in the maxima can be had with heating rates well within the practical range. Different workers (2, 3) have used rates of 0.03 to 3.0 degrees/sec. With the 0.67 ev. trap in KCl(Tl), for example, such a difference should cause a shift of nearly 50 degrees in the position of the maximum. This is, in fact, borne out experimentally in the references given, the peaks being at about 300° and 350°K. respectively.

In principle one should be able to obtain all trap depths from quite complex curves, although the relative contributions of peak and subpeaks may often be difficult to analyze. The assumption of first order kinetics seems to be generally valid for each individual trap, but a number of traps lying close together in depth may have decay rates which, in sum, obey an inverse power law (3). The identification of individual traps is then not feasible in any event.

1. Bünger, W. and Flechsig, W. Z. Physik, 67: 42. 1931.
2. Johnson, P. D. and Williams, F. E. J. Chem. Phys. 21: 125. 1953.
3. Randall, J. T. and Wilkins, M. H. F. Proc. Roy. Soc. (London), A, 184: 366. 1945.
4. Urbach, F. *In* Solid luminescent materials. (Cornell Symposium of American Physical Society). Chap. 6. John Wiley & Sons, Inc., New York. 1948.

Received November 4, 1953.
Chemistry Branch,
Atomic Energy of Canada Limited,
Chalk River, Ontario.

REACTIONS OF SYRINGALDEHYDE INVOLVING HALOGENATION

By K. R. Kavanagh and J. M. Pepper

In a manner similar to that whereby vanillin may be prepared by the oxidation of softwood lignins, a mixture of vanillin and syringaldehyde would be so obtained by the oxidation of hardwood lignins. The value of this preparation of these aromatic aldehydes as pure chemicals would be increased if their separation could be achieved readily. Pearl and Dickey (8) have summarized the various laboratory methods that have been used. A paper chromatographic separation has subsequently been described by Stone and Blundell (12). The aim of the present work, in part, was to determine whether syringaldehyde (VIII) could be separated from vanillin (VII) by bromination or iodination of the VII under conditions wherein no reactions occurred with the VIII. The halogenation of vanillin in the reactive 5-position is well established, but there have been no reports on any similar introduction of halogen into the syringaldehyde molecule. Any such reaction would be expected to be minimized owing to the absence of any such activated position ortho to the phenolic hydroxyl group. The decreased ortho-directing tendency of methoxyl groups, due likely to steric effects, has been pointed out by Rosenwald (11). Syringaldehyde was treated with iodine under similar conditions to those used for the preparation of 5-iodovanillin (9), that is, iodine dissolved in a potassium iodide solution was added slowly to an alkaline solution of the aldehyde. A dense, black, iodine-containing product resulted which gave no definite melting point. A similar iodination of a 1:1 molar mixture of vanillin and syringaldehyde was then attempted using an amount of iodine equimolar to the vanillin with which it was thought reaction would be more rapid. The same black product resulted and was not studied further. In the attempts to brominate syringaldehyde according to the procedure for the preparation of 5-bromovanillin (6), the previously unreported 2-bromosyringaldehyde (I), m.p. 186–187°C., was obtained. On repeating this reaction with equimolar amounts of vanillin, syringaldehyde, and bromine, a precipitate resulted which consisted of a mixture of 5-bromovanillin (m.p. 164°C.) and I. Neither of the halogenation methods appeared to be a practical means of separation of mixtures of VII and VIII. The 2-bromosyringaldehyde (I) was identified by analyses and conversion to the known derivatives.

Repeated attempts to convert syringic acid (III) to the reference compound 2-bromosyringic acid (II) according to the direct bromination procedure of Levine (5) were unsuccessful. It is interesting to note that Bogert and Plaut (1) reported a similar failure. 2-Bromo-3,4,5-trimethoxybenzoic acid (V) was made from 3,4,5-trimethoxybenzoic acid (IV) according to the method of Feist and Dschu (3) only if the powdered iron catalyst that they recommend was omitted; otherwise, unchanged IV was recovered. The oxidation of I with silver oxide according to the method used by Pearl (7) for the oxidation of vanillin gave a product having the required properties

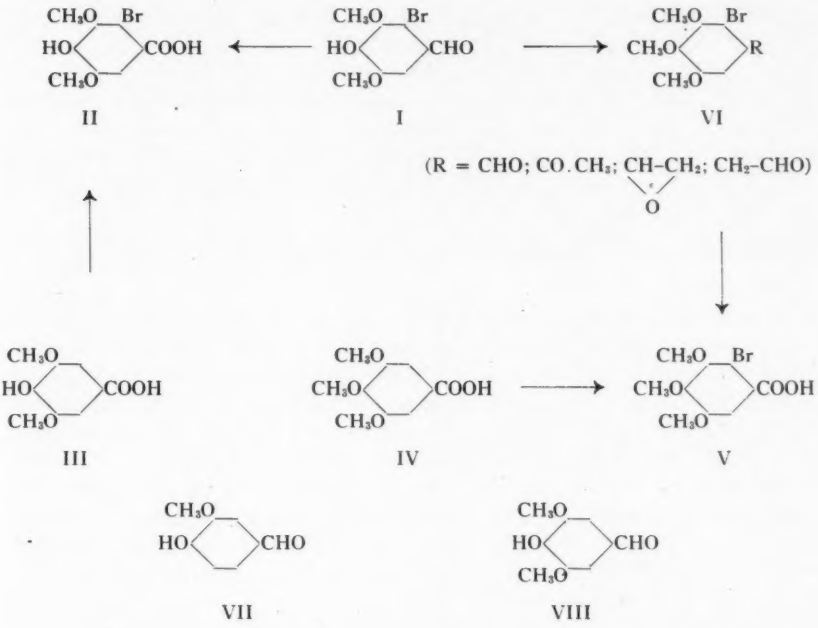

of II. Other structure proof of I was obtained by its methylation with diazomethane to VI, which was subsequently oxidized with potassium permanganate to a product V, identical with that obtained from IV. Since the reaction of aromatic aldehydes with diazomethane may give rise to the mixture of products shown as VI (2), no purification was attempted at this stage in the belief that all such products would be oxidized to V.

Two derivatives, the oxime and the acetate of 2-bromosyringaldehyde, were prepared as pure compounds and their analyses reported.

EXPERIMENTAL

A. Iodination Studies

Syringaldehyde (5 gm.) (9) was reacted with iodine under the same relative conditions as those used for the preparation of 5-iodovanillin (9). A black residue (5.5 gm.) resulted, which gave a positive Beilstein test, had no definite melting point but charred slowly to leave a residue. A similar treatment of equimolar amounts of syringaldehyde (5 gm.), vanillin (4.2 gm.), and iodine (7 gm.) again resulted in a similar black precipitate (9.3 gm.).

B. Bromination Studies

Syringaldehyde (6 gm.) was reacted with bromine under the same relative conditions as those used for the preparation of 5-bromovanillin (6). The resulting light yellow product (4.7 gm.) was recrystallized three times from glacial acetic acid; colorless needles, m.p. 186–187°C. A similar treatment of

equimolar (0.017 mole) amounts of syringaldehyde (3 gm.) and vanillin (2.5 gm.) with bromine (1.4 gm.) (0.0087 mole) gave rise to a white product (1.5 gm.) which, after two recrystallizations from ethanol, yielded a product (m.p. 152–155°C.) (0.9 gm.) whose mixed melting point (159–161°C.) with an authentic sample (m.p. 164°C.) indicated that it was mainly 5-bromovanillin. A further experiment using an equimolar (0.017 mole) amount of bromine yielded a product which, after recrystallization from ethanol, weighed 2.0 gm., m.p. 135–143°C.

C. Preparation and Identification of 2-Bromosyringaldehyde

Preparation

Several runs were made to study the optimum conditions of preparation of this new compound. Neither decreasing the rate of addition of bromine nor refluxing the reaction mixture for from 15 min. to six hours after complete addition materially affected the yield. The following procedure illustrated the sythesis. Syringaldehyde (6 gm.) was dissolved, with warming, in glacial acetic acid (15 ml.). To this hot solution was added, dropwise, over a period of 20 min., a solution of bromine (5.3 gm.) in acetic acid (10 ml.). The crude reaction product which separated was removed by filtration; weight, 6.2 gm. After recrystallization from glacial acetic acid, then ethanol, colorless needles resulted. Yield, 3.8 gm., m.p. 186–187°C. Calc. for $C_9H_9O_4Br$: mol. wt. 261; C, 41.4; H, 3.48; Br, 30.6; OCH_3, 23.8%. Found: mol. wt. (Rast) 262, 265; C, 41.55, 41.60; H, 3.65, 3.60; Br, 30.7, 30.86; OCH_3, 23.2, 23.6%.

2-Bromosyringaldehyde oxime.—The oxime was prepared in the usual way; m.p. 132–133° C.* Calc.for $C_9H_{10}O_4BrN$: C, 39.2; H, 3.65; OCH_3, 22.5%. Found: C, 39.9, 39.2; H, 4.1, 4.0; OCH_3, 22.2%.

2-Bromosyringaldehyde acetate.—This monoacetate was prepared according to the method used for the preparation of the analogous derivative of vanillin (10). Recrystallization from ethanol gave white needles, m.p. 113.5–114.5°C. Calc. for $C_{11}H_{11}O_5Br$: C, 43.62; H, 3.66; OCH_3, 20.4%. Found: C, 43.70; H, 3.82; OCH_3, 20.4, 19.9% .

Identification

Synthesis of 2-bromo-3,4,5-trimethoxybenzoic acid (IV).—Starting with 3,4,5-trimethoxybenzoic acid the method of Feist and Dschu (3) was followed but the required product, m.p. 148.5–150°C. (reported (3), 148°C.) was obtained only if the powdered iron catalyst, mentioned in their procedure, was omitted.

Oxidation of 2-bromosyringaldehyde to 2-bromosyringic acid.—To the washed silver oxide prepared from silver nitrate (2.4 gm.) (7) was added water (24 ml.), sodium hydroxide (2.8 gm.), and 2-bromosyringaldehyde (2 gm.). After gentle heating with stirring for 20 min., the solution was filtered and the

**It was observed that this oxime, after recrystallization from either ethanol–water or water alone, melted at 100–102°C. after air-drying. Further drying in an Abderhalden drier or in a vacuum desiccator raised the melting point to 132–133°C. This suggested that the oxime forms a stable hydrate of unknown exact composition. Calc. for $C_9H_{10}O_4BrN.3/2\ H_2O$: OCH_3, 20.4%. Found for the product, m.p. 100–102°C: OCH_3, 20.4, 20.2, 20.8%.*

residue washed with hot water. The combined filtrate was acidified with sulphur dioxide gas but no precipitate formed. To recover any unreacted aldehyde, dilute sulphuric acid (7 ml.) was added and the solution boiled until the sulphur dioxide had been removed. After standing, a precipitate was removed and was shown to be starting material (35% recovery). The remaining filtrate was extracted with ether. This extract was dried and the excess solvent removed to leave a residue (1.0 gm.). Two recrystallizations from dilute acetic acid gave pale yellow crystals (0.6 gm.) m.p. 153–155°C. in good agreement with that of 155°C. reported by Levine (5). Calc. for $C_9H_9O_5Br$: C, 39.0; H, 3.28; OCH_3, 22.4%. Found: C, 39.2; H, 3.38; OCH_3, 22.2%.

Conversion of 2-bromosyringaldehyde to 2-bromo-3,4,5-trimethoxybenzoic acid.—To a suspension of 2-bromosyringaldehyde (4 gm.) in ether (300 ml.) was added an ethereal solution of diazomethane prepared from nitrosomethylurea (20.6 gm.). After 2.5 hr. stirring at around 0°C. a clear solution resulted after which the ether and excess diazomethane were allowed to evaporate at room temperature. The residual yellow oil was dissolved in ether (100 ml.) and this solution extracted with 5% sodium hydroxide (2 × 100 ml.). The ether layer, after drying, was concentrated to leave an orange-colored oil (4.3 gm.) which was used directly in the next step.

The method of Head and Robertson (4) for the oxidation of a substituted benzaldehyde to the corresponding acid was first tested by the successful conversion of veratraldehyde to veratric acid in 60% yield, after recrystallization from dilute acetone. To the methylated product (4.3 gm.) obtained above, dissolved in acetone (100 ml.), was added with swirling a solution of potassium permanganate (1.62 gm.) in water (50 ml.) over a period of one hour at 50–55°C. During the next hour, further permanganate (0.38 gm. in 10 ml. water) was added. The mixture was cooled to 0°C., cleared with sulphur dioxide, and the acetone evaporated. Some white crystals and a yellow oil separated, which, after decantation of the water, were treated with saturated sodium bicarbonate (50 ml.) which dissolved only the crystals. From this solution, after acidification, a white precipitate (0.8 gm.) was obtained. Reoxidation of the oil resulted in a further amount (0.2 gm.) of product. These were combined and after recrystallization from dilute ethanol gave the required product, m.p. 146–148°C. A mixed melting point with synthetic V was undepressed. Calc. for $C_{10}H_{11}O_5Br$: C, 41.3; H, 3.81; OCH_3, 31.9%. Found: C, 42.1, 41.6; H, 3.94, 4.16; OCH_3, 31.6, 31.8%.

ACKNOWLEDGMENT

The authors wish to thank the Saskatchewan Research Council for the award of a Graduate Research Fellowship to one of them (K. R. K.). The Howard Smith Chemicals Limited, kindly donated the vanillin used in this investigation.

1. BOGERT, M. T. and PLAUT, E. J. Am. Chem. Soc. 37: 2729. 1915.
2. Die Chemie. Newer methods of preparative organic chemistry. Interscience Publishers Inc., New York. 1948. p. 522.

3. FEIST, K. and DSCHU, G. L. Festschr. A. Tschirch, 23–29. 1926. (Chem. Abstr. 22: 3405. 1928.)
4. HEAD, F. S. H. and ROBERTSON, A. J. Chem. Soc. 2432. 1931.
5. LEVINE, A. A. J. Am. Chem. Soc. 48: 797. 1926.
6. MCIVOR, R. A. and PEPPER, J. M. Can. J. Chem. 31: 298. 1953.
7. PEARL, I. A. J. Am. Chem. Soc. 68: 429. 1946.
8. PEARL, I. A. and DICKEY, E. E. J. Am. Chem. Soc. 73: 863. 1951.
9. PEPPER, J. M. and MACDONALD, J. A. Can. J. Chem. 31: 476. 1953.
10. PISOVSCHI, T. J. Ber. 43: 2137. 1910.
11. ROSENWALD, R. H. J. Am. Chem. Soc. 74: 4602. 1952.
12. STONE, J. E. and BLUNDELL, M. J. Anal. Chem. 23: 771. 1951.

RECEIVED SEPTEMBER 29, 1953.
DEPARTMENT OF CHEMISTRY,
UNIVERSITY OF SASKATCHEWAN,
SASKATOON, SASK.

CANADIAN JOURNAL OF CHEMISTRY

Notes to Contributors

Manuscripts

(i) ***General.*** Manuscripts should be typewritten, double spaced, on paper 8½×11 in. **The original and one copy are to be submitted.** Tables (each typed on a separate sheet) and captions for the figures should be placed at the end of the manuscript. Every sheet of the manuscript should be numbered.

Style, arrangement, spelling, and abbreviations should conform to the usage of this journal. Names of all simple compounds, rather than their formulas, should be used in the text. Greek letters or unusual signs should be written plainly or explained by marginal notes. Superscripts and subscripts must be legible and carefully placed.

Manuscripts should be carefully checked before they are submitted; authors will be charged for changes made in the proof that are considered excessive.

(ii) ***Abstract.*** An abstract of not more than about 200 words, indicating the scope of the work and the principal findings, is required, except in Notes.

(iii) ***References.*** References should be listed **alphabetically by authors' names,** numbered, and typed after the text. The form of the citations should be that used in this journal; in references to papers in periodicals, titles should not be given and only initial page numbers are required. All citations should be checked with the original articles and each one referred to in the text by the key number.

(iv) ***Tables.*** Tables should be numbered in roman numerals and each table referred to in the text. Titles should always be given but should be brief; column headings should be brief and descriptive matter in the tables confined to a minimum. Numerous small tables should be avoided.

Illustrations

(i) ***General.*** All figures (including each figure of the plates) should be numbered consecutively from 1 up, in arabic numerals, and each figure referred to in the text. The author's name, title of the paper, and figure number should be written in the lower left corner of the sheets on which the illustrations appear. Captions should not be written on the illustrations (see Manuscript (i)).

(ii) ***Line Drawings.*** Drawings should be carefully made with India ink on white drawing paper, blue tracing linen, or co-ordinate paper ruled in blue only; any co-ordinate lines that are to appear in the reproduction should be ruled in black ink. Paper ruled in green, yellow, or red should not be used unless it is desired to have all the co-ordinate lines show. All lines should be of sufficient thickness to reproduce well. Decimal points, periods, and stippled dots should be solid black circles large enough to be reduced if necessary. Letters and numerals should be neatly made, preferably with a stencil (**do NOT use typewriting**) and be of such size that the smallest lettering will be not less than 1 mm. high when reproduced in a cut 3 in. wide.

Many drawings are made too large; originals should not be more than 2 or 3 times the size of the desired reproduction. In large drawings or groups of drawings the ratio of height to width should conform to that of a journal page but the height should be adjusted to make allowance for the caption.

The original drawings and one set of clear copies (e.g. small photographs) are to be submitted.

(iii) ***Photographs.*** Prints should be made on glossy paper, with strong contrasts. They should be trimmed so that essential features only are shown and mounted carefully, with rubber cement, on white cardboard.

As many photographs as possible should be mounted together (with a **very** small space between each photo) to reduce the number of cuts required. Full use of the space available should be made and the ratio of height to width should correspond to that of a journal page; however, allowance must be made for the captions. Photographs or groups of photographs should not be more than 2 or 3 times the size of the desired reproduction.

Photographs are to be submitted in duplicate; if they are to be reproduced in groups one set should be mounted, the duplicate set unmounted.

Reprints

A total of 50 reprints of each paper, without covers, are supplied free. Additional reprints, with or without covers, may be purchased.

Charges for reprints are based on the number of printed pages, which may be calculated approximately by multiplying by 0.6 the number of manuscript pages (double-spaced typewritten sheets, 8½ in.×11 in.) and making allowance for illustrations (not inserts). The cost per page is given on the reprint requisition which accompanies the galley.

Any reprints required in addition to those requested on the author's reprint requisition form must be ordered officially as soon as the paper has been accepted for publication.

Contents

Printed in Canada *by* University of Toronto Press